URBAN DEVELOPMENT DIRECTORATE (UDD)

Government of the People's Republic of Bangladesh

Final Report on
Engineering Geological and Geo-Physical Surveys

Under

Preparation of Payra-Kuakata Comprehensive Plan Focusing on Eco-Tourism

Package No. 7 (Seven)

December, 2020

Submitted by

Environmental & Geospatial Solutions (EGS)

Suite No.-6, 12th Floor, 218, Sahera Tropical Center, Elephant Road, Dhaka-1205

Abbreviations

ASTM:	American Society for Testing and Materials
AVS30:	Average Shear Wave velocity of 30 meter depth
BH:	Borehole
DSHA:	Deterministic Seismic Hazard Assessment
EGL:	Existing Ground Level
GWL:	Ground Water Level
MASW:	Multi-Channel Analysis of Surface Wave
N value:	Soil resistance or compactness
PGA:	Peak Ground Acceleration
PS logging:	Primary and Shear wave logging (Down-hole seismic test)
SA:	Spectral Acceleration
SPT:	Standard Penetration Tests
UDD:	Urban Development Directorate
PSHA:	Probabilistic Seismic Hazard Assessment

EXECUTIVE SUMMARY

Urban Development Directorate (UDD) has decided to introduce suitable development plan for Amtali, Taltoli, Barguna Sadar and Pathargata upazila of Barguna dristrict and Galachipa, Rangabali and Kalapara upazila of Patuakhali dristrict. As such, UDD has initiated the project titled 'Preparation of Payra-Kuakata Comprehensive Plan Focusing on Eco-Tourism'. Engineering Geological and Geo-Physical study is one of the important development module of this project. In this development plan, subsurface geological and geotechnical information's consider as an important tool for a durable and sustainable urbanization.

In this project work, both the geophysical and geotechnical investigations have been conducted. In geotechnical survey 100 numbers of SPT boring (up to 30m) has been conducted in the field and the soil samples also collected from the field and laboratory tests have been completed. And in geophysical Survey, sixteen (16) Downhole Seismic (PS Logging), twenty seven (27) Multi-channel analysis of surface wave (MASW), and forty four (44) Microtremor (single array) have been investigated by using some sophisticated instruments.

However, subsurface 3D model of different layers has been developed through Geotechnical investigation, which have been updated eventually by integrating other data set. According to Standard Penetration Test's (SPT) N-value, layer 4 and layer 6 are considered as a foundation layer.

This study is an attempt towards refinement in seismic hazard calculation of Bangladesh using PSHA and DSHA methods. New approaches in seismic source zone delineations, consideration for local site effects and incorporating inherent certainties in different source parameters as well as attenuation relationship are some of the improvements applied in this study. Results are presented in form of hazard maps and curves showing PGA and SA. Peak ground acceleration has been computed with 2% and 10% probability exceedance in 50 years. In this study both peak ground acceleration (PGA) and peak spectral acceleration (PSA) have been estimated considering with site effect. However, the ground motion has found slight higher than all other previous studies. The reason might be due to the utilization of appropriate Ground Motion Prediction Equation for different fault zones and utilization of Vs30 information of project area to account for the site effect.

Moreover, the project area is relatively liquefaction hazard prone. Liquefaction hazard map is showing approx. 67.79% areas are at very high risk, 29.80% have moderate risk and 2.41 % areas are at low and very low risk respectively. Overall the area lies in very high to moderate liquefaction hazard prone area. Most of the area lies within very highly liquefaction hazard prone area (about 67.79%). The remaining project area is mostly in moderate liquefaction hazard prone zone (about 29.80%).

According to Geological suitability map, most of the area is moderately suitable (approx. 33.31%) to poorly suitable (approx. 35.35%) for infrastructure development, mainly in the western part, central part and southern part of the study area as well as north part of the Amtali upazila. Approximately 3.57% (good) area represents very suitable for infrastructure development in the study area. And very poorly (approx. 27.77% of the total area) suitable area for the infrastructure development are along with eastern part as well as north-eastern part of the study area.

Nasim Ferdous

Nasim Ferdous
Team Leader and Coordinator
Engineering Geology and
Geotechnical Unit Email:
egs.bd.2014@gmail.com
Environmental & Geospatial
Solutions (EGS)

CONTENTS

LIST OF FIGURES

1. INTRODUCTION

1.1. Background

Bangladesh can earn money in local and also in foreign exchange by opening an environmental friendly tourist recourse at Barguna and Patuakhali dristrict. The spot, if properly developed, would become an excellent holiday resort and tourist center. The success of developing Barguna and Patuakhali district as a tourist center, seaport land area and industrial zone depends much on good communication facilities and availability of modern amenities. Moreover, the proposed sea port and industrial zone would generate lots of new financial activities including huge vehicular traffic such as air, rail, road and water. This phenomenon would have both positive and negative impacts on the socio-economic condition and existing land use pattern of the region. The proposed planning package would guide such probable changes in the socio-economic condition and landuse pattern of the region, and would also address the adverse impact of such changes.

Landuse planning is an impotent component for a modern urban development. A paradigm shift in landuse planning has been taken place by mainstreaming disaster risk reduction in landuse planning in Bangladesh. This phenomenon involves integrating earthquake risk investigation in landuse planning in particular. Therefore attempt has been taken to incorporate a rigorous geological and geotechnical site characterization, including a potential risk analysis in preparing Payra-Kuakata Comprehensive Plan Focusing on Eco-Tourism.

Urban development is being increasing very fast in Bangladesh. The government has planned to develop Barguna and Patuakhali district as a tourist center, seaport and industrial zone. However, risk sensitive urban planning is very important in such a disaster prone country like Bangladesh for a risk resilient urban development in these cities and surrounding area. Among those cities Amtali, Taltoli, Barguna Sadar and Pathargata upazila of Barguna district and Galachipa, Rangabali and Kalapara upazila of Patuakhali dristrict is most disaster prone area because of the area is located near coastal area and relatively less seismo-tectonically active zones. So this area covers the assessment and management of Geohazard like; earthquake and ground subsidence, and hydrometorological hazards in predominantly urban context. Considering the geohazard threat of the populated urban and rural areas of the project, UDD has taken many initiatives for a rigorous geological and geotechnical (engineering geology) site characterization of the 7 (Seven) upazilas, including Amtali, Taltoli, Barguna Sadar,

Pathargata, Galachipa, Rangabali and Kalapara upazila under 'Preparation of Payra-Kuakata Comprehensive Plan Focusing on Eco-Tourism'.

Therefore the geological and geotechnical site characterization of the areas including potential seismic hazard assessment and ground subsidence risk analysis are an important component for rick sensitive landuse planning of the populated urban and rural area. In here, Environmental & Geospatial Solutions (EGS) has been entrusted to conduct this project work.

1.2. Location and Accessibility

Barguna district (Barisal division) area 1831.31 sq km, located in between 21°48' and 22°29' North latitudes and in between 89°52' and 90°22' East longitudes. It is bounded by Jhalokati, Barisal, Pirojpur and Patuakhali districts on the North, Patuakhali district and Bay of Bengal on the South, Patuakhali district on the East, Pirojpur and Bagerhat districts on the West. Amtoli, Taltoli, Patharghata and Barguna Sadar upazila are selected as a project area from Barguna district.

On the other hand, Patuakhali district (Barisal division) area of 3220.15 sq km, located in between 21°48' and 22°36' North latitudes and in between 90°08' and 90°41' East longitudes. It is bounded by Barisal district on the North, Bay of Bengal on the South, Bhola district on the East, Barguna district on the West. The land of the district is composed of alluvial soil of the meghna basin and of a number of small char lands. Galachipa (Including New Created Rangabali Upazila) and Kalapara upazila are selected as a project area from Patuakhali District.

Kuakata a scenic sea beach on the South of Bangladesh. The most important attraction of the beach is that one can see both sunrise and sunset from some of its locations. Situated 320 km from Dhaka and 70 km from the Patuakhali district headquarters, Kuakata is part of Latachapli and Dhulasar unions of Kalapara upazila. On the other hand, Amtali upazila of Barguna District is on the way to Kuakata from Barisal. The only highway towards Kuakata from Barisal is running through Amtali upazila. Due to the reason, both Kalapara and Amtali upazila have been undertaken for "Preparation of Eco-Tourism Development Plan for Kuakata Coastal Region" to develop tourism in the area in an integrated and comprehensive manner on a regional planning concept. The best way to reach Kuakata from Dhaka is to first travel to Barisal by road, water, or air, and then to take the bus or boat/launch for the destination. The Bangladesh Road Transport Corporation introduced a direct bus service from Dhaka to Kuakata via Barisal. Besides, on the west of Kuakata, there is a reserve forest, Fatrar Char by

name, which is part of Sundarbans and is a unique location for tourism development. Sonar char of Rangabali upazila is also a place of panoramic beauty. There is ample opportunity for tourism development in the area. Moreover, Paira Bandar, the third sea port has already been established at Ravnabad Channel near Kuakata, which would act as catalyst for radical change in the overall urbanization in the region (Location of Project Area Figure 1.1).

Table: Area, Population and Density of the Project Area:

Name of District	Name of the Upazila	Area		Population	Density of total Population per Sq.Km
		Sq. Km	Acre		
Barguna	BargunaSadarUpazila	454.38	112279.74	261343	575
Barguna	PathargataUpazila	387.36	95718.74	163927	423
Barguna	AmtaliUpazila (Including TaltoliUpazila)	720.75	178101.2	270802	376
Patuakhali	Galachipa (Including New Created RangabaliUpazila)	1268.37	313421.05	361518	285
Patuakhali	KalaparaUpazila	491.89	121548.67	237831	484
Total		**3322.77**	**821074**	**1295421**	**389.86**

Source: BBS, 2011

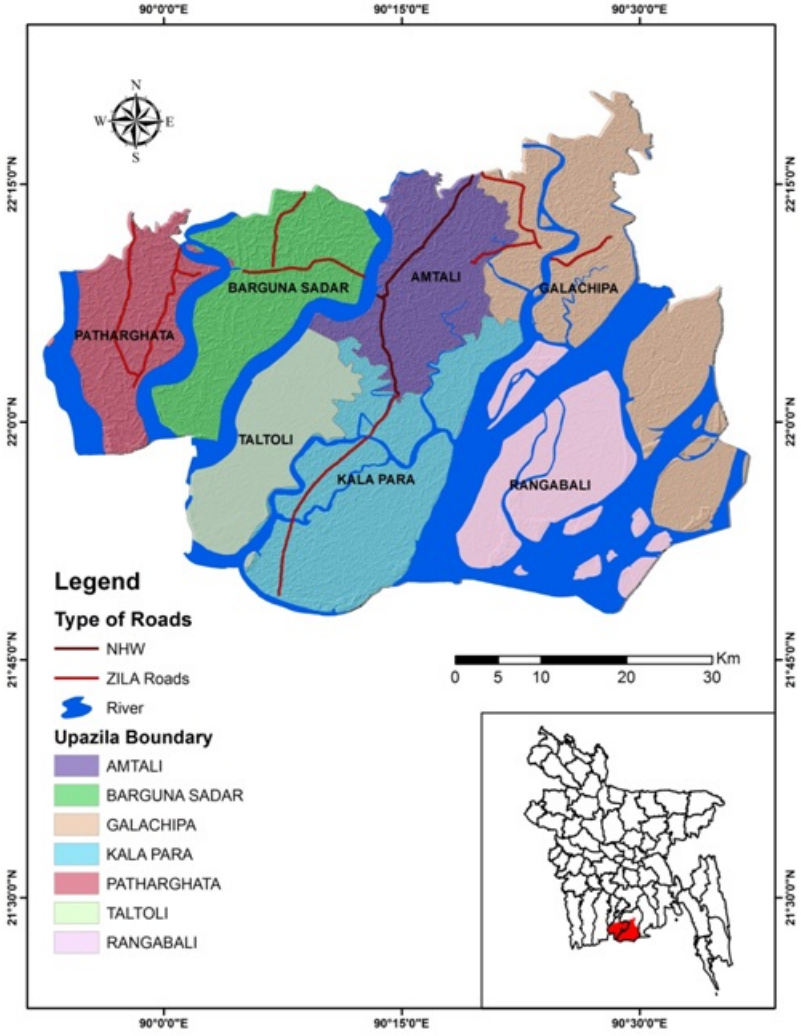

Figure 1.1 Location map of the project area

1.3. Aims and Objectives

The main objective of the research is to carry out a Engineering Geological and Geo-Physical Survey of the 7 (Seven) upazila including Amtoli, Taltoli, Barguna Sadar and Patharghata of Barguna district and Galachipa, Rangabali and Kalapara upazila of Patuakhali district under Preparation of Payra-Kuakata Comprehensive Plan Focusing on Eco-Tourism. The main objective will be achieved through accomplishment of the following sub-objectives:

i. Preparation of Geological unit map of the study area.

ii. Sub-surface lithological 3D model development of the study area.

iii. Preparation of Soil classification map by using geophysical and geotechnical investigations of the study area.

iv. Development of engineering geological map based on AVS30 values of the study area.

v. Foundation layers delineation and determination of engineering properties of the sub-soil.

vi. PGA, Sa (T) Maps of 5% damping at 0.3 and 1.0 second periods values of 10% exceedance probability during next 50 years for local site condition determination of the study area.

vii. Risk Sensitive Building Height determination of the study area.

viii. Formulation of Policies and plans for mitigation of different types of hazards, minimizing the adverse impacts of climate change and recommend possible adaptation strategies for the region.

2. METHODOLOGY

2.1. Strategic Methodology

The methodology consists of both field and laboratory investigations. To conduct this project work, geotechnical and geophysical data of soil need to be collected, analysed and interpreted. Geotechnical data should be collected from field investigations *i.e.,* boring, standard penetration test (SPT), and laboratory investigations *i.e.,* soil physical properties test, consolidation test, direct shear test and triaxial test of undisturbed soil sample. Geophysical data should be collected from down-hole seismic test (PS logging); Multi-channel analysis of surface wave (MASW) and Singles Microtremor survey. The total works have been conducted through the following methodology-

2.1.1. Geophysical Investigation

Field geophysical investigation is conducted to achieve the purpose of seismic hazard assessment. Seismic site characterization by analyzing seismic wave propagation velocity from acquired shallow seismic wave form data is the main objective. P-S logging, Multi Channel Analysis of Surface Wave (MASW) and Microtremor tools are involved in geophysical investigation.

- General purposes of the geophysical survey:

- To estimate shear wave velocity and measure soil/rock properties (i.e. shear modulus, bulk modulus, compressibility, and Poisson's ratio)
- Engineering geological map development based on AVS30
- To Seismic site response study
- Risk Sensitive Building Height
- Characterization of strong motion sites
- Utilize this information for seismic hazard analysis

2.1.2. Geotechnical Investigation

Geotechnical investigations have become an essential component of every construction to ensure safety of human beings and materials. It includes a detailed investigation of the soil to determine the soil strength, composition, water content, and other important soil characteristics. Geotechnical investigations are executed to acquire information regarding the physical characteristics of soil and rocks. The purpose of geotechnical investigations is to design earthworks and foundations for structures, and to execute earthwork repairs necessitated due to changes in the subsurface environment. A geotechnical examination includes surface and subsurface exploration, soil sampling, and laboratory analysis. Geotechnical investigations are also known as foundation analysis, soil analysis, soil testing, soil mechanics, and subsurface investigation. The samples are examined prior to the development of the location. Geotechnical investigations have acquired substantial importance in preventing human and material damage due to the earthquakes, foundation cracks, and other catastrophes. Geotechnical investigations can be as simple as conducting only a visual assessment of the site or as detailed as a computer-aided study of the soil using laboratory tests.

General purposes of the geotechnical survey:

- Sub-surface lithological 3D model development
- Foundation layers delineation and developing engineering properties of the sub-soil
- Liquefaction susceptibility or Liquefaction potential index (LPI) map have been constructed from study data

However, following investigations have been conducted for collecting both geotechnical and geophysical data in the Project area:

SL No	Test Name	Numbers of tests were required	Numbers of tests were done
In Field			
1	Borelog Drilling with SPT (upto 30m)	100	100
2	PS logging (30m depth)	16	16
3	MASW (30m depth)	27	27
4	Single Microtremor	43	44
In Laboratory			
1	Particle/Grain Size Analysis	100	200
2	Atterberg Limits Determination	100	100
3	Specific Gravity Determination	90	100
4	Direct Shear Test	38	38
5	Unconfined Compression strength Determination	37	37
6	Consolidation Test	37	37
7	Moisture Content Determination	-	100
8	Triaxial Test	35	36

2.2. Detail Procedures Of Survey/Testing

The method of testing/surveying, application, Instrumentation and previous works of Geophysical and Geotechnical investigation are given below-

2.2.1. Test Detail and Procedure of Downhole Seismic Test (Ps Logging)

Seismic down hole test is a direct measurement method for obtaining the shear wave velocity profile of soil stratum. The seismic down hole test aims to measure the travelling time of elastic wave from the ground surface to some arbitrary depths beneath the ground. The seismic wave was generated by striking a wooden plank by a 7kg sledge hammer. The plank was placed on the ground surface at around 1 m in horizontal direction from the top of borehole. The plank was hit separately on both ends to generate shear wave energy in opposite directions and is polarized in the direction parallel to the plank.

The shear wave emanated from the plank is detected by a tri-axial geophone. The geophone was lowered to 1 m below ground surface and attached to the borehole wall by inflating an air bladder. Then, the measurements were taken at every 1 m interval until the geophone was lowered to 30 m below ground surface. For each elevation, 9 records were taken and then used

to calculate the shear wave velocity. The first arrival time of an elastic wave from the source to the receivers at each testing depth can be obtained from the downhole seismic test.

Figure 2.1 Field Data Acquisition by PS logger

When two geophones are used (in special case) at that situation, two geophones are lowered in the hole by keeping them 1.5m apart. There exists two ways of moving geophone either upward or downward. Say, if the hole is 30m then the bottom geophone is kept at 30m and then the top geophone will be at 28.5m and then we bring these geophones upward by taking reading after each meter and for downward is vice versa. In Downhole Seismic, an accelerometer mounted to a wooden plank source is used to trigger data collection.

Figure 2.2 Main Component of the Freedom Data PC

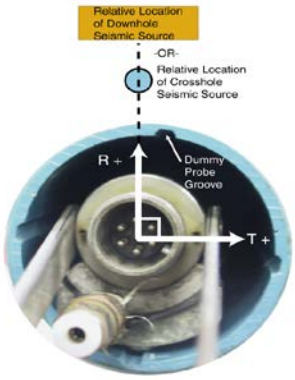

Figure 2.3 Receiver Orientation in Sinco casing

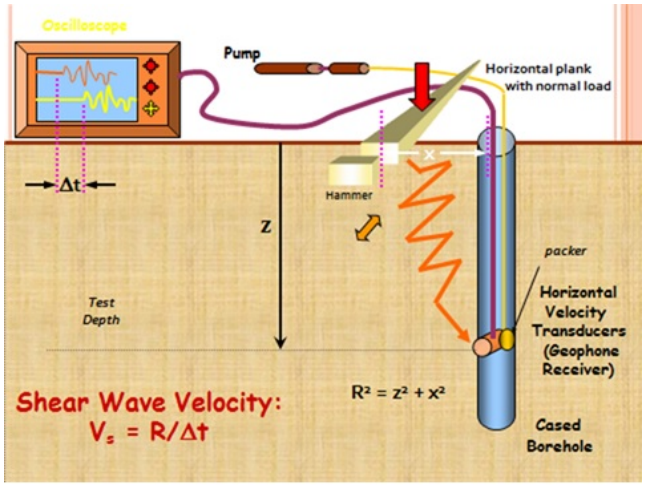

Figure 2.4 Calculation of Shear Wave Velocity by Down hole Seismic, where R=Distance between source to geophone

Figure 2.5 To set the wooden plank 1.0 meters from a borehole

Figure 2.6 To attach the trigger to a hammer.

Figure 2.7 To connect the air pump with a battery.

Figure 2.8 To connect the computer with cables which are connected to the geophone.

Figure 2.9 Make sure the geophone works. Then, put the geophone into the borehole and fix the safety rope with the holder

Figure 2.10 Hit the wooden plank in 3 directions which are on the left, right and vertical directions.

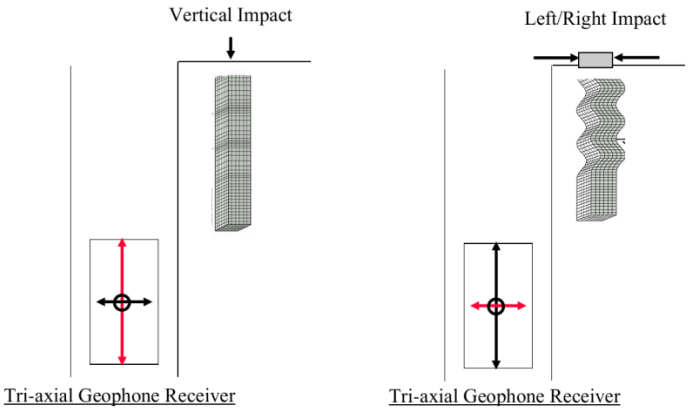

Figure 2.11 Triaxial geophone behavior.

Analysis and Calculation from PS Logging

P-wave travel time is calculated by the first arrival of either peak or trough in the seismic trace and P-wave is characterized by higher frequency and lower amplitude. On the other hand, shear wave is characterized by lower frequency but high amplitude.

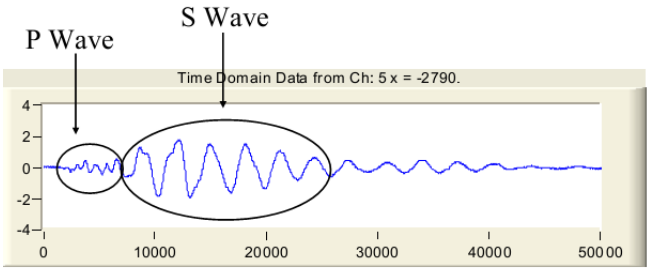

Figure 2.12 P wave and S wave in the Computer Window

S wave travel time is calculated from the first cross as we hit in both direction of the wooden plank so there generate opposite phase shear waves in radial and transverse direction and cross at some points.

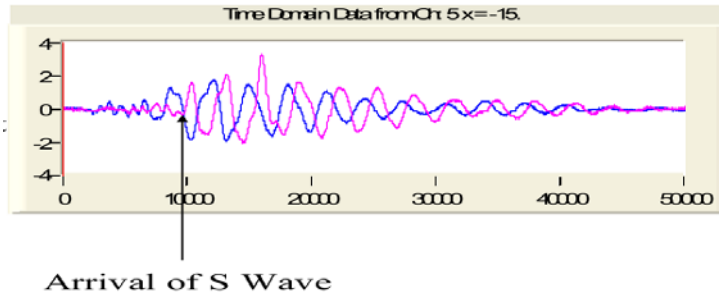

Figure 2.13 Arrival of S wave

Moreover, bounty of engineering geological parameters of soil can be determined whenever shear wave and compressional wave velocity is known. The Shear Modulus (G), Constrained Modulus (M) , Poisson Ratio (ν) and Young Modulus(E) of the soil profiles are calculated using the following formula:

$$G = \rho V_S^2$$

$$M = \rho V_P^2$$

$$\nu = [0.5(\frac{V_P}{V_S})^2 - 1]/[(\frac{V_P}{V_S})^2 - 1]$$

$$E = 2G(1+\nu)$$

Where, *p*is the local soil mass density (unit weight divided by gravity) obtained from the boring log information is taken 2 gm/cc for based on SPT results.

Besides, the average shear wave velocity upto 30 m depth has been determined using the following equation.

$$T_{30} = \sum \frac{Hi}{Vi}$$

$$AVS\ 30 = \frac{30}{T_{30}}$$

Where, Hi : Thickness of i th layer and $30 = \sum Hi$

Vi: S-wave velocity of i th layer

Instrument List

The PS logging test equipments are listed below-

1. One Freedom NDT PC
2. Two High Sensitive Tri-axial Geophones.
3. Two set Cable/Air lineSpool
4. Wooden Plank.
5. 7kg weight Hammer.

Figure 2.14 Freedom Data PC with P-SV Downhole Source and 1 Tri-axial Geophone Receiver used in Crosshole Seismic Investigations

Application of PS Logging Test

Downhole Seismic (PS Logging) system is useable for providing information on dynamic soil and rock properties for earthquake design analyses for structures, liquefaction potential studies, site development, and dynamic machine foundation design. The investigation determines shear and compressional wave depth versus velocity profiles. Other parameters, such as Poisson's ratios and moduli, can be easily determined from the measured shear and compressional wave velocities. The PS Logging is a downhole method for the determination of material properties of soil and rock.

2.2.2. Test Detail and Procedure of Multi-Channel Analysis of Surface Wave (MASW)

MASW utilizes the frequency dependent property of surface wave velocity, or the dispersion property, for Vs profiling. It analyses frequency content in the data recorded from a geophone array deployed over a moderate distance.

MASW utilizes the frequency dependent property of surface wave velocity, or the dispersion property, for Vs profiling. It analyses frequency content in the data recorded from a geophone array deployed over a moderate distance.

The processing of MASW is schematically summarized in Figure 2.15. The principle MASW is to employ and arrange a number of sensors on the ground surface to capture propagating Rayleigh waves, which dominates two-thirds of the total seismic energy generated by impact sources. If the tested ground is not homogeneous, the observed waves will be dispersive, a phenomenon that waves propagate towards receivers with different phase velocities depending on their respective wavelength (see Figure 2.16).

From field observation, the data in space-time domain (for instance, the left plot in Figure 2.15) is transformed to frequency-velocity domain by slant-stack and Fast Fourier transform using

$$S(\omega,c)=\int e^{-i\frac{\omega}{c}x}U(x,\omega)\,dx$$

where U(x,ω) is the normalized complex spectrum obtained from the Fourier transform of $u(x,t)$, ω is the angular frequency, c is the testing-phase velocity and $S(\omega,c)$ is the slant-stack amplitude for each ω and c, which can be viewed as the coherency in linear arrival pattern along the offset range for that specific combination of ω and c. When c is equal to the

true phase velocity of each frequency component, the $S(\omega,c)$ will show the maximum value. Calculating $S(\omega,c)$ over the frequency and phase-velocity range of interest generates the phase-velocity spectrum where dispersion curves can be identified as high-amplitude bands. The dispersion curve is, then, used in inversion process to determine the shear wave velocity profile of the ground.

In theory, a phase-velocity spectrum can be calculated for a known layer model **m** and the field setup geometry. This process is called forward modeling. The inversion process tries to adjust assumed layer model as much as possible through several iterations in order to make the calculated spectrum looks similar to the dispersion curve obtained from the field test. Once the algorithm can match the calculated with the measured one, the assumed model will be considered as the true profile.

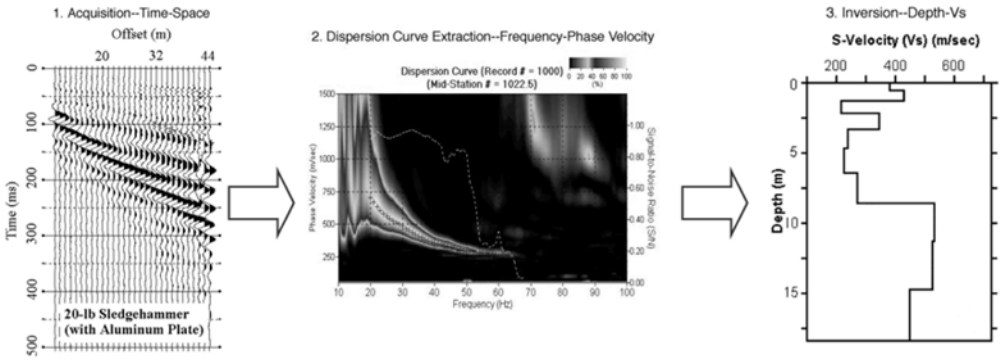

Figure 2.15 MASW data processing (Park et al., 1999)

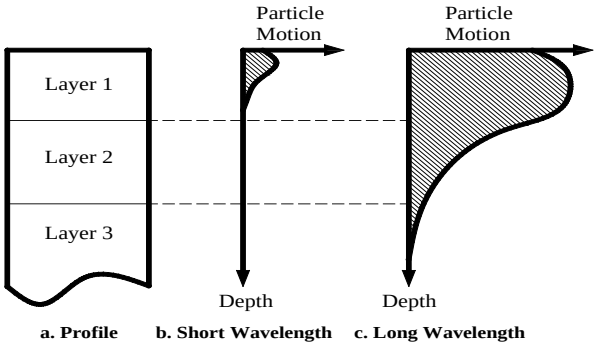

Figure 2.16 Rayleigh wave dispersion in layer media (Rix, 1988)

Active Source Data Acquisition

The active MASW method was introduced in GEOPHYSICS in 1999. This is the most common type of MASW survey that can produce a 2D VS profile. It adopts the conventional mode of survey using an active seismic source (e.g., a sledge hammer) and a linear receiver array, collecting data in a roll-along mode. It utilizes surface waves propagating horizontally along the surface of measurement directly from impact point to receivers. It gives this VS information in either 1D (depth) or 2D (depth and surface location) format in a cost-effective and time-efficient manner. The maximum depth of investigation (z max) is usually in the range of 10–30 m, but this can vary with the site and type of active source used.

Seismic energy for active source surface wave surveys can be created by various ways, but we used a sledgehammer to impact a striker plate on the ground since it is a low-cost, readily available item. To signal to the seismograph when the energy has been generated, a trigger switch is used as the interface between the hammer and the seismograph. When the sledgehammer hits the ground, a signal is sent to the seismograph to tell it to start recording.

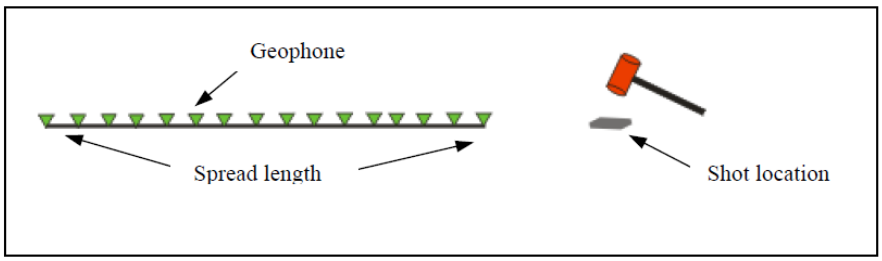

Figure 2.17 Schematic of linear active source spread configuration

And the source spread configuration like below:

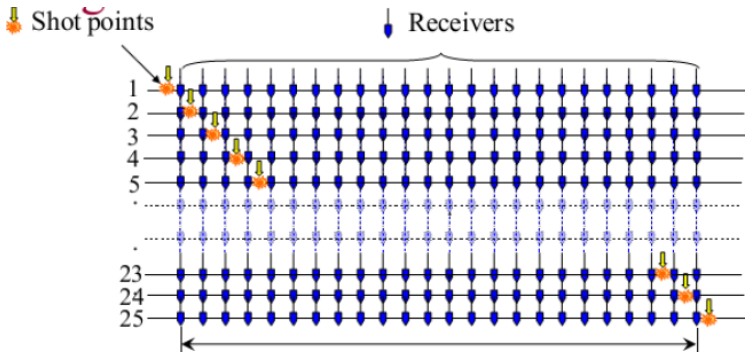

Survey Line Length

(Number of Sources= Number of Receivers + 1)

Figure 2.18 MASW Field Data Acquisition

At every station one data was acquired by stacking (3 times hammer hit) to enhance the data quality.

Analysis of MASW

In the phase velocity analysis, SPAC (Spatial Autocorrelation) method (Okada, 2003) is employed. Okada (2003) shows Spatial autocorrelation function $\rho(\omega,r)$ is expressed by Bessel function.

$$\rho(\omega,r) = J_0(\omega r / c(\omega)) \quad \text{----------(1)}$$

Where, r is the distance between receivers, ω is the angular frequency, c(ω) is the phase velocity of the waves, J_0 is the first kind of Bessel function. The phase velocity can be obtained at each frequency using equation (1). Figure 2.19 shows an example of dispersion curve of the survey, the frequency range between 15 and 50 Hz.

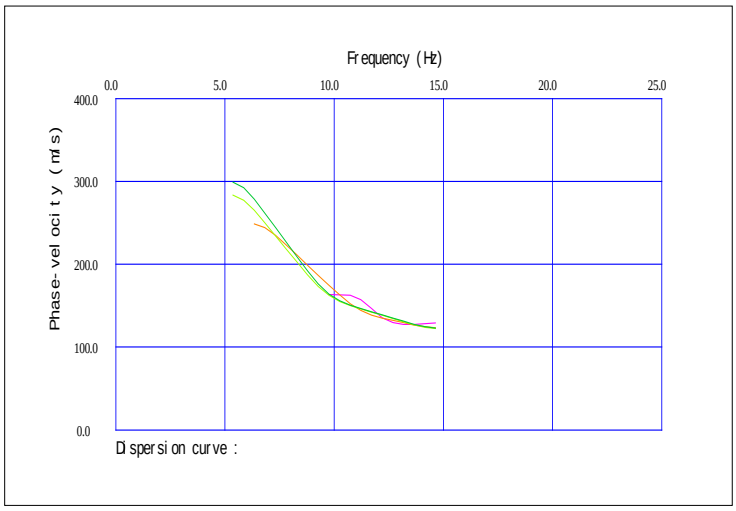

Figure 2.19 Dispersion Curve

A one-dimensional inversion using a non-linear least square method has been applied to the phase velocity curves. In the inversion, the following relationship between P-wave velocity (Vp) and Vs (Kitsunezaki et. Al.., 1990):

$$Vp = 1.29 + 1.11Vs \quad \text{---------- (2)}$$

Where Vp and Vs are the P-wave velocity and S-wave velocity respectively in (km/sec).

These calculations are carried out along the measuring line, and the S-wave velocity distribution section was analyzed, then summarized to one dimensional structure; SeisImager software can also give a 2-D velocity model a sample of which is shown in Fig. 2.20.

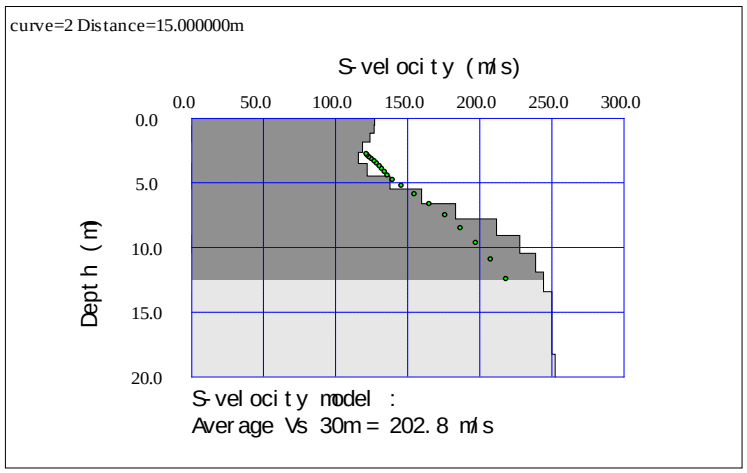

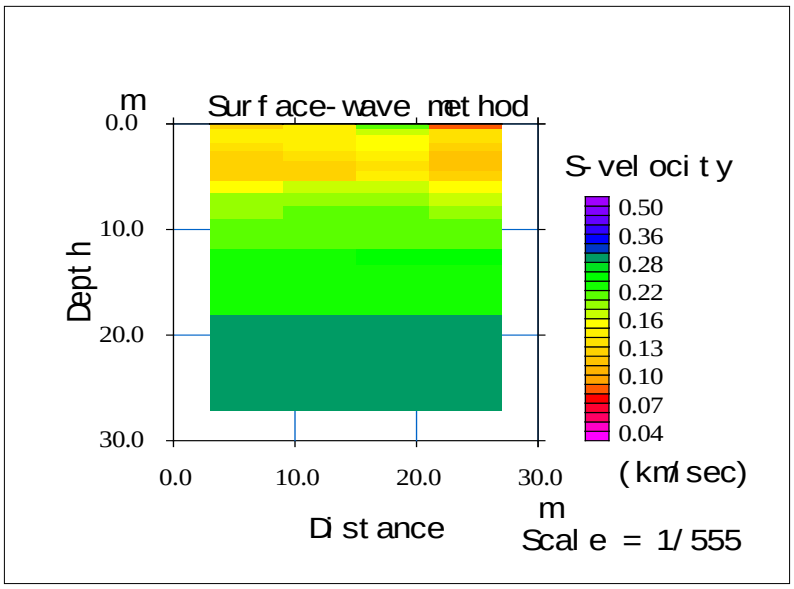

Figure 2.20 One dimensional Velocity Structure and 2 D velocity Model

Figure 2.21 shows an example of dispersion curve for MASW and phase velocity versus frequency as a sample. A one dimensional inversion using a non-linear least square method has been applied to the phase velocity curves and one dimensional S-wave velocity structures down (Figure 2.22).

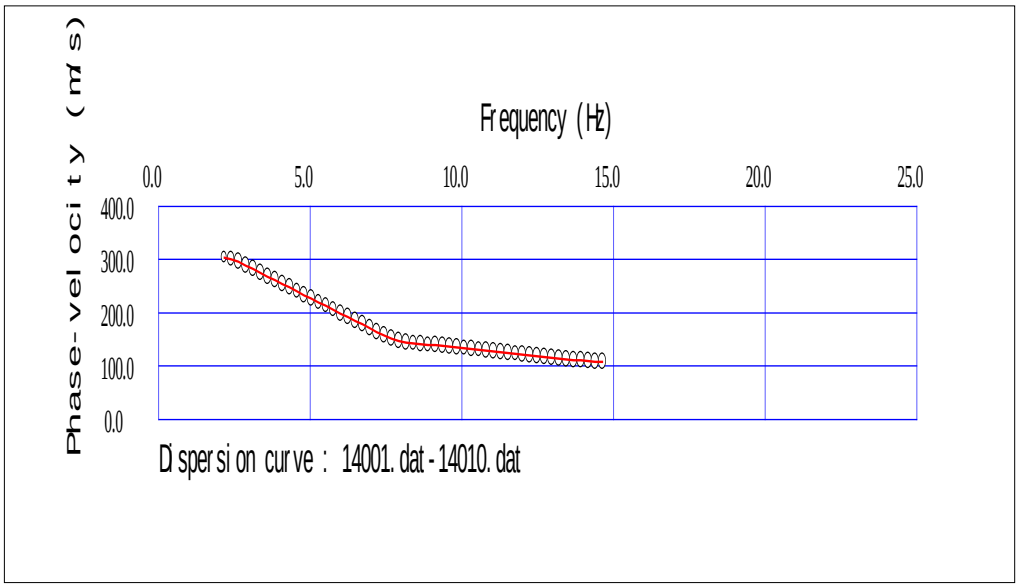

Figure 2.21 Dispersion Curve for MASW

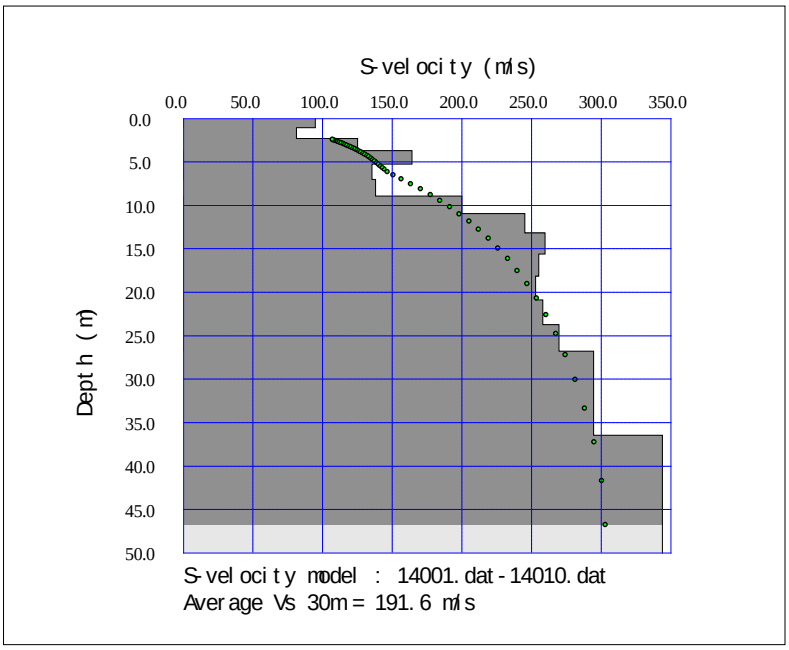

Figure 2.22 One dimensional velocity structure for MASW

Calculation of AVS 30

The AVS30 can be calculated as follows:

$T_{30} = \sum(Hi/Vi)$

AVS 30= $(30/ T_{30})$

Where, Hi= Thickness of the i th layer and $\sum Hi= 30$

Vi= S wave velocity of the I th layer

2.2.3. Test Detail And Procedure Of Microtremor Measurement (Single Microtremor)

Microtremor method is a practical and economical seismic survey since it has potential to explore deep soils without a borehole. Microtremors are the phenomenon of very small vibrations of the ground surface even during ordinary quiet time as a result of a complex stacking process of various waves propagating from remote man-made vibration sources caused by traffic systems or machineries in industrial plants and from natural vibrations caused by tidal and volcanic activities. Observation of microtremors can give useful information of dynamic properties of the site such as predominant period, amplitude, peak ground acceleration and shear wave velocity.

Single Microtremor observation

Method

1) The transfer function of surface layer

$$S_T = \frac{\text{Hor. spectrum at surface}}{\text{Hor. spectrum at base}} = \frac{S_{HS}}{S_{HB}}$$

2) Vertical component of MT is affected by Rayleigh wave at surface, but no effect at base and no amplification of vertical waves. Define the effect of Rayleigh wave as;

$$E_S = \frac{\text{Ver. spectrum at surface}}{\text{Ver. spectrum at base}} = \frac{S_{VS}}{S_{VB}}$$

3) To eliminate the effect of Rayleigh wave, define new transfer function as;

$$S_{TT} = \frac{S_T}{E_S} = \left(\frac{S_{HS}}{S_{VS}}\right) x \left(\frac{S_{VB}}{S_{HB}}\right) = \left(\frac{S_{HS}}{S_{VS}}\right)$$

(1.0)

$$H/V spectrum = \frac{Hs}{Hv} = \frac{\sqrt{F_{NS} x F_{EW}}}{F_{UD}}$$

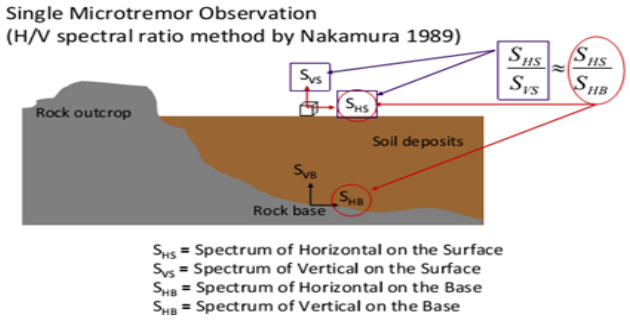

Figure 2.23 Fundamental of Single Microtremor observation

Field Data Acquisition System

Microtremor observations are performed using portable equipment, which is equipped with a super-sensitive sensor, a wire comprising a jack in one site and USB port in another site, and a laptop computer is also used. The microtremor equipment has been set on the free surface on the ground without any minor tilting of the equipment. The N-S and E-W directions are properly maintained following the directions arrowed on the body of the equipment. The sampling frequency for all equipments is set at 200Hz. The low-pass filter of 40Hz is set in the data acquisition unit. Like the seismometer or accelerometer, the velocity sensor used can measure three components of vibrations: two horizontal and one vertical. The natural period of the sensor is 2 sec. A global positioning system (GPS) is used for recording the coordinates of

the observation the available frequency response range for the sensor is 0.5-20Hz. The length of record for each observation was 10min.

Figure 2.24Field data acquisition of Single microtremor

2.2.4. Standard Penetration Test (SPT) Method

The Standard Penetration test (SPT) is a common in situ testing method used to determine the geotechnical engineering properties of subsurface soils. The test procedure is described in the British Standard BS EN ISO 22476-3, ASTMD1586. A short procedure of SPT N-value test is described in the following paragraph.

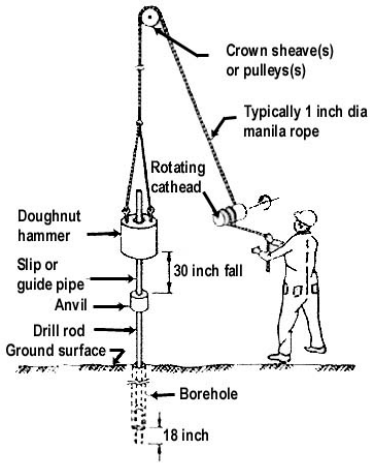

Figure 2.25 The SPT sampler in place in the boring with hammer, rope and cathead (Adapted from Kovacs, et al., 1981)

The test in our field uses a thick-walled sample tube, with an outside diameter of 50 mm and an inside diameter of 35 mm, and a length of around 650 mm. This is driven into the ground at the bottom of a borehole by blows from a slide hammer with a weight of 63.5 kg (140 lb)

falling through a distance of 760 mm (30 in). The sample tube is driven 150 mm into the ground and then the number of blows needed for the tube to penetrate each 150 mm (6 in) up to a depth of 450 mm (18 in) is recorded. The sum of the number of blows required for the second and third 6 in. of penetration is termed the "standard penetration resistance" or the "N-value". In cases where 50 blows are insufficient to advance it through a 150 mm (6 in) interval the penetration after 50 blows is recorded. The blow count provides an indication of the density of the ground, and it is used in many empirical geotechnical engineering formulae.

a) The main objective of SPT is as follows:
b) Boring and recording of soil stratification.
c) Sampling (both disturbed and undisturbed).
d) Recording of SPT N-value
e) Recording of ground water table.

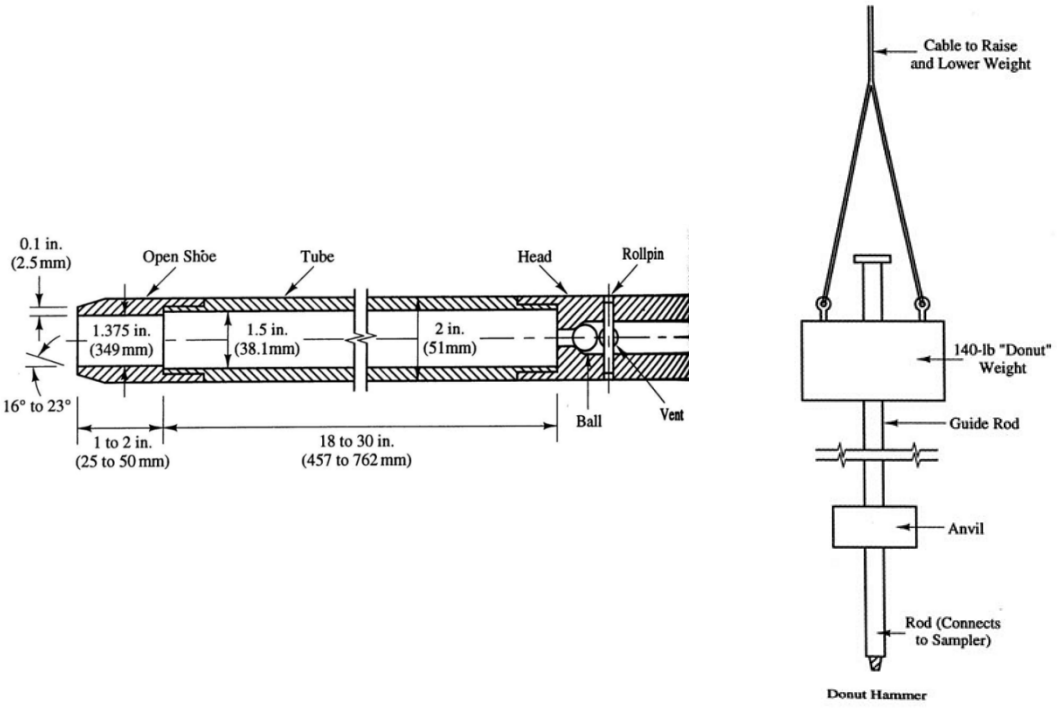

Figure 2.26 SPT Sampler and Donut Hammer

3. GEOLOGY OF THE STUDY AREA

3.1. Surface Geology

Geology focuses on the nature and properties of rocks and sediments. A good knowledge on the geology of the rocks and sediments is indispensable to understand the nature and properties of the parent materials. It is essential to understand the processes of formation of major soils of the country. Geomorphological knowledge is also important to visualize the processes and methods well. Bangladesh lies in an active seismic location. Moreover being a riverine country, the sediments are much affected by the combination of river process and seismic activity. The rivers are the most significant features of Bangladesh geology. They constantly change course, sometimes so rapidly that it cannot be predicted. As a result the topological features of Bangladesh are ever changing and it gives a spectacular feature of Surface geology (Figure 3.1).

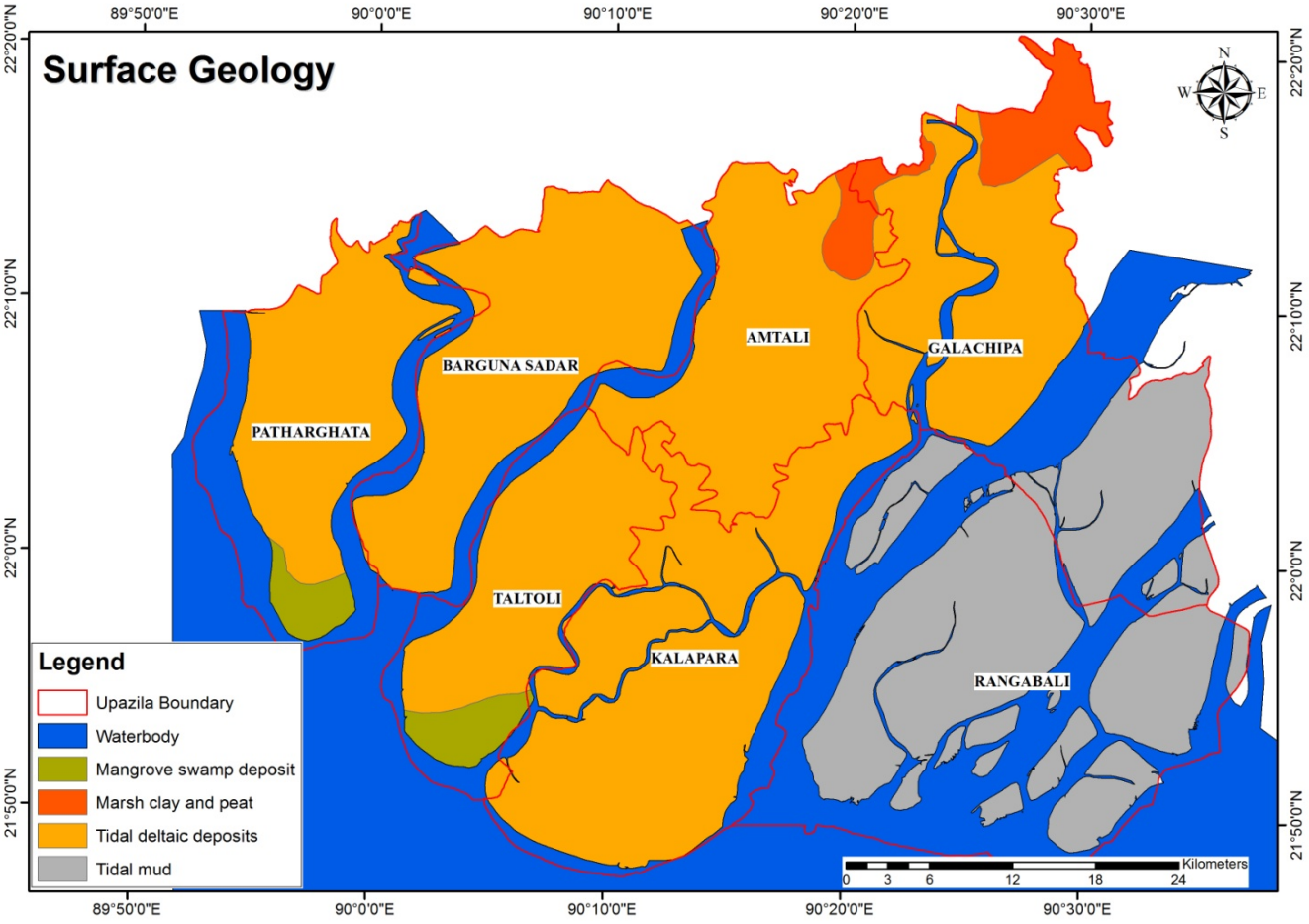

Figure 3.1 Surface Geology Map of Study Area (Source: After GSB 2001)

Mangrove Swamp Deposit:

These alluvial deposits are geologically very recent and deep. The soil is a silty clay loam with alternate layers of clay, silt and sand. The surface is clay except on the seaward side of islands in the coastal limits, where sandy beaches occur.

Marsh Clay and Peat:

Peat soils and Marshy clays in the surface geology of the area is indication of swampy and humid environment of present active river plain deposits. In these soils, partially or wholly decomposed organic matter are present. These soils have a low infrastructure and of low quality on engineering value. Peat and muck layers are black to dark brown, strongly reduced, and neutral in reaction under persisting conditions. When these layers are allowed to dry, they become extensively acidic. The unit is seasonally flooded by both increased river water and rainwater hence, remains wet around this time. During the dry season where mineral topsoil is present, they become dry. Under dry condition mineral top-soils are mainly grey or dark grey and become strongly acidic. The soil has generally low agricultural productivity. The land is used for reed production and fishing under natural conditions.

Tidal Deltaic Deposit:

Tide-dominated deltas are the most variable and difficult to characterize because of fluvial systems play in defining their delta, with rivers differing widely in discharge, sediment load, seasonality, and grain size. Tide dominated deltas has characteristics that they can extend hundreds of kilometers across and along the continental margin. The associated sediment transport regimes are typically high energy, but they vary considerably at the scale of tidal cycles and seasonal river discharge. The sedimentary successions formed in tide-dominated deltaic settings tend to be hetero-lithic, with interbedded sands, silts, and clays and both fining- and coarsening upward facies associations. It is because of varying transport energy.

Tidal Mud:

They consist mainly of soft mud with admixtures of sand in some places. Generally, mud is deposited near highwater mark, silty or sandy mud in areas of intermediate water, and fine sand near the position of the water at low tide. In some places the sediments are laminated and cross-bedded. Lenticular bedding is a structure of the muddy heteroliths facies displaying 2.5-7 m thick of alternating layers mud and sand. The ripples and sand lenses in lenticular bedding are

discontinuous and isolated. The genesis of lenticular bedding is related to the tidal rhythm (tidal currents alternating with periods of quiescent or slack water).

3.2. Subsurface 3D model of different layers through Geotechnical investigation

Description of different layer of the soil, its sedimentary characteristics, structure, and lithology are reflected in 3D model. Engineering properties of different soil layer: SPT value, soil strength and foundation layer etc are also being described. Computing all the results of soil properties and geotechnical properties preparation of 3D model for sub surface information of different layers of the area can be done by using GIS.

Lithological succession has been encountered in the boreholes reveal that geologically the study area is very common for its sand and silt alteration almost throughout the whole area. Based on distinct lithological characteristics, Standard Penetration Test blow counts (SPT-N) the borelogs encompasses seven distinct lithofacies, denoted as layers1 to layer7 as described in Figure-3.2a.

a.

Layer_No	Description
Layer-1	Brownish Gray to Grey Very Soft to Medium Stiff Clayey SILT/Silty CLAY with Very Fine Sand
Layer-2	Light Grey to Gray Very Loose to Medium Dense Very Fine to Fine SAND with Silt/Clay
Layer-3	Gray Medium Stiff to Stiff SILT/Claye SILT/Silty CLAY with Very Fine Sand
Layer-4	Light Grey to Gray Medium Dense to Dense Very Fine to Medium SAND with Silt/Clay
Layer-5	Grey Medium Stiff to Hard Silty CLAY/SILT
Layer-6	Grey Medium Dense to Very Dense Very Fine to Medium SAND
Layer-7	Grey Medium Stiff to Very Stiff Silty CLAY/Claye SILT/SILT

b.

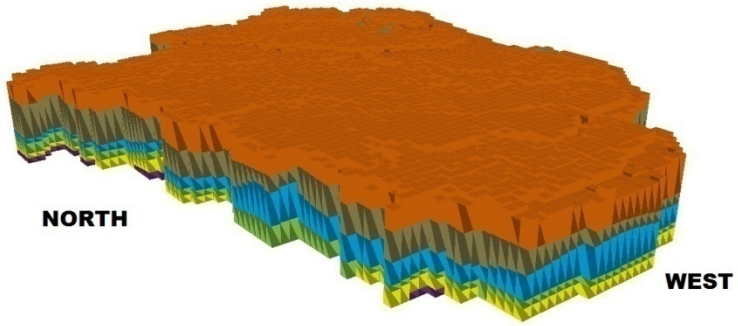

c.

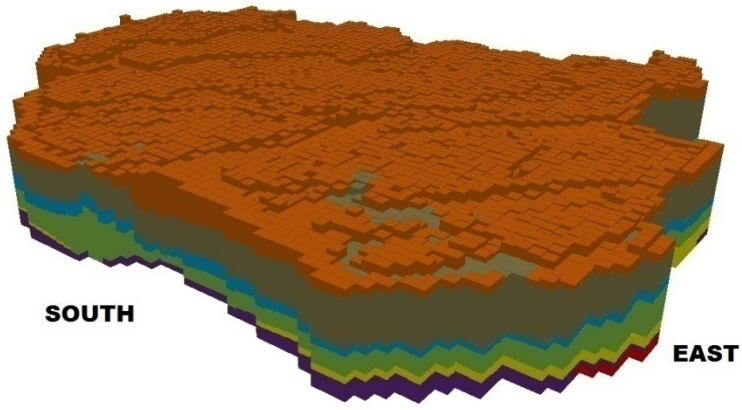

Figure 3.2(a) Legend and Lithologic characteristic of subsurface of PKCP Study area; (b) Subsurface 3-D model showing Northwestern part; (c) Subsurface 3-D model in Southeastern direction

Subsurface 3D model was prepared showing Southeastern part and along Northwestern direction using ArcGIS to elucidate the subsurface geological conditions of the study area as shown in Figure 3.2b & c respectively. All 100 boreholes of 30m depth were carefully has been examined to delineate the spatial distribution of the subsurface lithological units of the area.

Among the 7 layers, 4 layers are sand dominate and 3 layers are silt/clay dominant. From the Figure 3.2b & c, it can observe that Layer 1 is presented the top of the study area. The thickness of the layer increases from southeast to northwest and maximum thickness of the layer encounter at western part of the area. Layer2 underlay by layer1 is present throughout the study area and thickness of the layer increases toward northeast from southwest direction. Layer 3 which is underlay by layer2 is also present almost throughout the area (except few discrete places at eastern part of the area). The layer is thin compare to layer 1 & 2 and maximum thickness encounter at western part of the area. Layer4 is consider as foundation layer for the study area and is present throughout the study areas. Maximum thickness of the layer encounters at the southern part and eastern part of the area. Layer5 underlay by layer4 is absent at the middle part of the study areas. A thin strata of Layer6 is present at southeastern part of the area. There are 5 discrete places at southern part of the study area where layer7 has been found.

Engineering layer suitability attributes of the project area has been determined by means of 100 sample points covering three major soil textures (e.g., sand, silt and clay).

Based on SPT N-Value of boreholes layer4 and layer6 are considered as foundation layer for the study area and a foundation depth map (Figure 3.3) is produced which is categorized into 6 classes based on the depth of the foundation layer. Green color zones (Northeastern Rangabali Upazila) of the study area suggest foundation layer depth ranging from 7.3 to 10m. The blue color areas of Galachipa, Rangabali, Taltoli and Kalabpara upazila represents foundation layer depth ranges from 10.01 to 15m. From the map it can be observed that the Southwestern half of Kalapara upazila, eastern half of Ragabali upazila, northeastern part of Galachipa upazila, middle part of the Taltoli upazila and a small part of southern Barguna Sadar Upazila suggest foundation layer at depth ranging from 15.01 to 20m which represents by cyan color. The light green color zones of northern and southwestern Galachipa, northwestern Rangabali, northeastern Kalapara and some discrete zones of Amtoli, Taltoli and Barguna Sadar suggest foundation layer depth in between 20 to 25m. The orange zones of southern half of Amtoli, northern half of Taltoli, Barguna Sadar and Patharghata; and few discrete places of Kalapara;

Galachipa and Rangabali upazila suggest foundation layer depth ranging from 25.01 to 30m. Rest of the area shows red colour, which indicates the foundation layer depth more than 30m represented by red color.

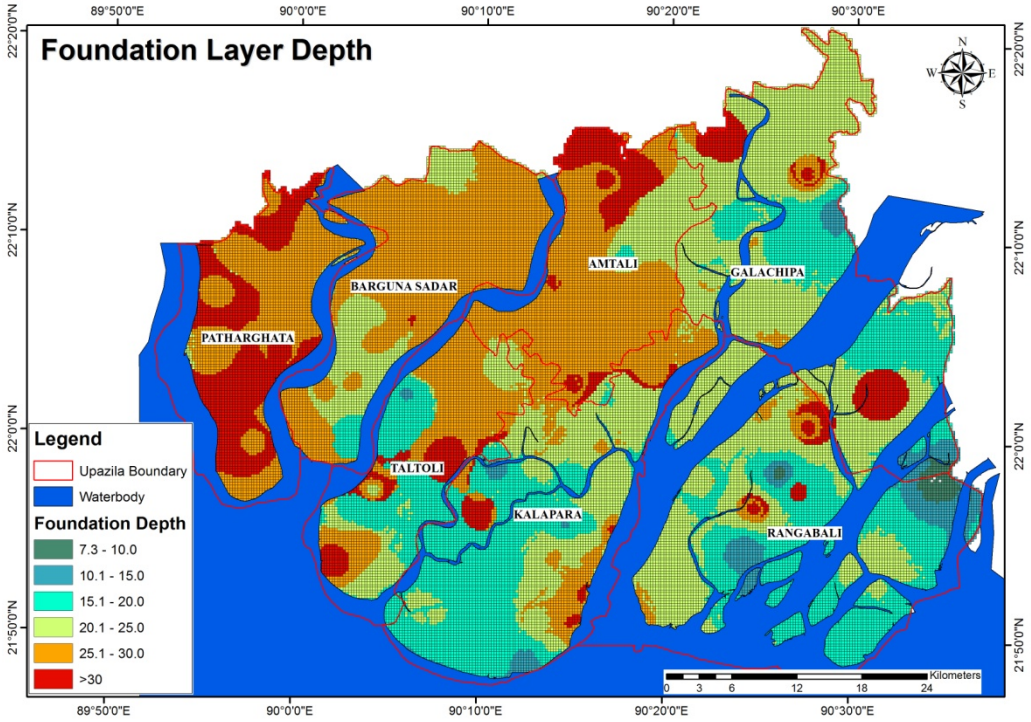

Figure 3.3 Foundation depth of Study Area

Although the possible foundation layer depth of the area has been proposed, the necessity of the individual foundation depth identification is highly recommended. Pile foundations are most often used in the various situations; when there is a layer of weak soil at the sub surface. This layer cannot support the weight of the building, so the loads of the building have to bypass this layer and be transferred to the layer of stronger soil or rock that is below the weak layer.

3.3. Subsurface cross-section

Eight (8) cross section have been prepared for payra-kuakata area based on borlog information. Cross sections are AA', BB', CC', DD', EE', FF', GG' and HH'. Payra-Kuakata project area represents Seven (7) lithological layer upto 30m. Lithological description of the Seven layers are following-

Layer_No	Description
Layer-1	Brownish Grey to Grey Very Soft to Medium Stiff Clayey SILT/Silty CLAY with Very Fine Sand
Layer-2	Light Grey to Grey Very Loose to Medium Dense Very Fine to Fine SAND with Silt/Clay
Layer-3	Grey Medium Stiff to Stiff SILT/Clayey SILT/Silty CLAY with Very Fine Sand
Layer-4	Light Grey to Grey Medium Dense to Dense Very Fine to Medium SAND with Silt/Clay
Layer-5	Grey Medium Stiff to Hard Silty CLAY/SILT
Layer-6	Grey Medium Dense to Very Dense Very Fine to Medium SAND
Layer-7	Grey Medium Stiff to Very Stiff Silty CLAY/Clayey SILT/SILT

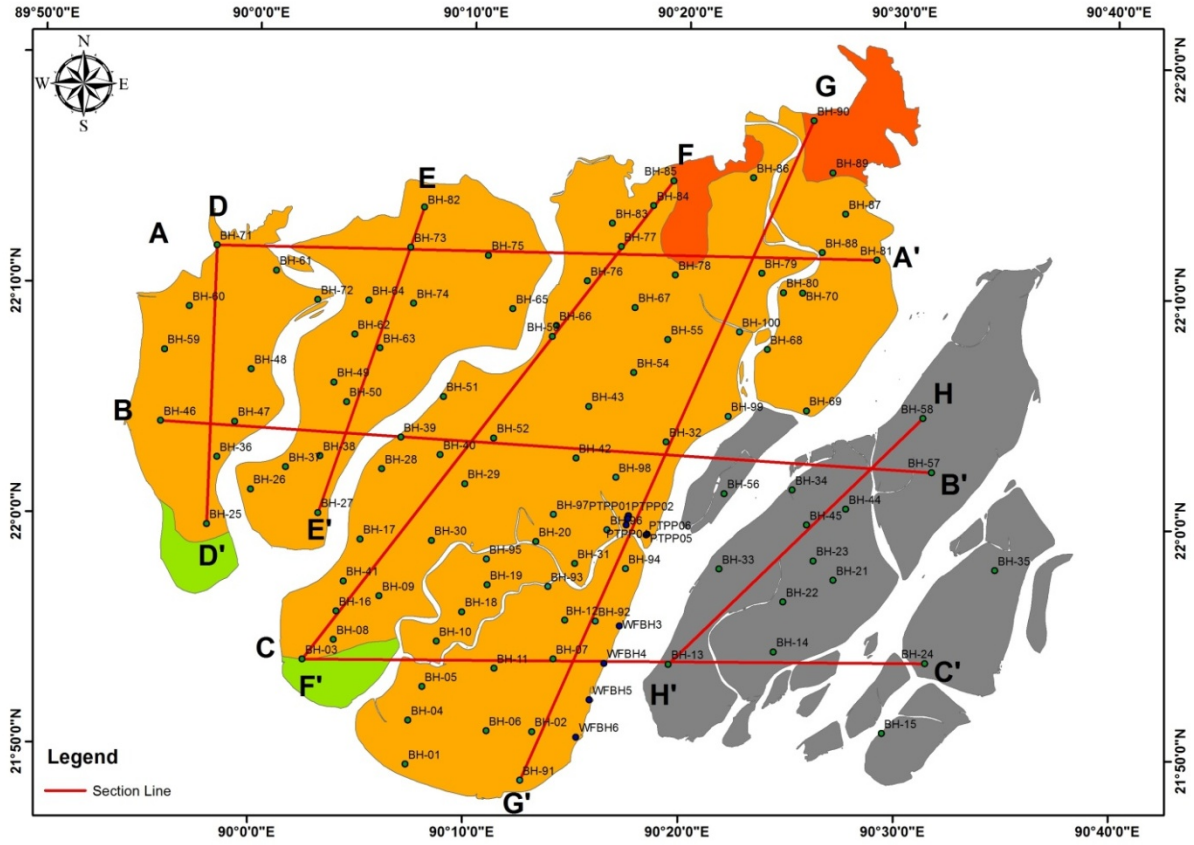

Figure 3.4 Lithological cross section line in the BH location map

Cross-section A-A'

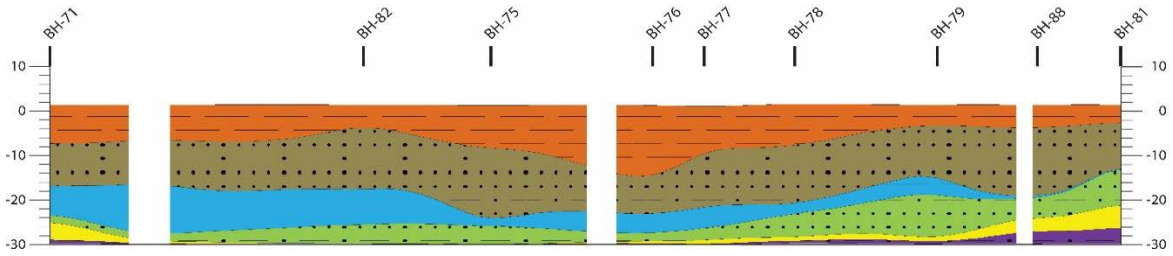

Figure 3.5 Cross section A-A'

Cross Section **AA**' Comprises about 52.91km from BH-71 to BH-81.Layer 6 is last encountered strata in this section with maximum thickness of 4m in the east. It vanishes in middle and appeared again in West side. It then underlies by Layer 6 that follows the same trend as layer 7 with maximum thickness of 4m. Then Layer 5 underlines it, which have average thickness of 8m and maximum 13m near BH-79. It is pinched toward west and underlined by Layer 4, which is pinched toward east. Layer 3 have a maximum thickness of 13m with an average of 10m in west and 3-5m in east. Layer 2 and Layer1 underlies all these layers. Layer2 have an average thickness of about 10 m while Layer 1 have 7m. Layer 1 thickness increased in the middle near BH76 and Layer 2 decreased a bit.

Cross-section B-B'

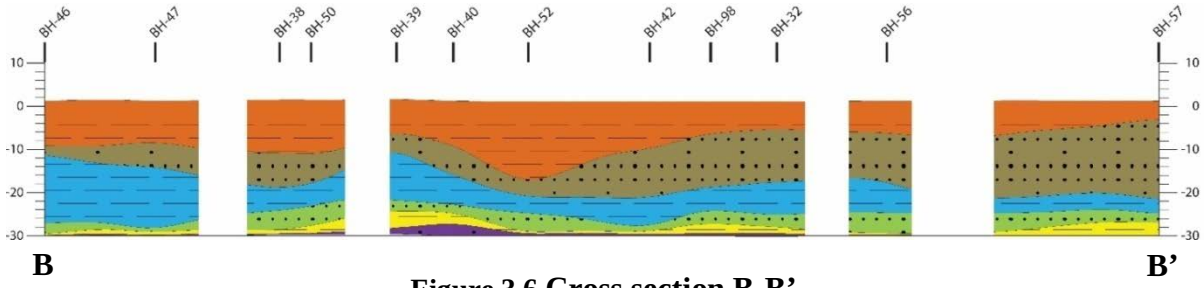

Figure 3.6 Cross section B-B'

Section **BB'** Covers about 61.95 km from BH-46 to BH-57. Here lowermost layer is Layer 6 though most of the area have Layer 4 and Layer 5 as the lowest layer up to 30m depth. Layer5 and Layer 6 have maximum thickness of 4m while layer 4 have 6m and continued from west to east with a thickness average of 3m. Layer 1, 2, 3 also continued throughout the section where Layer 1 and Layer 3 thinned near BH 57, but layer 2 pinched near BH 46. Layer 3 have on average 15m thickness in western most portion and decreased to 7-8m in center and 3-4m in east. Layer 2 have average thickness of 18m in east 5-10m in center and 2-3m in west. Layer 1 have 10m in average thickness in west and center with maximum of 15m.

Cross-section C-C'

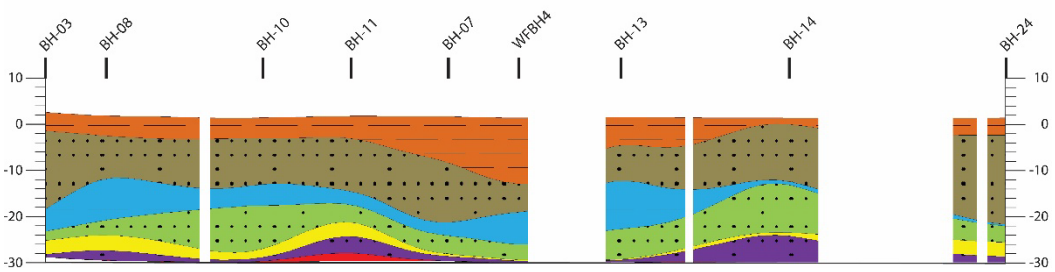

C **Figure 3.7 Cross section C-C'** **C'**

Section **CC'** Comprises about 49.91 km from BH-03 to BH-24. In this section, Layer 7 is encountered though it only covers a small area with maximum thickness of 2m. Then thinned Layer 6 and Layer 5 underlined it. Both have average thickness of 3m where both thinned in center near BH 13. This two layer then underlined by layer 4 that varies from 2 to 10m in thickness. Layer 3 that underlines the layer 3 have thickness varies from .5m to 8m in places. These two layer are covered by Layer 2 and Layer 1. Layer 2 have an average thickness of 13m narrowing near WFBH14 where Layer 1 increased. Average 4m thick Layer 1 envelops the area but in reached maximum of 15m near WFBH14.

Cross-section D-D'

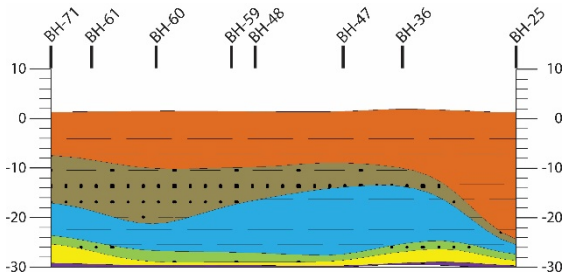

D **Figure 3.8 Cross section D-D'** **D'**

Section **DD'** Covers about 22.37 km from BH-71 to BH-25. Very thin Layer 6 is encountered at the bottom of 30m depth boreholes. These layers underlined by layer 5 and layer 4, which is not more than 2-4 m in thickness. And Layer 4 covered by layer 3,2,1 which are very thick. Layer3 is about 8-10 m in thickness from North to center where Layer 2 is 5-10m and Layer 1 is about 10m. Layer 3 and 2 are pinched near BH25 and Layer 1 thickness is maximized to about 25m.

Cross-section E-E'

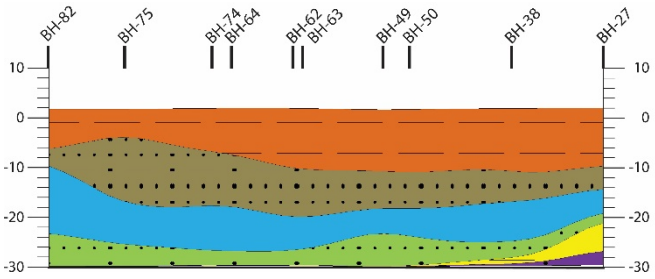

E **Figure 3.9 Cross section E-E'** **E'**

Section **EE'** Comprises about 25.94 km from BH-82 to BH-27.Layer6 and Layer 5 appears in the bottom of the borehole of South, but covers a small area and maximum thickness reached about 2m for Layer 6 and 9m for layer 5. Layer 4 is also pinched in south but continued in north with an average thickness of 5m. It then underlined by Layer 3 which thickness varies from 5 to12m place to place. Layer 2 slightly pinched near BH 82 but holds a thickness ranging from 2 to 17m. Layer 1 have a average of 10m in thickness though slightly pinched near BH 75.

Cross-section F-F'

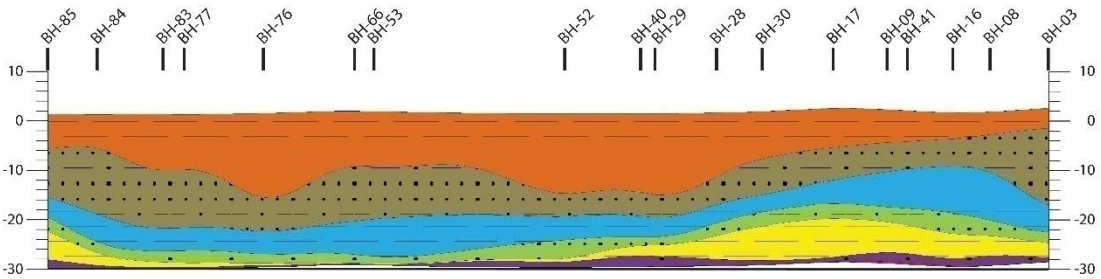

F **Figure 3.10 Cross section F-F'** **F'**

Section **FF'** Comprises about 48.56 km from BH-85 to BH-03. Bottom of this section is defined Layer 6 which have 2-3m thickness. Layer 5 and Layer 4 have higher thickness near BH 28, BH-30 and Bh-17 but pinched in the center portion. The overall thickness of the Layer 4 is ranging from 4m to 10m. Layer 2 and Layer 1 is very thick ranging from 5 to 10m for Layer2 and 4m to 15m for Layer 1.

Cross-section G-G'

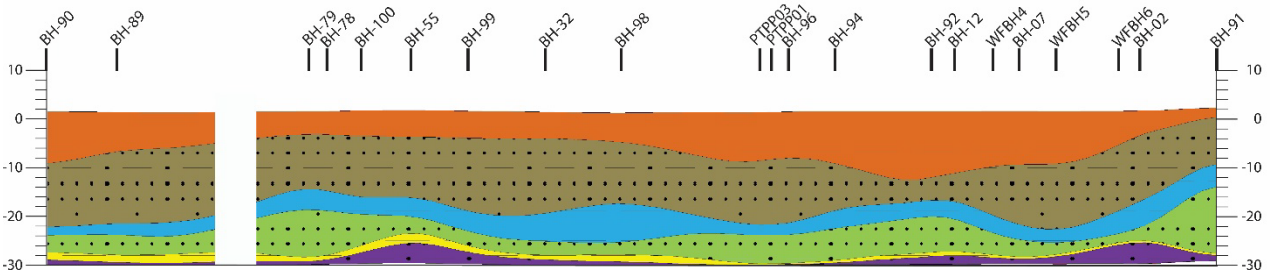

G **Figure 3.11 Cross section G-G'** **G'**

Section **GG'** Covers about 57.90 km from BH-90 to BH-91. Layer 6 have about 4m thickness near BH 02, BH 55 and Layer 5 underlines it with maximum thickness of 2m. Layer 4 covers these having thickness ranging from 4 to 17m. Layer 3 has average 3m thickness. The Average thickness of Layer 2 is about 10m and Layer 1 also has average of 8m with value ranging from 2m to15m.

Cross-section H-H'

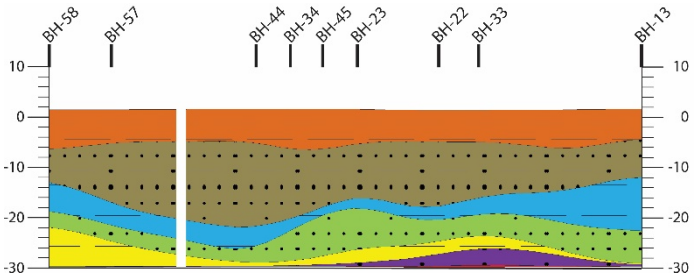

H **Figure 3.12 Cross section H-H'** **H'**

Section **HH'** Comprises about 28.38 km from BH-58 to BH-13. Layer 6 is the lower most layer with maximum thickness of 4m. Layer 5 underlines it and have its maximum thickness about 8m in north side and pinches in the south. Layer 3 have thickness ranging from 4m to 8m where layer 3 have thickness of 5m to 10m. Layer 2 is most abundant here having average 8 to 10m in thickness. Layer 1 have thickness ranging from 6m to 8 m here.

4. SEISMIC HAZARD ASSESSMENT

Earthquakes can be one of the most catastrophic disasters resulting in mass causality and immense destruction and damages to physical assets and the environment. The geologic and tectonic settings of Bangladesh, especially the northern and eastern regions, render the country at moderate seismic risk. Indian plate moving northeast collides with the Eurasian plate thus generating frequent earthquakes in the region encompassing Bangladesh, North-East India, Myanmar and Nepal. The country is exposed to significant seismic hazard due to its proximity to seismically active tectonic plates and because of rapid haphazard urbanization, over the past few decades, and high population density, it can experience massive damage and loss, if an event of a large enough magnitude were to occur. Taking this into consideration, along with the recent claims by researchers about the threat of an impending big seismic event affecting Bangladesh and surrounding regions, there is a necessity to assess the seismic risk of the country.

Seismic hazard assessment of a region or site can be done primarily by two basic methods, namely deterministic methods and probabilistic methods. The deterministic approach is scenario based and involves determining the ground motion at a particular site for a given magnitude earthquake and a known fault. On the other hand, probabilistic seismic hazard assessment (PSHA) (Cornell, 1968) method deals with determining the probability of exceeding different levels of ground motion over a specified time period. The PSHA approach involves identifying and defining all the seismic sources and determining their recurrence relationships i.e. their seismicity rates. Finally the hazard at a site can be assessed by estimating the earthquake effects or ground motion resulting from earthquakes of different sizes and from different sources using attenuation relationships. The final hazard curves shows the probability of exceeding different levels of ground motion at a site over a certain period of time.

Several seismic hazard studies have been conducted for Bangladesh by various researchers over the past years. In 1979, Committee of Experts on Earthquake Hazard Minimization published the first official seismic hazard-zoning map for Geological Survey of Bangladesh (GSB, 1979), which was later revised during the development of the Bangladesh National Building Code (BNBC) in 1993. The country was divided into three zones (Ali and Choudhury, 1994) with coefficients which were based on PGA values for a return period of 200 years. The central and north-eastern parts of the country showed the highest PGA of 0.25g followed by Zone 2 with a PGA of 0.15g which includes the major cities of Dhaka, Chittagong, Comilla

and Rangpur. The southwestern parts of the country showed lower PGA values of 0.075g. Furthermore, the concept of Maximum Considered Earthquake (MCE) motion with 2475 return period has been introduced in the new seismic zone map for revised building codes where the country has been divided into four zones having Z values of 0.12, 0.20, 0.28 and 0.36. The predictions are mostly consistent with that of neighboring country, India, but some cities show a significant increase in motion compared to the previous seismic maps. In the works of (Ansary and Sharfuddin, 2002), modifications were made to the seismic zones, however, the assumptions regarding the site magnitude-frequency recurrence relationships were not fully justified. This assumption may not generally be justified for two reasons. The PGA at a site depends not only on the magnitude but also on the epicentral distance from the site. In addition, different earthquake sources are most likely to possess different frequency characteristics.

4.1. Probabilistic seismic hazard analysis (PSHA)

More recently, standard PSHA for Bangladesh has been conducted using the software CRISIS (Ordaz et al. 2013) where the country was divided into seven seismic zones and recurrence characteristics of each of the zones were estimated. Different attenuation laws developed for different regions were applied to estimate the PGA for various return periods separately, including the one developed for Bangladesh from isoseismals of historical events by Islam et al. (2010). Spectral acceleration results (SA) for 0.2s and 1.0s were also presented in the study. However, the accuracy seems to be limited because there is no clear justification in delineating the source zones as well as no consideration for site effects. In addition, Neo-Deterministic Seismic Hazard Assessment (NDSHA) has also been conducted in Bangladesh which is based on structural models, seismic source zones, focal mechanisms, magnitude and locations of historical earthquakes rather than overly simplified empirical attenuation laws (Al-Hussaini et al. 2015).

Neighboring countries such as India, Nepal and Myanmar, which are under seismic hazard threat have also been carrying out their seismic hazard assessments for years and improving their methodological approaches over time. Similar attempts have also been taken to conduct seismic hazard assessments in Bangladesh and the necessity of accurately predicting ground motion levels to determine appropriate building code provisions for earthquake-resistant design of structures in a country like ours cannot be stressed enough. This is an intensive task which requires thorough analyses and development of appropriate seismological models; namely, seismogenic sources, ground motion predictions and seismic site conditions. Both gaps and a

lack of understanding in the existing seismic studies of the country such as limited consideration for site effects, uncertainties in source parameters and zonation, lack of a complete catalogue, selection of region appropriate GMPEs amongst others, still remain. Consequently, an updated seismic hazard model for the country is imperative and necessitated by new data, recent findings, and improved methodologies. In this study we attempt to perform a new probabilistic seismic hazard analysis (PSHA) of Bangladesh addressing some of the existing shortcomings. This includes using revised seismic source zones based on the recent study of Wang et al. (2014), declustering the events with two established methods, tackling uncertainties with the logic-tree approach as well as applying seismic zone specific GMPEs and accounting for site conditions throughout the country. Comparisons in results are also made by carrying out the PSHA calculations with uniform site conditions of stiff rock while keeping all other variables constant. In addition, deterministic seismic hazard assessment has also been carried out for the project area taking into account the source parameters and source to site distance of two most potential neighboring fault zones.

Study Area

The area of concern for this study is the tectonic regime in and around Bangladesh as shown in Fig. 4.1. Detailed seismology, geodesy, and tectonics study has revealed that Bangladesh is surrounded by five major potentially active seismotectonic regimes (Wang et al., 2014) and one Stable Continental Crust (SCC) section Nath & Thingbaijam (2011).The complex interaction of Indian plate with Eurasian and Burma Silverplate, results in a great threat of earthquakes for Bangladesh The country has experienced five major destructive earthquakes with Richter magnitude 7.0 and above (Ambraseys, 2004; Bilham, 2004; ADPC and OYO, 2009) over the past 150 years.

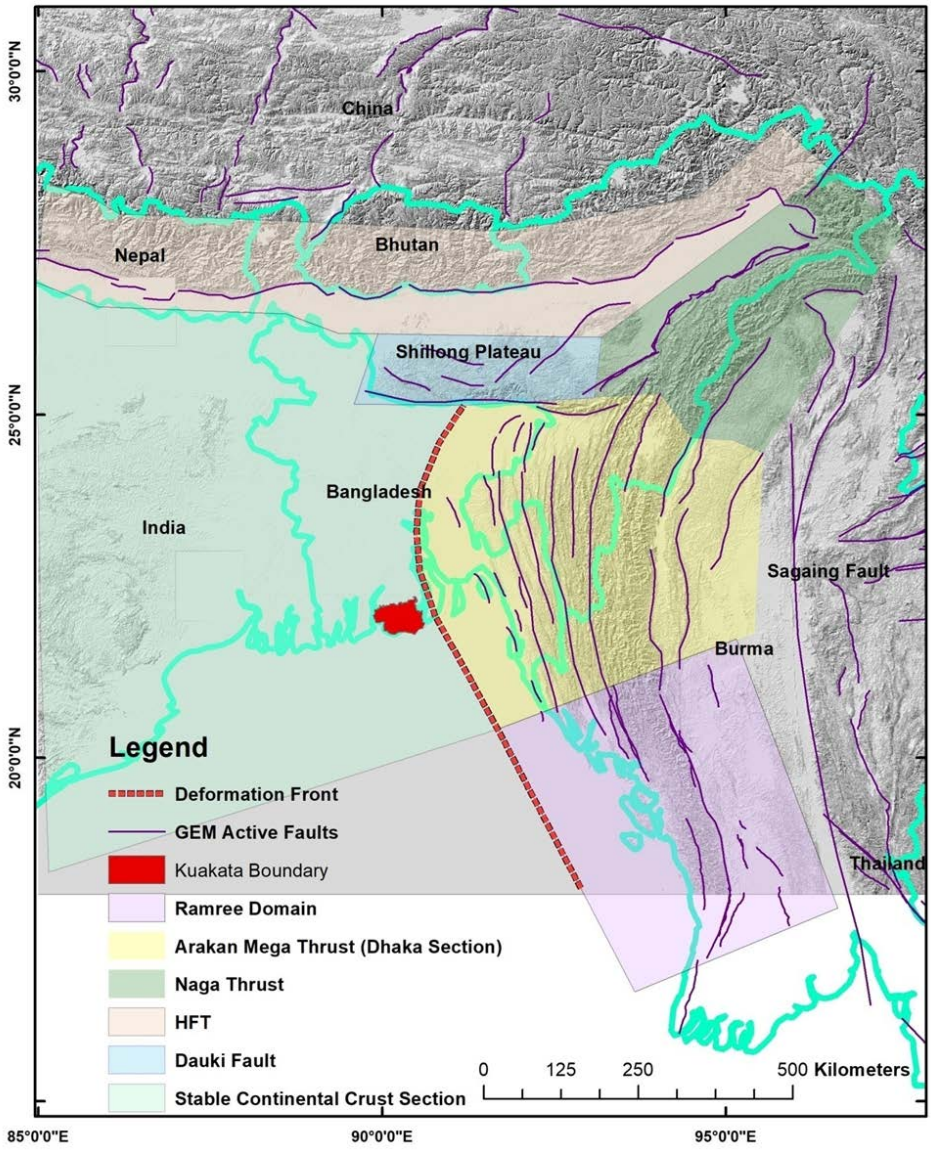

Figure 4.1 Major Seismotectonic regimes in and around Bangladesh. It has been overlaid on a hillshaded SRTM Digital Elevation Model (DEM) of 30m resolution (Source:https://earthexplorer.usgs.gov/) Adopted from Wang (2014).

The Himalayan Thrust Fault (HTF) marked by the collision between Indian plate and Eurasian plate in the north, extends to almost 2000km from the Kashmir in the west to the Himalayan syntaxes in the Assam (Yu and Sieh, 2013). Just south of the HTF lies the 270km long north dipping reverse Dauki fault running along the southern flank of Shillong plateau. Arakan megathrust runs as concave folded thrust belt on the other side of Bangladesh from south to northeast. The Ramree domain is characterized by sustained convergence and pronounced seismicity in the northern part as opposed to its southern counterpart and is 450km long (Wang et al., 2014). This tectonic regime has produced a deformation belt that increases its width

from about 170km in the south to about 250km in the north. The north of Ramree domain, the Dhaka section (~500km long & ~400km maximum width) of Arakan Mega Thrust is formed due to the collusion of Burma silver plate and thick sediment laden Ganges-Brahmaputra delta (Wang et al., 2014). Recent studies by Steckler et al. (2016) have revealed the presence of locked megathrust deformation front boundary underneath the Dhaka, the densely populated capital of the country. Numerous thrust faults exist in the Chittagong Tripura Folded Belt (CTFB) of this region. A 430km long and 160-240km wide section of the NE and SW trending Naga Trust regime is present between the Shilling plateau and Himalayan syntaxis, formed by the Indo-Burman plates collision (Wang et al., 2014). In addition, the 1400 km long Sagaing fault system is another likely source of major earthquake and it lies between Andaman sea ridge spreading zones in the south to the eastern Himalayan syntaxes in the north. In the past a few seismic events have also originated from the western parts of the country which can be characterized as a Stable Continental Crust (SCC) section according to studies of Nath and Thingbaijam (2012).

The probability of occurrence of a major earthquake and the recurrence interval for each tectonic regime from the fault zone length and slip rate has been estimated by Yu & Sieh (2013). The Arakan megathrust (Dhaka section), HTF and Ramree show the highest potentiality of generating major earthquake. The maximum magnitude earthquake that can be generated from each of the source regimes has also been estimated. The relationship of Strasser et al. (2010) used is as follows:

$$Mw=4.868+1.392\log(L)$$

Here L is the length of fault rupture that would produce an earthquake and Mw refers to moment magnitude converted from seismic moment using Hanks & Kanamori (1979) relation,

$$\log(M_o)=1.5M_w+16.1 \text{ , where } M_o=\mu AD$$

Here the recurrence intervals are just a coarse approximation of the time between maximum sized earthquakes for the five major faults (Yu and Sieh, 2013). Some of the important source parameters of the six tectonic regimes are given in Table 4.1. The focal mechanism of events in the stable continental region has been inferred from the study of Nath and Thingbaijam (2012) and the subsequent dip and strike parameters from events with similar focal mechanism (Brandt and Saunders, 2011). A rake value of 90 degrees is assumed for reverse faults. Thus, defined six seismic source zones based on the previous studies might have a simplification effect on probabilistic seismic hazard assessment. However, defining the seismic zones in much improved manner is beyond the scope of the present study.

Table 4.1 Source Zone Parameters

	Length(km)	**Dip (°)**	**Rake**	**Strike**	**Hypocentral Depth(km)**	**M_{max}**	**Slip Rate**	**Recurrence Interval (yr)**	**Date of Last Event**
CTBF	~500	<10	90	345	20	8.6	10	760	Unknown, perhaps 1500
HTF	~500	~10	90	90	20	8.6	21	5000	1100 (?)
Dauki	~270	~45	75	90	35	8.3	11	1200	1897
Naga	~400	~23	90	48	20	8.5	5	920	Unknown
Ramree	~500	~16	90	325	30	8.6	23	730	1762
SCC	~500	~50	90	340	18	7.3	?	?	Unknown?

Source: Yu & Sieh (2013) and Nath & Thingbaijam (2011)

Methods

The PSHA is carried out following the Hazard Modelers Toolkit (Weatherill, 2014) of OpenQuake engine developed by GEM. This is a free and open source software written in the Python programming language for calculating seismic hazard and risk at variable scales (from single sites to large regions) (Silva et al., 2014).

Earthquake Catalogue and Magnitude Homogenization

The initial step involves gathering seismicity data from earthquake catalogue for in and around Bangladesh. The records of 3472 events, within a geographical limit of 18°-30° N latitude and 85°-96° E longitude, between years 1505 and 2018 has been collected from the USGS, GEM-ISC, BSSA, and BMD (Bangladesh Meteorological Department) catalogue. All the events are arranged in a chronological order and checked for redundancy.

Since the catalogue contains different magnitude scales such as surface-wave magnitude (Ms), body-wave magnitude (Mb), local or Richter scale Magnitude (Ml) and moment magnitude (Mw), magnitude conversion for all the events is performed to homogenize the unit of measurement. The magnitudes are all expressed as moment magnitude, Mw, because it does not saturate for large events (Hanks and Kanamori, 1979). The conversion relationships between various types of magnitudes (Ms/Mb/Ml) and moment magnitude that are used is given below. Out of the 3472 events, those that fall within the source zones are shown in Fig 4.2 with their magnitude distribution.

Table 4.2: Magnitude conversion empirical relations

Magnitude	Magnitude Range	Magnitude Conversion Relation	References
Ms	3.0 to < 6.2	$Mw = 0.67\ Ms + 2.07\ (\sigma = 0.17)$	(Scordilis 2006)
	6.2 to 8.2	$Mw = 0.99\ Ms + 0.08\ (\sigma = 0.20)$	(Scordilis 2006)
M_b	3.5 to 5.5	$Mw = 0.85\ m_b + 1.03\ (\sigma = 0.20)$	(Scordilis 2006)
	5.5 to 7.3	$Mw = 1.46 m_b - 2.42$	(Sipkin 2003)
M_L	M_L </= 6	$Mw = M_L$	(Heaton & Tajima 1986)

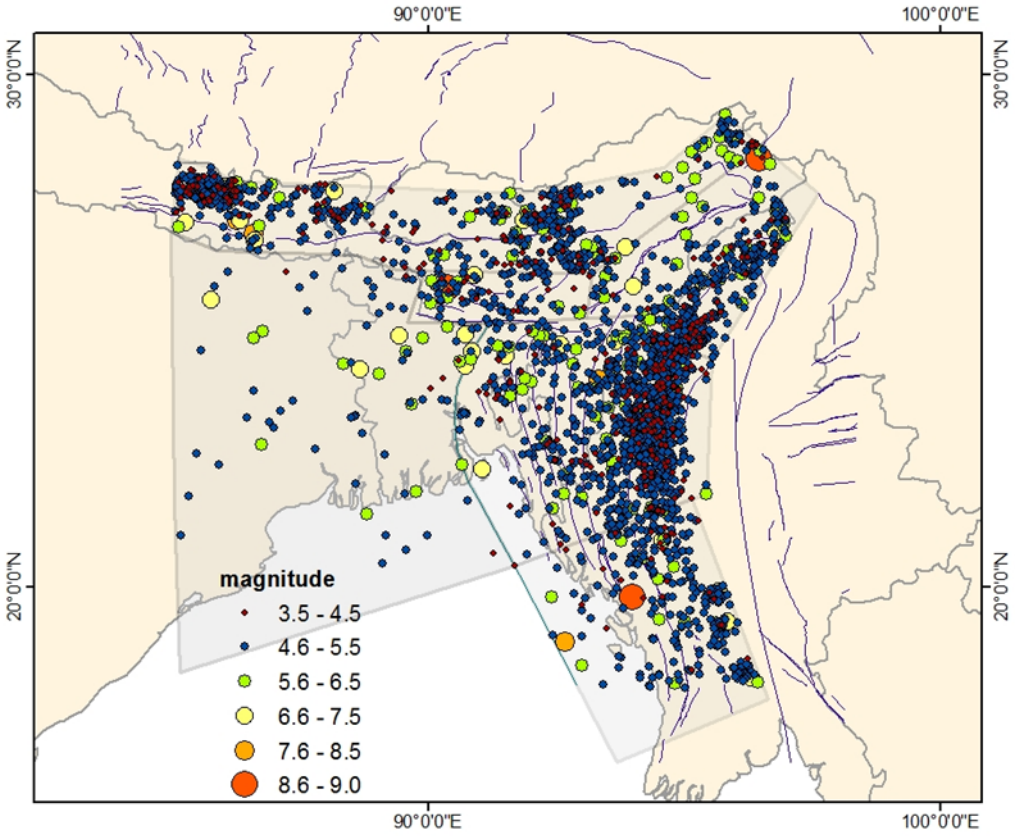

Figure 4.2 Map showing the earthquake events in and around Bangladesh between 1505-2018

Declustering

This catalogue is then declustered because PSHA based on the Cornell (1968) approach assumes a Poissonian process, where seismic events are considered temporally independent. Thus the dependent events (foreshocks, aftershocks or swarms) are separated from the mainshocks. In this study, two different algorithms for declustering are applied to the catalogue separately, namely the Garnder & Knopoff (1974) method and the algorithm used in AFTERAN program (Musson, 1999).

Gardner and Knopoff (1974)

In the first method, the events are sorted in descending order of magnitude and dependent events within fixed temporal and spatial windows which depend on the magnitude of the events are identified. The algorithm thus identifies foreshocks and aftershocks by considering the

windows forwards and backwards in time from the main shock. The original windows suggested by Garnder & Knopoff (1974) are approximated by:

$$\text{distance (km)} = 10^{0.1238M+0.983}$$

$$\text{time (decimal years)} \begin{cases} = 10^{0.032M+2.7389} & \text{if } M \geq 6.5 \\ 10^{0.5409M-0.547} & \text{otherwise} \end{cases}$$

There have been some modifications to the original window and while declustering using the GK algorithm, in this study we apply the one proposed by Uhrhammer [1986] which is as follows:

$$\text{distance (km)} = e^{-1.024+0.804M}$$

$$\text{time (decimal years)} = e^{-2.87+1.235M}$$

Out of the 3472 events, the GK declustering method leaves us with 2584 events. Among these events, 2065 (i.e. 59% of the total events) of them are considered finally because the rest fall outside the six seismic source zones (as shown in table 4.2 and figure 4.3).

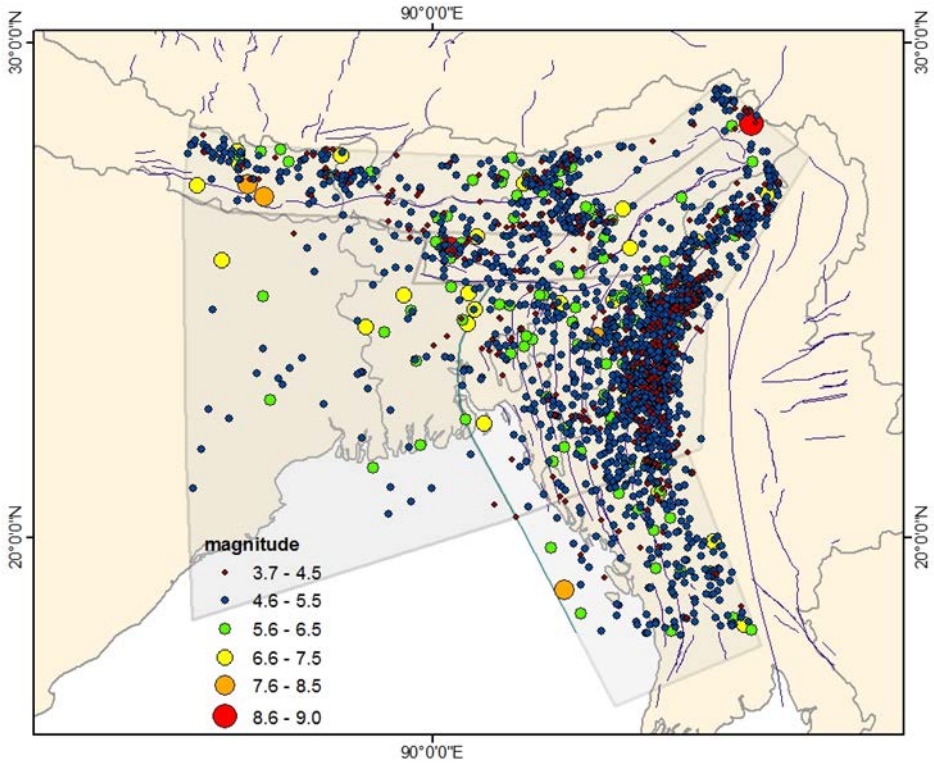

Figure 4.3 Events after declustering using GK method

AFTERAN (Musson 1999)

The AF approach is a modification of the GK approach but is slightly more computationally complex. Here, instead of a fixed time window, a moving-time window is used. At first the events are arranged into their magnitude-descending order after which the events within fixed distance windows are identified using a moving time window of T days. The events which fall both within the distance window and the T days' time-window are declared as dependent ones. The time window is then shifted to the next event, and the process is repeated. In this study, in order to retain a significant number of events and also ensure a Poissonian process, the AF algorithm with an Uhrhammer [1986] distance window and 100 days' time-window is used to decluster the catalogue.

This procedure leaves us with a total of 3229 events out of the initial 3472. Again, we only consider the events which lies within the perimeters of the six source zones and that filters out a final of 2500 events which constitutes 72% of the original dataset (shown in table 4.3 and figure 4.4).

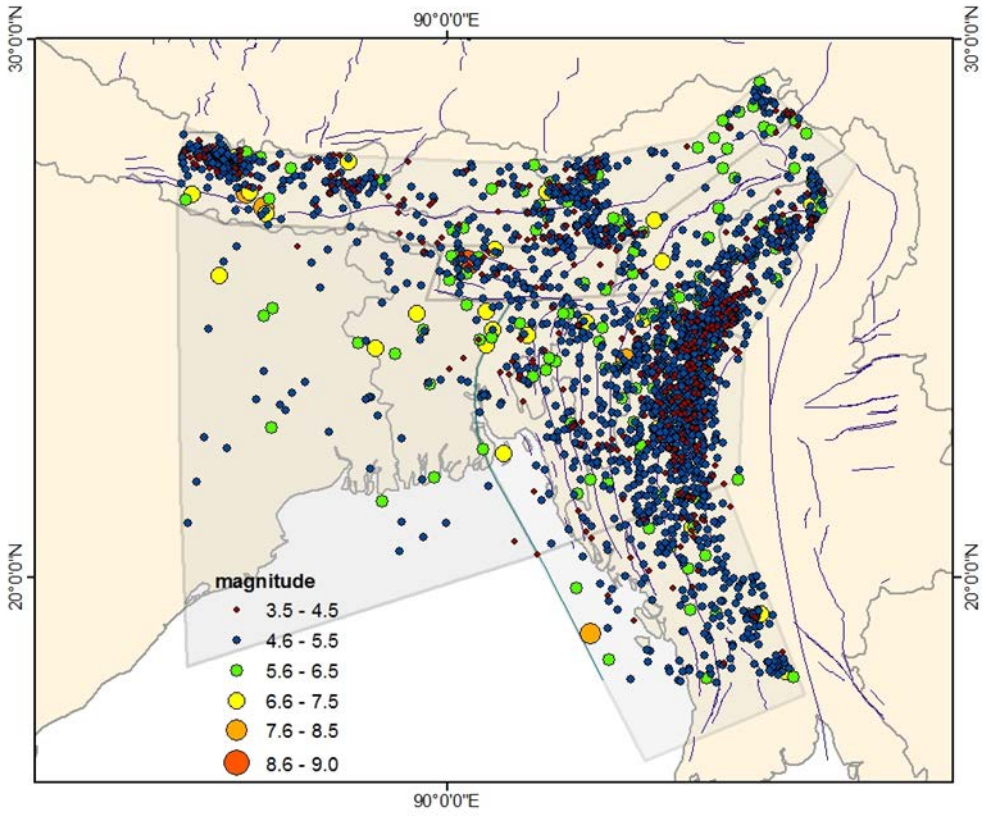

Figure 4.4 Events after declustering using Musson method

Table 4.3 Summary of seismic events

	Before Declustering	After Declustering
Gardener and Knopoff	3472	2065
AFTERAN (Musson)		2500

Both the methods resulted in different number of events for each of the six seismic zones as shown in table 4.4

Table 4.4 Number of events in each seismic zone after declustering

	GK	Musson
CTFB	916	1017
Dauki	89	90
HTF	395	610
Naga	379	445
Ramree	216	262
SCC	70	76
Total	**2065**	**2500**

Depth distribution of the events from both methods of declusting is shown in figure 4.5.

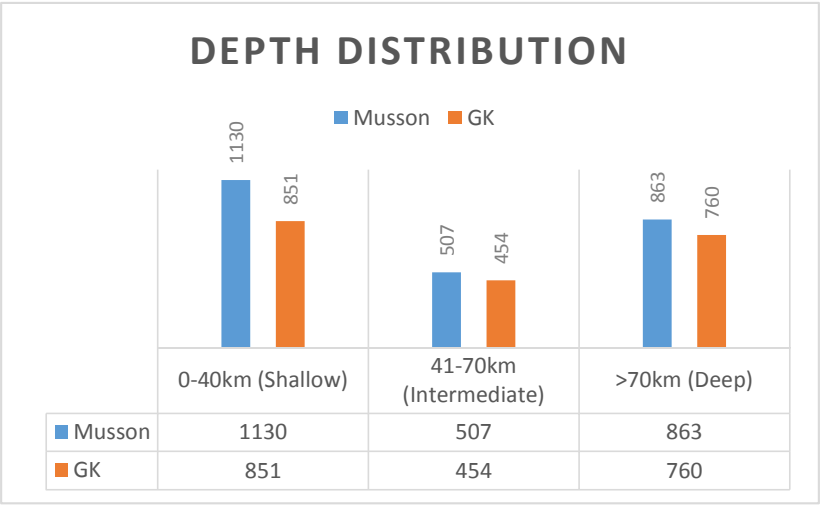

Figure 4.5 Bar chart showing the depth distributions of earthquake events

Catalogue Completeness

The completeness of the catalogue is estimated using the Stepp (1972) method to determine the smallest magnitude at which all of the earthquakes in space and time have been detected (i.e. magnitude of completeness, Mc). The Stepp (1972) method uses the standard deviations of empirical annual occurrence rates of events of different magnitudes classes for different time intervals, identifying the Mc when the observed rate of earthquakes above Mc starts to show deviation from the expected rate.

The unbiased estimate of the mean rate of events per unit time interval of a given sample, if a time interval, Ti is taken and Poissonian distribution of n events assumed, is:

$$\lambda = \frac{1}{n}\sum_{i=1}^{n} T\mathrm{i}$$

with variance $\sigma_i^2 = \lambda/n$. For unit time interval of 1 year, the standard deviation of the estimate of the mean is

$$\sigma_\lambda = \sqrt{\lambda}/\sqrt{T}$$

where T is the sample length.

Identification of the Mc is a very crucial step for seismic hazard analysis because incomplete catalogues can affect the recurrence parameters of the source zones which in turn may significantly impact the estimation of hazard at a site. The following magnitude and years are considered to be complete in the earthquake catalogue and the Step plots for both methods are shown in Figure 4.6.

Table 4.5 Years of Magnitude Completeness

Completeness Magnitude	Year of Completeness	
	Gardner	**Musson**
3.0	1982	1981
4.0	1982	1981
5.0	1970	1975
6.0	1942	1908
7.0	1815	1804

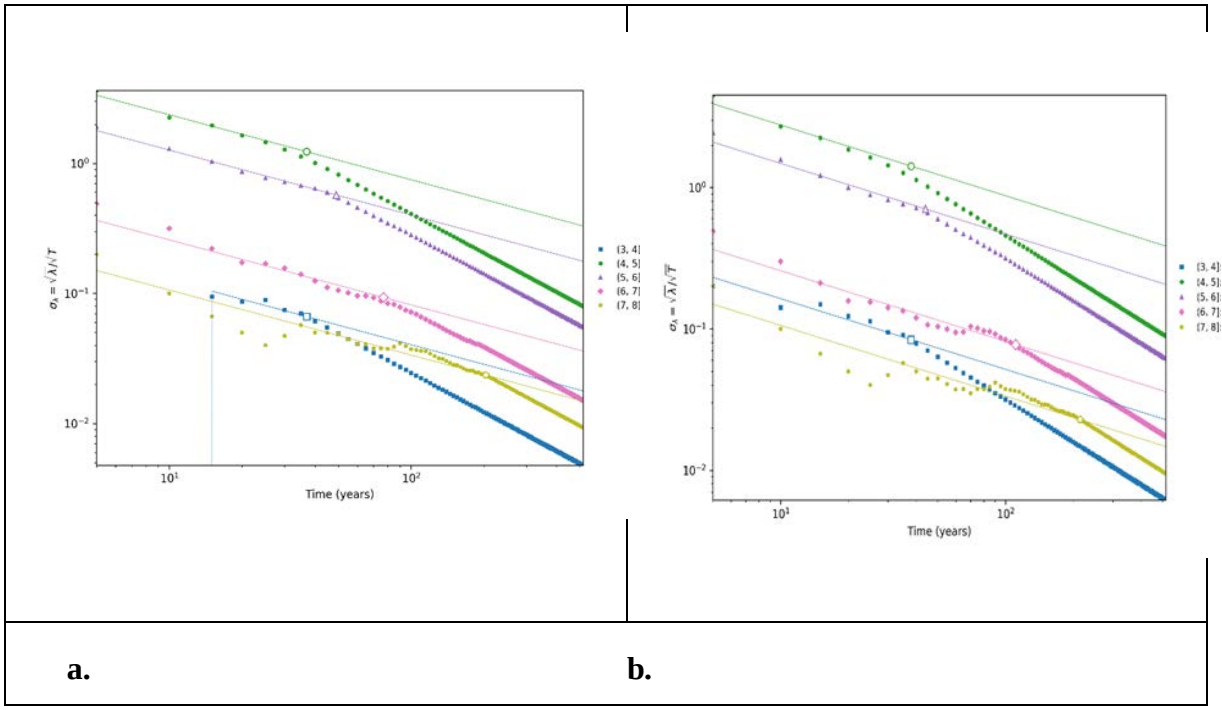

a. **b.**

Figure 4.6 Step plots of completeness magnitudes for (a) Gardner (b) Musson

It is clear that events of small magnitudes are complete from recent years (around 30 years ago) most likely due to lack of devices to detect them while events of larger magnitudes are complete from a longer period of time as they were easy to detect.

Recurrence Relationships

Gutenberg-Richter (GR) recurrence relationship for each source zones in obtained the form:

$$\mathrm{Log}_{10}(N) = a\text{-}b\mathrm{M}$$

where, N represents the cumulative number of earthquakes above magnitude M, and *a* and *b* are two constants (Gutenberg & Richter 1944). Constant *b* is the measure of the relative abundance of large to small shocks. The GR parameters for the zones were estimated by the Maximum Likelihood (ML) method in this study. This method is an adjustment of the Aki (1965) and Bender (1983) approach to incorporate for time variation in completeness. The catalogue is divided into S sub-catalogues, where each sub-catalogue corresponds to a period with a corresponding Mc. The mean of the a- and b-values of each sub-catalogue, weighted by the number of events in each sub-catalogue, is taken to give the average a and b-values along with their uncertainties.

The *a* (intercept) and *b*-values (slope) of the magnitude-frequency for the five sources is shown in the table 4.6 below

Table 4.6 Recurrence 'a' and 'b' values for each zone

	GK		**Musson**	
	a-value	**b-value**	**a-value**	**b-value**
CTFB	3.4	0.68	3.5	0.69
HTF	3.1	0.66	3.2	0.63
Dauki	3.4	0.77	3.3	0.75
Naga	4.4	0.84	3.6	0.80
Ramree	2.6	0.49	2.6	0.48
SCC	4.97	1.13	4.8	1.08

The *b* value is usually 1 for seismically active regions. Higher values of b denotes that smaller magnitude events are more abundant than the larger ones for that particular region.

Maximum Magnitude

The source parameter maximum magnitude, Mmax, simply defined as the largest possible earthquake that can occur in a certain region is associated with considerable epistemic uncertainties due to the evident limitations in its observability (Cornell, 1968). For this study, the cumulative moment method is employed to estimate the maximum magnitude. This method has been adapted from the cumulative strain energy release method for estimating Mmax which was initially proposed by Makropoulos & Burton (1983) where the Mmax is derived from a plot of cumulative moment release against time. The average slope of this plot indicates the mean moment release for the fault which is enveloped by two further straight lines with gradients equal to that of the slope of mean cumulative moment release. The vertical distance between these two lines indicates the potential total amount of moment that could be released in that fault source if no earthquakes were to occur in the corresponding time

The table below shows the Mmax values for the six seismogenic source zones in this study. Generally, intraplate regions have maximum moment magnitudes varying between 6.5 and 7.0 whereas, for plate boundary regions it is between 8.0 and 9.0. The resulting Mmax values are compared with those obtained from the magnitude-scaling relationships of Strasser et al. (2010) and consistency is found for most of them. Source regions CTFB, Dauki and Ramree show almost same values as the ones obtained from the empirical relationship while HTF and Naga faults show slightly lower maximum magnitudes then the ones derived from the scaling relationship. For both declustering methods similar maximum magnitudes were obtained.

Table 4.7 Maximum magnitudes for each zone using cumulative moment method

	Maximum Magnitude
CTFB	8.6
HTF	8.6

Dauki	8.3
Naga	8.5
Ramree	8.6
SCC	7.3

Ground Motion Prediction Equation (GMPEs)

Selection of appropriate ground motion prediction equations to account for the attenuation of seismic energy is a rather challenging task which depends on the regional tectonic characteristics of the site of interest. Generally, three GMPEs are developed for three broad categories of regions, namely, shallow crustal events in active tectonic regimes (e.g. Western North America), shallow crustal earthquakes in stable continental regions such as that in Central and Eastern North America and finally for subduction zones (e.g. Pacific Northwest).Attenuation models relate the effect Y at a site to magnitude and distance, so that in general

$$Y=Y\ (M,r)$$

Where M is usually moment magnitude and 'r' can refer to the various types of distances. Some models use epicentral distance (R_{epi}), some use closest distance to fault rupture (R_{rup}), and some models use Joyner-Boore distance (R_{JB}).

No specific GMPE has been developed for Bangladesh which is why GMPEs used in neighboring regions or those in areas having similar geologic and tectonic attributes are used in the study. Nath & Thingbaijam (2011) have characterized the CTFB and Ramree as subduction zone. This study is in line with the recent findings (Steckler et al. 2016; Wang et al. 2014). The Dauki fault zone is recognized as active intraplate margin (Nath & Thingbaijam 2011). The other two concerned seismotectonic zones namely HFT and Naga have been treated as active continental crust based on the study of (Avouac, 2015). Since some earthquakes may also be generated from the western parts of the country, that region has been characterized as a stable continental region to account for background seismicity. In recent years, numerous GMPEs have been developed for active continental crust, subduction zones and active intraplate margin. For active continental crustal zones (HTF and Naga zones), Abrahamson &

Silva (2008), Chiou & Youngs (2014), Campbell and Bozorgnia (2014) and Akkar & Bommer (2010) relations have been used. The CTFB and Ramree regions are characterized as subduction zones for which Youngs et al (1997), Atkinson & Boore (2003), Lin & Lee (2008), and Zhao et al. (2016) have been applied. For the active intraplate margin of Dauki zone, Atkinson and Boore (2006) and Nath (2012) empirical relationships (Gregor et al., 2014) are used and for the Stable Continental Region Atkinson and Boore (2011) and Tavakoli and Pezeshk (2005). The GMPEs utilized in this study were carefully selected based on the studies of (Nath & Thingbaijam 2011) and the GMPE pre-selection criteria of Global Earthquake Model (Douglas et al. 2013).

Site Effects

Taking site effects into account is a very important requirement for accurate estimation of seismic ground motion at site. For this study, Vs30 which is the average shear wave velocity at 30m depth is considered. This has been measured (CDMP 2012 & UDD 2018) for various locations throughout the country using PS-logging and other methods. Moreover, the Vs30 information retrieved from the current project has also been utilized. Most of the country falls under site class SC (Vs30 ranging from 180-360 m/s) or site class SD (Vs30 less than 180 m/s) (BNBC 2015).

The relationship between Z1.0 and Vs30 given by Chiou & Youngs (2008) and Campbell and Bozorgnia (2007) is used to estimate the depth to shear wave velocity VS = 1.0 km/s (Z1.0) while depth to Vs = 2.5 km (Z2.5) is found using the relationship proposed by (Kaklamanos, Baise and Boore, 2011) where,

$$Z_{2.5} = 519 + 3.595Z_{1.0}$$

Logic Tree Formulation

Logic tree approach has been used to tackle the epistemic uncertainties within certain source parameters (a and b- values of recurrence relationships) as well as for different GMPEs that were used for different tectonic regimes. Equal weights have been assigned to all branches because we have found no reason to prefer one option over the other. The GMPE and source logic trees are shown in 4.7 and 4.8, respectively.

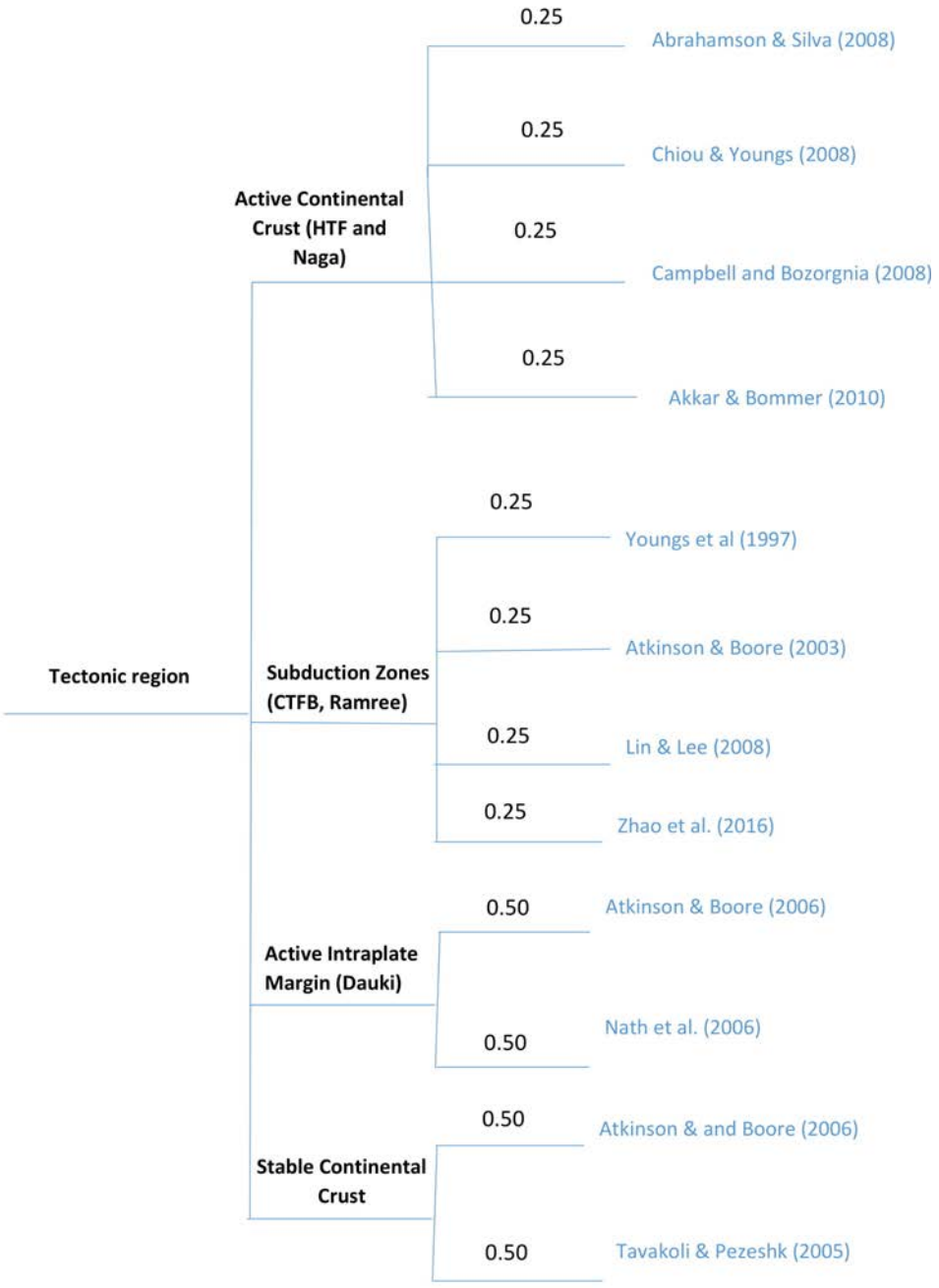

Figure 4.7 GMPE Logic Tree

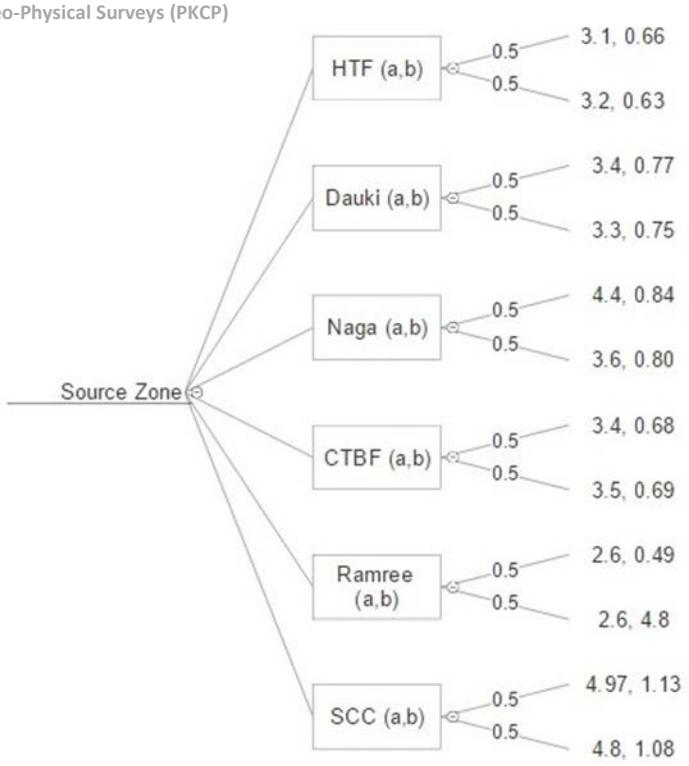

Figure 4.8 Source Logic Tree for a- and b-values

PSHA calculation

In the probabilistic seismic hazard assessment (PSHA) method, the ground motion at a site is estimated for a specified probability of being exceeded in a given time period (Cornell, 1968). The results of PSHA can be expressed in many ways all of which involves some level of probabilistic computations combining uncertainties in earthquake size, distance, frequency and effects to estimate seismic hazard. A common approach involves the development of hazard curves which indicate the annual probability of exceedance of a ground motion parameter, which can then be used to calculate the probability of exceeding that parameter in a specific period of time. The standard Cornell-McGuire approach which is the basic calculation to find the probabilities is as follows:

$$E(z) = \sum_{i=1}^{Ns} Vi \int_{r=0}^{\infty} \int_{Mmin}^{Mmaxi} fm\,(m)\, fri(r)\, P(Z>z \mid m,r)\, drdm$$

where,

E(z) = mean annual rate of exceedance of ground motion level "z" during a specified time period "t";

Ns = number of seismogenic sources;

ν_i = mean rate of occurrence of earthquakes between lower/upper bounds magnitude "m" being considered for the "ith" source

$fm_i(m)$ = probability density distribution of magnitude within the "ith" source, which is obtained using the Gutenberg-Richter relationship;

$fr_i(r)$ = probability density distribution of epicentral distance "r" between various locations within source "ith" and the site where hazard is estimated;

$P(Z > z \mid m,r)$ = probability that a given earthquake of magnitude "m" and epicentral distance "r" will exceed ground motion level "z", which is obtained employing the selected attenuation relationships.

In this study, the OpenQuake software is used to perform classical PSHA calculations for Bangladesh by specifying the region grid coordinates. Hazard maps, curves and uniform hazard spectra are investigated for 50 years' time period and calculated at 10% and 2% probabilities of exceedance. Spectral accelerations are computed for periods ranging from 0 to 1.0 seconds. Region gird-spacing of 10km is used to obtain a balance between the precision and computational demand and time. A pragmatic truncation value of 3 sigma (σ) for GMPEs is used because it was seen that values less than 3 were inappropriate (e.g. Strasser et al. (2010) and Bommer & Abrahamson (2006).

Results and Discussion

The seismic hazard maps for Kuakata are presented in figures below displaying spatial distribution of PGA and PSA at 0.2s, 0.3s, and 1s computed for 10% and 2% probability of exceedance in a 50 year time period, which correspond to 475 and 2475 years respectively. These return periods are considered because they are the most commonly used parameters to express the PGA values thus making it easier for comparison while calculation of spectral accelerations at 0.2s, 0.3s, and 1s periods for return periods of 475 and 2,475 years is consistent with building codes.

The results (Fig 4.9) show that the PGA estimates in Kuakata range from 0.16g to a maximum of 0.25g for 10% probability of exceedance in 50 years and range from 0.33g to 0.54g for 2% probability of exceedance in 50 years.

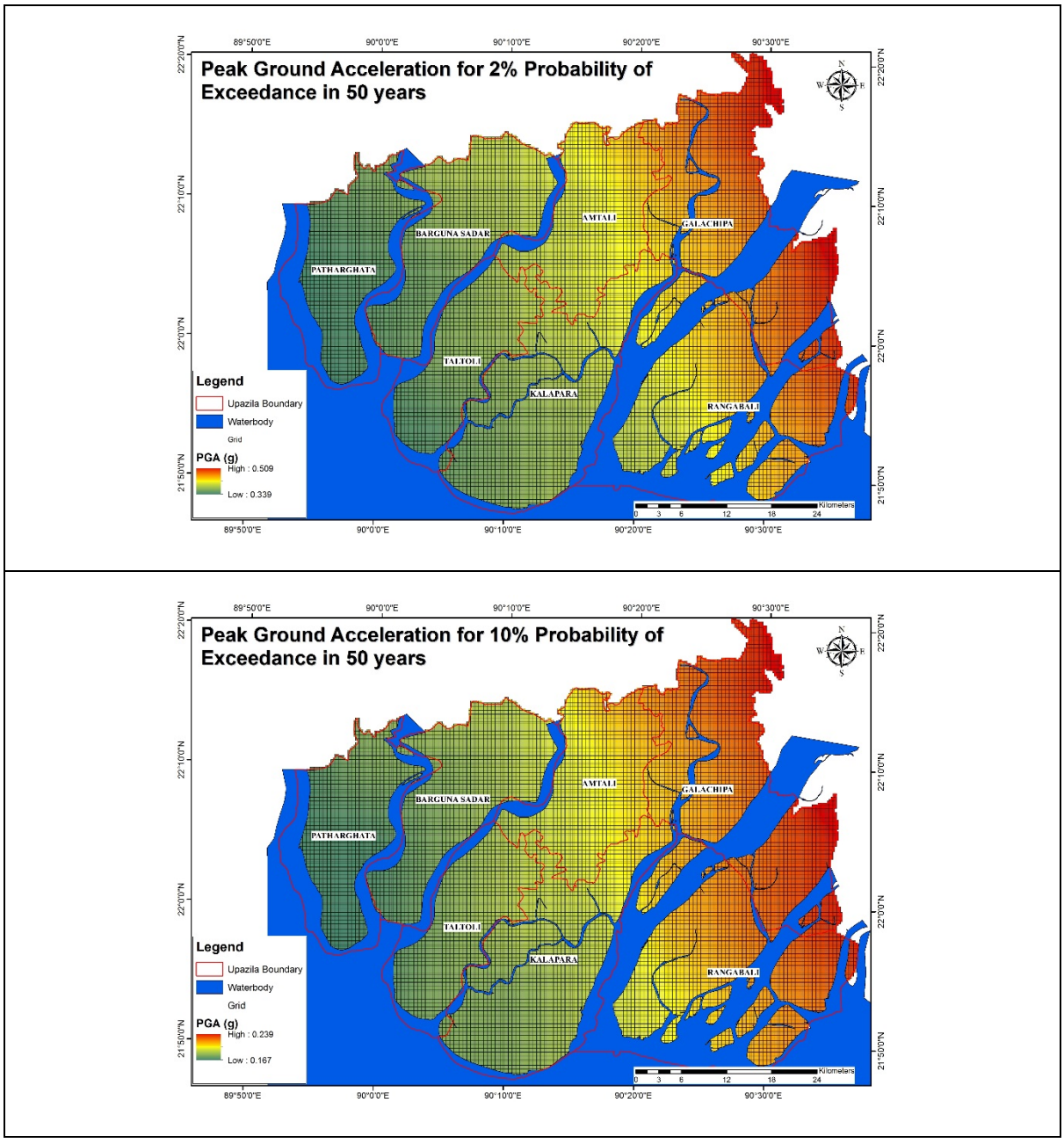

Figure: 4.9 PGA maps for (a) 2% and (b) 10% probabilities of exceedance in 50 years with site effect

The maps for the peak spectral accelerations (Figs 4.10, 4.11, and 4.12) show the possible ground motion scenario of Kuakata. The values for period 0.2 seconds are the highest with a

maximum of 1.42g for 2% probability of exceedance (Fig 4.10a). The spatial distribution of PSA at 0.2s is similar to that of the PGA distribution however, that of 1.0s shows some variation. This difference in pattern was also found in the studies of Al-Hussaini & Al-Noman (2010).

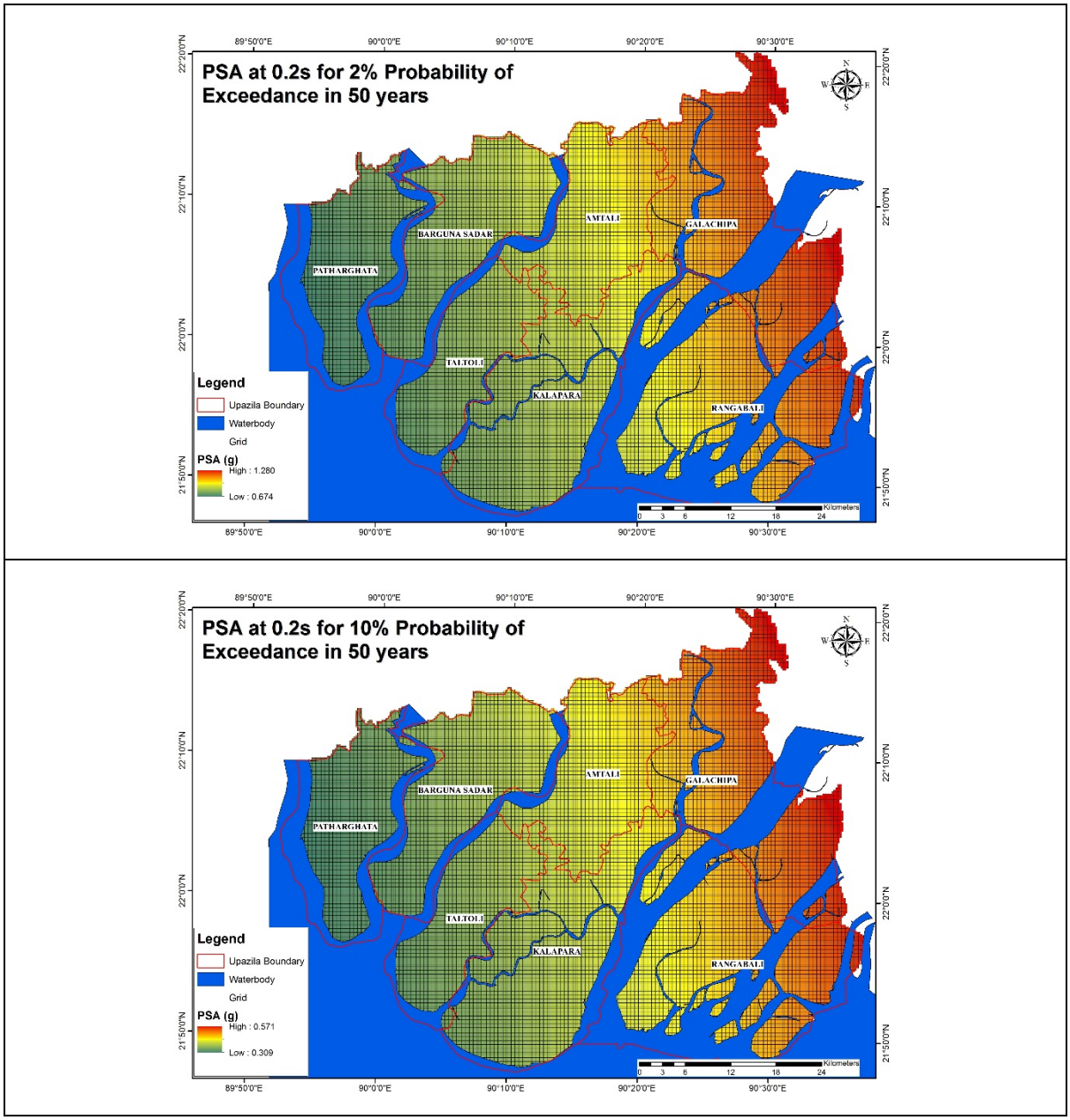

Figure: 4.10 PSA at 0.2 seconds maps for (a) 2% and (b) 10% probabilities of exceedance in 50 years with site condition

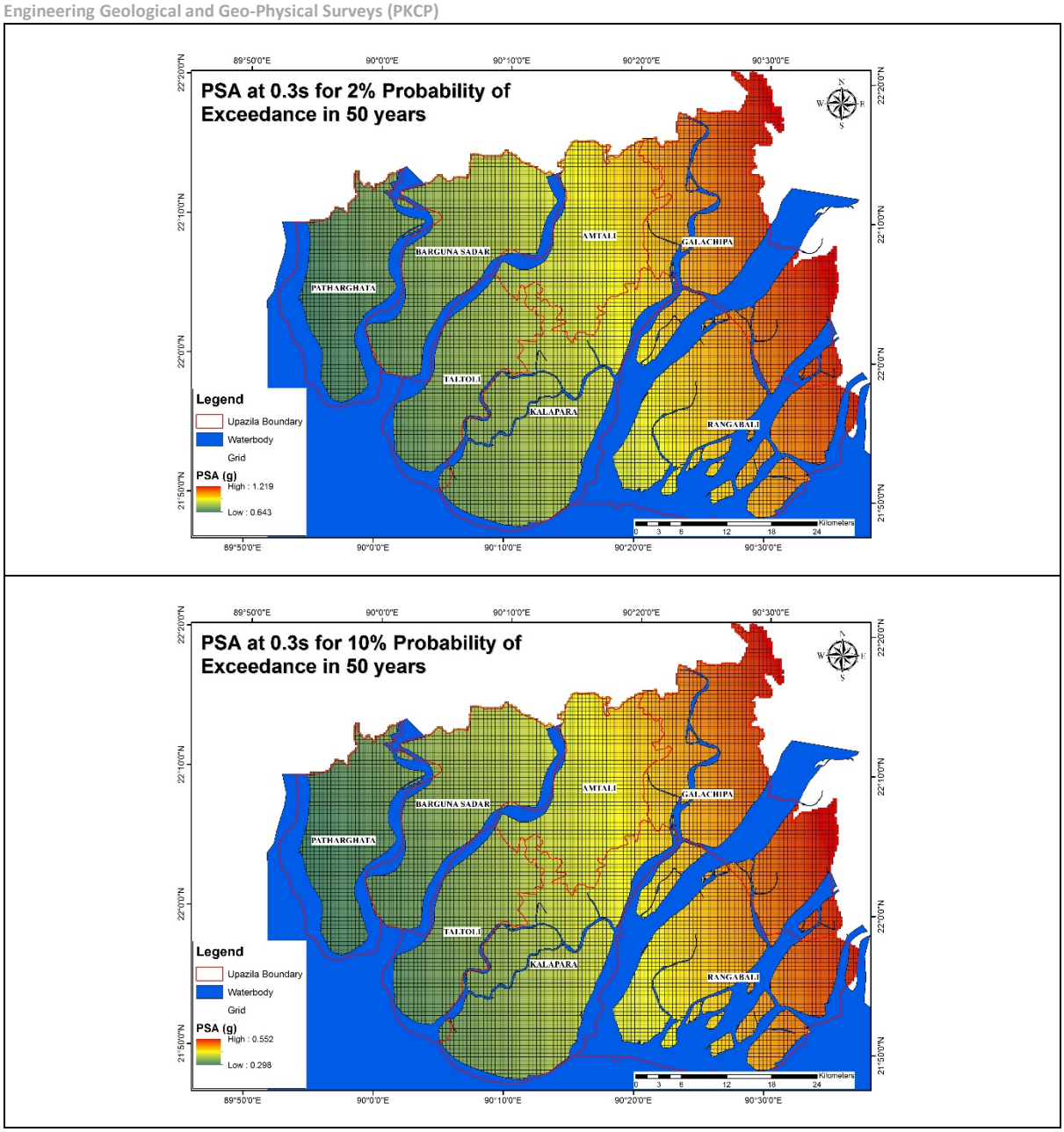

Figure: 4.11 PSA at 0.3s maps for (a) 2% and (b) 10% probabilities of exceedance in 50 years with site effect

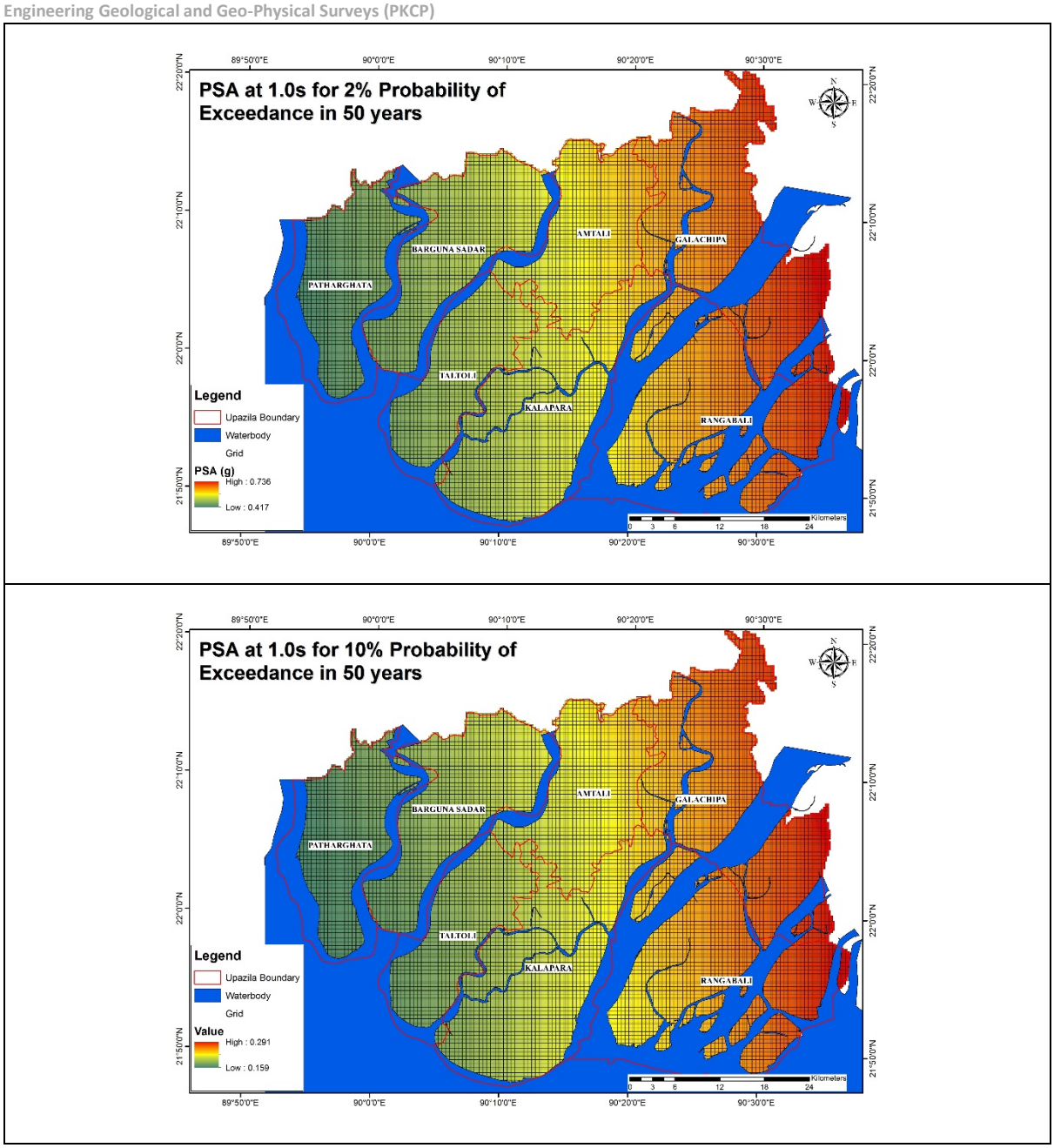

Figure: 4.12 PSA at 1.0s maps for (a) 2% and (b) 10% probabilities of exceedance in 50 years with site effect

The peak spectral accelerations at 0.3s, and 1s periods for 10% probability of exceedance in 50 years and 2% probability of exceedance in 50 years are being shown in the figure 4.11, and 4.12.

Hazard curves showing the probability of exceedance against intensty measure levels (PGA and SA) for 50 years return period for Payra-Kuakata project area.

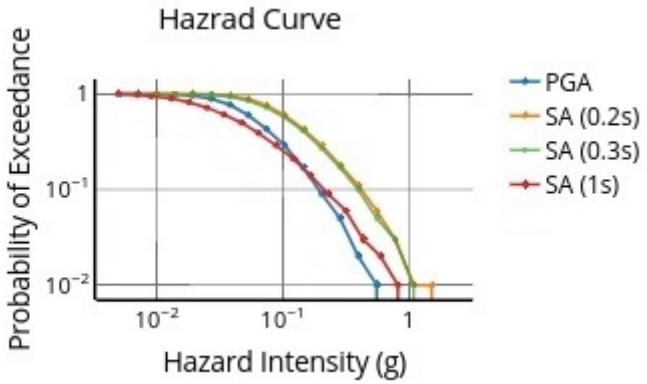

Figure 4.13 Hazard Curves for Payra-Kuakata project area(with site effect)

For all the hazard curves, it is clear that as the probability of exceedance decreases (*i.e.* the return period increases) the level of intensity measure subsequently increases. For all cases, the SA for 0.2s has the highest values for each corresponding exceedance probability while SA for 1 seconds has the lowest. Thus, structures with a natural frequency of 0.2s can be assumed to be at high risk. A summary of the PGA and SA estimates for the three cities are givien in Table 4.8.

Table 4.8 Maximum PGA and SA values for Kuakata

Area	10% Probability of Exceedance				2% Probability of Exceedance			
	PGA	SA (0.2s)	SA (0.3s)	SA (1.0s)	PGA	SA (0.2s)	SA (0.3s)	SA (1.0s)
Payra-Kuakata	0.25	0.63	0.60	0.31	0.54	1.42	1.34	0.77

4.2. Deterministic Seismic Hazard Assessment (DSHA)

Deterministic Seismic Hazard Assessment

There are two basic approaches to seismic hazard analysis. Both use the same basic body of information to determine what the "design earthquake" should be. The main difference is that the probabilistic approach systematically examines the uncertainties and includes the likelihood of an actual earthquake exceeding the design ground motion whereas the deterministic approach opts for the worst case earthquake possible. All of the elements of a deterministic analysis are included in the probabilistic approach. However, the deterministic method is strongly recommended in projects where consequences of failure are inexcusable and protection is needed against the worst earthquake that has the rational possibility of occurrence.

Commonly used steps in Deterministic Seismic Hazard Analysis are as follows:

1. Identification of possible sources
2. Characterization of the controlling earthquake
3. Estimation of ground motion from source to site
4. Assessment of seismic hazard at site

The first step is to identify all the possible sources of ground motion. Some of these will be easy to identify (e.g., a known active fault); others may be more difficult to describe. Next, the controlling earthquake needs to be defined and this involves engineering judgment. As the known earthquakes will have occurred at a distance that is not likely to be the same as the distance to the site, some correction needs to be made. This is done through the use of established ground motion prediction equations. In deterministic analysis, it is traditional to use the closest distance from a source to a site. It is very important to use ground motion prediction equations that are characteristic to the local geology as the resulting hazard statement is merely a scenario. So the more relevant the equation to the local geology, the realistic the resulting scenario. Characterization of the principal seismotectonic regimes in and around the area and determining the principal earthquake mechanism for each regime is conducted for this study. The ground motion prediction equations are selected with keen consideration for local ground conditions.

Potential Seismotectonic Regimes

The attenuation relation is usually developed for different tectonic regimes. Currently, subduction zone, an active tectonic region with the shallow crustal earthquake and stable continental region are typically considered for attenuation relation (Abrahamson & Silva, 1997).

The combined study of seismology, geodesy, and tectonics has revealed that Bangladesh is surrounded by five major potentially active seismotectonic regimes (Wang et al. , 2014). Due to the complex tectonic interaction of Indian plate with Eurasian and Burma Silverplate, Bangladesh is under threat of major earthquakes. Historically, over the last 150 years, this country was rocked by five major destructive earthquakes with Richter magnitude 7.0 and higher (GOB, 2009; Ambraseys, 2004; Bilham, 2004).To the north, the Himalayan mountain belt is formed by the collision of the Indian plate with Eurasian plate and the collision boundary (figure 4.14) is marked by the Himalayan Frontal Thrust Fault (HFT). This north-dipping thrust fault runs nearly 2000km from the Kashmir in the west to the Himalayan syntaxes in the Assam (Yu & Sieh, 2013). Just immediate southern proximity of HFT, about 270km long north dipping reverse fault, the Dauki fault lies along the southern flank of Shillong plateau. Arakanmegathrust runs as concave folded thrust belt on the eastern side of Bangladesh from south to northeast. The 450km long Ramree domain characterized by sustained convergence and pronounced seismicity in the northern part compared to its southern counterpart (Wang et al., 2014). This tectonic regime has produced a deformation belt that increases its width from about 170km in the south to about 250km in the north. The north of Ramree domain, the Dhaka section (~500km long & ~400km maximum width) of Arakan Mega Thrust is resultant from the collision of Burma silver plate and thick sediment covered Ganges-Brahmaputra delta (Wang et al., 2014). Recently Steckler et al (2016) have identified the presence of locked megathrust deformation front boundary just beneath the mega city Dhaka. Chittagong Tripura Folded Belt (CTFB) present in this tectonic region lies within Bangladesh exhibiting several thrust faults. The NE and SW trending Naga Trust regime results from the Indo-Burman collision are located between Shilling plateau and Himalayan syntaxis. This 430km long section exhibits a width from 160 to 240km (Wang et al., 2014). The study area of KPCP (edit please) is in close proximity of two of the aforementioned seismotectonic regimes viz. Arakan Thrust (Dhaka Section) and the Ramree Domain.

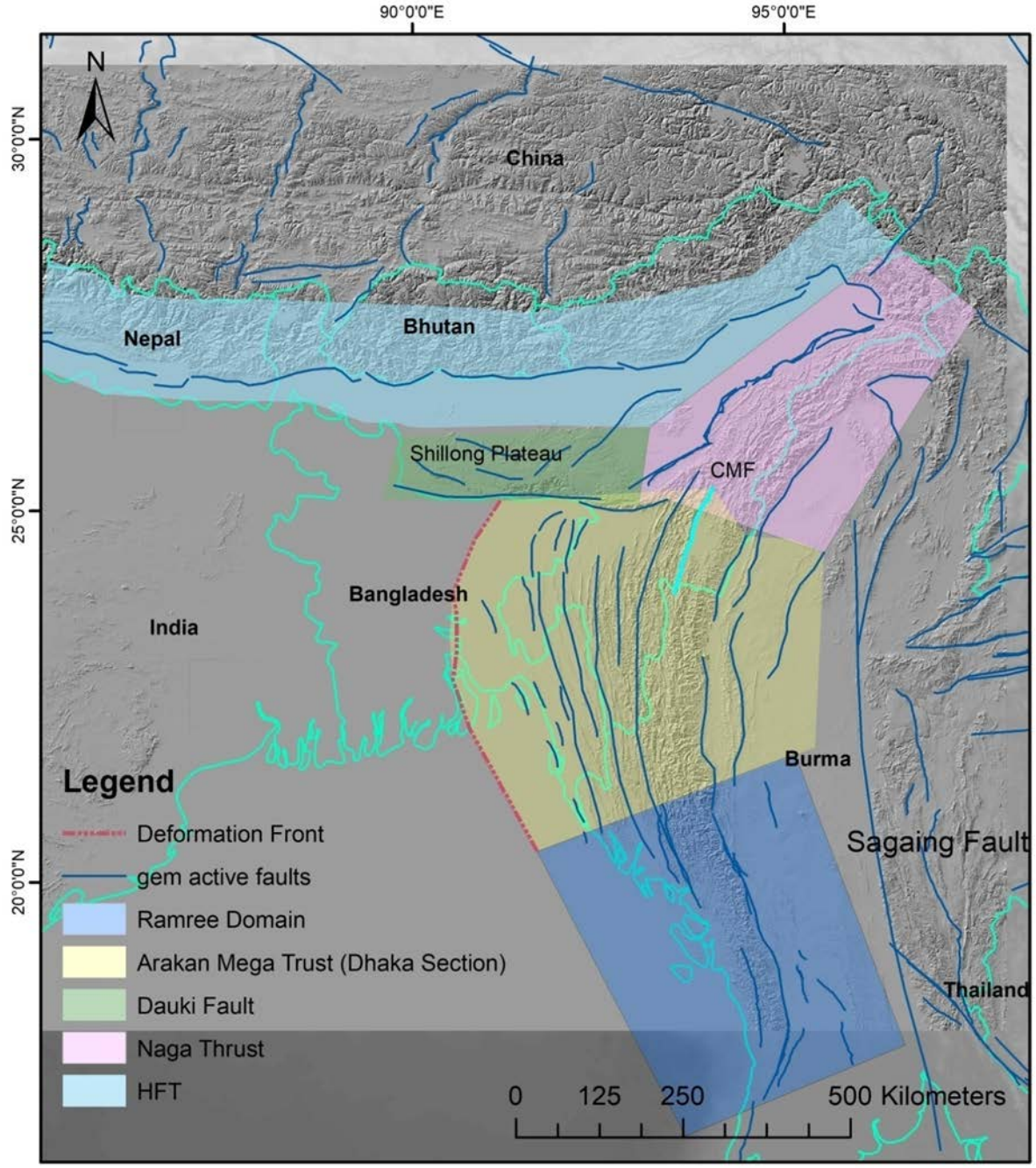

Figure 4.14 Major seismotectonic regimes in and around Bangladesh (adapted from (Wang et al., 2014))

The blue straight lines are the Global Earthquake Model (GEM) active faults (Christophersen et al., 2015). The shaded relief map retrieved from SRTM 1 ARC SEC is used as the background image; HFT is for Himalayan Frontal Thrust and CMF is Churachandpur Mao fault

Yu & Sieh (2013) has estimated the probability of occurrence of a major earthquake and the recurrence interval for each tectonic regime from the fault zone length and slip rate. The Arakanmegathrust (Dhaka section), HFT and Ramree show the highest potentiality of generating major earthquake (table 4.9 & 4.10)

Table 4.9 Potential seismicity scenarios of the major seismotectonic regimes in and around Bangladesh based on the empirical equation of Blaser et al.(2010) in Stirling & Goded (2012)**.**

Name	**Length(km)**	**Dip °**	**Locking Depth (km)**	**Slip Rate(mm/yr)**	**M_{max}**	**Average Slip (mm/yr)**	**Recurrence Interval (yr)**	**Date of Last Event (AD)**
Main Frontal Trust (MFT)	~500	~10	20	21	8.9	16	760	1100 (?)
Naga Trust	~400	~23	20	5	8.7	25	5000	unknown
DaukiFault	~270	~45	35	11	8.4	13	1200	1897
Arakan Megathrust(Dhaka Section)	~500	<10	20	10	8.9	9	920	Unknown, but perhaps 1548
Arakan Megathrust(Ramree Section)	~500	~16	30	23	8.9	17	730	1762

Source: (Yu & Sieh, 2013)

Table 4.10 Potential seismicity scenarios of the major seismotectonic regimes in and around Bangladesh based on the empirical equation of Strasser et al. (2010) inStirling & Goded (2012)**.**

Name	**Length (km)**	**Dip °**	**Locking Depth (km)**	**Slip Rate (mm/yr)**	**M_{max}**	**Average Slip (mm/yr)**	**Recurrence Interval (yr)**	**Date of Last Event (AD)**
Main Frontal Trust (MFT)	~500	~10	20	21	8.6	6.3	300	1100 (?)
Naga Thrust	~400	~23	20	5	8.5	11	2200	unknown
DaukiFault	~270	~45	35	11	8.3	7.5	680	1897
Arakan Megathrust(Dhaka Section)	~500	<10	20	10	8.6	3.6	360	Unknown, but perhaps 1548

Arakan Megathrust(Ramree Section)	~500	~16	30	23	8.6	6.7	290	1762

Source: (Yu & Sieh, 2013)

The source parameter maximum magnitude, $M_{max,}$ simply defined as the largest possible earthquake that can occur in a certain region is associated with considerable epistemic uncertainties due to the evident limitations in its observability (Cornell, 1968). Yu & Sieh (2013)have estimatedthe maximum magnitude earthquake that can be produced from each seismotectonic regime. The maximum magnitudes were derived from the relations established by Blaser et al., (2010)and Strasser et al.,(2010). The first one is suitable for the subduction zone and the other one is for the interface event. For example, the highest magnitudes calculated in HFT are 8.9 with a recurrence interval 760 years and 8.6 with a recurrence interval of 300 years from the respective equations. The first one having a higher recurrence interval and higher slip value (~16m) shows consistency with a paleoseismic observation from the westernmost part of the fault. In another literature, it is proposed that more than 500 years ago the last rupture occurred where the fault slip was about 12 m. The other parts of the fault also went through a similar amount of slips (Kumar et al., 2010). The coherence in the observations makes the estimation acceptable. The accepted distance parameter from source to the site for this study is the epicentral distance. The controlling design earthquake is set to have its epicentre 50 kilometres away from the site, within the Arakan Megathrust regime and in accordance with the potential seismicity scenario of the respected regime(s).

Ground Motion Prediction Equations

Ground Motion Prediction Equations (GMPEs) or attenuation relationships or ground motion models, provide a means of predicting the level of ground shaking and its associated uncertainty at any given site or location, based on an earthquake magnitude, source-to-site distance, local soil conditions, fault mechanism, etc. GMPEs are efficiently used to estimate ground motions for use in both deterministic and probabilistic seismic hazard analyses.

The colossal number of published ground motion prediction equations emphasizes the importanceof proper criteria for the selection of appropriate equations for seismic hazard assessment in a given region. Cotton et al (2006) suggest the following exclusion criteria.

1. The model is not from the correct tectonic regime;

2. The model hasn't been published in an international peer-reviewed journal;
3. Inadequate documentations and lackluster dataset;
4. For the same tectonic regime, there is another publication following up on that model;
5. The frequency range of the model does not meet engineering requirements;
6. The model has an inappropriate functional form (magnitude scaling taken into account), or the regression method or regression coefficients are judged to be inappropriate.

In addition to the exclusion criteria, the selection criteria proposed by Stewart et al, (2015) were taken into account, stipulating that,

- GMPEs derived from international datasets are to be prioritized over the ones derived from local datasets.
- GMPEs having attributed, multifaceted functional forms are to be emphasized.
- If there are multiple GMPEs, all well-endowed in terms of data but show different trends, the selected GMPEs should incorporate the different trends to showcase epistemic uncertainty.

With these criteria in place, the following three ground motion prediction equations have been selected for the hazard assessment:

1. Youngs et al (1997)
2. Atkinson and Boore (2003)
3. Zhao et al (2016)

Seismic Hazard Assessment at Site

The preceding survey conducted the testing for local site conditions with the parameter being AVs30 i.e. average velocity of shear wave propagating through the top 30 meters of the ground. The survey incorporated two techniques: PS Logging and Multichannel Analysis for Surface Wave (MASW). The resulting AVs30 values are as follows:

Table 4.11 AVs30 values in different locations (exploration points) within the study area obtained by PS Logging and Multichannel Analysis for Surface Wave (MASW)

ID	Lat	Long	AVS30	PS_ID	Lat	Long	AVS30
MASW-01	21.896922	90.096240	160.4	PS01	21.822277	90.122042	158.733
MASW-02	21.856878	90.133068	173.1	PS02	21.908114	90.405833	172.69
MASW-03	22.064133	90.233002	158.9	PS03	21.98446	90.083894	148.302
MASW-04	21.947628	90.177573	148.9	PS04	21.98503	90.22015	149.315
MASW-05	21.930813	90.421332	163.7	PS05	22.025535	90.418347	153.866
MASW-06	21.829242	90.515129	153.9	PS06	22.067503	89.927283	153.891
MASW-07	22.088547	89.921828	169.9	PS07	22.044112	90.051524	158.31
MASW-08	22.133985	90.012633	168.8	PS08	22.059275	90.186166	137.419
MASW-09	22.185166	89.987518	164.9	PS09	22.168115	90.408955	161.707
MASW-10	22.142274	90.078016	170.9	PS10	22.141493	90.233098	164.723
MASW-11	22.036876	90.172085	169.9	PS11	22.05873	90.31988	134.44
MASW-12	22.012223	90.447358	154.4	PS12	22.177767	90.015177	134.026
MASW-13	22.052923	90.066759	153.4	PS13	22.155764	90.122003	146.708
MASW-14	22.168417	90.149975	169.9	PS14	22.247763	90.322332	127.998
MASW-15	21.972921	90.088349	172.8	PS15	22.22561	90.45629	139.106
MASW-16	22.072886	90.302790	177.4	PS 16	21.994316	90.275292	169.387
MASW-17	22.102038	90.218399	180				

MASW-18	21.978473	90.233746	177.8
MASW-19	22.163421	90.493973	166.4
MASW-20	22.210745	90.111824	172.2
MASW-21	22.218119	90.301839	168.6
MASW-22	22.091300	90.415183	170.2
MASW-23	21.858442	90.236906	170.5
MASW-24	22.267794	90.476066	145.6
MASW-25	22.160346	90.413511	177.4
MASW-26	21.942536	90.255428	165
MASW-27	22.013511	90.288996	170.9

The ground motion prediction equations are not overly sensitive to the soil/rock conditions. Typically, these equations contain 4 to 6 soil categories (Douglas, 2018). Among the equations used in this study, Atkinson and Boore (2003) recognizes 4 soil categories with Vs30<180, 180<Vs30<760, 760<Vs30<2000 and Vs30>2000 (Douglas, 2018) whereas Zhao et al (2016) recognizes 4 categories but the limiting values differ slightly (Vs30<200, 200<Vs30<760, 760<Vs30<2000 and Vs30>2000) in units of m/s (Douglas, 2018). This trait of the equations implies that they would generate a single value of design acceleration across all the exploration points. So the spatial distribution of earthquake ground motion could not be displayed as there would be a single value of peak ground acceleration (PGA) throughout the study area.

Deterministic Seismic Hazard Assessment Results

As spatial distribution of design peak ground acceleration could not be mapped in an effective manner, so instead of said maps, the individual PGA values for each equation in each potential seismicity scenario which are characteristic of the respective seismotectonic regimes are displayed in addition with

the ground motion scenario of the said regimes. In each case, the source is placed at a distance of 50 km from the site.

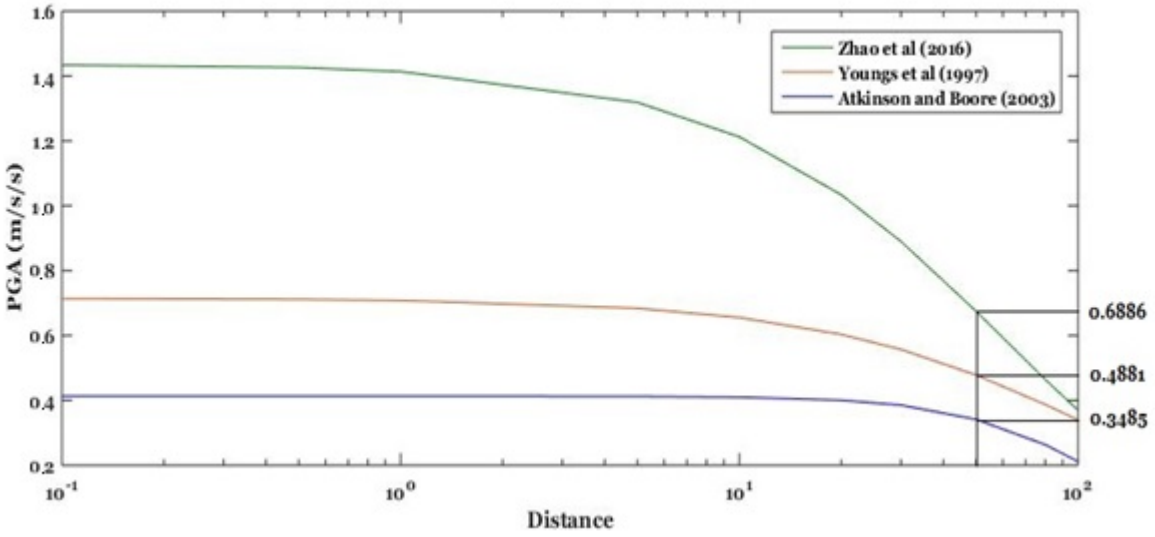

Figure 4.15 Propagation of earthquake ground motion shown as a function of Peak Ground Acceleration (ms^{-2}) based on the potential seismicity scenarios of the ArakanMegathrust (Ramree Domain) based on the empirical equation of Blaser et al. (2010) in Stirling & Goded (2012).

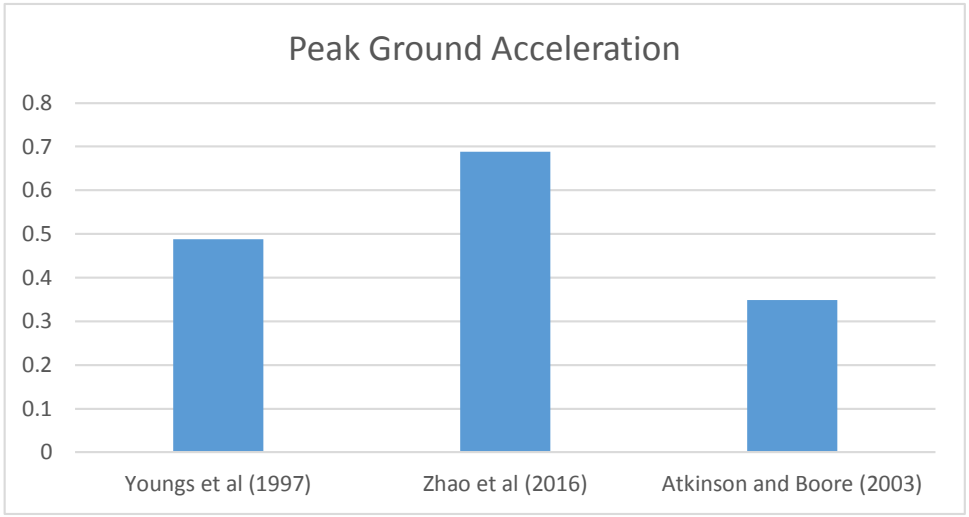

Figure 4.16 Estimated peak ground acceleration (PGA) based on the potential seismicity scenarios of the ArakanMegathrust (Ramree Domain) based on the empirical equation of Blaser et al. (2010) in Stirling & Goded (2012).

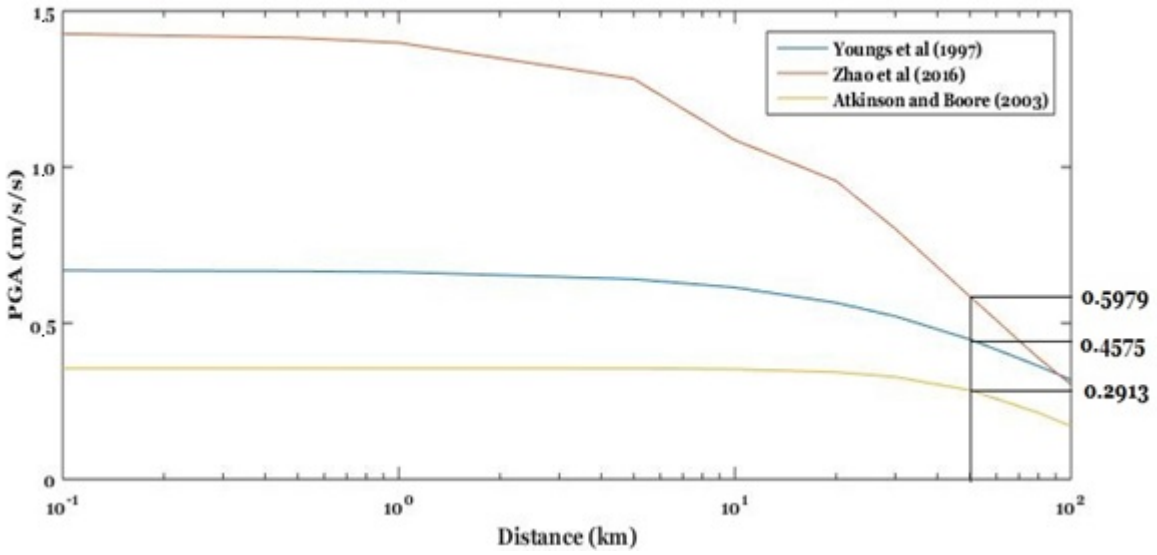

Figure 4.17 Propagation of earthquake ground motion shown as a function of Peak Ground Acceleration (ms^{-2}) based on the potential seismicity scenarios of the Arakan Megathrust (Dhaka Section) based on the empirical equation of Blaser et al. (2010) in Stirling & Goded (2012).

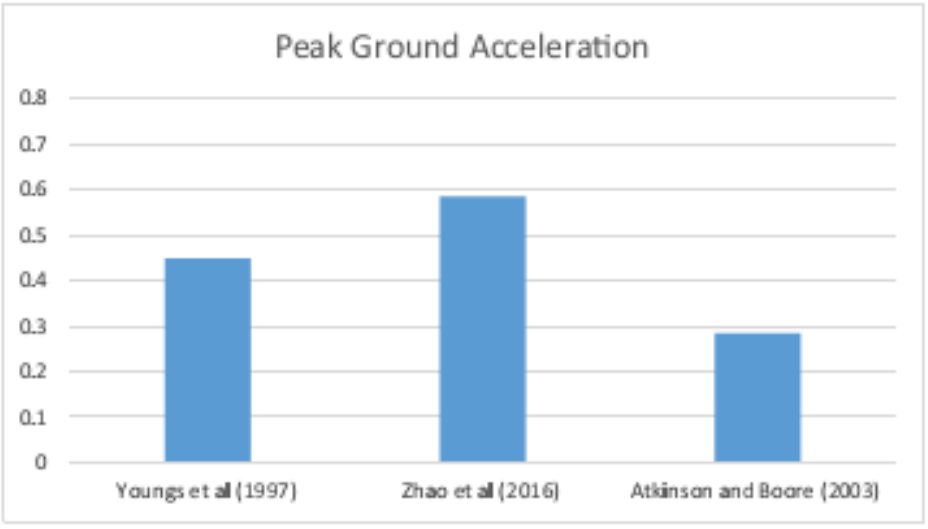

Figure 4.18 Estimated peak ground acceleration (PGA) based on the potential seismicity scenarios of the ArakanMegathrust (Dhaka Section) based on the empirical equation of Blaser et al. (2010) in Stirling & Goded (2012).

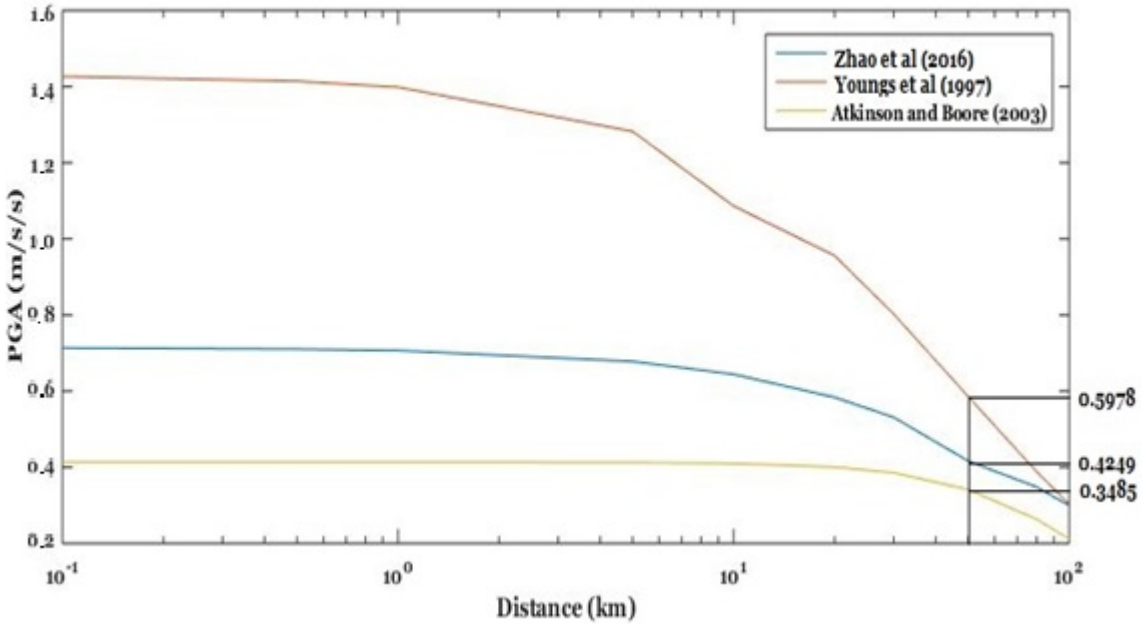

Figure 4.19 Propagation of earthquake ground motion shown as a function of Peak Ground Acceleration (ms^{-2}) based on the potential seismicity scenarios of the ArakanMegathrust (Ramree Domain) based on the empirical equation of Strasser et al. (2010) in Stirling & Goded (2012).

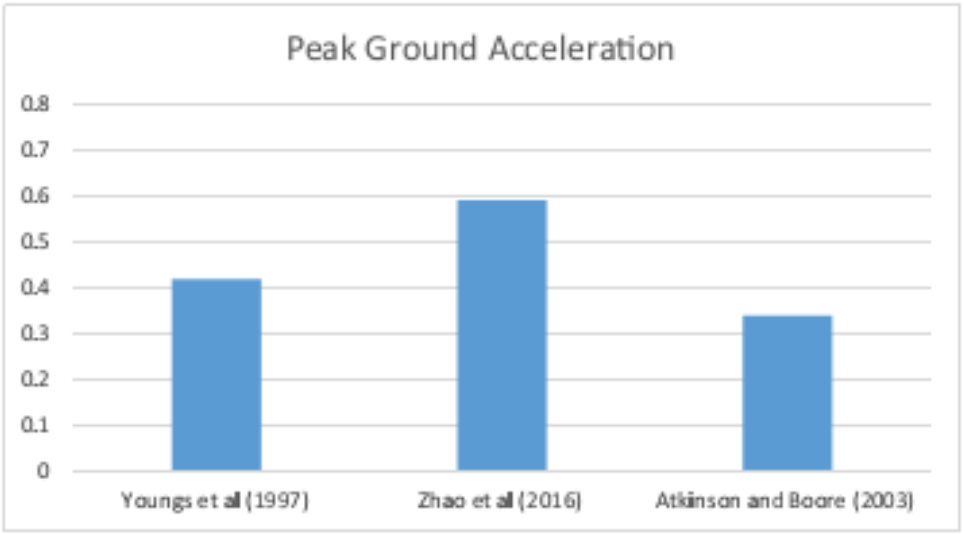

Figure 4.20 Estimated peak ground acceleration (PGA) based on the potential seismicity scenarios of the ArakanMegathrust (Ramree Domain) based on the empirical equation of Strasser et al. (2010) in Stirling & Goded (2012).

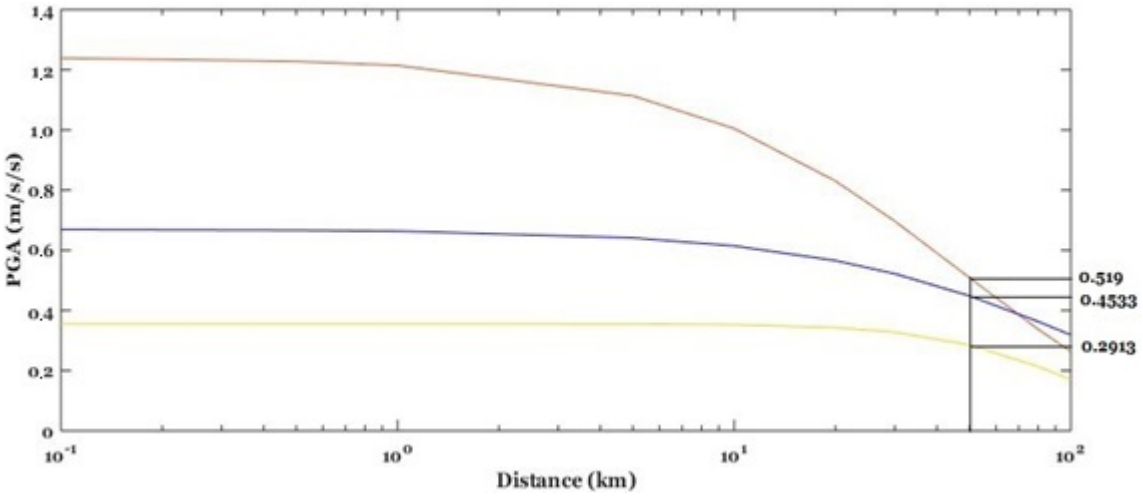

Figure 4.21 Propagation of earthquake ground motion shown as a function of Peak Ground Acceleration (ms^{-2}) based on the potential seismicity scenarios of the Arakan Megathrust (Dhaka Section) based on the empirical equation of Strasser et al. (2010) in Stirling & Goded (2012).

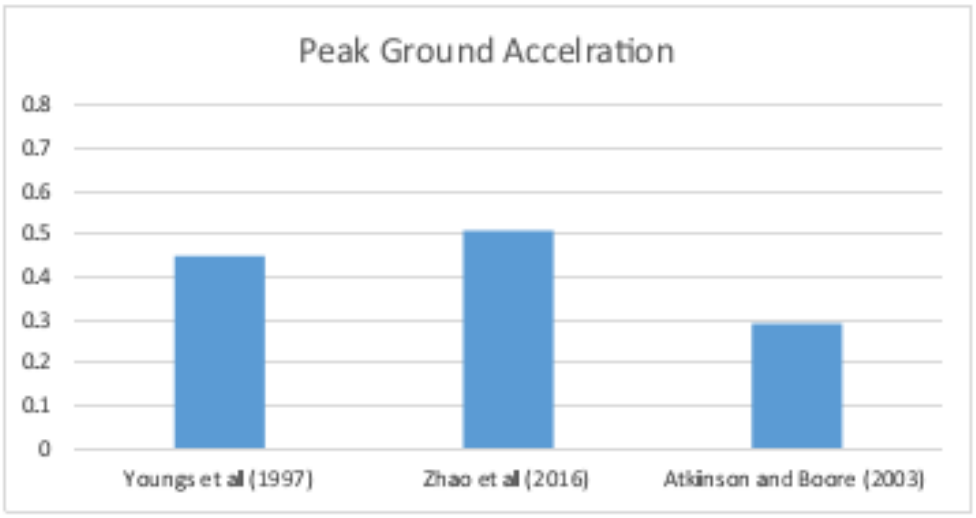

Figure 4.22 Estimated peak ground acceleration (PGA) based on the potential seismicity scenarios of the ArakanMegathrust (Dhaka Section) based on the empirical equation of Strasser et al. (2010) in Stirling & Goded (2012).

The individual seismic hazard scenarios are summarized in Table 4.12. The different estimations are for the same geographic locations and hence from the table we can determine a worst case scenario for the deterministic hazard assessment.

Table 4.12 Estimated peak ground acceleration (PGA) based on the potential seismicity scenario of the major seismotectonic regimes in and around Bangladesh based on the empirical

equation of Blaser et al. (2010) and Strasser et al. (2010) in Stirling & Goded (2012) considering 50km distance of Payra-Kuakata from Ramree and Dhaka section

Potential Seismicity Scenario		**Seismotectonic Regime**	**Peak Ground Acceleration (g)**		
			Youngs et al (1997)	Zhao et al (2016)	Atkinson and Boore (2003)
Blaser et al (2010)	M_{max}=8.9 Locking Depth = 20km	ArakanMegathrust (Dhaka Section)	0.4575	0.5979	0.2913
	M_{max} =8.9 Locking Depth = 30km	ArakanMegathrust (Ramree Domain)	0.4881	*0.6886*	0.3485
Strasser et al (2010)	M_{max} =8.6 Locking Depth = 20km	ArakanMegathrust (Dhaka Section)	0.4533	0.519	0.2913
	M_{max} =8.6 Locking Depth = 30km	ArakanMegathrust (Ramree Domain)	0.4249	0.5978	0.3485

After careful observation of different seismotectonic setting and ground motion scenario the worst case event was identified to be the one occurring from the ArakanMegathrust (Ramree Domain) at a distance of 50 kilometers from the site and the predicted seismic hazard is 0.6886 ms^{-2}.

The minimum physical distance from the ArakanMegathrust (both Ramree Domain and Dhaka Section) to the site is approximately 80 kilometers. So the ground motion scenario at 80 kilometers from site need an assessment.

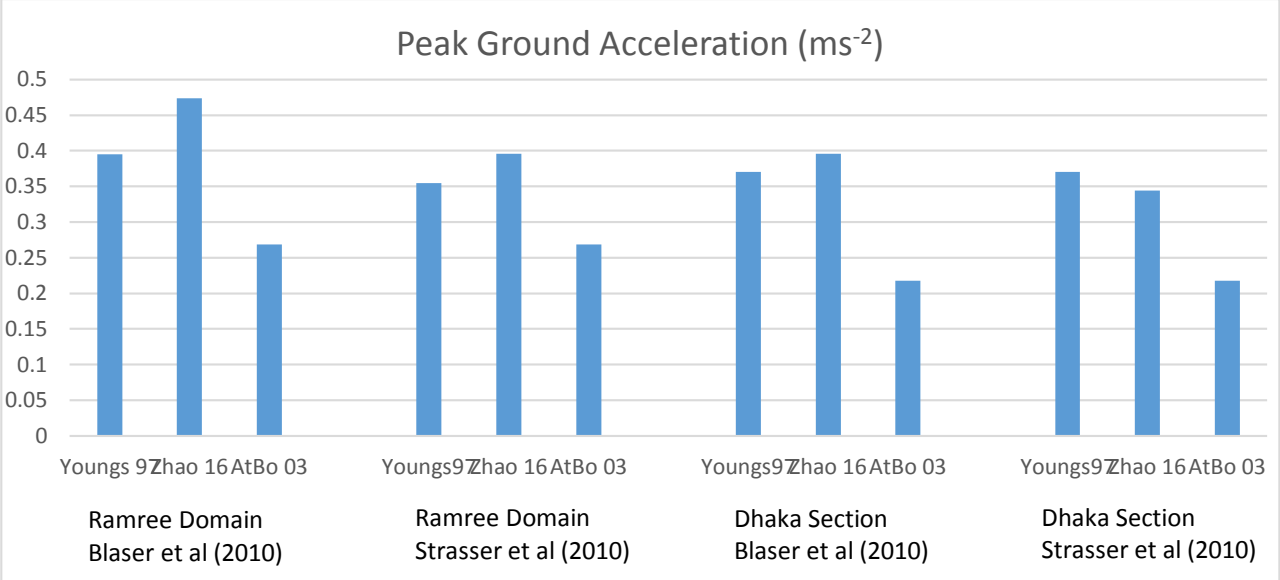

Figure 4.23 Estimated peak ground acceleration (PGA) based on the potential seismicity scenarios of the ArakanMegathrust based on the empirical equations of Blaser et al (2010) and Strasser et al. (2010) in Stirling & Goded (2012), set at a minimum physical distance of 80 km from the source.

The assessment is summarized in Table 4.13. The source to site distance is set at 80 kilometers which is the minimum physical distance. The seismotectonic setting i.e. source type, locking depth etc. are taken from the empirical equations as shown in Table 4.9 and 4.10.

Table 4.13 Estimated peak ground acceleration (PGA) based on the potential seismicity scenario of the major seismotectonic regime of ArakanMegathrust (Both Ramree Domain and Dhaka Section) in Bangladesh based on the empirical equations of Blaser et al. (2010) and Strasser et al. (2010) in Stirling & Goded (2012) considering 80km distance from Ramree and Dhaka Section

Potential Seismicity Scenario		**Seismotectonic Regime**	**Peak Ground Acceleration (g)**		
			Youngs et al (1997)	Zhao et al (2016)	Atkinson and Boore (2003)
Blaser et al (2010)	M_{max}=8.9 Locking Depth = 20km	ArakanMegathrust (Dhaka Section)	0.3704	*0.3961*	0.2175

	M_{max} =8.9 Locking Depth = 30km	ArakanMegathrust (Ramree Domain)	0.3952	0.4739	0.2689
Strasser et al (2010)	M_{max} =8.6 Locking Depth = 20km	ArakanMegathrust (Dhaka Section)	0.3704	0.344	0.2175
	M_{max} =8.6 Locking Depth = 30km	ArakanMegathrust (Ramree Domain)	0.355	0.3961	0.2689

After careful observation of different seismotectonic setting and ground motion scenario the worst case event was identified to be the one occurring from the Arakan Megathrust (Ramree Domain) at a distance of 80 kilometers (minimum physical distance) from the site and the seismic hazard is 0.4739 ms^{-2}.

4.3. Engineering Geological Mapping

There are many types of "Engineering Geological Map" depending on intended purpose. For instance, when the target is to know suitable foundation soil layer for a planned building, an engineering geology map should have a property of some geotechnical strength, in another case, when it is necessary to know groundwater potential for a water resource development, a map is created on the basis of permeability of soil as a focal point.

In this study, the target is estimation/evaluation of earthquake phenomenon; so seismic and engineering characteristic of soil is required for the engineering geology map to analyze seismic hazard. To understand seismic hazard assessment the necessary basin information are ground motion at the ground surface; the ground motion can be usually calculated using S-wave velocity. Hence, the engineering geological map is created on the basis of S-wave velocity.

It is notable that in seismic ground motion analysis, especially calculation of amplification of soil, is examined by an empirical method that uses average S-wave velocity of ground in the top 30m depth (hereinafter referred to as "V_{s30}"), because the limited point data that is boring/PS logging data should be expanded to the study area in order to make ground model.

Therefore, "soil type map based on V_{s30}" is defined as the "Engineering Geological Map" in this study.

4.3.1 Shear Wave Velocity Estimation

Estimation of shear wave velocity (Vs) and mapping is a way to characterize varying site conditions, and it can also be used to model earthquake-related ground shaking. Estimation of Vs aims to generate a map of estimated shear wave velocities for the upper 30m of the subsurface, Vs30. Field measurement of Vs of near surface layers implying near surface seismic surveys alike Downhole seismic test (PS Logging) and multi channel analysis of surface wave (MASW) can serve the purpose. V_s of subterranean layers can be obtained by another mean — determination of shear wave velocity from SPT N value from empirical relation between V_s and N value. Because of near surface seismic tests are expensive and so limited numbers of seismic tests are done while SPT tests could be done more extensively, a probabilistic correlation between V_s obtained from near surface seismic and SPT tests are used for to depict extrapolated gestalt picture of V_{s30} distribution throughout the study area from point data (V_{s30} at each borehole). The resulting velocities can be more confidently used for V_{s30} mapping. Further this map can be useful for seismic site response analysis i.e., to determine peak ground acceleration (PGA) and spectral acceleration (SA) values of both bedrock and ground surface.

As a part of engineering geological or V_{s30} mapping, as mentioned earlier, of the Study Area, shear wave velocity (Vs) of the local near surface geological units can be obtained by PS Logging and SPT test. The shear wave velocity is a fundamental parameter required to define the dynamic properties of soils. A viable formula for velocity determination at the study area has been adopted by probabilistic correlation between Vs yielded from PS Logging and SPT tests. Then the V_{s30} categories assigned to the generalized geologic units were used to generate a V_{s30} map. Finally, the hybridized V_{s30} map has been used for seismic site response analysis — PGA and SA mapping, which is hopefully believed to pave the way to the structural engineers and planners to sustainable infrastructure development at Study Area.

N Value and V_s Correlation

Correlations between SPT resistance and shear wave velocity have been proposed for a number of different soil types (Ohba and Toriumi,1970; Imai and Yoshimura, 1970; Fujiwara, 1972; Ohsaki and Iwasaki, 1973; Imai, 1977; Ohta and Goto, 1978; Seed and Idriss, 1981; Imai and Tonouchi, 1982; Sykora and Stokoe, 1983; Jinan, 1987; Lee, 1990; Sisman, 1995; Iyisan, 1996;

Kayabalı, 1996; Jafari et al., 1997; Pitilakis et al., 1999; Kiku et al., 2001; Jafari et al., 2002; Andrus et al., 2006; Hasançebi and Ulusay, 2007; Hanumantharao and Ramana, 2008; Dikmen, 2009). A summary of empirical relationships between SPT resistance and V_s in the literature is presented in for different soil types. In these relationships, SPT-N_{60} blow count is mostly considered. It should be noted that the empirical relationships use a power–law relationship between Vs and SPT N-value. In these relationships, the values of the exponent, which control the curvature of the relationship, are more consistent than the constant that controls the amplitude. This accounts for the generally similar shapes of the curves.

The shear wave velocity of the Study Area soil has been determined from down-hole seismic (PS Logging) method using at 16 locations and MASW at 27 point. The shear wave velocities (V_{s30}) determined from SPT blow counts (N) and down-hole seismic tests are considered during the development of empirical relationship. The following power–law expression based on regression has been obtained to derive V_s from N (red dashed line in Figure 4.24).

$V_s = 90.03N^{0.285}$…….. (4.1)

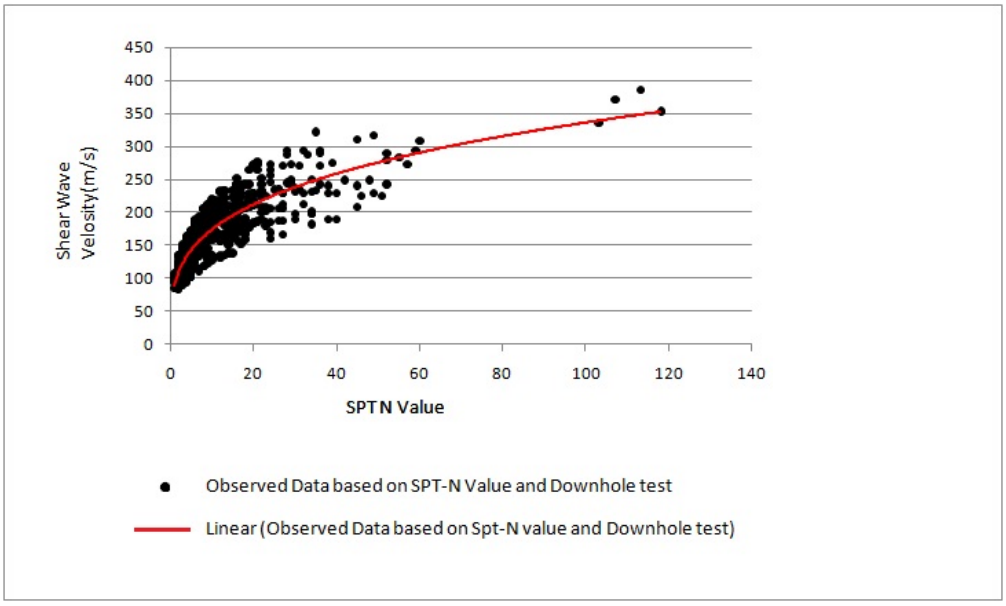

Figure 4.24 Regression analysis between measured SPT-N value and shear wave velocity (Vs) obtained from down-hole seismic test (PS Logging)

The shear wave velocities measured in down-hole tests can be compared with those estimated using empirical models for different soil types. The relationship proposed for study area soil in this study (red dash line in Figure 4.25) is quite compatible with the following equation

(Equation – 4.2), which has similar trend, introduced by Ohba and Toriumi (1970)(Green bold line in Figure 4.25).

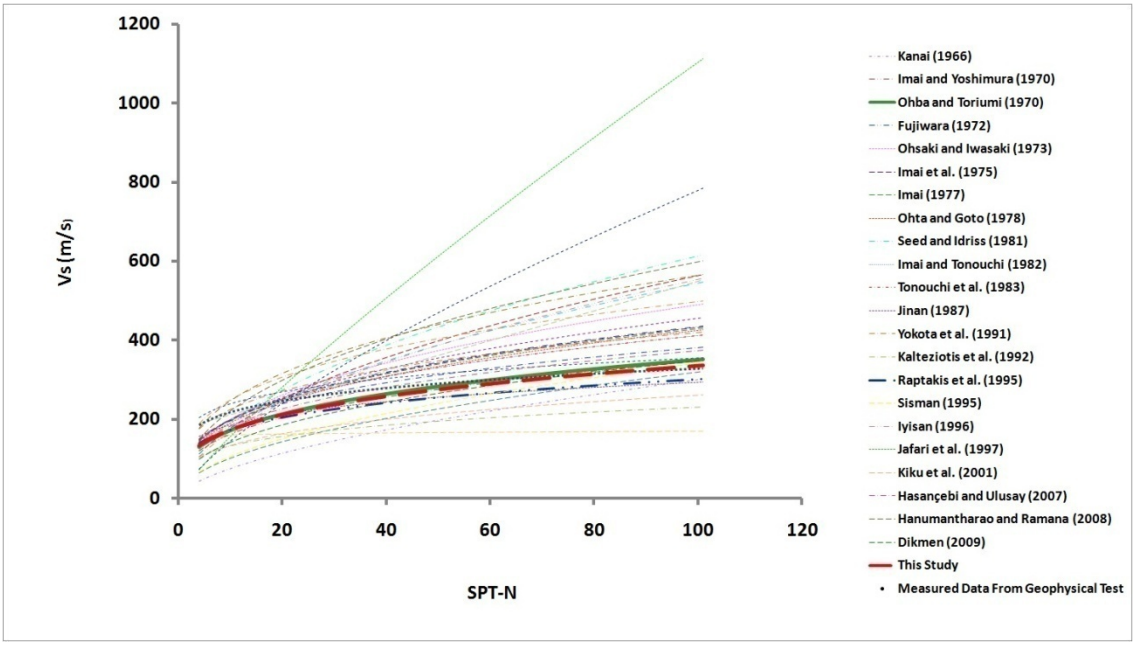

Figure 4.25 SPT-N value and Vs empirical relations for all soils in study area

The distribution of the shear wave velocity data with respect to SPT-N value at the same depth with SPT application and SPT-based geophysical test is considered in the interpretations.

$V_s = 84N^{0.31}$……. (4.2)

Based on this equation 4.2, shear wave velocity (V_s) at every 1.5m interval has been calculated at every boreholes drilled within study area.

Vs 30 Calculation

Near surface shear wave velocity is crucial for earthquake-hazard assessment studies (Wald & Mori 2000; Kanli et al. 2006). The average shear wave velocity of the upper 30 m (V_{s30}) can be computed in accordance with the following expression:

$$V_s{}^{30} = \frac{30}{\sum_{i=1}^{N}(h_i/v_i)} \quad \text{…….(4.3)}$$

where h_i and v_i denote the thickness (in meters) and shear-wave velocity of the i^{th} formation or layer respectively in a total of N existing in the top 30 m. V_{s30} was accepted for site classification in the USA (NEHRP) by the UBC (Uniform Building Code) in 1997 (Dobry et

al, 2000). Using the aforementioned equation 4.3, V_{s30} at every borehole has been calculated. Figure 4.26 represent Vs30 map of the study Area.

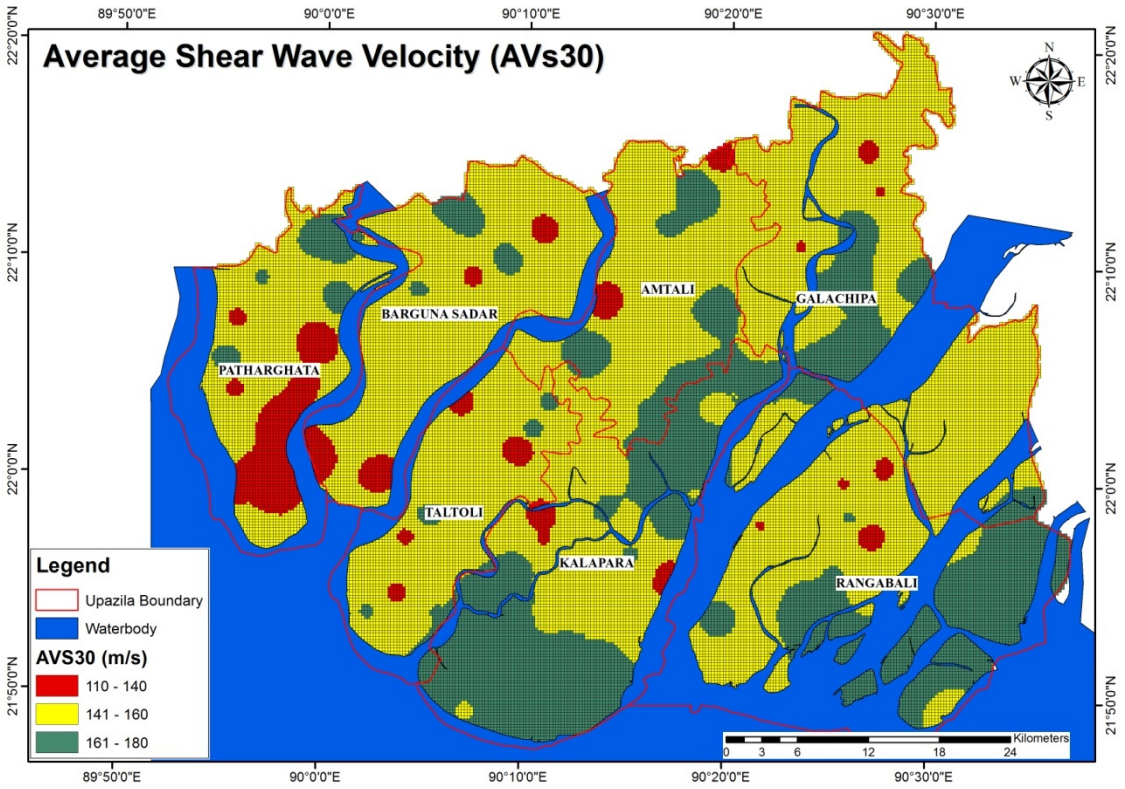

Figure 4.26 Engineering geological map of the Study Area

From the figure 4.26 it can be clearly visualize that the red color areas (northern part of Patharghata, northern most part of Barguna Sadar with few discrete parts of the project area) represents the Low shear wave velocity zone ranging from 110 to 140.00 m/s; Most of the area is comprising with the yellow color areas represents shear wave velocity range of 141 to 160 m/s and the green color areas (maximum part of Kalapara, Galachipa and Rangabali Upazila) have comparatively High shear wave velocity ranges from 161 to 180 m/s. Vs30 of soil is a very use full tool for soil type classification.

4.3.2. Soil Type Determination based on Vs30

An important part of this study is the soil classification of the study area. The area has been investigated and classified according to a method provided by NEHRP (stands for National Earthquake Hazard Reduction Program, USA) Provisions. NEHRP Provisions describes; at first to define the site class based on V_{s30}, and secondly to set the amplification factors by the selected site class, as shown in Table 4.14.

Table 4.14: Definition of site class based on Vs30 — according to NEHRP (National Earthquake Hazard Reduction Program, USA) provisions.

Site Class	Site class description	Shear wave velocity (m/sec)	
		Minimum	**Maximum**
A	**HARD ROCK** Eastern United States only	1500	
B	**ROCK**	760	1500
C	**VERY DENSE SOIL AND SOFT ROCK** Unstrained shear strength u_s> 2000psf ($u_s \geq$ 100kPa) or N ≥ 50 blows/ft	360	760
D	**STIFF SOILS** Stiff soil with undrained shear strength 1000psf ≤ u_s ≤ 2000psf (50KPa < u_s< 100KPa) or 15 ≤ N ≤ 50 blows/ft	180	360
E	**SOFT SOILS** Profile with more than 10 ft (3m) of soft clay defined as soil with plasticity index Pl > 20, moisture content w > 40% and undrained shear strength u_s< 1000psf (50kpa) (N ≤ 15 blows/ft)	>100	180
F	**SOILS REQUIRING SITE SPECIFIC EVALUATIONS** **1. Soils vulnerable potential failures or collapse under seismic loading:** e.g., liquefiable soils, quick and highly sensitive clays, collapse weakly connected soils. **2. Peats and/or highly organic clays:**		100

	(10ft (3m) or thicker layer) **3. Very high plasticity clays:** (25ft (8m) or thicker layer with plasticity index > 75) **4. Very thick soft/medium stiff clays:** (120ft (36m) or thicker layer)		

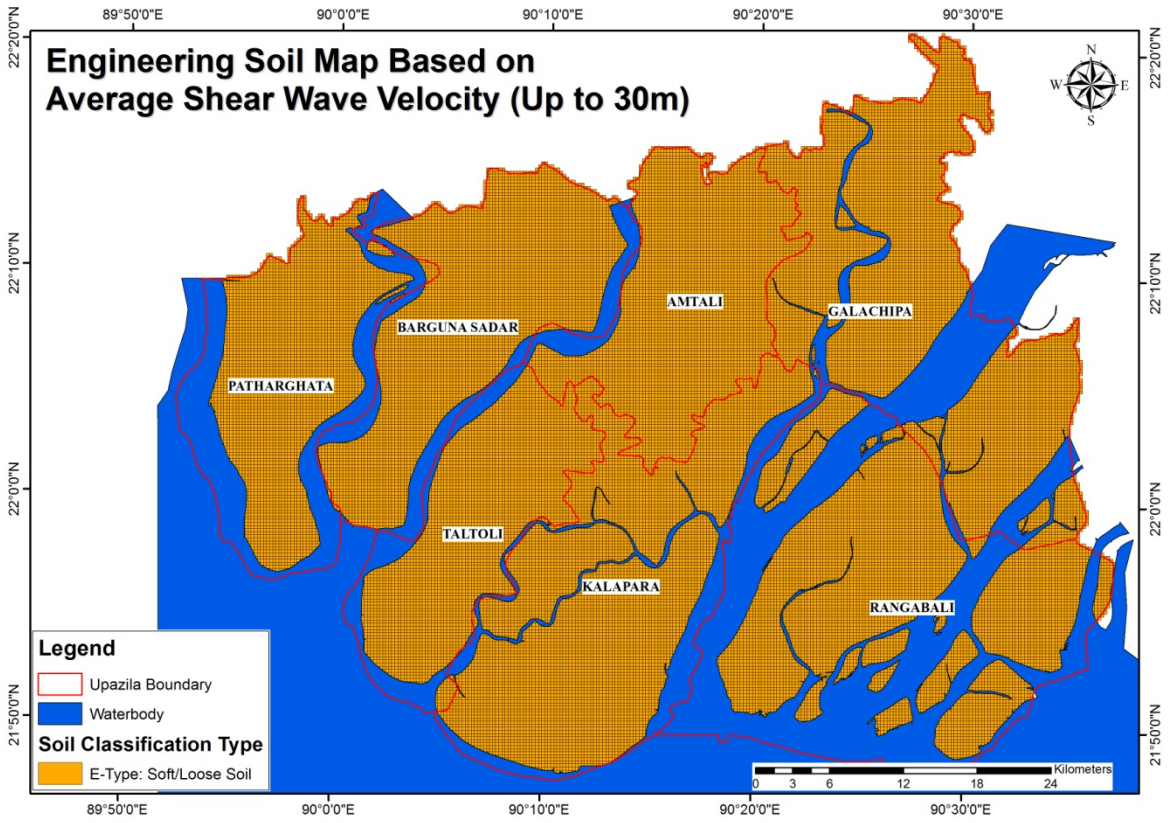

Figure 4.27 Soil classification map of Study Area according to NEHRP (stands for National Earthquake Hazard Reduction Program, USA) provisions based on the average shear wave velocity distribution down to 30 m

Velocity range of the soils of the project area is 110 to 180 m/s i.e., they belongs to the class E according to the provision. That means the soils within the area are soft/loose. Figure 4.27 shows the engineering soil condition of the project area based average shear wave velocity (AVs30).

4.4. Building Height Map

Ground Motion Parameters at Ground Surface

Peak ground acceleration (PGA) is equal to the maximum ground acceleration that occurred during earthquake shaking at a location. PGA is equal to the amplitude of the largest absolute acceleration recorded on an acclerogram at a site during a particular earthquake and Peak Spectral Acceleration (PSA) for 0.3 Sec and 1 sec were measured to identify comparative suitable land for low and high rise building respectively. Suitable land can be identified using following equation.

F = ma……. (4.4)

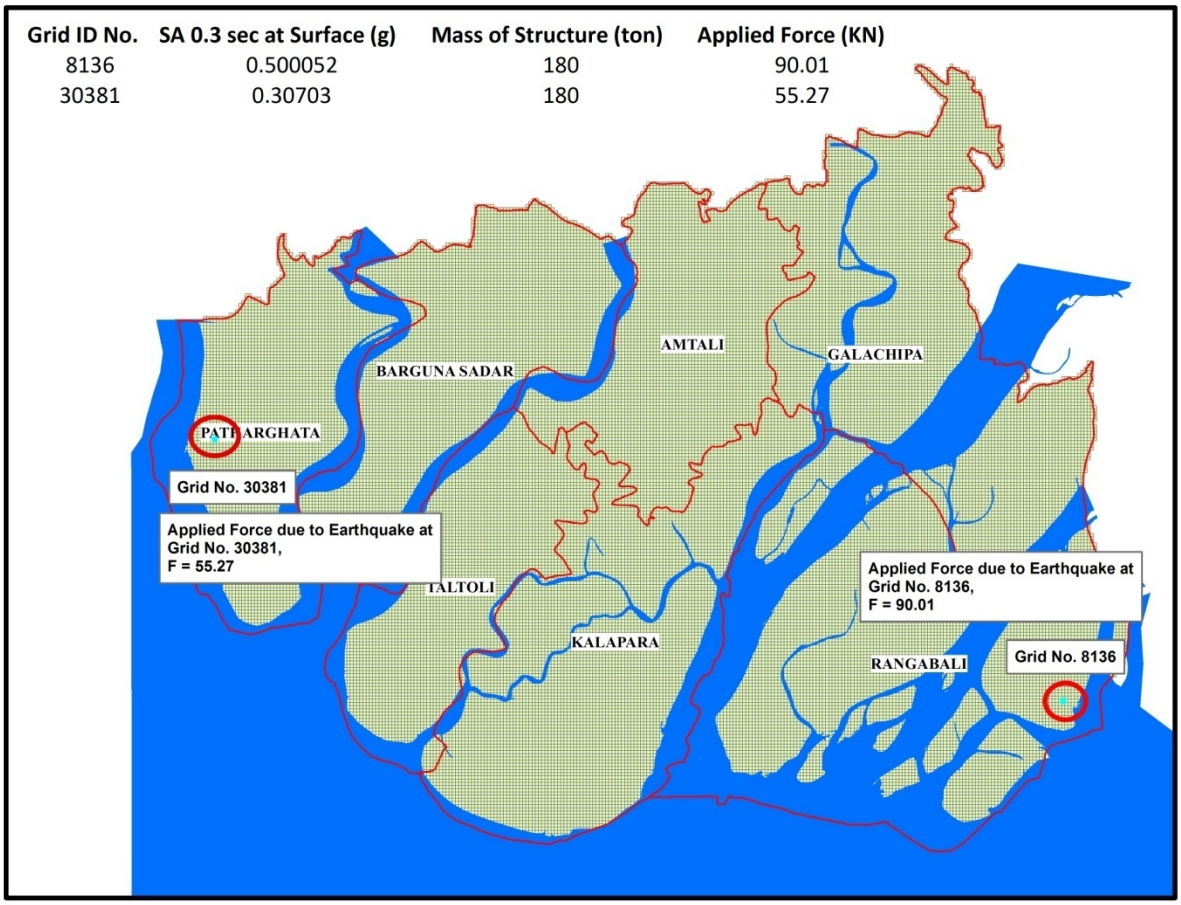

Figure 4.28 Example showing importance of land suitability microzoning in response of earthquake

Here, F is the applied force due to measure earthquake intensity from PGA or PSA value in a grid; m is the mass of the structure and a is Peak Spectral Acceleration. For example three storied building with a mass(m) of 180 ton will be constructed within the area and primarily

two possible location, Grid no. 8136 at Rangabali upazila with a PSA 0.3 sec value of 0.500052g and at grid no. 30381 of Patharghata upazila with a PSA 0.3 sec value of 0.30703g (Figure 4.28) has been selected for this building. The building will be constructed one of these two location based of their ground strength in response of earthquake.

Hence the figure shows that the applied force at grid no. 8136 is 90.01kN which is 34.74kN more than the applied force of 55.27kN at grid no. 30381. The applied force value of two grid suggest that, if earthquake occurs in this area, than grid no. 30381 will experience 34.74kN less load than at grid no. 8136. Finally we can conclude that grid no.30381 is more suitable for three storied building construction comparison to grid no. 8136. Same way we can use SA 1.0sec value for identifying a suitable area for high rise building.

From the amplification analysis, PGA, SA 0.3s and SA 1.0s at ground surface calculation maps the study area were prepared (Figure 4.29, 4.30 and 4.31).

PGA at Ground surface

The PGA value of the project area ranges from 0.16730 to 0.23859g (Figure 4.29). Purple coloured areas of Patharghata, Barguna Sadar, Taltoli, Amtoli & Kalapara Upazila has Low PGA value indicating relatively 3rd degree sensitive for earthquake. The PGA value of the area ranges from 0.1673 to 0.1911g. Light brown colour areas of Barguna Sadar, Amtali, Taltoli, Kalapara, Galachipa and Rangabali upazila has PGA value in between 0.19111 to 0.21482 and are relatively 2nd degree earthquake sensitive zone. The rest of the areas of Galachipa and Rangabali upazila represents with green colour and are comprises 1st degree earthquake sensitive zone having PGA value ranging from 0.21483 to 0.23859g.

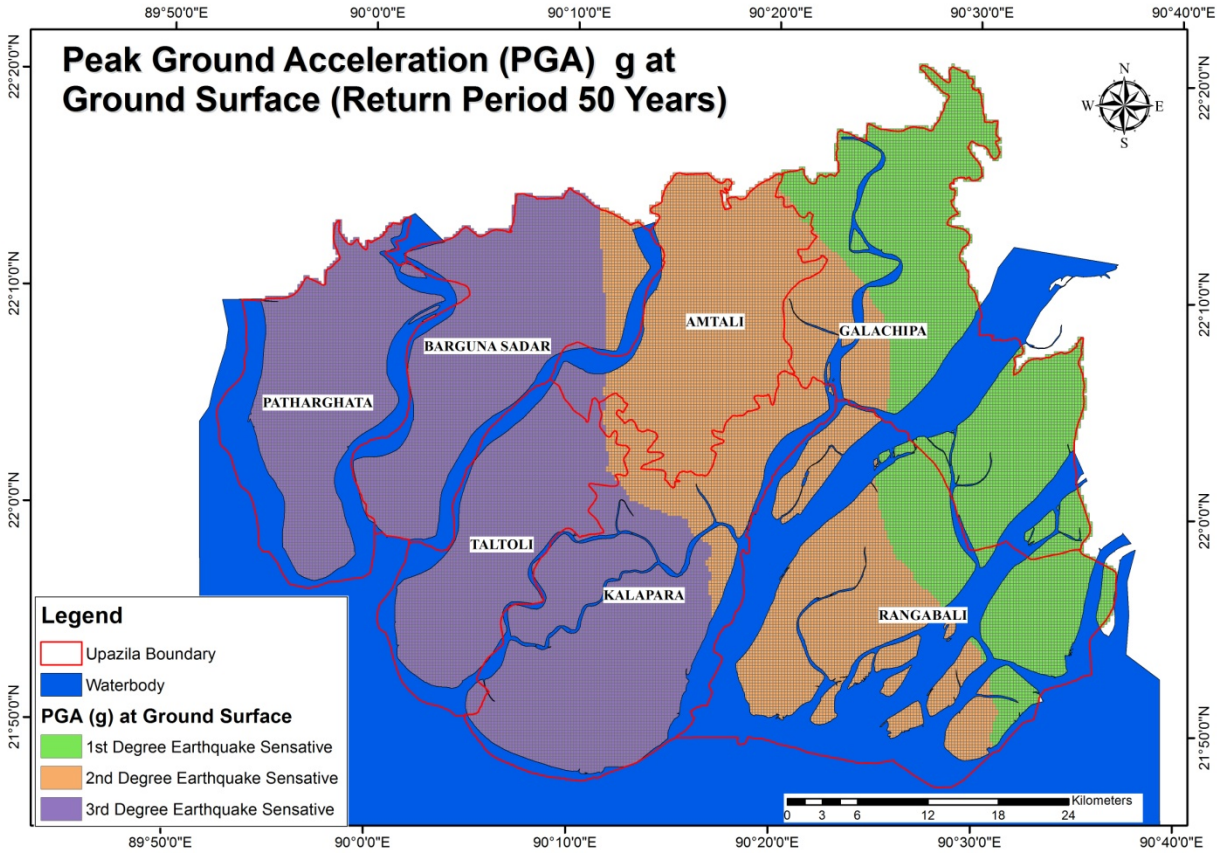

Figure 4.29 Distribution of PGA acceleration of ground surface at Study Area

SA 0.3s at Ground Surface

In figure 30 of Spectral Acceleration for 0.3 Sec structural period of the project area shows that the SA value (for 0.3 sec period) of the area increases from west to east. Spectral acceleration g for 0.3 sec structural period suggest that Cyan colour area of Patharghata, Barguna Sadar, Taltoli, Kalapara and Amtoli upazila is relatively 3rd degree sensitive for low rise buildings and have SA (0.3 sec) g value ranging from 0.297665 to 0.382515g. Barguna Sadar, Taltoli, Kalapara, Amtoli, Galachipa and Rangabali upazila is relatively 2nd degree sensitive for low rise buildings and SA for 0.3 sec ranging from 0.382516 to 0.467364g, which represents by yellow colour. Rest of the area of Galachipa and Rangabali are represented by red colour and relatively 1st degree sensitive for low rise buildings and also SA 0.3 sec value ranges from 0.467365 to 0.552214g.

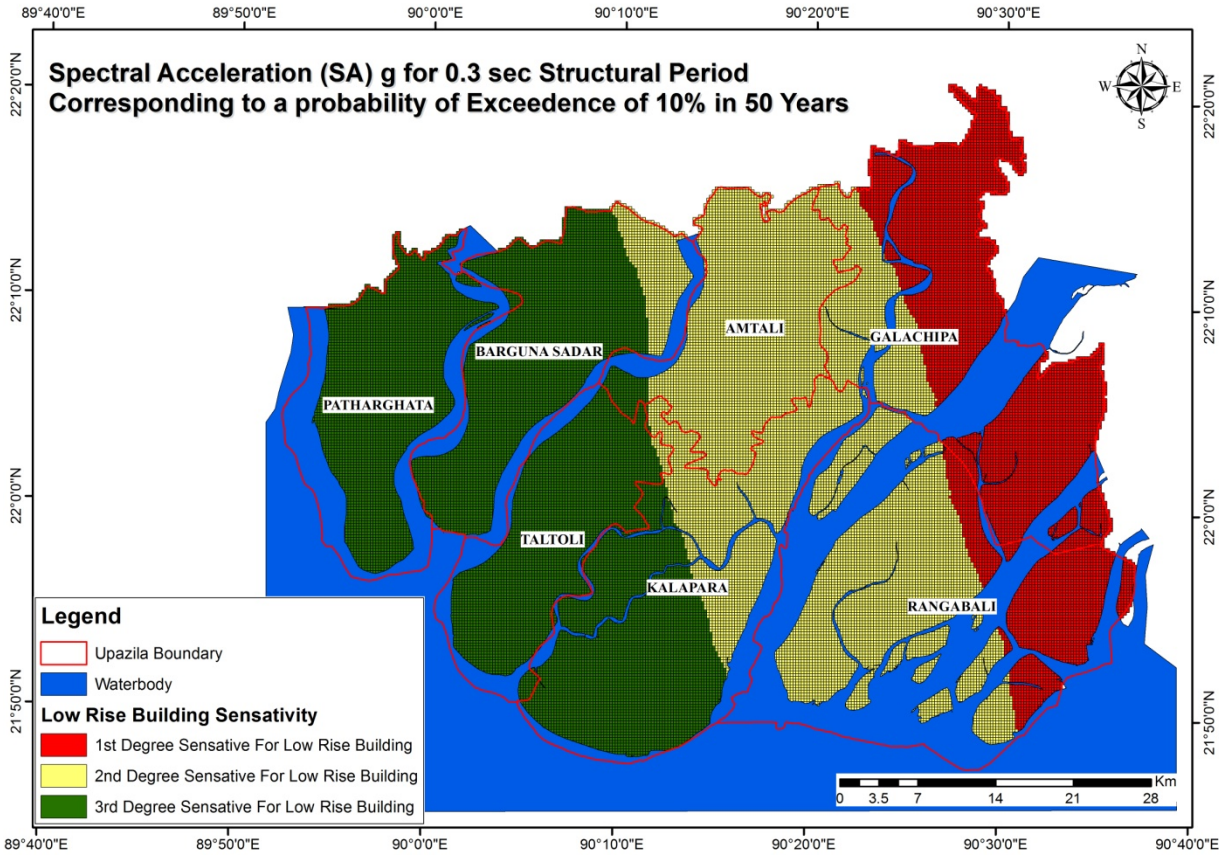

Figure 4.30 Represents calculated distribution of spectral acceleration (SA) for short period (0.3s) of ground surface at Study Area

SA 1.0 sec at Ground Surface

The SA value (for 1.0s period) is used to identify the earthquake sensitive zone for high rise buildings. Here in the study area, the SA value (for 1.0s period) ranges from 0.158551 to 0.290725g. The green colour area of Patharghata, Barguna Sadar, Taltoli, Kalapara and Amtoli upazila having relatively Low SA value for 1 sec and are ringing from 0.158551 to 0.202606g as shown in figure 4.31 suggesting that the area is relatively 3rd degree earthquake sensitive for high rise buildings. From the figure it can be also observed that the orange colour areas of Galachipa and Rangabali upazila have high SA value for 1 sec (0.246671 to 0.290725g) suggest that the area is relatively 1st degree earthquake sensitive for high rise buildings. The olive colour area with SA value of 0.202607 to 0.246670g suggest that the area is relatively 2nd degree earthquake sensitive for high rise buildings

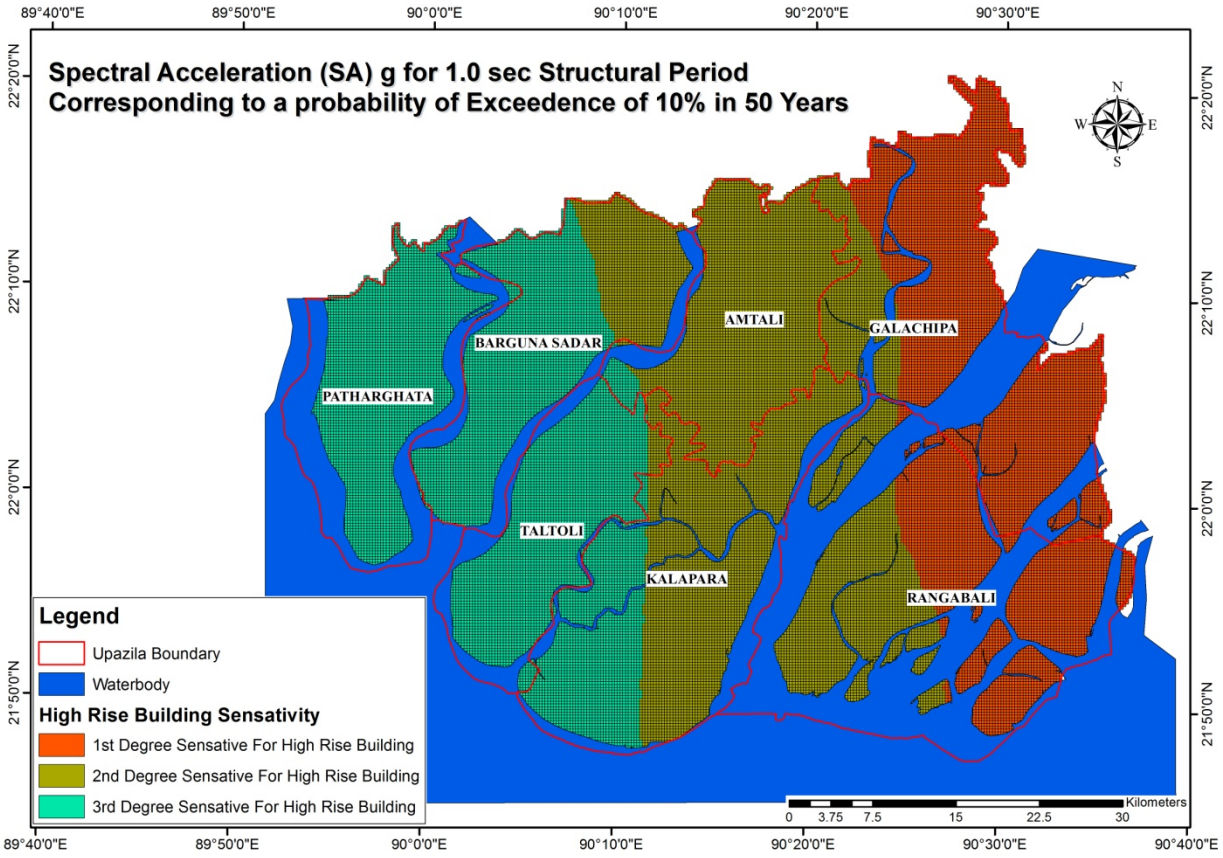

Figure 4.31 Soil cIllustrates calculated distribution of spectral acceleration (SA) — for long period (1.0s) — of ground surface at Study Area

Peak spectral acceleration (PSA) is an important tool for determining the building height of an area. Here PSA for 1.0 and 0.3 sec is used for identifying the appropriate location for high rise and low rise building respectively. A building height map is produced for the study area using PSA (Figure 4.32), which represent low rise building and high rise building. Low rise indicate 3 stories building and high rise represents 10 stories building (Ishiyama y. 2011).

Building Height

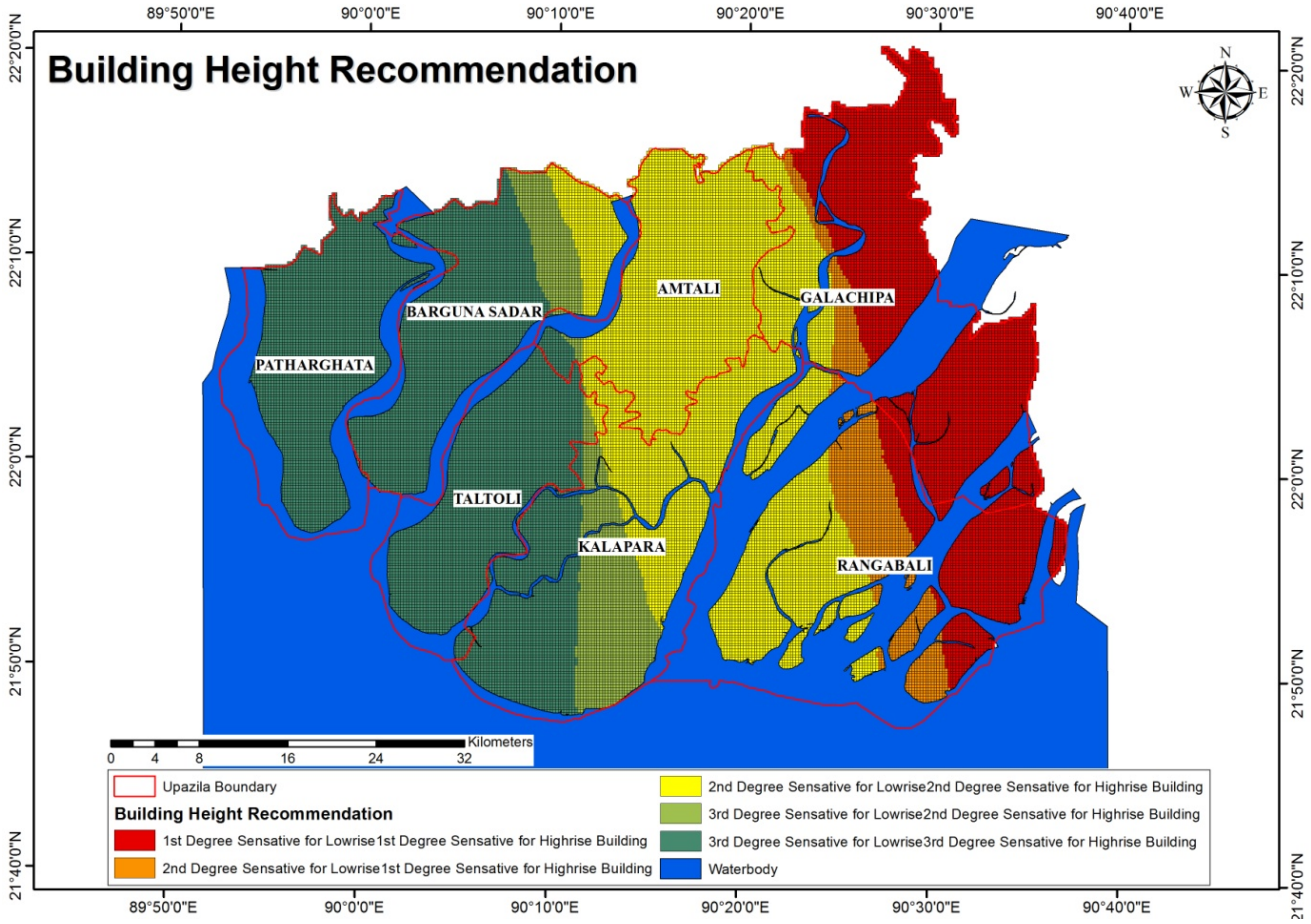

Figure 4.32 Building Height Map of Study Area

From the map it can be observed that the dark green coloured areas of Patharghata, Barguna Sadar, Taltoli, Kalapara and Amtali upazilas area relatively 3rd degree risk sensitive zones for low rise building and 3rd degree risk sensitive for high rise buildings. The map also shows that the yellowish green coloured areas of Barguna Sadar, Taltoli, Kalapara and Amtali upazilas are relatively 3rd degree risk sensitive for low rise buildings but 2nd degree risk sensitive for high rise buildings. The yellowish coloured zones of Barguna Sadar, Galachipa, Rangabali, Taltoli, Kalapara and Amtali upazila are relatively 2nd degree risk sensitive for low rise buildings and 2nd degree risk for high rise buildings. The orange coloured zones of Galachipa and Rangabali upazila are relatively 2nd degree risk sensitive for low rise buildings but 1st degree risk for high rise buildings. Rest of the study area with red colour is relatively 1st degree risk sensitive for low rise buildings and 1st degree risk sensitive for high rise buildings.

Moreover, Uniform Hazard Spectra (UHS) for the Payra-Kuakata are also plotted in Fig 4.33 for 10% and 2% probabilities of exceedance. The SA is seen to peak around periods 0.2s and 0.4s and then gradually decreasing till up to period of 2 seconds.

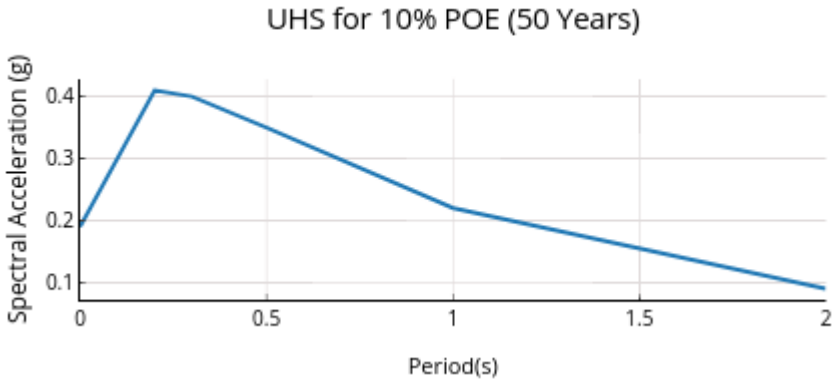

(a)

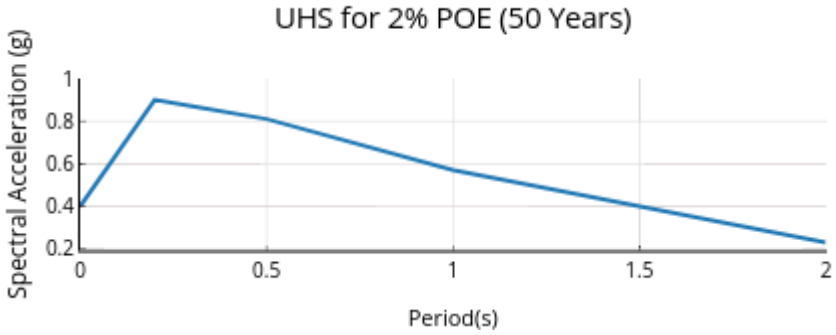

(b)

Figure 4.33 Uniform Hazard Spectra for Kuakata for (a) 10% and (b) 2% probabilities of exceedance

In addition, Peak period distribution map has been prepared from single Microtremor test. This map shows most of the area covered by 0.5 to 0.7s peak period (Figure 4.34), which indicates that 5 to 7 storey building will be affected by earthquake. On the other hand, 44 nos single Microtremor test have been conducted, where 18 points contain more than 0.6s peak period. Then 11 and 8 points have more than 0.5 and 0.7s peak period respectively (Figure 4.35).

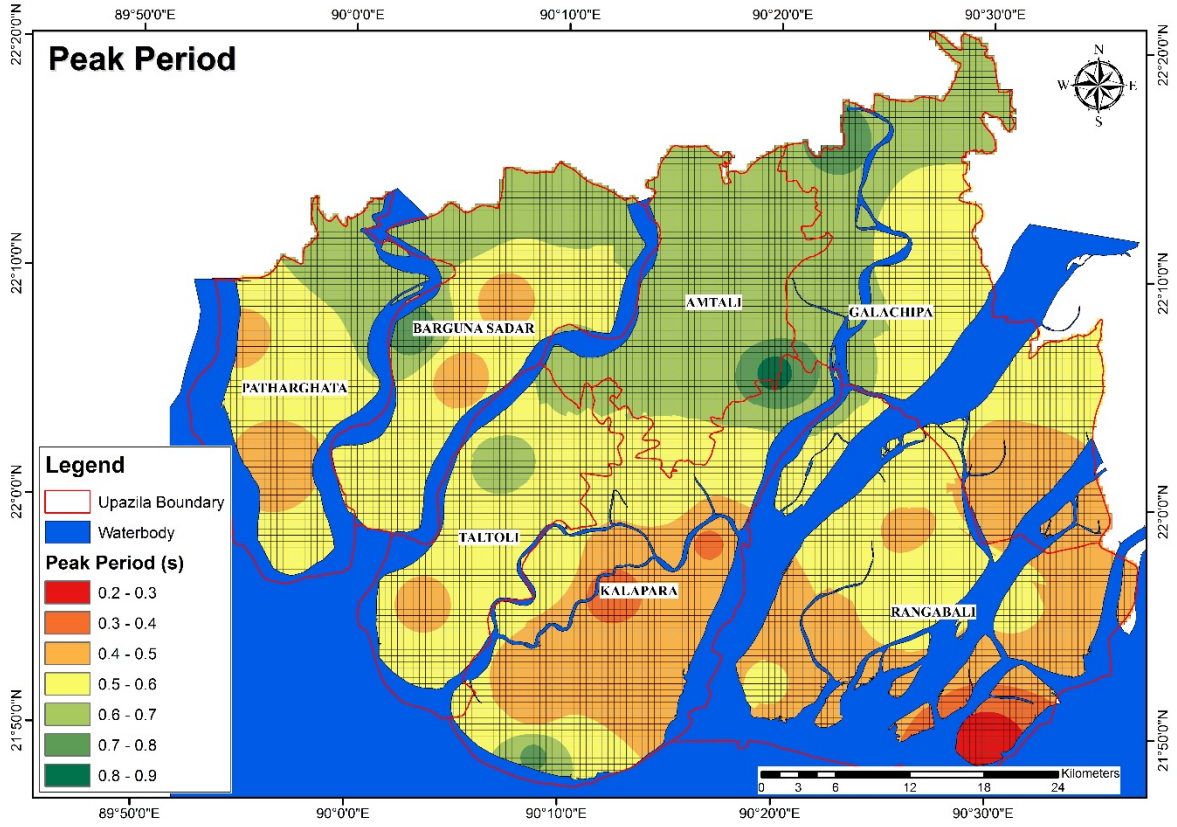

Figure 4.34 Peak Period distribution map of the project area

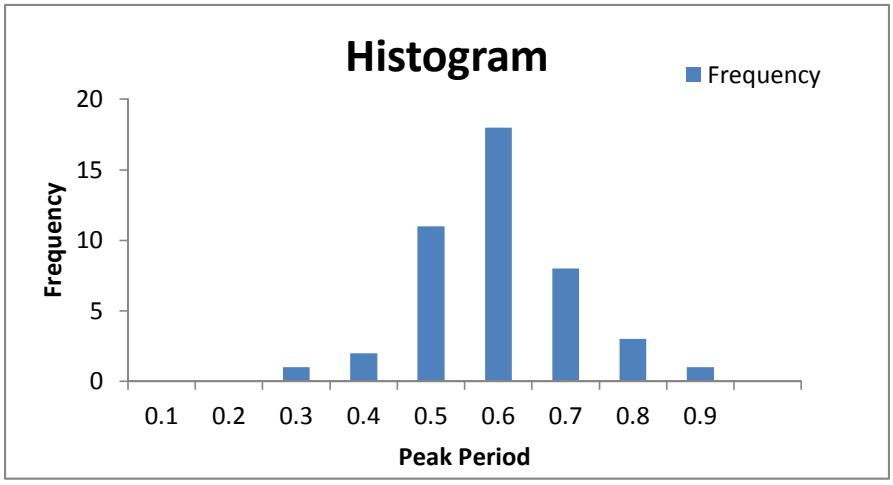

Figure 4.35 Peak Period data frequency of the project area

According to Uniform Hazard Spectra (for 10% probabilities) SA value is more than 0.3 g for 0.2s to 0.7s which indicates that 2 to 7 storey building will be affected by earthquake (Figure 4.33). Whereas peak period data indicates 5 to 7 storey building will be affected by earthquake (Figure 4.34). To reduce the damage, Spectral acceleration (SA) value should be considered for building and/or infrastructure development. And national building code should be considered as well.

5. LIQUEFACTION POTENTIAL INDEX (LPI) ASSESSMENT

The liquefaction phenomenon provides an unsupportive environment of built structures by altering previously solid ground into a liquefied softened condition (Palacios et al., 2012). Due to exposing structures to hazardous ground failure, soil liquefaction has become major concern for civil engineers for over forty years (Sadek et al., 2014). Apart from ground deformation like sand boils and lateral movement, soil liquefaction can also render structural damages like settlement and failure of bearing capacity of civil structures (Papathanassiou et al., 2006). Notably, these damages increase during earthquakes (Rahman et al., 2015). The Alaska and Japan earthquakes of 1964 triggered rigorous studies on the phenomenon of liquefaction among geotechnical engineers; in which included were field evaluations of major earthquakes and laboratory studies applying cyclic loading devices (Coduto et al., 2010).

Rather than occurring randomly, the liquefaction phenomenon abides by some geological and hydrological conditions of subterranean soil deposits (Youd, 1973). Generally, potentially liquefiable areas are within 15 to 20 m of the ground surface, where soils there are dominantly cohesion less and granular, and simultaneously saturated by water. Another factor instrumental for this phenomenon to take place is the magnitude of ground shaking, which needs to be substantially strong for liquefying susceptible soils. Preferably, moderate to great earthquakes effectively trigger liquefaction, which commonly induce ground failure and deformation (Palacios et al., 2012).

Soil's resistance to liquefaction gives the measurement of liquefaction potential. Liquefaction susceptibility range from not susceptible to highly susceptible, implying no effect of seismic energy and high enough effect of even very little seismic energy for liquefaction initiation, respectively (Palacios et al., 2012). However, so far, rapid and significant progresses have been achieved in measuring liquefaction susceptibility (Seed et al., 2003). Vulnerability to earthquake induced soil liquefaction of an area is generally calibrated following Simplified Procedure of Seed and Idriss (1971) on the basis of standard penetration test (SPT) blow counts (Maugeri and Monaco, 2006; Papathanassiou et al., 2006; Heidari, 2011). The original simplified method is now more updated due to a number of researchers' further tuning by modifications, improvements, calibration, and validation (Youd et al., 2001; Juang et al., 2003; Cetin et al., 2004; Lee et al., 2004; Sonmez and Gokceoglu, 2005; Sawicki andMierczyński, 2006; Groot et al., 2006; Sawicki and Swidzinski, 2007; Cox et al., 2007; Papathanassiou et al., 2006; Papathanassiou, 2008; Holzer, 2008;Jha and Suzuki, 2009; Heidariand Andrus, 2010; Noutash et al., 2012; Tan et al., 2013; Kang et al., 2014; Boulanger and Idriss, 2014; Sadek et

al., 2014; Palacios et al., 2014; Rahman et al., 2015; Sawicki and Sławińska, 2015). This empirical procedure aids researchers while estimating factor of safety, FL, against liquefaction, where value of FL>1 designates a soil layer as non-potential to liquefaction while value of FL<1 is indicate a layer as potential for liquefaction initiation (Papathanassiou et al., 2006). But, this method cannot estimate the surface effect of liquefaction induced ground failure other than determining soil's aptitude during cyclic seismic loading. In order to overcome this limitation, Iwasaki et al. (1982) introduced liquefaction potential index (LPI), where FL acts as a function while computation.

The geological location of Bangladesh, i.e. it's stand on the northeastern margin of the Indian plate, where there surrounding some major faults like the Indian-Burman plate boundary fault, the Dauki fault, etc., and a number of active faults within the Chittagong-Tripura Fold Belt (CTFB) (Morino et al., 2013), along with the soil condition impose specter of impending destructive earthquakes around Bangladesh (Bilham and England, 2001; Ambraseys and Bilham, 2003; Bilham and Wallace, 2005; Steckler etal., 2008; Rahman et al., 2015; Rahman et al., 2017; Farazi et al., 2018). In addition, the easily accessible historical record (likely, Banglapedia, http://banglapedia.search.com.bd/HT/E_0002.htm) of earthquakes further supports the anticipation (Steckler et al., 2008; Rahman et al., 2015). Moreover, according to Comprehensive Disaster Management Program (CDMP) 2009 report and Rahman et al. 2015, earthquake of moderate to large magnitude is possible in this region as a result of continuing tectonic distortion along the active plate-boundary faults. Albeit, a compact scenario of earthquake risk, it's impacts, and related strategies, policies, and action plans for provision, response and mitigation are still not fully formulated (Bangladesh Urban Earthquake Resilience Project report, 2014).

Payra -Kuakata Comprehensive Eco-tourism project has an aim to prepare a Disaster Risk sensitive land use planning for the upazila's under this project as the region is near to Sundarbans, Sea beach and there lies our one of the important and Largest port. As the region lies on recent or Holocene deposit but there are some subsurface anticline and also close to plate boundary or mega thrust fault. Although the surface geology says that the region has low liquefaction probability but this surface layer is very thin and the region is lies in an unstable sediment deposition. And the PGA value found is also moderate says that it liquefaction can occur if there a huge or 7.5 magnitude earthquake occur near the region. Notably, so far there is no such study on earthquake triggered liquefaction hazard potential evaluation of the geological materials in this region. From these perspectives, this study attempts to prepare an

earthquake induced liquefaction susceptibility map of the said area, of which the main objective is to determine the liquefaction potential of the area. To attain this goal, we followed Simplified Procedure of Seed and Idris (1971) to figure out liquefaction potential index (LPI) of the subterranean geological materials. Further, we prepared a liquefaction susceptibility map, representing the zone wise degree of hazard, and cumulative frequency distribution (CFD) of LPI of subterranean geological matters. So far in this town, there is no record of identification of the liquefaction phenomenon.

5.1. Methodology

Use of the standard penetration test (SPT) yielded N value soil resistance for a designed earthquake triggered liquefaction severity evaluation of soil up to 20 m of the subsurface is ubiquitous worldwide (Seed and Idriss, 1971; Seed et al., 1985, 2001, 2003;Youd et al., 2001;Sonmez, 2003; Cetin et al., 2004; Sonmez and Gokceoglu, 2005; Maugeri and Monaco, 2006; Papathanassiou et al., 2006;Sonmez et al., 2008;Idriss and Boulanger, 2010; Boulanger and Idriss, 2012, 2014; Sadek et al., 2014; Rahman et al., 2015). As per assessment of susceptibility to liquefaction of the seven Upazila's of Payra-Kuakata Eco tourism Project, here we followed the Simplified Procedure. Furthermore, SPT N values and other required engineering parameters of 100 boreholes at various sites of the area were considered to serve the purpose. Later on were calculated the liquefaction potential index (LPI) of each SPT profile to engender a hazard map, presenting liquefaction potential, for the study area.

For this study, 100 boreholes, alongside SPT, up to 20m depth were completed at various sites of the study area. The data of the subterranean geological materials from these boreholes were used for LPI estimation. Decision on boring sites has been made following the subterranean geological units of the area. The locations of the boreholes are manifested in the surface geological map of the study area (Fig. 3.1). Among them, 83 boreholes were in the Tidal Deltaic Deposits, 15 in Tidal Mud Deposits, and 2 in Marshy Clay & Peat deposit but no borehole investigation could be conducted in Mangrove Swamp deposit area. Information regarding the boreholes, with their respective LPI values, has been provided as thumbnail in the following table 5.1.

Table 5.1: Calculated liquefaction potential index (LPI) of every SPT profile for a scenario seismic event of M_W = 7.5 and PGA of 0.167 to 0.239g.

Bore hole No	Coordinates		Ground Water Table(m)	Liquefaction Potential Index (LPI)	Surface Geologic Unit
	Latitude (N)	Longitude (E)		PGA 0.167 to 0.239g	
BH-01	21.822277	90.122042	1.33	21.85	Tidal Deltaic Deposit
BH-02	21.847410	90.219710	0.67	42.76	Tidal Deltaic Deposit
BH-03	21.896795	90.040669	1.67	25.95	Tidal Deltaic Deposit
BH-04	21.854020	90.123620	1.33	11.26	Tidal Deltaic Deposit
BH-05	21.878603	90.133850	1.33	29.12	Tidal Deltaic Deposit
BH-06	21.847390	90.184280	1	27.17	Tidal Deltaic Deposit
BH-07	21.900240	90.235110	0.67	20.86	Tidal Deltaic Deposit
BH-08	21.911389	90.064722	0.67	36.54	Tidal Deltaic Deposit
BH-09	21.943614	90.099477	3	7.06	Tidal Deltaic Deposit
BH-10	21.911690	90.144440	1	26.70	Tidal Deltaic Deposit
BH-11	21.892820	90.189570	1.33	26.98	Tidal Deltaic Deposit
BH-12	21.928450	90.243640	0.67	35.64	Tidal Deltaic Deposit
BH-13	21.897865	90.324560	1.5	16.55	Tidal Mud
BH-14	21.908114	90.405833	1.67	38.29	Tidal Mud
BH-15	21.850446	90.490652	1.5	32.69	Tidal Mud
BH-16	21.932089	90.066250	1	24.09	Tidal Deltaic Deposit
BH-17	21.984460	90.083894	0.33	17.74	Tidal Deltaic Deposit
BH-18	21.933220	90.163820	1.33	12.86	Tidal Deltaic Deposit
BH-19	21.953080	90.183010	1.33	16.88	Tidal Deltaic Deposit

BH-20	21.985030	90.220150	0.67	15.66	Tidal Deltaic Deposit
BH-21	21.960680	90.451320	1	44.27	Tidal Mud
BH-22	21.944397	90.412697	1	34.89	Tidal Mud
BH-23	21.974417	90.435536	1	36.09	Tidal Mud
BH-24	21.901461	90.523381	2	35.34	Tidal Mud
BH-25	21.993467	89.964499	2	0.00	Tidal Deltaic Deposit
BH-26	22.019223	89.998116	0.67	12.00	Tidal Deltaic Deposit
BH-27	22.003005	90.050841	0.33	0.00	Tidal Deltaic Deposit
BH-28	22.035618	90.099704	0.67	1.18	Tidal Deltaic Deposit
BH-29	22.025846	90.164284	0.33	0.00	Tidal Deltaic Deposit
BH-30	21.984438	90.139164	0.33	29.88	Tidal Deltaic Deposit
BH-31	21.969520	90.250604	1.67	0.01	Tidal Deltaic Deposit
BH-32	22.058730	90.319880	1	26.49	Tidal Deltaic Deposit
BH-33	21.967460	90.362603	0.67	23.05	Tidal Mud
BH-34	22.025535	90.418347	1	10.25	Tidal Mud
BH-35	21.969547	90.576594	1.33	36.87	Tidal Mud
BH-36	22.042219	89.971430	0.67	4.79	Tidal Deltaic Deposit
BH-37	22.035766	90.025007	1	2.69	Tidal Deltaic Deposit
BH-38	22.044112	90.051524	1.67	5.98	Tidal Deltaic Deposit
BH-39	22.058749	90.114047	0.33	28.71	Tidal Deltaic Deposit
BH-40	22.046608	90.144795	0.67	12.77	Tidal Deltaic Deposit
BH-41	21.953924	90.071331	0.33	29.52	Tidal Deltaic Deposit

BH-42	22.045890	90.250250	1.33	1.84	Tidal Deltaic Deposit
BH-43	22.083448	90.259355	1	30.03	Tidal Deltaic Deposit
BH-44	22.012220	90.460230	0.67	35.33	Tidal Mud
BH-45	22.000280	90.430060	0.67	16.18	Tidal Mud
BH-46	22.067503	89.927283	1.33	10.97	Tidal Deltaic Deposit
BH-47	22.067929	89.984847	0.67	15.35	Tidal Deltaic Deposit
BH-48	22.106045	89.996869	1.33	7.18	Tidal Deltaic Deposit
BH-49	22.097637	90.061310	0.33	7.81	Tidal Deltaic Deposit
BH-50	22.083612	90.071353	2	0.32	Tidal Deltaic Deposit
BH-51	22.088656	90.146443	0.67	31.26	Tidal Deltaic Deposit
BH-52	22.059275	90.186166	0.67	0.00	Tidal Deltaic Deposit
BH-53	22.133484	90.230084	0.33	5.94	Tidal Deltaic Deposit
BH-54	22.108494	90.293883	0.33	11.83	Tidal Deltaic Deposit
BH-55	22.132797	90.319892	1.67	26.72	Tidal Deltaic Deposit
BH-56	22.022000	90.365601	1.33	21.29	Tidal Mud
BH-57	22.039678	90.526369	1.67	40.18	Tidal Mud
BH-58	22.078819	90.518992	1	21.94	Tidal Mud
BH-59	22.119288	89.929288	0.33	5.75	Tidal Deltaic Deposit
BH-60	22.150878	89.947985	1	1.17	Tidal Deltaic Deposit
BH-61	22.177767	90.015177	1.33	7.22	Tidal Deltaic Deposit
BH-62	22.132510	90.076761	1.33	4.96	Tidal Deltaic Deposit
BH-63	22.122942	90.096608	1.33	4.94	Tidal Deltaic Deposit

BH-64	22.157271	90.087346	2.5	11.99	Tidal Deltaic Deposit
BH-65	22.153119	90.199123	0.33	28.26	Tidal Deltaic Deposit
BH-66	22.141493	90.233098	1.33	11.21	Tidal Deltaic Deposit
BH-67	22.155550	90.294022	1.5	14.38	Tidal Deltaic Deposit
BH-68	22.126798	90.397147	0.67	43.65	Tidal Deltaic Deposit
BH-69	22.082895	90.428391	1.67	20.13	Tidal Deltaic Deposit
BH-70	22.167904	90.424019	0.33	32.96	Tidal Deltaic Deposit
BH-71	22.195257	89.968453	1.33	17.56	Tidal Deltaic Deposit
BH-72	22.157138	90.047608	1.33	10.06	Tidal Deltaic Deposit
BH-73	22.196093	90.119071	1.33	15.03	Tidal Deltaic Deposit
BH-74	22.155764	90.122003	1.67	12.53	Tidal Deltaic Deposit
BH-75	22.191372	90.179425	1.67	12.60	Tidal Deltaic Deposit
BH-76	22.174278	90.256693	1.67	0.00	Tidal Deltaic Deposit
BH-77	22.199496	90.282488	0.67	32.31	Tidal Deltaic Deposit
BH-78	22.179485	90.324827	1	13.77	Tidal Deltaic Deposit
BH-79	22.181953	90.391907	1.33	44.01	Tidal Deltaic Deposit
BH-80	22.168115	90.408955	0.33	33.81	Tidal Deltaic Deposit
BH-81	22.192693	90.481211	1.67	40.56	Tidal Deltaic Deposit
BH-82	22.225376	90.129198	1	15.64	Tidal Deltaic Deposit
BH-83	22.216233	90.275309	1.5	0.00	Tidal Deltaic Deposit
BH-84	22.229500	90.307035	1	27.40	Tidal Deltaic Deposit
BH-85	22.247763	90.322332	1.33	25.84	Tidal Deltaic Deposit

BH-86	22.250839	90.384350	0.67	19.37	Tidal Deltaic Deposit
BH-87	22.225610	90.456290	1	34.31	Tidal Deltaic Deposit
BH-88	22.197535	90.438764	0.33	28.57	Tidal Deltaic Deposit
BH-89	22.255466	90.445988	0.5	28.54	Marshy Clay & Peat
BH-90	22.292854	90.430606	0.67	11.77	Marshy Clay & Peat

Borehole No	Coordinates		Ground Water Table (m)	Liquefaction Potential Index (LPI)	Surface Geologic Unit
	Latitude (N)	Longitude (E)			
BH-91	21.812062	90.210988	1.52	29.68	Tidal Deltaic Deposit
BH-92	21.928189	90.267361	1.52	24.33	Tidal Deltaic Deposit
BH-93	21.95257	90.230187	1.37	17.05	Tidal Deltaic Deposit
BH-94	21.966536	90.290073	1.07	16.46	Tidal Deltaic Deposit
BH-95	21.971627	90.182075	1.22	16.38	Tidal Deltaic Deposit
BH-96	21.994316	90.275292	1.52	11.71	Tidal Deltaic Deposit
BH-97	22.004768	90.233541	1.22	12.47	Tidal Deltaic Deposit
BH-98	22.03246	90.281358	1.37	13.51	Tidal Deltaic Deposit
BH-99	22.07797	90.367705	1.83	24.99	Tidal Deltaic Deposit
BH-100	22.139093	90.375344	1.68	34.23	Tidal Deltaic Deposit

In this study, we have considered magnitude 7.5 (M_W) for liquefaction susceptibility estimation. Additionally, peak horizontal ground acceleration (PGA) for the study area was estimated considering around 400 years of seismicity record of this region. It was found that PGA varies from 0.167g to 0.239g in the whole area.

For more than four decades geotechnical earthquake engineers all over the world have been using in situ tests and deterministic procedure—more popularly known as the Simplified

Procedure of Seed and Idriss (1971) — to predict the likelihood of a soil layer to liquefy under expected seismic stress of a given seismic shaking. By the way, Seed and Idriss (1982), Seed et al. (1985), etc. brought more modification and improvement to this shining original method of Seed and Idriss (1971) which, furthermore, was analyzed, redacted, and tuned by Seed et al. (2001), Youd et al. (2001), Idriss and Boulanger (2004), etc. However, in this research, we used the updated Simplified Procedure updated by Youd et al. (2001) for assessment of resistance to lquefaction of subsurface soils of the selected area.

In current practice of liquefaction susceptibility evaluation, factor of safety (F_L) against liquefaction is defined considering cyclic stress ratio (CSR), the cyclic resistance ratio (CRR), and a magnitude scaling factor (MSF) (Eq. 1) — was originally proposed by Seed and Idriss (1971) as CRR to CSR ratio.

$$F_L = (CRR7.5/CSR)\ MSF \quad (1)$$

F_L>1 implies a non-liquefiable soil layer whereas FL<1 implies a liquefiable one.

The cyclic stress ratio, being proportional to the peak ground acceleration (amax), implies the cyclic stress generated by a seismic event. The cyclic resistance ratio, in contrary, is the required stress for changing the condition of a soil to eventually turn it into liquefied state, and can be calibrated for Mw = 7.5 seismicity ($CRR_{7.5}$) using standard penetration resistance (N1)60cs of clean sand equivalent. Here, the use of a magnitude scaling factor is in adjusting $CRR_{7.5}$ to calculate CRR for variable earthquake magnitudes. The detailed procedure is documented in Youd et al. (2001).

Factor of safety (FL) lacks efficacy because it has no application other than determining whether a layer is susceptible to liquefaction or not. But the introduction of liquefaction potential index (LPI) by Iwasaki et al. (1978, 1982) brought the opportunity to quantify and categorize the severity of a liquefaction prone layer; also provided a tool for representative liquefaction hazard mapping by geographic information system (GIS) (Holzer et al., 2003; Sonmez and Gokceoglu, 2005). Iwasaki et al. (1978, 1982) introduced thickness and depth of the susceptible layer with FL in LPI calculation. According to them, LPI is proportionally related to:

i. the liquefiable layer's thickness,
ii. distance between the layer and the surface, and
iii. difference of the factor of safety value (when, FL < 1) from 1.0.

They defined the LPI by following equation:

$$L_I = \int_0^{20} \mathbf{F(z)W(z)d(z)} \quad (2)$$

$$F(z) = 1 - F_L \text{ for } F_L<1.0 \quad (3a)$$

$$F(z) = 0 \text{ for } F_L \geq 1.0 \quad (3b)$$

$$W(z) = 10—0.5z \text{ for } z<20 \text{ m} \quad (3c)$$

$$W(z) = 0 \text{ for } z>20 \text{ m} \quad (3d)$$

where z is the distance of the layer from the surface in meters.

Based on the studies of case history data, Iwasaki et al (1982) and Toprak and Holzer (2003) did comparison of LPI values to liquefaction rigorousness. According to Iwasaki et al. (1982), liquefaction would be severe where LPI>15 whereas implausible where LPI<5. Further, Toprak and Holzer (2003) found that liquefaction triggered sand boils and lateral spreading correspond to the values of LPI≥5 and LPI≥12 respectively. In addition, following the values of LPI, Iwasaki et al (1982) classified in four categories based on liquefaction severity. Classification schemes by several other authors, e.g., Luna and Frost (1998), Microzonation for Earthquake Risk Mitigation (MERM, 2003), Sonmez (2003), Sonmez and Gokceoglu (2005), etc., are also available. However, herein, for hazard mapping, we adopted the LPI based liquefaction hazard categories of Iwasaki et al. (1982).

Later, following the calibration of Toprak and Holzer (2003),Holzer et al. (2003), and Holzer et al. (2006) we assumed that surface manifestation of liquefaction would occur if LPI ≥ 5. So, with a view to predicting the percentage area of every unit that might show surface manifestation of earthquake induced liquefaction failure, we regarded the cumulative frequency distribution value of LPI = 5 as threshold value (Holzer et al., 2006) (Fig. 5.1). The liquefaction hazard map (Fig. 5.2) of Payra Kuakata has been prepared combining the LPI values and the aforementioned percentages of each unit area.

5.2. Discussions of Liquefaction Hazard Map

Analyzing SPT blow-count in 100 boreholes, a liquefaction potential index has been produced for the study area. Approximately 60 % borehole has the LPI values more than 15 comes with the idea that this region has high liquefaction potential.

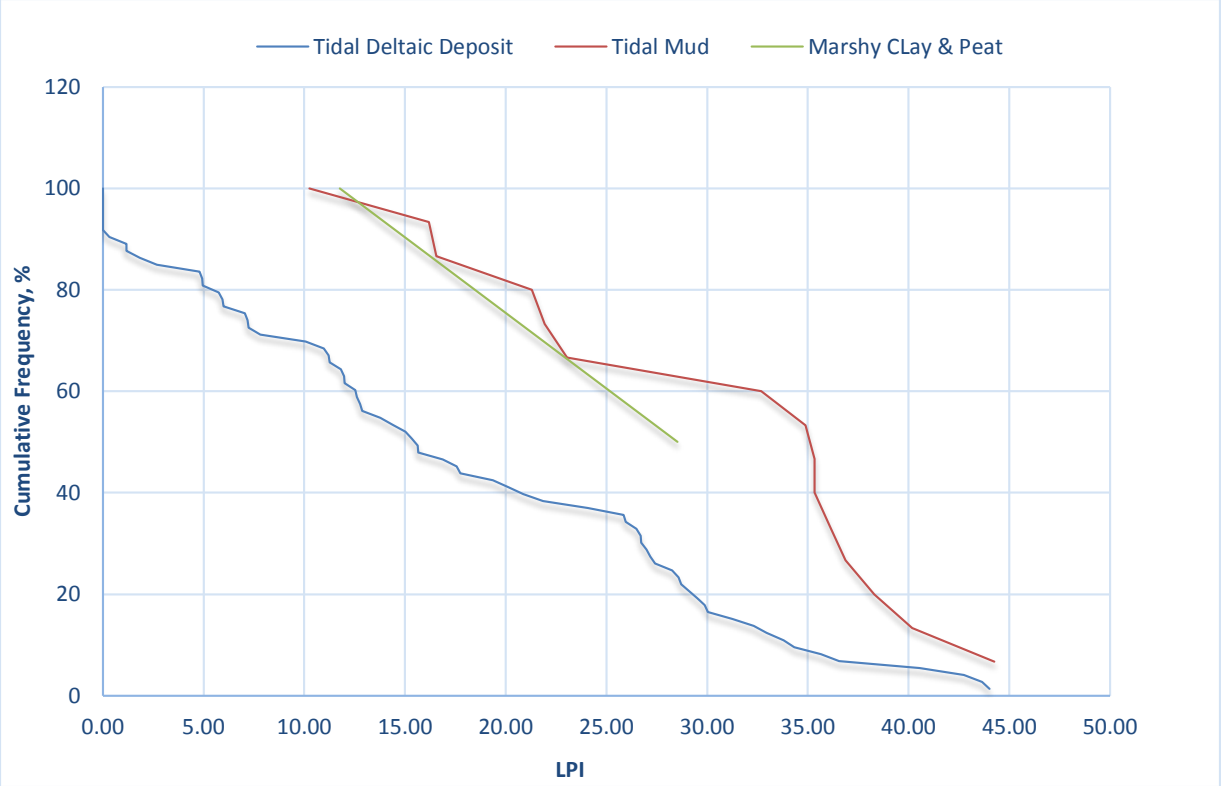

Figure 5.1 Cumulative frequency distributions of LPI for four surface geology units of Payra-Kuakata area

Figure 5.1 and 5.2 shows cumulative frequency distributions of LPI for three surface geology units and liquefaction hazard map of the study area respectively. In addition, the map shows the probable liquefaction prone area. It is produced for 7.5 (M_w) earthquake on the plate boundary faults or any nearest place considering a scenario of peak ground acceleration 0.167 to 0.239g.

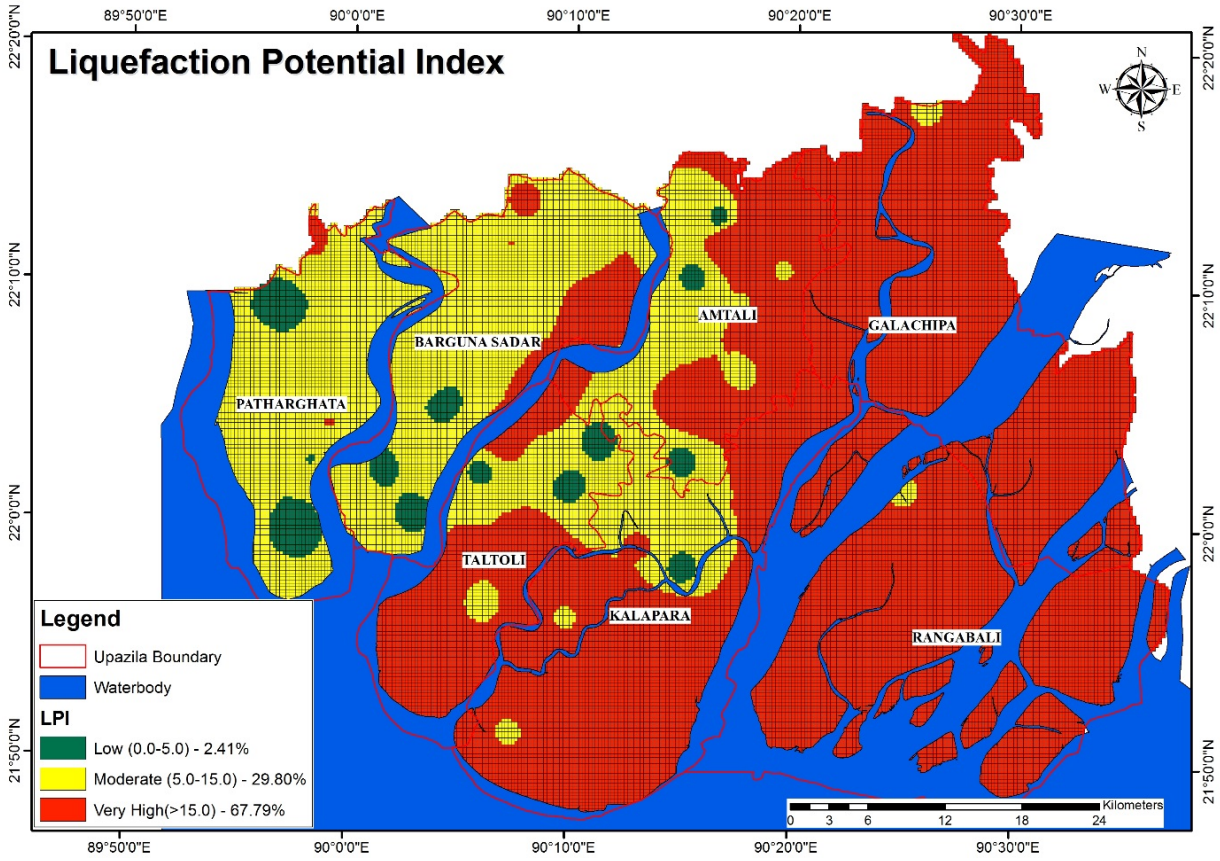

Figure 5.2 Liquefaction hazard map of Payra-Kuakata area

This study attempts a quantitative approach to stimulate a seismic soil liquefaction potential index for Payra-Kuakata Eco tourism Project, regarding a seismic event of M_W =7.5 and PGA = 0.167 to 0.239g. There are seven upazila lies under the project area. Demarcation of spatial variability in surface manifestation of soil liquefaction included the operation of placing LPI values of all of the SPT boreholes, and contouring by equal LPI lines on a map. The map indicates the places with low, moderate, high, very high vulnerability to liquefaction damage. This liquefaction hazard probability map, however, would be useful in estimating site specific degree of hazard and impact area (Holzer et al., 2006). The liquefaction possibility of a borehole is defined by summing the LPI of the layers within 20m. For marking each layer of a borehole as liquefiable some criteria like if a layer has plasticity less than 7%, have clay content less than 10% and also saturated are used.

Table 5.2 liquefaction severity assessed from the liquefaction potential index (LPI) from different Literatures (Cho *et al*., 2012)

LPI	Iwasaki *et al*. (1982)	Luna and Frost (1998)	Chung *et al*. (2011)	This study
0	Not likely	Little to none	None	Very low
0<LPI ≤ 5	Minor	Minor	Little to none	Low
5<LPI ≤ 15	-	Moderate	Moderate	Moderate
>15	Severe	Major	Severe	Very high

Subsurface geology of soils has a great importance for identifying liquefiable layers then the surface geology. The reason is surface geology may vary within few depths from the surface. In this region subsurface area is topped by the surface geology unit tidal deltaic deposit, tidal mud, marshy peat and clay, mangrove swamp. The subsurface soils are mainly silty sand and clayey silts. As the region lies on mainly tide dominated delta and also in the coastal regime variation in sediment deposit, size of sediments, different discharge rate can be seen which cause heterolytic geology in subsurface.

Total 100 SPT borehole investigations were conducted within this study region. Among those 83 SPT borehole investigations were done in tidal deltaic deposit, where LPI values vary from 0 to 43.65 indicating low to very high liquefaction potential. There is probability that 80% area topped by tidal deltaic deposits can faced liquefaction induced surface disruption for the designed seismic stress. As this subsurface geology is heterolytic with interbedded sands, silts, and clays and both fining- and coarsening upward facies association. Again, saturated as groundwater level is very close to surface. These areas show moderate low to very high liquefaction.

Only 2 SPT boreholes are constructed in the area with marshy clay and peat and so we can't properly describe its liquefaction potentiality.

The areas with surface geologic unit as tidal Mud have mud in the upper layers near banks but in the intermediate layers interbedding of soil and clay layers are seen from the bore log. 15 SPT boreholes investigations are conducted on this unit. And all the boreholes have LPI values more than 5. In fact, area with this geologic unit is in the downstream so finer particles are deposited here. And as the deposits are recent so compaction of sediments is very low. In addition, higher ground water level, tidal effect due to coastal morphology creates the statured

environment. Thus, deposition of finer particles with low plasticity and increased pore water pressure due to saturation creates an ideal condition for liquefaction.

With the composition of subsurface geology, its texture, plasticity, porewater pressure also plays a great role. Pore-water is the water remains in the void of fine grained soil and the pressure of it increases if the dry fine-grained soil becomes wet due to contact of water. As water table is very close to surface it plays as an important role for increasing the liquefaction potential in this region. So, it can say that groundwater level plays a crucial role while calibrating LPI by the Simplified Procedure. Here, depth of groundwater table (GWT) varies from 0.33 to 3 m in this region, but in most of the (approximately 77%) boreholes GWT was found within 1.5m from the surface. (see the Table 5.1).

Overall Liquefaction potential of the Payra-Kuakata, LPI values were performed without considering definite liquefaction evidence as there is no documentation on liquefaction record in the study region. Basically, from the calculation it has observed that cyclic resistance ratio of the layers of this region is less than the stress ratio so the higher liquefaction potential is found. Nevertheless, the prediction that approx. 80% and 100% area of tidal deltaic deposit and tidal mud, respectively, of Recent age shows liquefaction induced surface manifestation is much higher than those reported by Holzer et al. (2006). But higher thickness of fine-grained soft soils as well as occurrence of the ground water table at very shallow depths in all over the area further explains the resultant prediction. Another important factor could be added is periodic presence of very low consistency soils in both of the zones. But, most importantly, abundance of silty layers, and clay layers of low liquid and plastic limits—ultimately attributing these clayey soils as poorly drained—have significantly contributed to higher LPI values while summing up from SPT profiles, hence increasing prediction of liquefaction surface effect area.

6. SETTLEMENT OF SOIL (CLAY SOIL)

Payra-Kuakata, the study area, is situated in the Southern part of Bangladesh and is characterized by tidal deltaic deposits, tidal muds, marh and mangrove swamp deposits (figure 3.1). These clay soils are usually subjected to a time dependent strain under load and resulting settlement of clay soil. As a result number of structures is tilted and collapsed due to settlement of clay soil below the foundation of structures. Nowadays, the settlement failure has become a common phenomenon in many parts of the country. So the main focus of the study is to determine the consolidation characteristics of the clay layers in the study area to analyze the settlement characteristics.

Clay samples from 37 boreholes have been collected to understand the settlement scenario of the study area. The compressibility, compression index, pre-consolidation stress and permeability properties of undisturbed clay samples are evaluated. All of these consolidation characteristics of undisturbed clay samples are determined from the one dimensional consolidation test. The values of compression index, Cc were found to vary from 0.138 to 0.387 and the values of preconsolidation stress, Pc (Kpa) of the clay samples varies from 130 to 350.

6.1. Previous Works

The geological and geotechnical characteristics of soils of different regions of Bangladesh have been studied by many researches. Morgan and McIntire (1959) and Hunt (1976) investigated geological characteristics of soils of different regions of Bangladesh. Ameen (1985) and Bashar (2000) investigated the geotechnical characteristics of the Dhaka clay. Serajuddin et al. (2001) reported characteristics of uplifted Pleistocene deposits in Dhaka city.

Few research works were conducted in the past to evaluate compressibility of intact and reconstituted samples of Dhaka clay. A very brief description of few of these research works is given below.

Siddique (1986) investigated the compressibility properties of reconstituted Dhaka clay. The values of compression index (Cc) and void ratio at 1 tsf vetical stress were found to be 0.28 and 0.84, respectively. Siddique and Safiullah (1995) reported coefficient of permeability values of reconstituted Dhaka clay. Void ratio-permeability relationship for Dhaka clay was also investigated by Islam et al. (2004).

Uddin (1990) investigated the undrained shear strength, compressibility and expansibility of reconstituted Dhaka clay. . A comparative study showed that Dhaka clay possesses a lower

value of K (coefficient of permeability) than that of some other clay. Uddin (1990) also reported that for reconstituted Dhaka clay, under K_0 stress condition, the compression index (Cc) and swelling index (Cs) determined from e versus log σ′v curve are 0.25 and 0.025, respectively. Under isotropic stress condition compression index (Cc) and swelling index (Cs) were found to be 0.278 and 0.038, respectively.

Islam (1999) investigated the strength and deformation anisotropy of Dhaka clay. The coefficient for undisturbed clay varied between 1.01 (i.e., isotropic) to 1.55 (i.e., anisotropic). Deformation properties e.g., compression index (Cc), swelling index (Cs) and coefficient of volume compressibility (mv) and coefficient of permeability (k) obtained from one-dimensional consolidation tests on reconstituted Dhaka clay were directionally independent in a vertical plane. Natural clay was, however, anisotropic both in deformation and hydraulic characteristics. The indices Cc and Cs were maximum in vertical direction. The value of coefficient of permeability in horizontal direction, however, was higher than that in vertical direction.

6.2. Methodology

Sampling

The undisturbed cohesive soils (clay) are usually used for consolidation test. The undisturbed clay samples from different parts of the project area have been collected by using Sellby Tube Sampler during the execution of Standard Penetration Test. The samples have been transferred to the Engineering Geological Laboratory of the Geology Department of Dhaka University for Laboratory Test. The main purpose of the consolidation test is to obtain information on the compression properties of a saturated soil for use in determining the magnitude and rate of settlement of structures. Most of the sample collected from different locations at depth 2.55m (Table 6.1).

Table 6.1 Consolidation test sampling lacations

Bore hole No	Sample No	Depth in meter	Location	Latitude	Longitude	Layer Profile
BH-03	UD-01	2.55	Chokina Govt. Primary School, Taltoli	21.896795	90.040669	Brownish Grey Very Soft to Soft Silty CLAY little Very Fine Sand
BH-11	UD-01	2.55	Dalbuganj Bazar Govt. Primary School, Kalapara	21.892820	90.189570	Brownish Grey Soft Silty CLAY
BH-20	UD-01	2.55	Khapupara Model High School, Kalapara	21.985030	90.220150	Brownish Grey to Grey Very Soft to Soft SILT/Silty CLAY
BH-22	UD-01	3.95	Rangabali Niz Haowla Govt. Primary School, Rangabali	21.944397	90.412697	Brownish Grey to Grey Very Soft Clayey SILT with Very Fine Sand
BH-23	UD-01	2.55	Rangabali Model High School/Rangabali H A Govt. Primary School, Rangabali	21.974417	90.435536	Brownish Grey to Grey Soft to Medium Stiff Clayey SILT
BH-26	UD-01	2.55	Moddho Gazi Mahmud Govt. Primary School, Barguna Sadar	22.019223	89.998116	Brownish Grey to Grey Very Soft to Medium Stiff Silty CLAY/Clayey SILT
BH-29	UD-01	2.55	Nolbunia Govt. Primary School, Taltoli	22.025846	90.164284	Brownish Grey to Grey Very Soft to Medium Stiff Silty CLAY/SILT
BH-30	UD-01	2.55	Dokkhin Jharakhali High School, Taltoli	21.984438	90.139164	Brownish Grey to Grey Very Soft to Soft CLAY with Organics
BH-32	UD-01	2.55	Moddho Panchjunia Govt. Primary School, Kalapara	22.058730	90.319880	Brownish Grey to Grey Very Soft to Soft CLAY
BH-33	UD-01	2.55	Bara Baizdia A K Hakim Govt. Primary School, Rangabali	21.967460	90.362603	Brownish Grey to Grey Very Soft to Soft SILT with Very Fine Sand
BH-34	UD-01	2.55	Mirzabari Jame Mosque, Koralia Bazar, Rangabali	22.025535	90.418347	Brownish Grey to Grey Very Soft to Soft SILT/Silty CLAY with Very Fine Sand
BH-36	UD-01	2.55	Pathorghata K. M. High School, Patharghata	22.042219	89.971430	Brownish Grey to Grey Very Soft to Soft Silty CLAY/SILT with Very Fine Sand
BH-37	UD-01	2.55	Garjanbunia Govt. Primary School, Barguna Sadar	22.035766	90.025007	Brownish Grey to Grey Very Soft to Stiff Silty CLAY/Clayey SILT
BH-38	UD-01	2.55	Porirkhal Govt. Primary School, Barguna Sadar	22.044112	90.051524	Brownish Grey to Grey Soft to Medium Stiff Silty CLAY/SILT
BH-42	UD-01	2.55	Ultakhali Govt. Primary School, Amtali	22.045890	90.250250	Brownish Grey to Grey Very Soft to Medium Stiff Clayey SILT
BH-48	UD-01	2.55	Amratola Govt. Primary School, Patharghata	22.106045	89.996869	Brownish Grey to Grey Very Soft Silty CLAY
BH-49	UD-01	2.55	Khakbunia Fazil(Degree) Madrasha, Barguna Sadar	22.097637	90.061310	Brownish Grey to Grey Very Soft to Soft Silty CLAY/SILT
BH-51	UD-01	2.55	Ponchakoralia Sluice Shonglogno Govt. Primary School, Taltoli	22.088656	90.146443	Brownish Grey Very Soft to Medium Stiff Silty CLAY

BH-55	UD-01	2.55	Uttar Kolairchar Mosque, Amtali	22.132797	90.319892	Brownish Grey Soft to Medium Stiff Silty CLAY
BH-57	UD-01	2.55	Char Bishwas Janata High School, Galachipa	22.039678	90.526369	Brownish Grey to Grey Very Soft to Medium Stiff SILT with Very Fine Sand
BH-58	UD-01	2.55	Char Kazal Puran Bazar Govt. Primary School, Galachipa	22.078819	90.518992	Brownish Grey to Grey Soft to Medium Stiff SILT/Clayey SILT
BH-59	UD-01	2.55	Charduani Govt. Primary School, Patharghata	22.119288	89.929288	Brownish Grey to Grey Very Soft to Medium Stiff Silty CLAY/Clayey SILT/SILT
BH-60	UD-01	3.95	Shingrabunia Govt. Primary School, Patharghata	22.150878	89.947985	Brownish Grey to Grey Very Soft to Medium Stiff Silty CLAY
BH-63	UD-01	3.95	Heulabunia Govt. Primary School, Barguna Sadar	22.122942	90.096608	Brownish Grey to Gery Very Soft to Medium Stiff Silty CLAY/SILT with Very Fine Sand
BH-65	UD-01	2.55	Burirchor ASG High School, Barguna Sadar	22.153119	90.199123	Brownish Grey Very Soft Silty CLAY
BH-66	UD-01	2.55	Amtali A K Pailot High School, Amtali	22.141493	90.233098	Brownish Grey to Grey Soft to Stiff Silty CLAY and Organics
BH-71	UD-01	2.55	Shotkor Betmore Govt. Primary School, Patharghata	22.195257	89.968453	Brownish Grey to Grey Soft to Medium Stiff Silty CLAY
BH-73	UD-01	2.55	Lakurtola Shonar Bangla High School, Barguna Sadar	22.196093	90.119071	Brownish Grey to Grey Very Soft to Soft SILT little Sand
BH-76	UD-01	2.55	Khukuani School Centre, Amtali	22.174278	90.256693	Brownish Grey to Grey Soft to Medium Stiff SILT/Silty CLAY/Clayey SILT
BH-77	UD-01	2.55	Amragachia Salehiya Cyclon Centre, Amtali	22.199496	90.282488	Brownish Grey to Grey Soft to Medium Stiff Silty CLAY
BH-79	UD-01	2.55	Dakshin Gabua Govt. Primary School, Galachipa	22.181953	90.391907	Brownish Grey Very Soft Silty CLAY
BH-83	UD-01	2.55	Charkhali Community Clinic, Kukuya, Amtali	22.216233	90.275309	Brownish Grey to Grey Soft to Medium Stiff SILT/Silty CLAY
BH-85	UD-01	2.55	Shakhariya High School, Hajirhat, Amtali	22.247763	90.322332	Brownish Grey to Grey Very Soft to Soft SILT/Silty CLAY
BH-86	UD-01	2.55	Moddho Amkhola Dakhil Madrasa, Galachipa	22.250839	90.384350	Brownish Grey to Grey Very Soft to Medium Stiff Silty CLAY/Clayey SILT
BH-87	UD-01	2.55	Chiknikandi High School, Galachipa	22.225610	90.456290	Brownish Grey to Grey Very Soft to Soft SILT
BH-92	UD-01	2.55	Poshchim Hasnapara Govt. Primary School,Lalua, Kalapara	21.928189	90.267361	Brownish Grey to Grey Very Soft to Soft Silty CLAY with Very Fine to Medium Sand
BH-96	UD-01	2.55	Dakshin Tiakhali 2 Govt. Primary School, Kalapara	21.994316	90.275292	Brownish Grey Soft Silty CLAY/Clayey SILT Little Very Fine Sand

Consolidation characteristics and Settlement calculation
Compressibility of Clay

Coefficient of compressibility Av,

The coefficient of compressibility av, is the slope of the void ratio versus the effective pressure curve when plotted arithmetically. av can be found from

$$av = -\frac{\Delta e}{\Delta \sigma'} \quad \ldots\ldots 6.1$$

Coefficient of volume change mv,

The coefficient of volume change or the coefficient of volume compressibility is defined as the change in volume of a soil per unit of initial volume due to given unit increase in the pressure. (Singh,A,2011)

$$mv = -\frac{\Delta e}{(1+e_0)\Delta \sigma'}$$

Substituting $-\frac{\Delta e}{\Delta \sigma'} = av$, we get $mv = \frac{a_v}{(1+e_0)}$ …….6.2

.

When the soil is laterally confined, the change in the volume is proportional to change in the thickness, ΔH and the initial volume is proportional to the initial thickness H_0

Hence , $mv = -\frac{\Delta H}{H_0} * \frac{1}{\Delta \sigma'}$ …….6.3

(The minus sign in the above equation simply denotes that the voids ratio or thickness decreases with the increase in the pressure)

Some typical values of Mv suggested by Barnes, (2001) for different types of soil are given in Table 6.2

Table 6.2 Typical values of m_v (Barnes, 2001)

Types of clay	m_v (m2/ MN)
Very stiff heavily over - consolidated clay	< 0.05
Stiff over - consolidated clay	0.05 – 0.1
Firm over - consolidated clay, laminated clay, weathered clay	0.1 – 0.3
Soft normally consolidated clay	0.30 – 1.0
Soft organic clay, sensitive clay	0.5 – 2.0
Peat	> 1.5

Compression index C_c

It is the principal values obtained from the consolidation test and is calculated from test data. The compression index, (Singh,A,2011) Cc, is equal to the slope of the linear portion of the void ratio versus log pressure plot. Typical values of Compression index are given in table 6.3. The value of Cc for Bangladesh soils (silty clay) determined by Aminullah (2004) ranges from 0.11 to 0.43.

The empirical equations available for determinations of Cc

$$C_c = \frac{\Delta e}{\text{Log}\,(\sigma'2/\sigma'1)} \quad \text{or} \quad \frac{\Delta e}{\Delta\,(\text{Log}\,\sigma'_v)} \qquad \ldots\ldots\ldots\ldots\ldots\ldots\ldots\ldots 6.4$$

The dimensionless compression index is useful for the determination of the settlement in the field.

Table 6.3 Classification of soil Compressibility. (Coduto, D.P, 2002)

Compressibility	Classification
0-0.05	Very slightly compressible
0.05-0.10	slightly compressible
0.10-0.20	Moderately compressible
0.20-0.35	Highly compressible
>0.35	Very highly compressible

Determination of Permeability

The amount of water flowing through a certain area can be represented by the coefficient of permeability. The higher the permeability of the soil, the more quickly water will be able to flow out of the soil.

The coefficient of consolidation kv = cv*mv * .γw ……6.5

Different researchers have determined the k value for fine grained soils. Some typical values of k suggested by Aysen (2002) for different types of soil are given in Table 6.4

Table 6.4 Some typical values of coefficient of permeability for different types of soils (Aysen, 2002)

Types of soil	Coefficient of Permeability (m/s)
Clean gravels	$1 – 10^{-2}$
Clean gravels, Clean sand and gravel	$10^{-2} – 10^{-5}$
Very fine sands, organic and inorganic silts mixtures of sand, silt and clay.	$10^{-5}– 10^{-9}$
Clays	$10^{-9}– 10^{-11}$
Well drained soils	$1 – 10^{-6}$
Poorly drained soils	$10^{-6} – 10^{-8}$
Practically impervious	$10^{-8} – 10^{-11}$

Preconsolidation stress, σ'c

The stress at the point where the slope of the consolidation curve changes is preconsolidation stress σ'c. It is the greatest vertical effective stress the soil has ever experienced. The value of σ'c sometimes greater than σ′z0 that is the soil may have been preconsolidated during the geologic past by the weight of an ice which has melted away, or by other geologic overburden or and structural loads which no longer exist.

The preconsolidation stress obtains from the test represents only the conditions at the point where the sample was obtained. The relative amount of preconsolidation is usually reported as the overconsolidation ratio (OCR) defined as

$OCR = \sigma'c/\sigma'z_0$

Typical range of overconsolidation Margins are given in table 6.5

Table 6.5 Typical range of overconsolidation margin. (Coduto, D.P, 2002)

Overconsolidation margin,σ'_m in kPa	Classification
0	Normally consolidated
0-100	Slightly consolidated
100-400	Moderately consolidated
>400	Heavily consolidated

6.3. Test Results Interpretation

Clay samples from 37 boreholes have been collected to understand the settlement scenario of the study area. All of these consolidation characteristics of undisturbed clay samples are determined from the one dimensional consolidation test. The values of compression index, Cc have been found to vary from 0.138 to 0.387 and the values of preconsolidation stress, Pc (Kpa) of the clay samples varies from 130 to 350.

The summary of consolidation characteristics of sub-surface clay deposits of Kuakata City is given in the following table (table 6.7)

Table 6.7 Test Summary

SUMMARY OF THE TEST RESULTS

Client : Urban Development Directorate (UDD)

Project: Preparation of Payra-Kuakata Comprehensive Plan Focusing on Eco-Tourism

Bore hole No	Sample No	Depth in meter	Latitude	Longitude	Layer Profile	Consolidation Test	
						Compression Index, Cc	Preconsolidation Stress, Pc (Kpa)
BH-03	UD-01	2.55	21.896795	90.040669	Brownish Grey Very Soft to Soft Silty CLAY little Very Fine Sand	0.155	170
BH-11	UD-01	2.55	21.892820	90.189570	Brownish Grey Soft Silty CLAY	0.17	240
BH-20	UD-01	2.55	21.985030	90.220150	Brownish Grey to Grey Very Soft to Soft SILT/Silty CLAY	0.168	195
BH-22	UD-01	3.95	21.944397	90.412697	Brownish Grey to Grey Very Soft Clayey SILT with Very Fine Sand	0.16	155
BH-23	UD-01	2.55	21.974417	90.435536	Brownish Grey to Grey Soft to Medium Stiff Clayey SILT	0.153	220
BH-26	UD-01	2.55	22.019223	89.998116	Brownish Grey to Grey Very Soft to Medium Stiff Silty CLAY/Clayey SILT	0.15	185
BH-29	UD-01	2.55	22.025846	90.164284	Brownish Grey to Grey Very Soft to Medium Stiff Silty CLAY/SILT	0.22	280
BH-30	UD-01	2.55	21.984438	90.139164	Brownish Grey to Grey Very Soft to Soft CLAY with Organics	0.15	230
BH-32	UD-01	2.55	22.058730	90.319880	Brownish Grey to Grey Very Soft to Soft CLAY	0.16	270
BH-33	UD-01	2.55	21.967460	90.362603	Brownish Grey to Grey Very Soft to Soft SILT with Very Fine Sand	0.138	165
BH-34	UD-01	2.55	22.025535	90.418347	Brownish Grey to Grey Very Soft to Soft SILT/Silty CLAY with Very Fine Sand	0.22	305
BH-36	UD-01	2.55	22.042219	89.971430	Brownish Grey to Grey Very Soft to Soft Silty CLAY/SILT with Very Fine Sand	0.163	160
BH-37	UD-01	2.55	22.035766	90.025007	Brownish Grey to Grey Very Soft to Stiff Silty CLAY/Clayey SILT	0.14	130
BH-38	UD-01	2.55	22.044112	90.051524	Brownish Grey to Grey Soft to Medium Stiff Silty CLAY/SILT	0.147	180
BH-42	UD-01	2.55	22.045890	90.250250	Brownish Grey to Grey Very Soft to Medium Stiff Clayey SILT	0.205	220
BH-48	UD-01	2.55	22.106045	89.996869	Brownish Grey to Grey Very Soft Silty CLAY	0.188	180
BH-49	UD-01	2.55	22.097637	90.061310	Brownish Grey to Grey Very Soft to Soft Silty CLAY/SILT	0.155	170
BH-51	UD-01	2.55	22.088656	90.146443	Brownish Grey Very Soft to Medium Stiff Silty CLAY	0.387	330
BH-55	UD-01	2.55	22.132797	90.319892	Brownish Grey Soft to Medium Stiff Silty CLAY	0.245	160
BH-57	UD-01	2.55	22.039678	90.526369	Brownish Grey to Grey Very Soft to Medium Stiff SILT with Very Fine Sand	0.205	230
BH-58	UD-01	2.55	22.078819	90.518992	Brownish Grey to Grey Soft to Medium Stiff SILT/Clayey SILT	0.205	230
BH-59	UD-01	2.55	22.119288	89.929288	Brownish Grey to Grey Very Soft to Medium Stiff Silty CLAY/Clayey SILT/SILT	0.187	300
BH-60	UD-01	3.95	22.150878	89.947985	Brownish Grey to Grey Very Soft to Medium Stiff Silty CLAY	0.268	350
BH-63	UD-01	3.95	22.122942	90.096608	Brownish Grey to Gery Very Soft to Medium Stiff Silty CLAY/SILT with Very Fine Sand	0.213	200
BH-65	UD-01	2.55	22.153119	90.199123	Brownish Grey Very Soft Silty CLAY	0.242	300
BH-66	UD-01	2.55	22.141493	90.233098	Brownish Grey to Grey Soft to Stiff Silty CLAY and Organics	0.21	260

BH-71	UD-01	2.55	22.195257	89.968453	Brownish Grey to Grey Soft to Medium Stiff Silty CLAY	0.145	155
BH-73	UD-01	2.55	22.196093	90.119071	Brownish Grey to Grey Very Soft to Soft SILT little Sand	0.15	180
BH-76	UD-01	2.55	22.174278	90.256693	Brownish Grey to Grey Soft to Medium Stiff SILT/Silty CLAY/Clayey SILT	0.201	295
BH-77	UD-01	2.55	22.199496	90.282488	Brownish Grey to Grey Soft to Medium Stiff Silty CLAY	0.18	170
BH-79	UD-01	2.55	22.181953	90.391907	Brownish Grey Very Soft Silty CLAY	0.194	210
BH-83	UD-01	2.55	22.216233	90.275309	Brownish Grey to Grey Soft to Medium Stiff SILT/Silty CLAY	0.292	280
BH-85	UD-01	2.55	22.247763	90.322332	Brownish Grey to Grey Very Soft to Soft SILT/Silty CLAY	0.235	320
BH-86	UD-01	2.55	22.250839	90.384350	Brownish Grey to Grey Very Soft to Medium Stiff Silty CLAY/Clayey SILT	0.25	205
BH-87	UD-01	2.55	22.225610	90.456290	Brownish Grey to Grey Very Soft to Soft SILT	0.32	175
BH-92	UD-01	2.55	21.928189	90.267361	Brownish Grey to Grey Very Soft to Soft Silty CLAY with Very Fine to Medium Sand	0.237	195
BH-96	UD-01	2.55	21.994316	90.275292	Brownish Grey Soft Silty CLAY/Clayey SILT Little Very Fine Sand	0.227	170

Compression Index

There is a relation between compression index and water content of samples. If the water content of sample is high then the sample is highly compressible, because the sample contains large amount of void with water. The compression index of the clay samples collected from at depth 2.55m ranges from 0.138 to 0.387 which indicates that the clay layer is moderately to very highly compressible according to the table 6.3.

Preconsolidation Stress

Results show that the filling material of Clay samples is moderately consolidated (please see table 6.5) and presonsolidation stress (Kpa) is ranging from 130 to 350.

Recommendation

A generalized settlement scenario has been characterized in this current project; though, it was beyond the scope of the current project. The clay layers of project area is found to be moderately and very highly consolidated, however, it is not well representative to reach a concrete conclusion as the number of sampling needs to be increased and sampling should be carried out at different depth levels. In this project, most of the clay samples for consolidation test have been collected from 2.55m depth. This particular clay layer is found as moderately to very highly compressible and moderately consolidated based on the compression index and preconsolidation stress. These findings do not necessarily mean that the clay layers at greater depth will show similar settlement scenario as the deeper clay layer is usually highly compacted

and the probability of settlement usually get decreased. It is also possible to predict settlement; however, to do so, more spatially distributed samples at varying depth are necessary. Moreover, the settlement of any area of investigation can be validating by the time series InSAR analysis. Time series InSAR analysis necessitates multi-temporal SAR (synthetic aperture radar) imagery.

7. GEOLOGICAL SUITABILITY AND RECOMMENDATION

We use 2 step multi-criteria decision making (MCDM) technique to develop geological suitability map. In first step we select 5 major criteria (**PGA, Foundation layer depth, Soil Type, Liquefaction Potential Index, Building Height Recommendation**.), and to find out the relative weight of these criteria AHP pairwise comparison have been applied in decision making. The analytic hierarchy process (AHP) (Saaty, 1980 and 1994) decomposes a complex MCDM problem into a system of hierarchies (more on these hierarchies can be found in Saaty, 1980). After getting the weighted value, weighted sum model has been applied to find the final suitability map.

The weighted sum model (WSM) is probably the most commonly used approach, especially in single dimensional problems like this. In weighted sum technique, we first convert our criteria raster files to a common numerical system as the WSM need all data in same unit, a uniform calculation (Figure 7.1). For this we converts our values into rating based on their impact in scale of 1 to 5; where 1 being less effective and 5 being most effective. i.e., if LPI is 0 or <5 we can say it is safer than >15 one, so <5 value is given 5 where >15 is given 1 (Table 7.1).

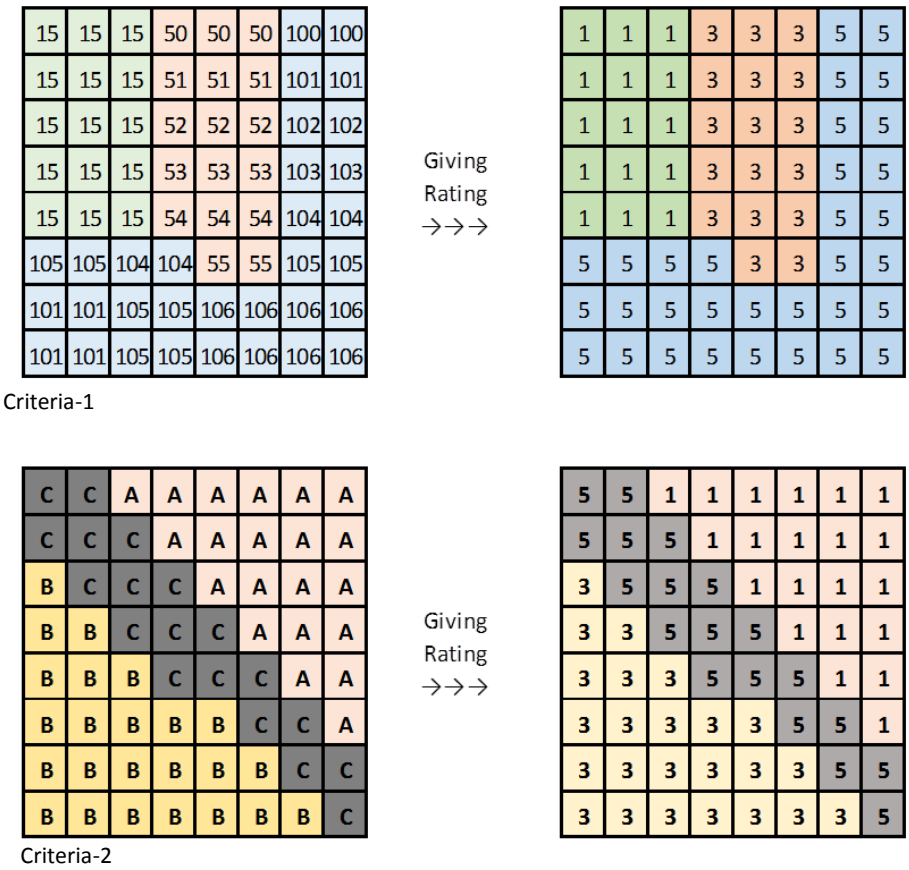

Figure 7.1 Preparation of weighted sum model (Step-1)

After rating the individual criterion, they have been given a weighted value, which is the impact of each criterion on the decision. This weighted value has been calculated from AHP method. Specialists were asked to participate in this AHP and give their pairwise rating. Afterward all the rating has been calculated in AHP model and the weight value identified. Then rating raster has been multiplied by the weighted value and afterward summed up for the final decision raster which returns value ranging from 100 to 500 (Figure 7.2). The decision raster is divided into 5 Classes i.e., Very Good, Good, Moderate, Poor, Very Poor from equally divided range of 100 to 500. The classes of suitability are relative to this area particularly.

Table 7.1: Rating and Weight Value for Geological suitability

Factors	Value	Rating	Weight
Peak Ground Acceleration	0.215 to 0.239	5	19.7
	0.191 to 0.215	3	
	0.215 to 0.239	1	
Foundation Depth	7.4 to 10	5	26.3
	10 to 15	4	
	15 to 20	3	
	20 to 25	2	
	>25	1	
AVS30	E-Type: Soft/Loose Soil	1	12.8
LPI	≤ 5	5	20.9
	5 to 15	3	
	>15	1	
Building Height Recommendation	3rd Degree Sensative for Lowrise& 3rd Degree Sensative for Highrise Building	5	20.3
	3rd Degree Sensative for Lowrise& 2nd Degree Sensative for Highrise Building	4	
	2nd Degree Sensative for Lowrise& 2nd Degree Sensative for Highrise Building	3	
	2st Degree Sensative for Lowrise&1st Degree Sensative for Highrise Building	2	

	1st Degree Sensative for Lowrise& 1st Degree Sensative for Highrise Building	1	

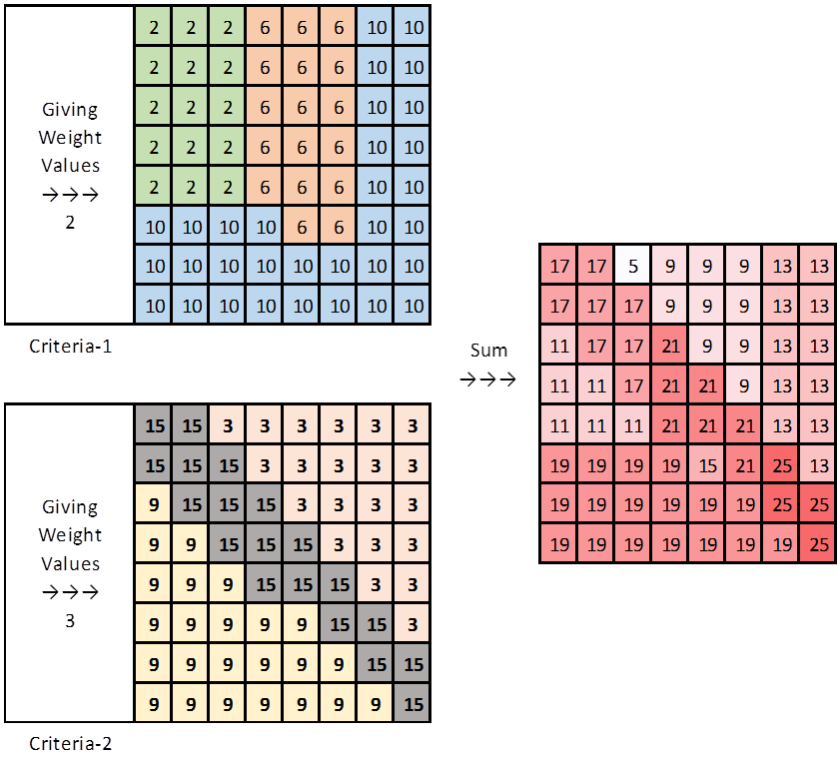

Figure 7.2 Preparation of weighted sum model (Step-2)

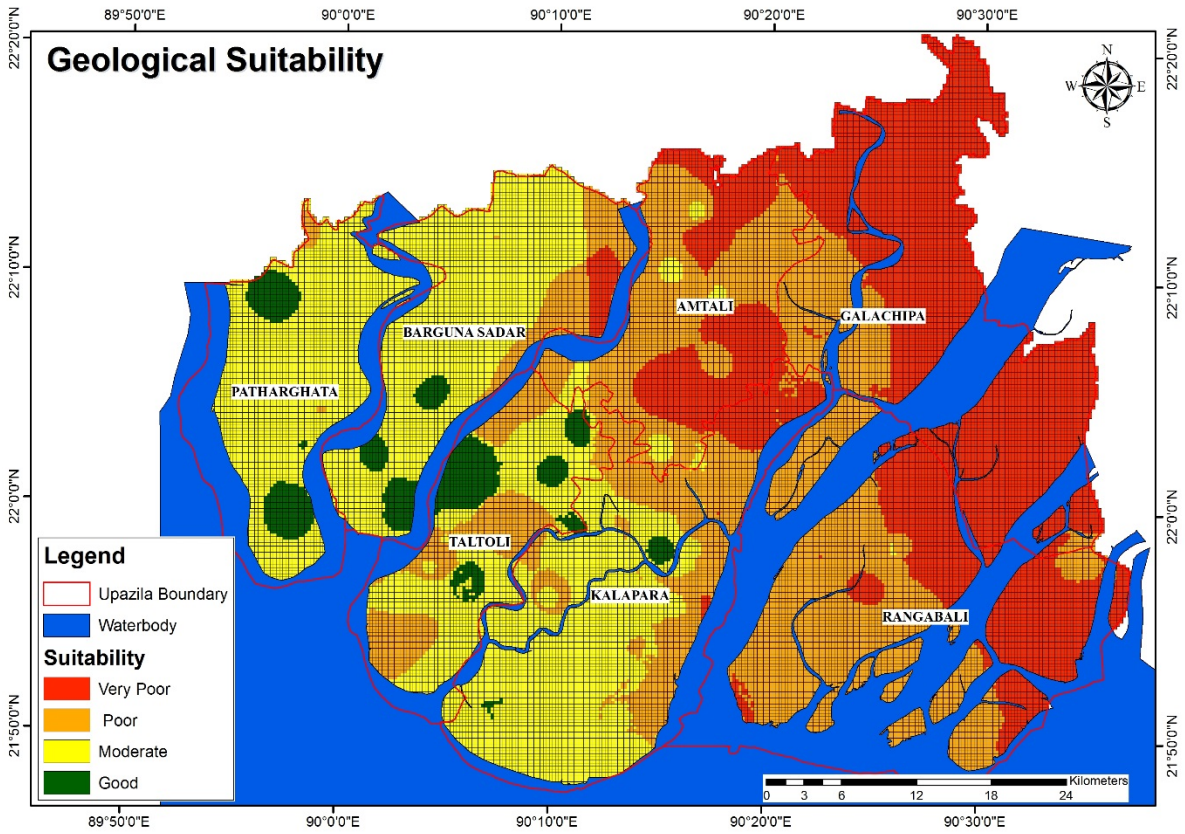

Figure 7.3 Geological Suitability map of Study Area

Figure 7.3 shows area delineated by Sage green colour areas of Patharghata, Barguna Sadar, Taltoli and Kalapara upazila is relatively good within this study area in terms of suitability and is suitable for light infrastructure with a foundation depth around 12 to 20m. Large and tall infrastructure requires pile foundation placed on Soil layer no 4 or 6. Those areas can be used for Commercial, Residential and Industrial Zone.

Yellow colour area of Patharghata, Barguna Sadar, Amtoli, Taltoli and Kalapara upazila is moderately suitable in comparison to other areas within the study area and for light infrastructure requires on-site subsoil investigation and proper foundation design. Deep pile foundation requires for large infrastructure. Such areas can be used as Industrial zone, Residential area, Commercial area, Agricultural Zone, Park and Recreation site.

Orange and Red colour area of Galachipa, Rangabali, Barguna Sadar, Amtoli, Taltoli and Kalapara upazila is poorly and Very poorly suitable in comparison to other areas within the study area for infrastructure development. Detail subsoil investigation and proper foundation design is require for all types of infrastructure, due to low suitability with hazard potential. Agricultural zone, rural settlement, Park and Recreation site are suggested for such sites.

Table 7.2 : Geological classification for infrastructure development

Sl No.	Geological Suitability	Infrastructure foundation suitability	Suggested Geological suitability
1	Good	4-6 story light infrastructure is suitable with a foundation depth of around 12 - 20m. Large and tall infrastructure requires pile foundation placed on layer no 4 or 6. Individual on-site subsoil investigation should be required.	Commercial area Residential area, Industrial zone
2	Moderate	4-6 story light infrastructure requires on-site subsoil investigation and proper foundation design. Deep pile foundation is needed for large infrastructure.	Industrial zone, Residential area, Commercial area, Agricultural Zone, Park and Recreation
3	Poor	Detail subsoil investigation and proper foundation design is required for all types of infrastructure, due to low suitability with hazard potential.	Agricultural zone, Wetland Rural settlement Park and Recreation
4	Very Poor	Detail subsoil investigation for deep pile foundation is essential, due to very low soil resistance and high hazard potential. Shallow foundation is not preferred.	Agricultural zone, Wetland Rural settlement Park and Recreation

8. POLICY BASED ON SEISMIC HAZARD ASSESSMENT

8.1. Policy Based on Foundation Depth Layer Map

Based on SPT N-Value (soil resistance) of boreholes layer4 and layer6 are considered as foundation layer for the study area and a foundation depth map (Figure 8.1) is produced which is categorized into 6 classes based on the depth of the foundation layer. Green color zones (Northeastern Rangabali Upazila) of the study area suggest foundation layer depth ranging from 7.3 to 10m and only 0.5% area of the study area belongs to this category. The blue color areas of Galachipa, Rangabali, Taltoli and Kalabpara upazila represents foundation layer depth ranges from 10.01 to 15m comprising only 2.77% of the total study area. From the map it can be observed that the Southwestern half of Kalapara upazila, eastern half of Ragabali upazila, northeastern part of Galachipa upazila, middle part of the Taltoli upazila and a small part of southern Barguna Sadar Upazila suggest foundation layer at depth ranging from 15.01 to 20m which represents by cyan color. This category covers 27.68% of the total land. About 30.85% of the total land mass represents with light green color suggest foundation layer depth in between 20 to 25m. The orange zones of southern half of Amtoli, northern half of Taltoli, Barguna Sadar and Patharghata; and few discrete places of Kalapara; Galachipa and Rangabali upazila suggest foundation layer depth ranging from 25.01 to 30m comprising 27.83% of the study area. Rest 10.37% of the area shows red colour, which indicatesthe foundation layer depth more than 30m.

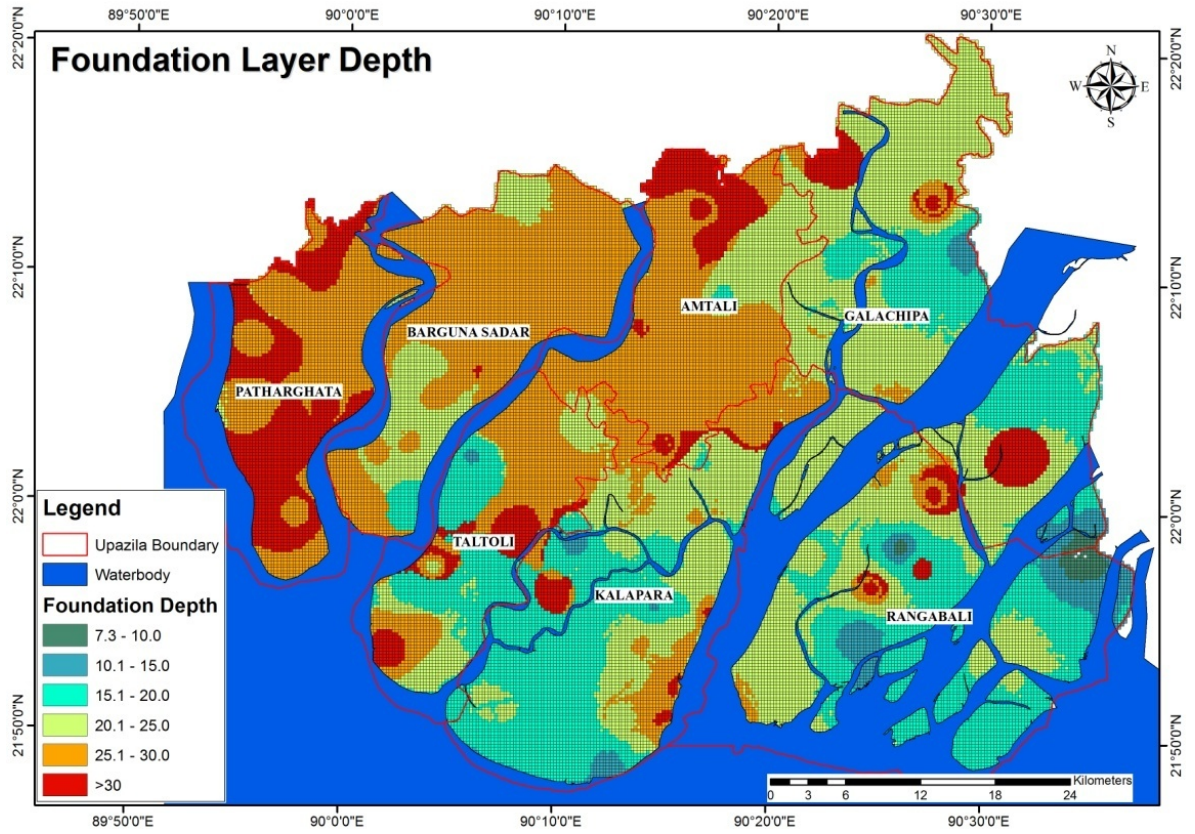

Figure 8.1 Foundation depth of Study Area

It is necessary to follow the national building code properly for any infrastructure development. For any infrastructure development in study area, everyone should be followed the suggested foundation depth layer.

8.2. Policy for Soil Type Determination based on Vs30

Velocity range of the soils of the project area is 110 to 180 m/s i.e., they belongs to the class E according to the provision. That means the soils within the area is soft/loose. Figure 8.2 shows the engineering soil condition of the project area based average shear wave velocity (AVs30). From the Figure 8.2 it can be observed that, the whole area belongs to category E suggesting soft/loose soil.

The purpose of this study was to generate guidelines to assist in the development of study area by estimating the soil type based on shear wave velocity of the top 30m (VS30). It is recommended that the suitable foundation depth layer should be considered for development as well as reduces the damages due to seismic hazards.

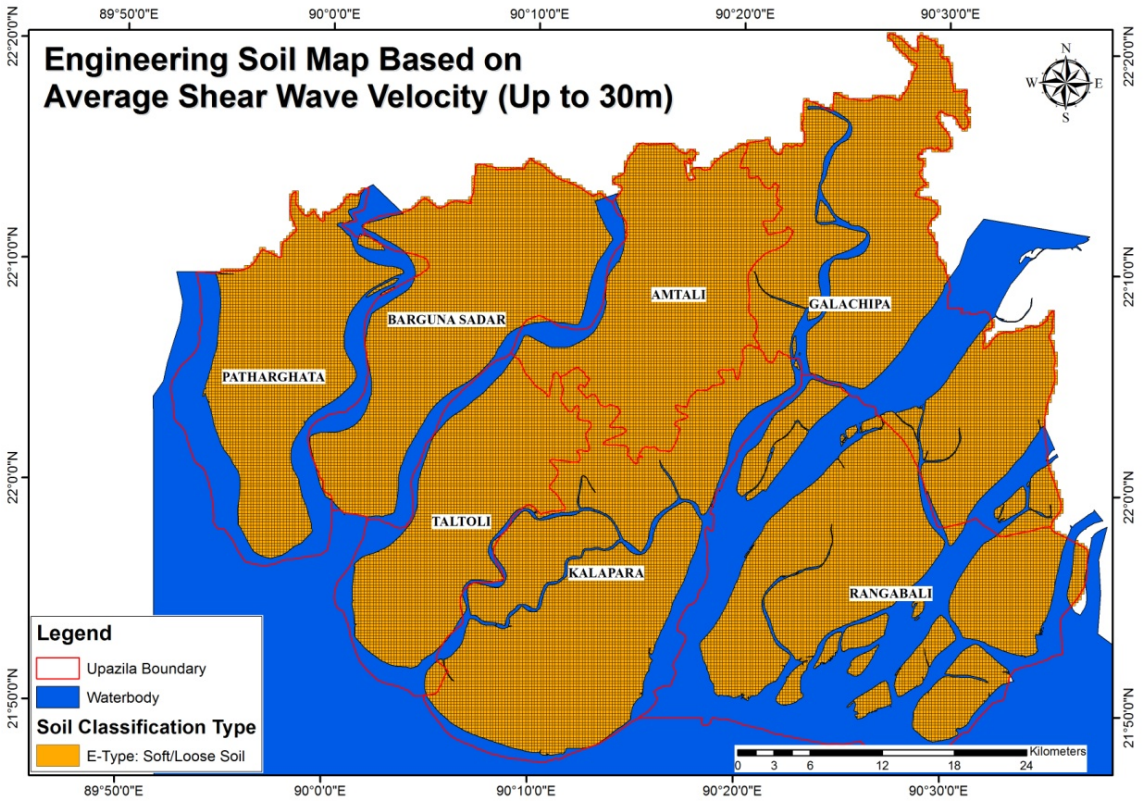

Figure 8.2 Soil classification map of Study Area according to NEHRP (stands for National Earthquake Hazard Reduction Program, USA) provisions based on the average shear wave velocity distribution down to 30 m

8.3. Policy Based on Building Height Map

Peak spectral acceleration (PSA) is an important tool for determining the building height of an area. Here PSA for 1.0 and 0.3 sec is used for identifying the appropriate location for high rise and low rise building respectively. A building height map is produced for the study area using PSA (Figure 8.3), which represent low rise building and high rise building. Low rise indicate 3 stories building and high rise represents 10 stories building.

Building Height Recommendation strategy should be considered during structural development of Study area. To prevent damages of property and human life, it is important to take proper measures for any kind of infrastructure development.

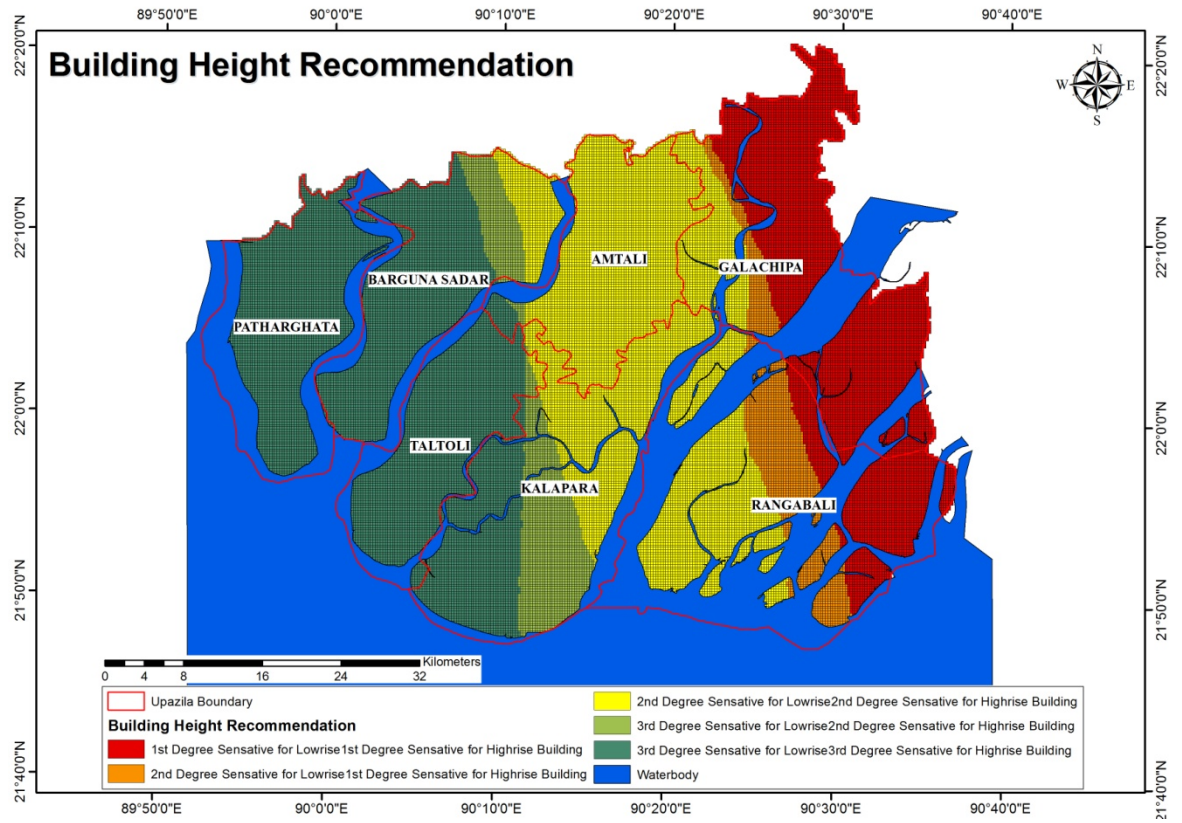

Figure 8.3 Building Height Map of Study area

From the map it can be observed that the dark green coloured areas of Patharghata, Barguna Sadar, Taltoli, Kalapara and Amtali upazilas area relatively 3rd degree risk sensitive zones for low rise building and 3rd degree risk sensitive for high rise buildings which represents approximately 34.59% of the total study area. The map also shows that the yellowish green coloured areas of Barguna Sadar, Taltoli, Kalapara and Amtali upazila, about 6.02% of the area is relatively 3rd degree risk sensitive for low rise buildings but 2nd degree risk sensitive for high rise buildings. The yellowish coloured zones of Barguna Sadar, Galachipa, Rangabali, Taltoli, Kalapara and Amtali upazila are relatively 2nd degree risk sensitive for low rise buildings and 2nd degree risk for high rise buildings comprising 32.78% of the whole study area. About 6.58% of total area represents by orange colour of Galachipa and Rangabali upazila are relatively 2nd degree risk sensitive for low rise buildings but 1st degree risk for high rise buildings. Rest of the 20.03% study area with red colour is relatively 1st degree risk sensitive for low rise buildings and 1st degree risk sensitive for high rise buildings.

In Addition, according to Uniform Hazard Spectra (for 10% probabilities) SA value is more than 0.3 g for 0.2s to 0.7s which indicates that 2 to 7 storey building will be affected by earthquake (Figure 4.33). Whereas peak period data indicates 5 to 7 storey building will be

affected by earthquake (Figure 4.34). To reduce the damage, Spectral acceleration (SA) value should be considered for building and/or infrastructure development. And national building code should be considered as well. There are several challenges for ensuring building safety and/or building code implementation i.e. Capacity of Local Government/ stakeholders, Lack of skill of building control officers, No professional trainings and lack of skill/ understanding in designers, petty contractors and artesian, Social /economic obstacles, Lack of awareness in Public, Large ratio of self-built construction in rural and urban area.

Suggestion for Government's Initiative for implementing building code

To improve the structural safety of houses to prevent damage and safeguard people's lives, property and livelihood from earthquakes through effective implementation of building safety regulations. Following objectives need to be achieved for proper building code-implementation:

- To raise awareness on the importance of implementing building safety regulation effectively to reduce risk of life and property losses caused by earthquakes
- To develop policy recommendations on improving the safety of houses, particularly that of traditional houses
- To develop capacity of national and local government officials to implement building safety regulations effectively
- To develop proper monitoring system for existing building safety in regular time interval

As an example (Role of Governments)

The role of government can best be exemplified by citing the initiatives undertaken by Government of India since after the super cyclone in Orissa and the major earthquake in Gujarat (UNCRD, 2008).

A National Disaster Management Act was adopted by the Indian Parliament in 2005 which have provided the establishment of National Disaster Management Authority at the Centre, the State Disaster Management Authorities in the States, as well as, the District Disaster Management Authorities in all Districts numbering more than 600. These authorities have to plan and execute all actions for advance preparedness as well as mitigation activities so that the future hazard occurrences may not impact the society as badly as before. The safety of non-engineered buildings will be one of the important issues to be taken up by the authorities. Already training of architects and engineers as well as training of masons and bar benders has

been initiated on sufficiently large scale which are proposed to be expanded to larger numbers and larger areas in the near future. Besides the earthquake safe elements to be provided in all new constructions actions are being taken towards retrofitting of all lifeline buildings such as schools, health centers, large community buildings and residences of government officials who will be taking care of post disaster management. Model Amendment to existing Acts and Building Byelaws in various levels of Local Bodies has been worked out at the Centre and being disseminated to States for implementation.

8.4. Geological suitability Policy

Geological suitability map of the area is produced (Figure) based on subsurface sediment criteria, foundation layer depth, Shear wave velocity (Vs) and PGA seismicity of the area (Table 8.1).

Figure 8.4 shows area delineated by Sage green colour areas of Patharghata, Barguna Sadar, Taltoli and Kalapara upazila is relatively good (approx. 3.57% of total area) within this study area in terms of suitability and is suitable for light infrastructure with a foundation depth around 12 to 20m. Large and tall infrastructure requires pile foundation placed on Soil layer no 4 or 6. Those areas can be used for Commercial, Residential and Industrial Zone.

Table 8.1: Geological classification for infrastructure development

Sl No.	Geological Suitability	Infrastructure foundation suitability	Suggested geological suitability
1	Good	4-6 story light infrastructure is suitable with a foundation depth of around 12 - 20m. Large and tall infrastructure requires pile foundation placed on layer no 4 or 6. Individual on-site subsoil investigation should be required.	Commercial area Residential area, Industrial zone
2	Moderate	4-6 story light infrastructure requires on-site subsoil investigation and proper foundation design. Deep pile foundation is needed for large infrastructure.	Industrial zone, Residential area, Commercial area, Agricultural Zone, Park and Recreation
3	Poor	Detail subsoil investigation and proper foundation design is required for all types of infrastructure, due to low suitability with hazard potential.	Agricultural zone, Wetland Rural settlement Park and Recreation
4	Very Poor	Detail subsoil investigation for deep pile foundation is essential, due to very low soil resistance and high hazard potential. Shallow foundation is not preferred.	Agricultural zone, Wetland Rural settlement Park and Recreation

Yellow colour area of Patharghata, Barguna Sadar, Amtoli, Taltoli and Kalapara upazila is moderately suitable in comparison to other areas within the study area and for light infrastructure requires on-site subsoil investigation and proper foundation design. Deep pile foundation requires for large infrastructure. Such areas can be used as Industrial zone, Residential area, Commercial area, Agricultural Zone, Park and Recreation site. Near about 33.31% area shows moderately suitable for infrastructure development in the study area.

Orange (approx. 35.35% of the total area) and Red (approx. 27.77% of the total area) colour area of Galachipa, Rangabali, Barguna Sadar, Amtoli, Taltoli and Kalapara upazila is poorly and Very poorly suitable in comparison to other areas within the study area for infrastructure development. Detail subsoil investigation and proper foundation design is require for all types of infrastructure, due to low suitability with hazard potential. Agricultural zone, rural settlement, Park and Recreation site are suggested for such sites.

Geological suitability classification has been prepared to reduce the damage of property and life due to seismic hazard by implementing above suggestion.

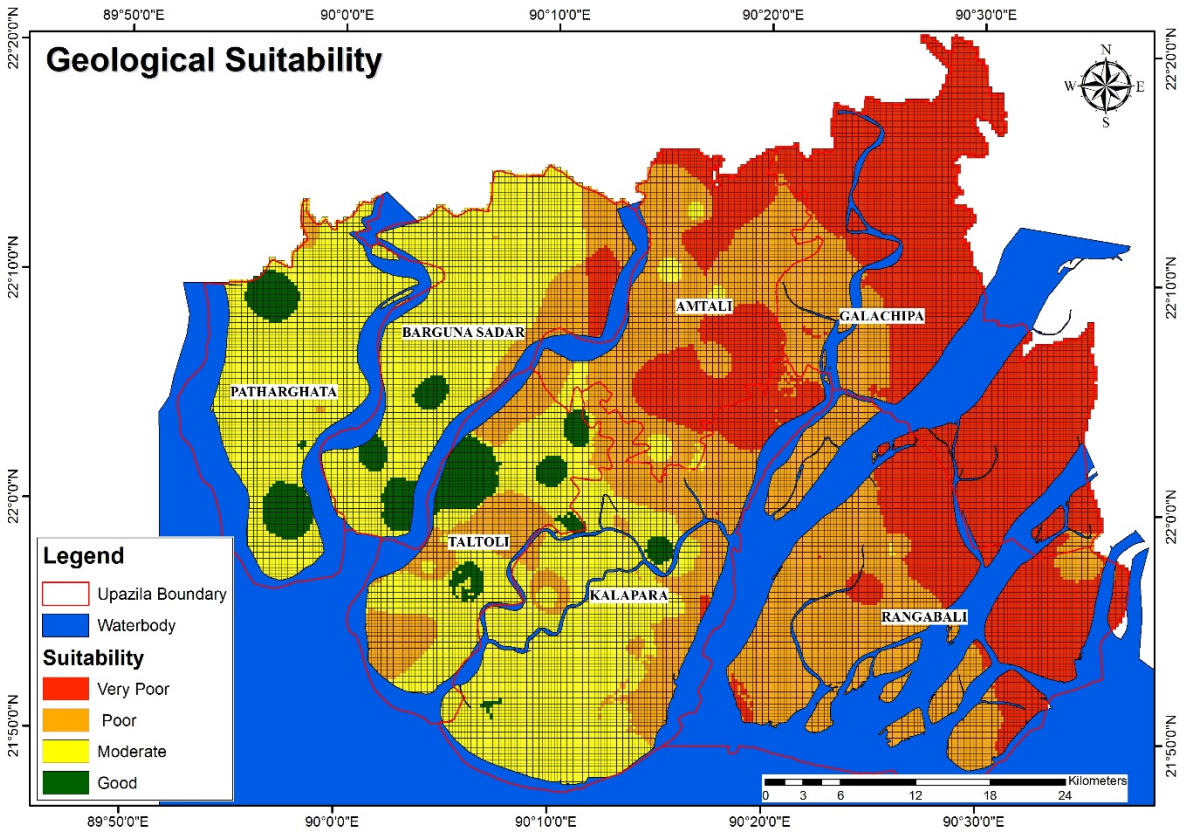

Figure 8.4 Geological Suitability map of Payra-Kuakata

9. CONCLUSION

Earthquakes are related to faulting and tectonic instability of an area. The overall tectonics of Bangladesh and adjoining region is conducive for the frequent and recurring earthquakes. The geo tectonic setting of the country is very active seismically. These are Himalayan Arc, Shillong Plateau and Dauki fault system in the North, Burmese arc and acrretionary wedges in the East, Naga-Disang-Haflong thrust zone in the Northeast. Threatened earthquake disaster inside Bangladesh may be expected from these active seismic zones outside the national boundary.

Seismically, Bangladesh is divided into three zones i.e. highly risk zone (zone 1), moderate risk zone (zone2) and less risk zone (zone3). Payra-Kuakata project area is situated in zone 3. Besides these, this area is located near Arakan Megathrust. So, Payra-Kuakata project area is less vulnerable compare to other zone in Bangladesh for earthquake. To propitiate the risk of earthquake some initiatives have been taken by the concerned authorities. One of the projects works named “Engineering Geological and Geo-Physical Surveys under Preparation of Payra-Kuakata Comprehensive Plan Focusing on Eco-Tourism” which has been initiated by Urban Development Directorate.

This study is an attempt towards refinement in sesimic hazard calculation of Bangladesh using PSHA and DSHA methods. New approaches in seismic source zone delineations, consideration for local site effects and incorporating inherent certainties in different source parameters as well as attenuation relationship are some of the improvements applied in this study.

Results are presented in form of hazard maps and curves showing PGA and SA. Peak ground acceleration has been computed with 2% and 10% probability excedance in 50 years. In this study both peak ground acceleration (PGA) and peak spectral acceleration (PSA) have been estimated considering with site effect. However, the ground motion has found slight higher than all other previous studies. The reason might be due to the utilization of appropriate Ground Motion Prediction Equation for different fault zones and utilization of Vs30 information of the project area to account for the site effect.

It should be noted that there is room for further improvement in tackling the uncertainties of many other source parameters and attenuation models. This study will contribute towards further seismic hazard assessments in Bangladesh and also facilitate in reducing seismic risk in structures by updating building codes in the country.

However, the project area is relatively liquefaction hazard prone. Liquefaction hazard map is showing approx. 67.79% areas are at very high risk, 29.80% have moderate risk and 2.41 % areas are at low and very low risk respectively. Overall the area lies in very high to moderate liquefaction hazard prone area. Most of the area lies within very highly liquefaction hazard prone area (about 67.79%). The remaining project area is mostly in moderate liquefaction hazard prone zone (about 29.80%).

According to Geological suitability map, most of the area is moderately suitable (approx. 33.31%) to poorly suitable (approx. 35.35%) for infrastructure development, mainly in the western part, central part and southern part of the study area as well as north part of the Amtali upazila. Approximately 3.57% (good) area represents very suitable for infrastructure development in the study area. And very poorly (approx. 27.77% of the total area) suitable area for the infrastructure development are along with eastern part as well as north-eastern part of the study area.

10. REFERENCES

i. Abbott, P. L. (2004). Natural Disasters (4th ed.). Boston: McGraw Hill.
ii. Anbazhagan P, Sitharam TG. Mapping of average shear wave velocity for Bangalore region: a case study. Journal of Environmental & Engineering Geophysics 2008;13(2):69–84.
iii. Anbazhagan P, Sitharam TG. Seismic microzonation of Bangalore. Journal of Earth System Science 2008; 117(S2):833–52.
iv. Anbazhagan P, Sitharam TG. Spatial variability of the weathered and engineering bed rock using multichannel analysis of surface wave survey. Pure and Applied Geophysics 2009;166(3):409–28.
v. Auld, B., 1977, Cross-Hole and Down-Hole Vs by Mechanical Impulse, Journal of Geotechnical Engineering Division, ASCE, Vol. 103, No. GT12, pp. 1381-1398
vi. Abrahamson, N.A. & Silva, W., Emperical Responce Spectral Attenuation Relations for Shallow Crustal Earthquakes.
vii. ADPC and OYO, 2009. Time-Predictable fault Modeling of Bangladesh,
viii. Aki, K., 1965. Maximum Likelihood Estimate of b in the formula log N = a - b M and its Confidence Limits. Bulletin of the Earthquake Research Institute, pp.237–239.
ix. Al-hussaini, T.M. & Al-noman, M.N., 2010. PROBABILISTIC ESTIMATES OF PGA AND SPECTRAL ACCELERATION IN BANGLADESH.
x. Al-hussaini, T.M., Al-noman, M.N. & Chowdhury, I.N., 2015. SEISMIC HAZARD ASSESSMENT FOR BANGLADESH - OLD AND NEW PERSPECTIVES.
xi. Ali, M.H. & Choudhury, J.R., 1994. Seismic Zoning of Bangladesh. In International Seminar on Recent Developments in Earthquake Disaster Mitigation. Dhaka. Available at: papers3://publication/uuid/D1250C05-2FC7-4954-A734-E33EBBEECB95.
xii. Ambraseys, N.N., 2004. Three little known early earthquakes in India. Current Science, 86(4), pp.506–508.
xiii. Aminullah, S.A. (2004); “Geotechnical Characteristics of Alluvial deposits of Bangladesh” M.Sc. Engineering thesis, Department of Civil Engineering, Bangladesh University of Engineering & Technology, Dhaka, Bangladesh.
xiv. Ameen (1985) and Bashar (2000) Ameen, S.F. (1985). “Geotechnical Characteristics of Dhaka Clay”. M. Sc. Engineering Thesis, Department of Civil Engineering, Bangladesh University of Engineering and Technology, Dhaka, Bangladesh.
xv. Anon, 2015. Bangladesh National Building Code, Housing and Building Research Institute.
xvi. Atkinson, G.M. & Boore, D.M., 2006. Earthquake ground-motion prediction equations for eastern North America. Bulletin of the Seismological Society of America.
xvii. Atkinson, G.M. & Boore, D.M., 2003. Empirical ground-motion relations for subduction-zone earthquakes and their application to Cascadia and other regions. Bulletin of the Seismological Society of America, 93(4), pp.1703–1729.
xviii. Atkinson, G.M. & Boore, D.M., 1995. Ground-motion relations for eastern north America. Bulletin of the Seismological Society of America, 85(1), pp.17–30.

xix. Aysen, A., 2002. Soil mechanics: basic concepts and engineering applications
xx. Barnes, G. (2001). "Soil Mechanics: Principles and Practice ". Second edition, MacMillan Press Ltd, Houndmills, Basingstoke, Hampshire and London
xxi. Bashar, A.(2000),"Geotechnical Characterization of Dhaka Metropolitan Area". M. Engineering Thesis, Department of Civil Engineering, Bangladesh University of Engineering and Technology, Dhaka, Bangladesh.
xxii. Boulanger, R.W., Idriss, I.M., 2012. Evaluation of overburden stress effects on liquefaction resistance at Duncan Dam. Canadian Geotechnical Journal 49 (9), 1052-1058.
xxiii. Boulanger, R.W., Idriss,I.M., 2014. CPT and SPT based liquefaction triggering procedures. Center for Geotechnical Modeling, Report No. UCD/CGM-14/01.Bender, B., 1983. Maximum likelihood estimation of b values for magnitude grouped data. Bulletin of the Seismological Society of America.
xxiv. Bilham, R., 2004. Historical Studies of Earthquakes in India. Annals of Geophysics, pp.1–26.
xxv. Bommer, J.J. & Abrahamson, N.A., 2006. Why do modern probabilistic seismic-hazard analyses often lead to increased hazard estimates? Bulletin of the Seismological Society of America.
xxvi. Boore, D.M. & Atkinson, G.M., 2008. Ground-motion prediction equations for the average horizontal component of PGA, PGV, and 5%-damped PSA at spectral periods between 0.01 s and 10.0 s. Earthquake Spectra.
xxvii. Banglapedia 2015 - http://en.banglapedia.org/index.php?
xxviii. Campbell, K.W. & Bozorgnia, Y., 2003. Updated near-source ground-motion (attenuation) relations for the horizontal and vertical components of peak ground acceleration and acceleration response spectra. Bulletin of the Seismological Society of America.
xxix. Chiou, B.S.J. & Youngs, R.R., 2008. An NGA model for the average horizontal component of peak ground motion and response spectra. Earthquake Spectra, 24(1), pp.173–215.
xxx. Chowdhury, I.N., 2016. Neo-Deterministic Studies for Seismic Hazard Assessment of Bangladesh. , (June).
xxxi. Cornell, C.A., 1968. Engineering seismic risk analysis. Bulletin of the Seismological Society of America, 58(5), pp.1583–1606. Available at: http://bssa.geoscienceworld.org/cgi/content/abstract/58/5/1583%5Cnhttp://bssaonline.org/cgi/content/abstract/58/5/1583.
xxxii. Comprehensive Disaster Management Program (CDMP II), 2013. Report of active fault mapping in Bangladesh: paleoseismological study of the Dauki fault and the Indo-Burman plate boundary fault. Final Report. Ministry of Disaster Management and Relief, Dhaka, Bangladesh.
xxxiii. Cetin, K.O., Seed, R.B., Der Kiureghian A. , Harder Jr. L. F. , Kayen R. E. , Moss R. E. S. , Tokimatsu K., 2004. Standard penetration test-based probabilistic and deterministic assessment of seismic soil liquefaction potential. J. Geotech. Geoenviron.
xxxiv. Coduto Donald P., 2002, Geotecnical Engineering Principles and Practices,California State Polytechnic University, Pomona, 372-393p, 424-425p.
xxxv. Garnder, J.K. & Knopoff, L., 1974. Bulletin of the Seismological Society of America. Bulletin of the Seismological Society of America, 64(5), pp.1271–1302. Available at: http://www.bssaonline.org/cgi/content/abstract/66/3/639.
xxxvi. Ghosh, B. et al., 2012. Seismic Hazard Assessment in India. 15th World Conference on Earthquake Engineering. Available at: http://www.iitk.ac.in/nicee/wcee/article/WCEE2012_2107.pdf.
xxxvii. GSB, 1979. Final report by the Committee of Experts on Earthquake Hazard Minimization,
xxxviii. Gutenberg, B. & Richter, C.F., 1944. Frequency of earthquakes in California. Bulletin of the Seismological Society of America, 34, pp.185–188.

xxxix. Fard M.Y., Babazadeh M., Yousefzadeh P., 2013. Soil liquefaction analysis based on geotechnical exploration and in situ test data in the Tabriz Metro Line 2. Seventh Int. Con. On Case Histories in Geotechnical Engineering, paper 31.
xl. Farazi, A.H., Nasim, F., Kamal, A.S.M.M., 2018. LPI Based Earthquake Induced Soil Liquefaction Susceptibility Assessment at Probashi Palli Abasan Project Area, Tongi, Gazipur, Bangladesh. Journal of Scientific Research (JSR). 10 (2), 105-116. DOI: http://dx.doi.org/10.3329/jsr.v10i2.34225
xli. Geological Map of Bangladesh (2001), Digitally compiled by F.M.Persits, C.J.Wandrey, R.C. Milici, (USGS), and Abdullah Manwar, (Director General, Geological Survey of Bangladesh)
xlii. http://gsb.portal.gov.bd/sites/default/files/files/gsb.portal.gov.bd/common_document/a515fee7_9cc5_44d3_bfc2_af21258155e1/Geological%20Map%20of%20Bangladesh.pdf
xliii. Groot, M.B.D., Bolton, M.D., Foray, P., Meijers, P., Palmer, A.C., Sandven, R., Sawicki, A., The T.C., 2006. Physics of liquefaction phenomena around marine structures.J. Waterw., Port, Coastal, Ocean Eng. 132, 227–243.
xliv. Hamada, M., Isoyama, R., Wakamatsu, K., 1995.The 1995 Hyogoken-Nanbu (Kobe)earthquake—liquefaction, ground displacement, and soil condition in the Hanshinarea.The School of Science and Engineering, Waseda University, Tokyo.
xlv. Hanks, T.C. & Kanamori, H., 1979. A moment magnitude scale. In Journal of Geophysical Research B: Solid Earth. pp. 2348–2350.
xlvi. Heaton, T.H. & Tajima, F., 1986. Estimating Ground Motions Using Recorded Accelerograms. , 8, pp.25–83.
xlvii. Holzer, T.L., Bennett, M.J., Noce, T.E., Padovani, A.C., Tinsley J.C. III.,2006. Liquefaction hazard mapping with LPI in the Greater Okland, California, area. Earthquake Spectra 22 (3), 693□708.
xlviii. Islam, M.S. et al., 2010. ATTENUATION OF EARTHQUAKE INTENSITY IN BANGLADESH. In Proceedings, 3rd International Earthquake Symposium, Bangladesh, Dhaka, March.5-6 2010.
xlix. Islam, M. S. (1999). “Strength and Deformation Anisotropy of Clays”. M. Sc. Engineering Thesis, Department of Civil Engineering, Bangladesh University of Engineering and Technology, Dhaka Bangladesh.
l. Idriss, I.M., Boulanger, R.W., 2004.Semi-empirical procedures for evaluating liquefaction potential during earthquakes. Proc. of 11th International Conf. on Soil Dynamics and Earthquake Engineering, and 3rd International Conf. on Earthquake Geotechnical Engineering, Berkeley, pp. 32–56.
li. Idriss, I.M., Boulanger R.W., 2010. SPT-based liquefaction triggering procedures. Center for Geotechnical Modeling, Report No. UCD/CGM-10-02.
lii. Ishiyama Y., (2011). Introduction to earthquake engineering and seismic codes in the world.
liii. Iwasaki, T., Tatsuoka, F., Tokida, K.-I., Yasuda, S., 1978.Apractical method for assessing soil liquefaction potential based on case studies at various sites in Japan. Proc. of 2nd International Conference on Microzonation, San Francisco, pp. 885–896.
liv. Iwasaki, T., Tokida, K., Tatsuoka, F., Watanabe, S., Yasuda, S., Sato, H., 1982.Microzonation for soil liquefaction potential using simplified methods. Proc. of 3rd International Earthquake Microzonation Conference, Seattle, pp. 1319–1330.
lv. Jha, S.K., Suzuki, K., 2009. Liquefaction potential index considering parameter uncer-tainties. Eng. Geol. 107, 55–60.
lvi. Juang, C.H., Yuan, H., Lee, D.H., Lin, P.S., 2003. A simplified CPT-based method for evaluating liquefaction potential of soils. J. Geotech. Geoenviron. Eng. 129 (1), 66–80.
lvii. Kienholz, H., Hafner, H., Schneider, G., & Tamrakar, R. (1983). Mountain Hazards Mapping

in Nepal's Middle Mountains Maps of Land Use and Geomorphic Damages (Kathmandu-Kakani Area). Mountain Research and Development, 3(3), 195–220.

lviii. Kitsunezaki. C. ,N. Goto, Y. Kobayashi., T. Ikawa, M. Horike, T. Saito, T. Kurota, K. Yamane, and K. Okuzumi, 1990, Estimation of P- and S- wave velocities in Deep Soil Deposits for Evaluating Ground Vibrations in Earthquake, SIZEN-SAIGAI-KAGAKU,9-3,1-17 (in Japanese).

lix. Kang, G.C., Chung, J.W., Rogers, J.D., 2014. Re-calibrating the thresholds for the classification of liquefaction potential index based the 2004 Niigata-ken Chuetsu earthquake. Eng. Geol. 169, 30–40.

lx. Le Dain, A.Y., Tapponnier, P., Molnar, P., 1984. Active faulting and tectonics of Burma andsurrounding regions. J. Geophys. Res. 89, 453–472.

lxi. Lee, D.H., Ku, C.S., Yuan, H., 2004.A study of the liquefaction risk potential at Yuanlin, Taiwan. Eng. Geol. 71, 97–117.

lxii. Luna, R. and Frost, J. D., 1998.Spatial liquefaction analysis system, J. Comput. Civil Eng. 12, 48–56.

lxiii. Ludwig, W.J., Nafe, J.E., and Drake, C.L., 1970, Seismic refraction, in The Sea, A.E. Maxwell (Editor), Vol. 4, Wiley-Interscience, New York, pp. 53-84

lxiv. Miller RD, Xia J, Park CB, Ivanov J. Multichannel analysis of surface waves to map bedrock. The Leading Edge 1999;18(12):1392–6.

lxv. Makropoulos, K.C. & Burton, P.W., 1983. Seismic risk of circum-pacific earthquakes I. Strain energy release. Pure and Applied Geophysics PAGEOPH.

lxvi. Musson, R.M.W., 1999. Probabilistic seismic hazard maps for the north Balkan region. Annals of Geophysics.

lxvii. Malczewski, J. (1999). GIS and multicriteria decision analysis. Engineering (Vol. 31).

lxviii. Noor, M.A., Yasin, M. & Ansary, M.A., 2005. Seismic Hazard Analysis of Bangladesh. In First Bangladesh Earthquake Symposium. Dhaka.

lxix. Okada, H., 2003, The microtremor survey method, Society of Exploration Geophysicist, Tulsa

lxx. Park CB, Miller RD, Xia J. Multi-channel analysis of surface waves. Geophysics 1999; 64(3):800–8.

lxxi. Papathanassiou, G., 2008. LPI-based approach for calibrating the severity of liquefaction induced failures and for assessing the probability of liquefaction surface evidence. Eng. Geol. 96, 94–104.

lxxii. Palacios, I.V., Espinosa, I.V., Vidal F., Chacon J., Irigaray C., 2012. Spatial variability of liquefaction susceptibility in the Metropolitan area of Granada (Spain).15 WCEE Proceedings.

lxxiii. Rahman, M.Z., Siddiqua, S., Kamal, A.S.M., 2015. Liquefaction hazard mapping by liquefaction potential index for Dhaka City, Bangladesh. Eng. Geol. 188, 137-147.

lxxiv. Rahman, M.Z., Hossain, M.S., Kamal, A.S.M.M., Siddiqua, S., Farazi, A.H., 2017. Seismic site characterization for Moulvibazar town, Bangladesh. Bulletin of Engineering Geology and the Environment. 1-21. DOI https://doi.org/10.1007/s10064-017-1031-6

lxxv. Sadek, S., Najjar, S., Mostapha, Y., Mostapha, M., 2014. Assessment of the potential for earthquake induced liquefaction in granular soils. Spreadsheets in in Education (eJSiE) 7 (2), 1-30.

lxxvi. Saaty, T.L. (1980) The Analytic Hierarchy Process. McGraw-Hill, New York.

lxxvii. Saaty, T. L. (1994). How to Make a Decision: The Analytic Hierarchy Process. Interfaces, 24, 19-43. https://doi.org/10.1287/inte.24.6.19

lxxviii. Scordilis, E.M., 2006. Empirical global relations converting MSand mbto moment magnitude. Journal of Seismology, 10(2), pp.225–236.

lxxix. Silva, V. et al., 2014. Development of the Open Quake engine, the Global Earthquake Model's

open-source software for seismic risk assessment. Natural Hazards, 72(3), pp.1409–1427.

lxxx. Sipkin, S.A., 2003. A Correlation to Body-wave magnitude mb Based on Moment Magnitude Mw. Seismological Reserch Letters, 74(6), pp.739–742.

lxxxi. Steckler, M.S. et al., 2016. Locked and loading megathrust linked to active subduction beneath the Indo-Burman Ranges. Nature Geoscience, 9(8), pp.615–618.

lxxxii. Stepp, J.C., 1972. Analysis of completeness of the earthquake sample in the Puget Sound area and its effect on statistical estimates of earthquake hazard. Proc. of the 1st Int. Conf. on Microzonazion, Seattle,Vol. 2, (July), pp.897–910.

lxxxiii. Strasser, F.O., Arango, M.C. & Bommer, J.J., 2010. Scaling of the Source Dimensions of Interface and Intraslab Subduction-zone Earthquakes with Moment Magnitude. Seismological Research Letters, 81(6), pp.941–950.

lxxxiv. Sawicki, A., and Mierczyński, J., 2006. Developments in modeling liquefaction of granular soils, caused by cyclic loads. Applied Mechanics Reviews 59, 91-106

lxxxv. Sawicki, A., and Swidzinski, W., 2007. Simple mathematical model for assessment of seismic induced liquefaction of soils. J. Waterw., Port, Coastal, Ocean Eng., 133, 50-54.

lxxxvi. Sawicki, A., and Sławińska, J., 2015. Liquefaction of saturated soil and diffusion equation.StudiaGeotechnicaetMechanica 37, 39-44.

lxxxvii. Seed, H.B., Idriss, I.M., 1971.Simplified procedure for evaluating soil liquefaction potential. J. Soil Mech. Found. Div. ASCE 97 (9), 1249–1273. Safety factor vs layer then lpi

lxxxviii. Seed, H.B., Idriss, I.M., 1982. Ground motions and soil liquefaction during earthquakes. Earthquake Engineering Research Institute Monograph, Oakland, CA.

lxxxix. Seed, H.B., Tokimatsu, K., Harder Jr., L.F., Chung, R., 1985. Influence of SPT procedures in soil liquefaction resistance evaluations. J. Geotech. Eng. ASCE 111 (12), 1425–1445.

xc. Seed, R.B., Cetin, K.O., Moss, R.E.S., Kammerer, A., Wu, J., Pestana, J., Riemer, M., 2001. Recent advances in soil liquefaction engineering and seismic site response evaluation. Proc. Of4th International Conference and Symposium on Recent Advances in Geo-technical Earthquake Engineering and Soil Dynamics, Univ. of Missouri, Rolla, Paper SPL-2.

xci. Seed R.B., Cetin K.O., Moss. R.E.S., Kammerer A.M., Wu J., Pestana J.M., Reimer M.F., Sanico R.B., Bray J.D., Kayen R.E., Faris A., 2003. Recent advances in soil liquefaction engineering: a unified and consistent framework. 26th Annual ASCE Los Angeles Geotechnical Spring Seminar.

xcii. Siddique, A. (1986). "Permeability and Consolidation Characteristics of Normally Consolidated Clays". M. Sc. Engineering Thesis, Department of Civil Engineering, Bangladesh University of Engineering and Technology, Dhaka, Bangladesh.

xciii. Steckler M.S., Akhter S.H., Seeber L., 2008. Collision of the Ganges-Brahmaputra Delta with the Burma Arc: Implications for earthquake hazard. Earth and Planetary Science Letters, 273, 367-378.

xciv. Tan C.S., Leong T.K., Teng L.S., 2013. The role of fines in liquefaction susceptibility of sand matrix soils.EJGE 18, 2355-2368.

xcv. U.S. Geological Survey, USGS. Available at: https://earthquake.usgs.gov/earthquakes/search/ [Accessed June 13, 2018].

xcvi. Uddin, K. M. (1990). "Compressibility and Shear Strength of Remoulded Clay". M. Sc. Engineering thesis, Department of Civil Engineering, Bangladesh University of Engineering and Technology, Dhaka, Bangladesh.

xcvii. UNCRD, 2008, From Code to Practice: Challenges for BuildingCode Implementation and the Further Direction of Housing Earthquake Safety.

xcviii. Wang, Y., 2014. Active tectonic and earthquake Myanmar region. Journal of Geophysical Research: Solid Earth, pp.3576–3822.

xcix. Wang, Y. et al., 2014. Active tectonic and earthquake Myanmar region. Journal of Geophysical Research: Solid Earth, 119, pp.3576–3822.

c. Weatherill, G.A., 2014. OpenQuake Hazard Modeller ' s Toolkit-User Guide,

ci. Youngs, R., 1997. Youngs et al_Strong Ground Motion Attenuation Relationships for Subduction Zone Earthquakes.pdf. Seismological Research Letters, 68(1), pp.58–73.

cii. Yu, W. & Sieh, K., 2013. Active tectonic features that pose a seismic threat to Bangladesh, Dhaka.

ciii. Youd, T.L., Idriss, I.M., Andrus, R.D., Arango, I., Castro, G., Christian, J.T., Dobry, R., Finn, W.D.L., Harder Jr., L.F., Hynes, M.E., Ishihara, K., Koester, J.P., Liao, S.S.C., MarcusonIII, W.F., Martin, G.R., Mitchell, J.K., Moriwaki, Y., Power, M.S., Robertson, P.K., Seed, R.B., Stokoe II, K.H., 2001.Liquefaction resistance of soils: summary report from the 1996 NCEER 14 and 1998 NCEER/NSF workshop on evaluation of liquefaction resistance of soils. J. Geotech. Geoenviron. Eng. 127 (10), 817–833.org/10.3390/su8040334

Appendix

Cross Section at 2500m Interval

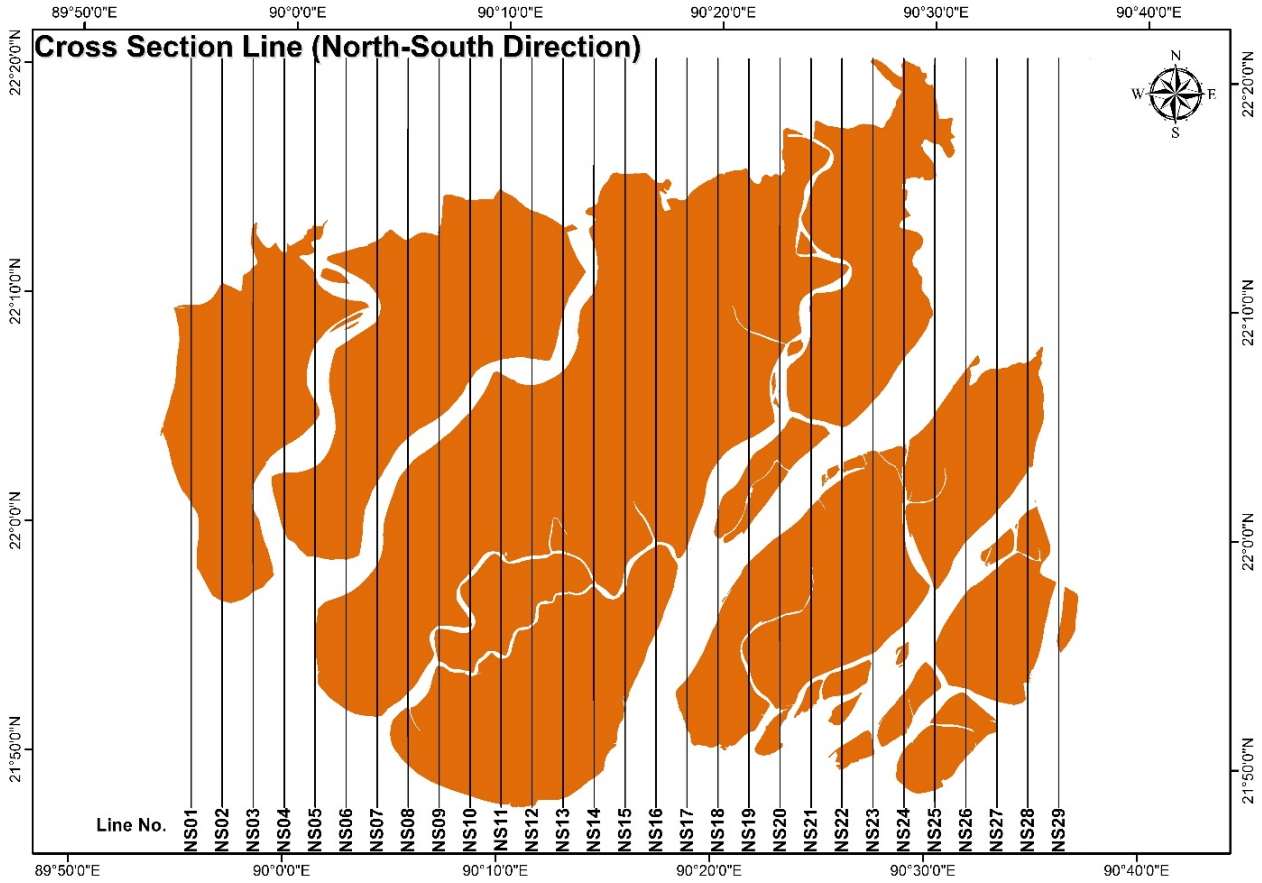

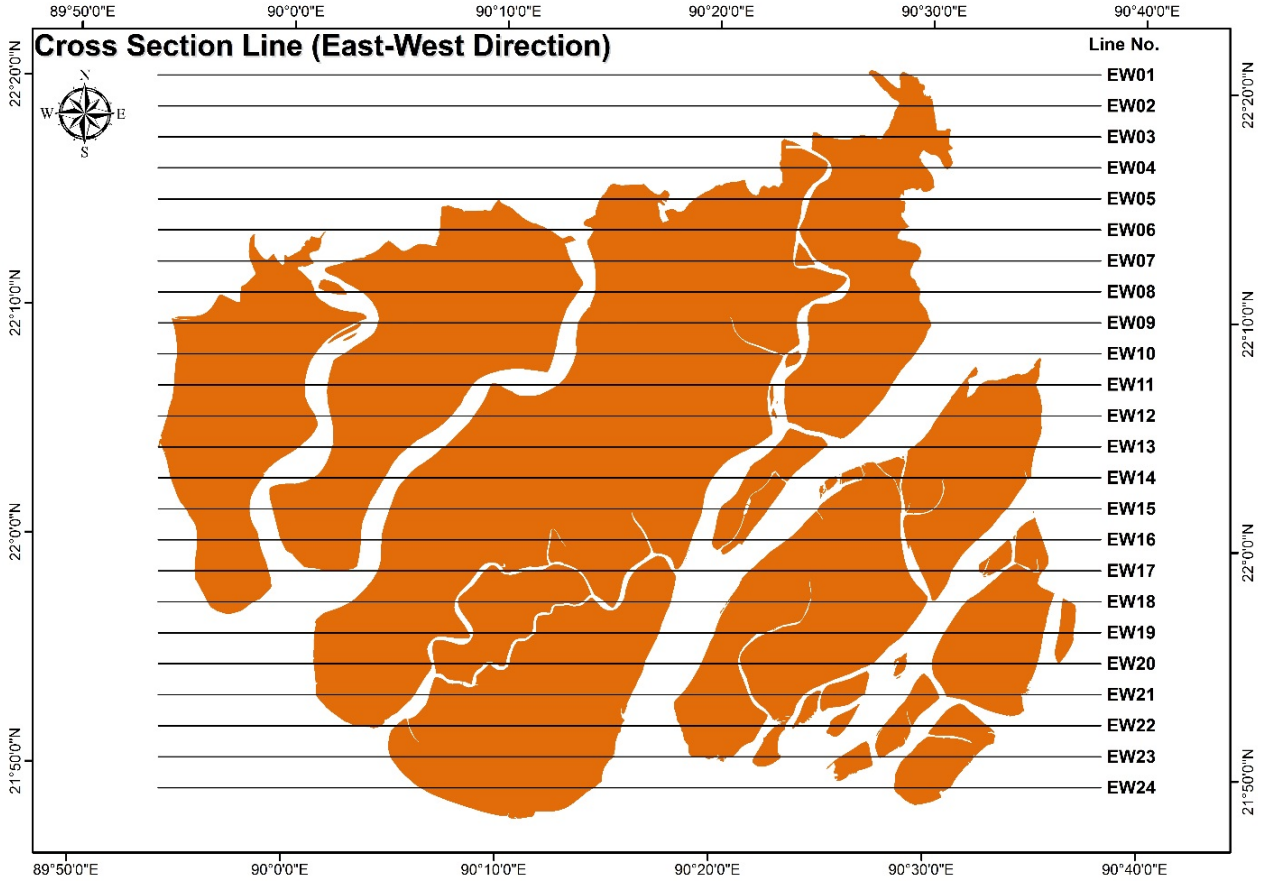

V.Soft to M.Stiff Clayey SILT/Silty CLAY	M.Stiff to Hard Silty CLAY/SILT
V.Loose to M.Dense V.Fine to Fine SAND	M.Dense to V.Dense V.Fine to M. SAND
M.Stiff to Stiff Clayey SILT/Silty CLAY	M.Stiff toV.Stiff Silty CLAY/Clayey SILT
M.Dense to Dense V.Fine to M. SAND	

Line: NS01

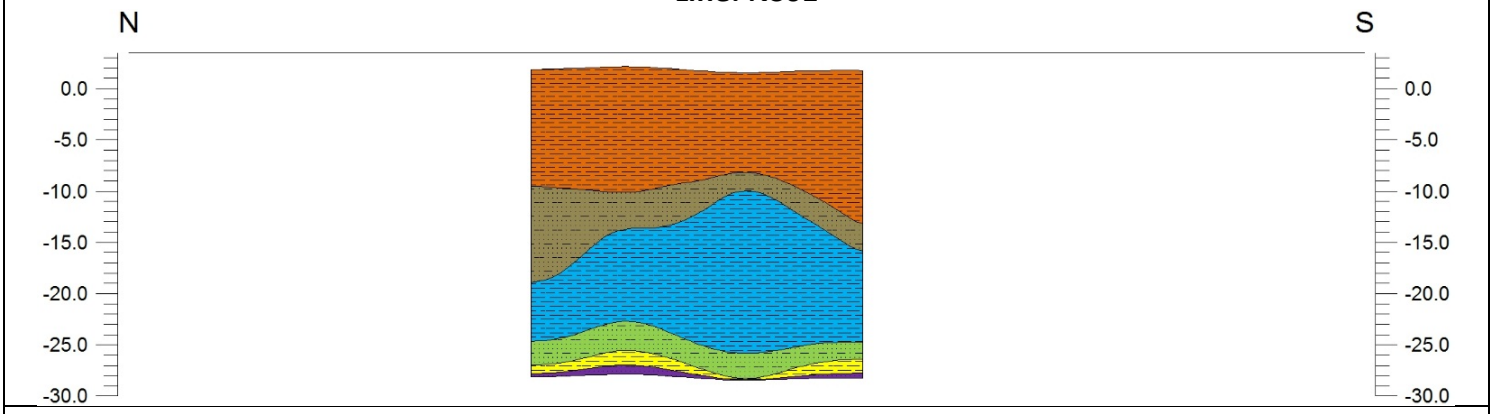

Line: NS02

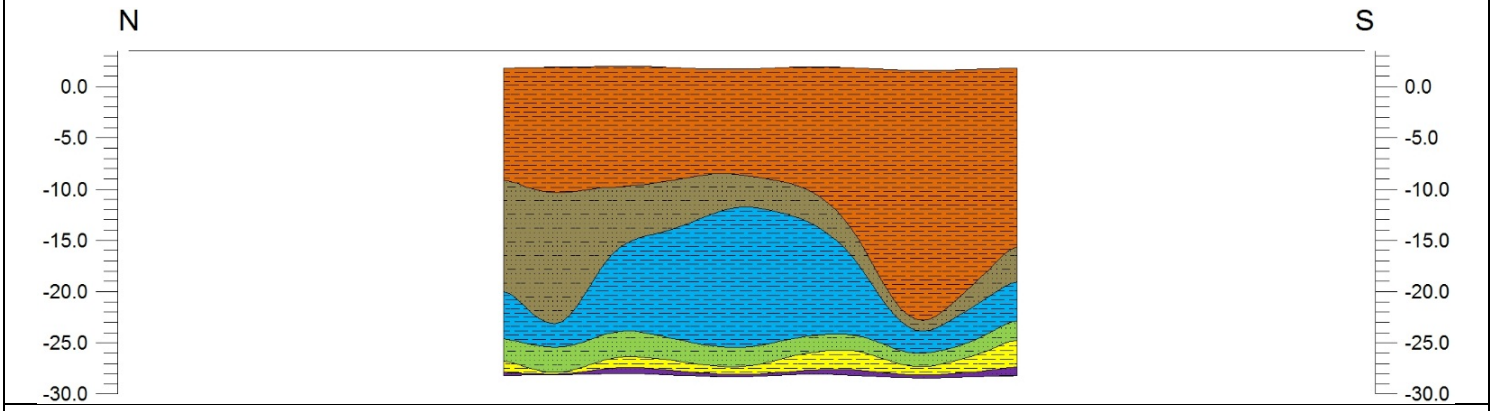

Line: NS03

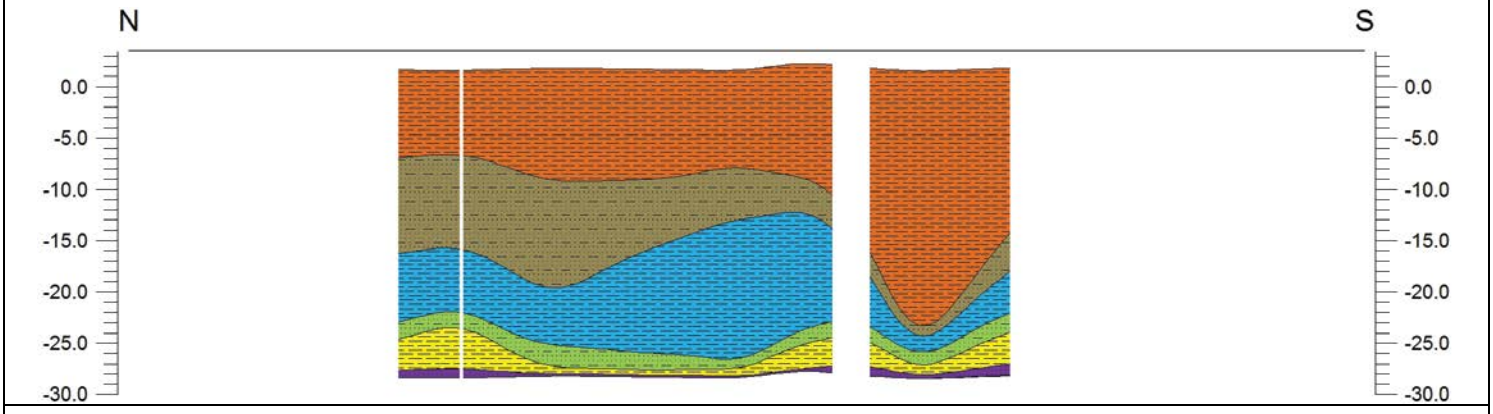

Line: NS04

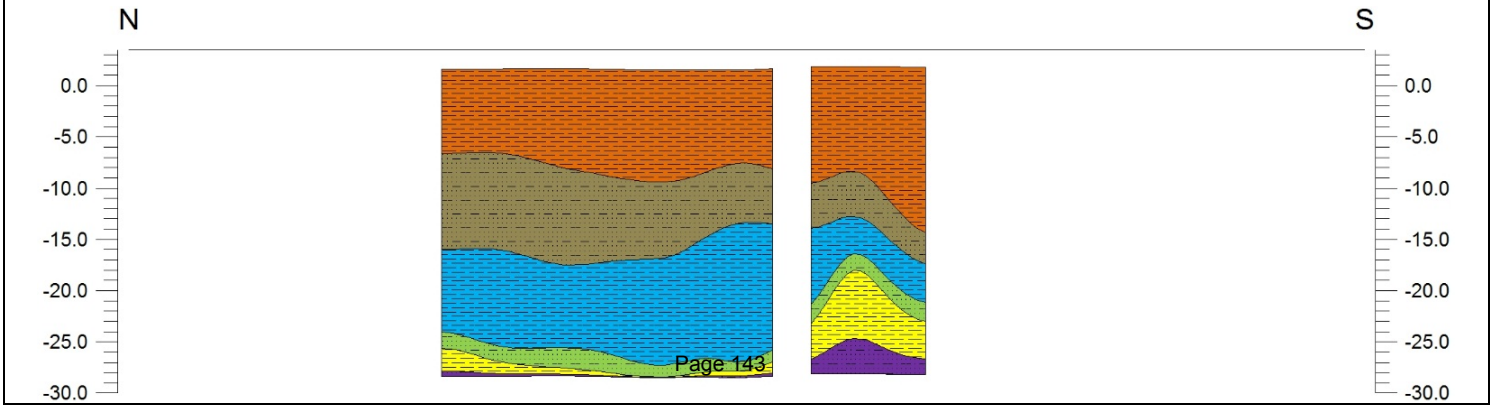

V.Soft to M.Stiff Clayey SILT/Silty CLAY	M.Stiff to Hard Silty CLAY/SILT
V.Loose to M.Dense V.Fine to Fine SAND	M.Dense to V.Dense V.Fine to M. SAND
M.Stiff to Stiff Clayey SILT/Silty CLAY	M.Stiff toV.Stiff Silty CLAY/Clayey SILT
M.Dense to Dense V.Fine to M. SAND	

Line: NS05

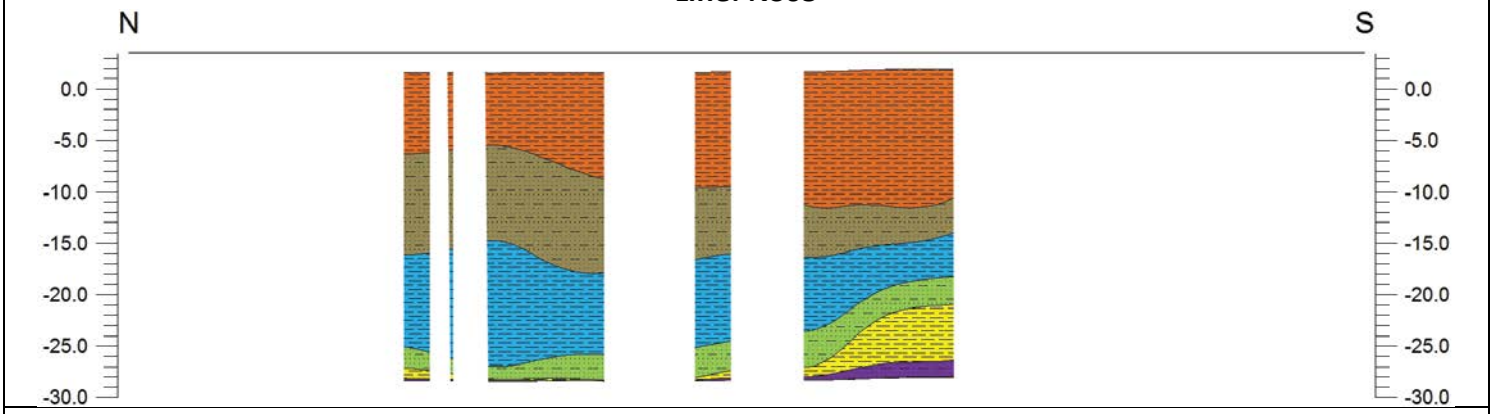

Line: NS06

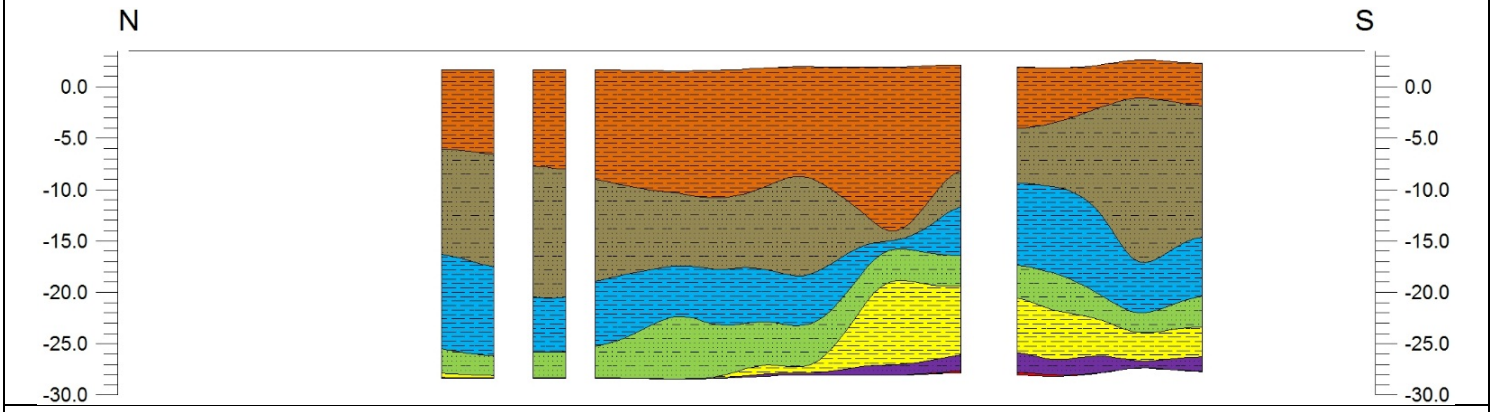

Line: NS07

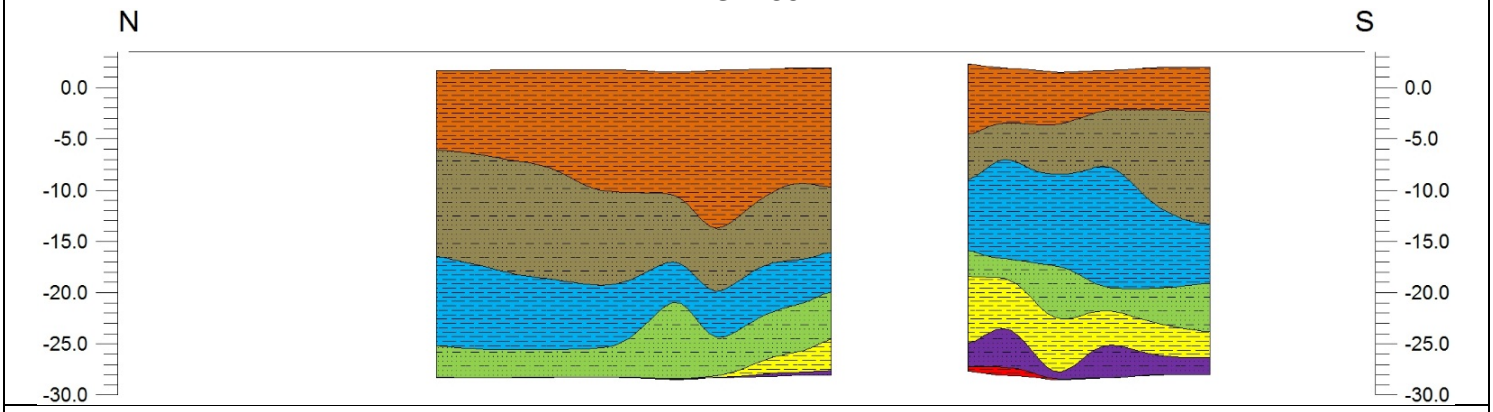

Line: NS08

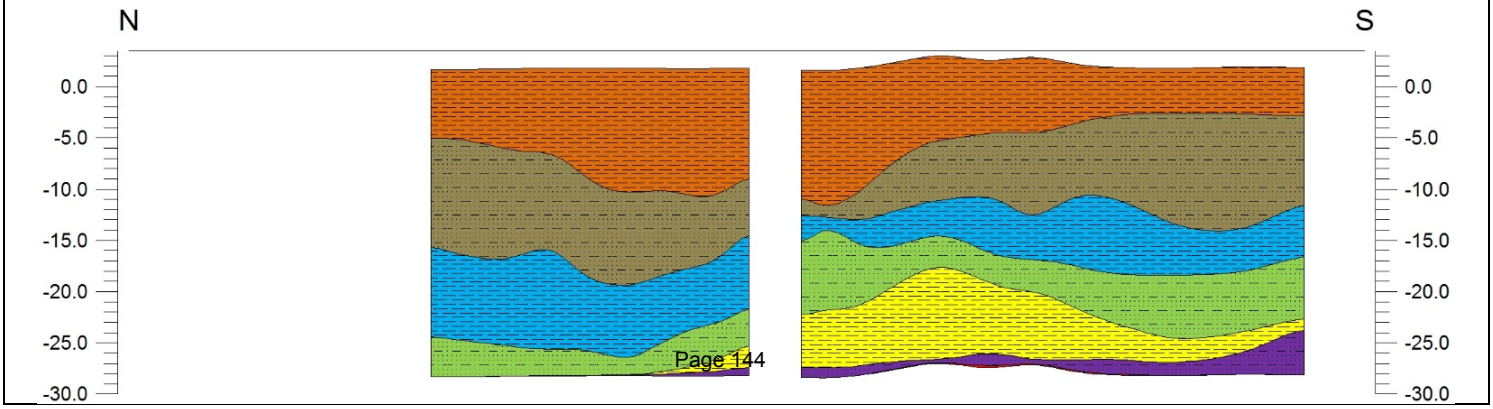

V.Soft to M.Stiff Clayey SILT/Silty CLAY	M.Stiff to Hard Silty CLAY/SILT
V.Loose to M.Dense V.Fine to Fine SAND	M.Dense to V.Dense V.Fine to M. SAND
M.Stiff to Stiff Clayey SILT/Silty CLAY	M.Stiff toV.Stiff Silty CLAY/Clayey SILT
M.Dense to Dense V.Fine to M. SAND	

Line: NS09

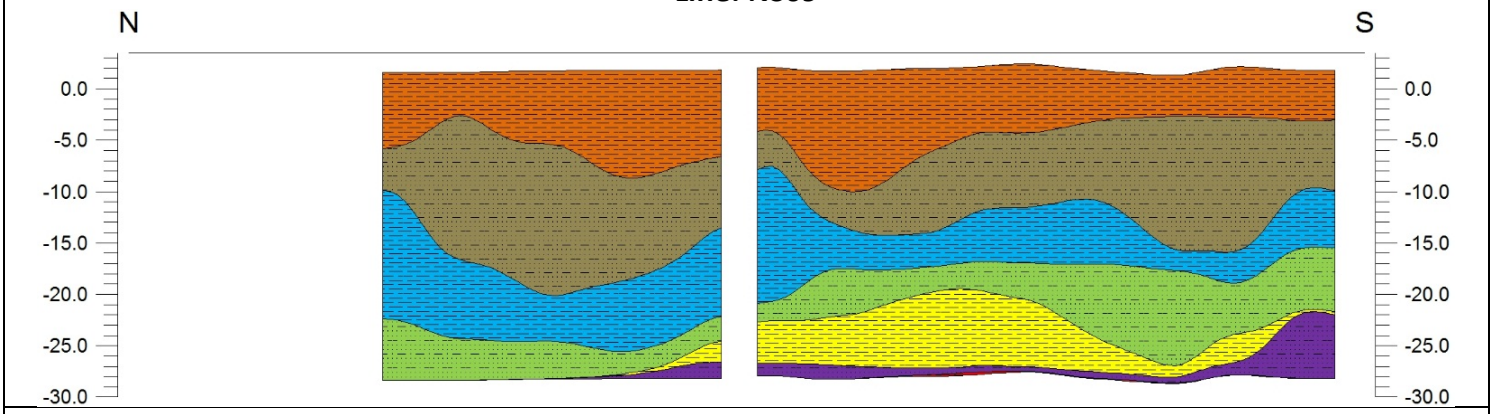

Line: NS10

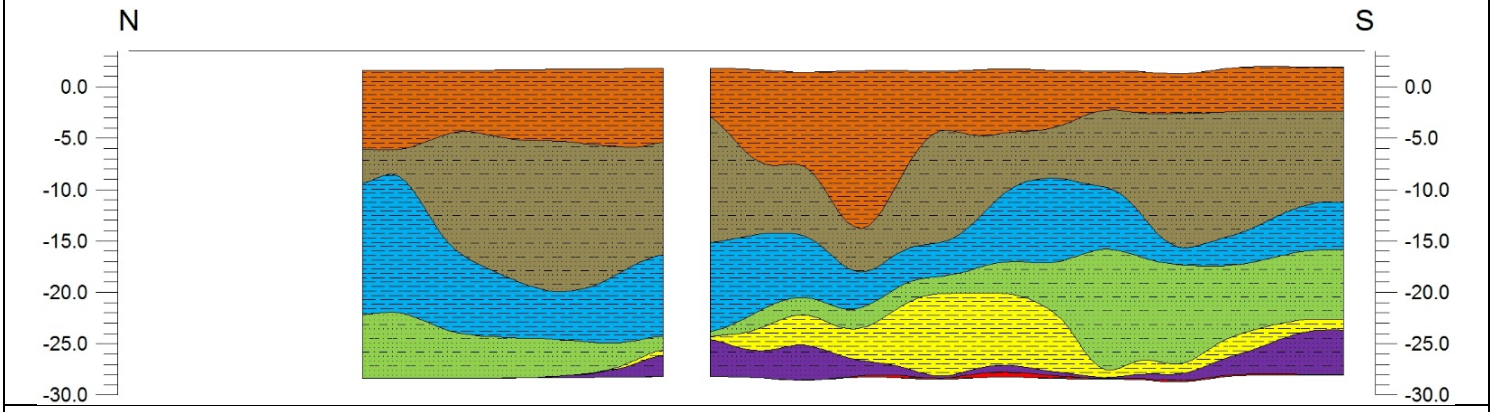

Line: NS11

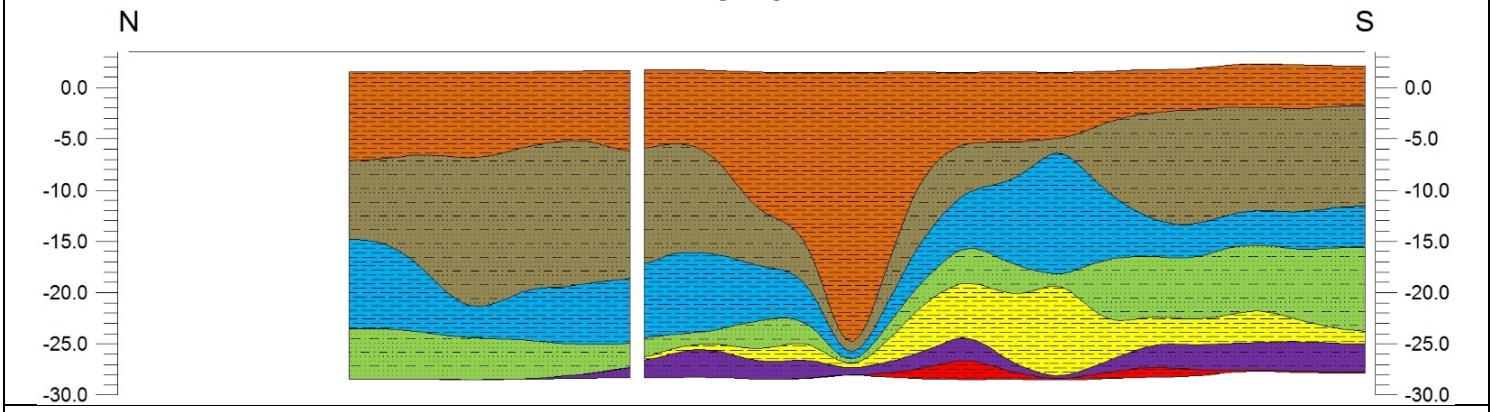

Line: NS12

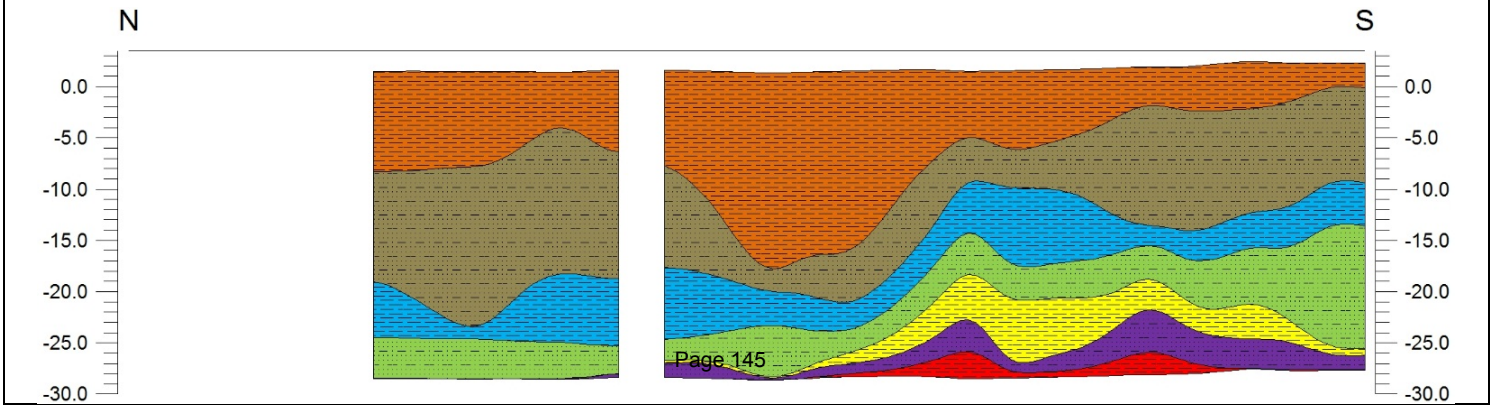

V.Soft to M.Stiff Clayey SILT/Silty CLAY	M.Stiff to Hard Silty CLAY/SILT
V.Loose to M.Dense V.Fine to Fine SAND	M.Dense to V.Dense V.Fine to M. SAND
M.Stiff to Stiff Clayey SILT/Silty CLAY	M.Stiff toV.Stiff Silty CLAY/Clayey SILT
M.Dense to Dense V.Fine to M. SAND	

Line: NS13

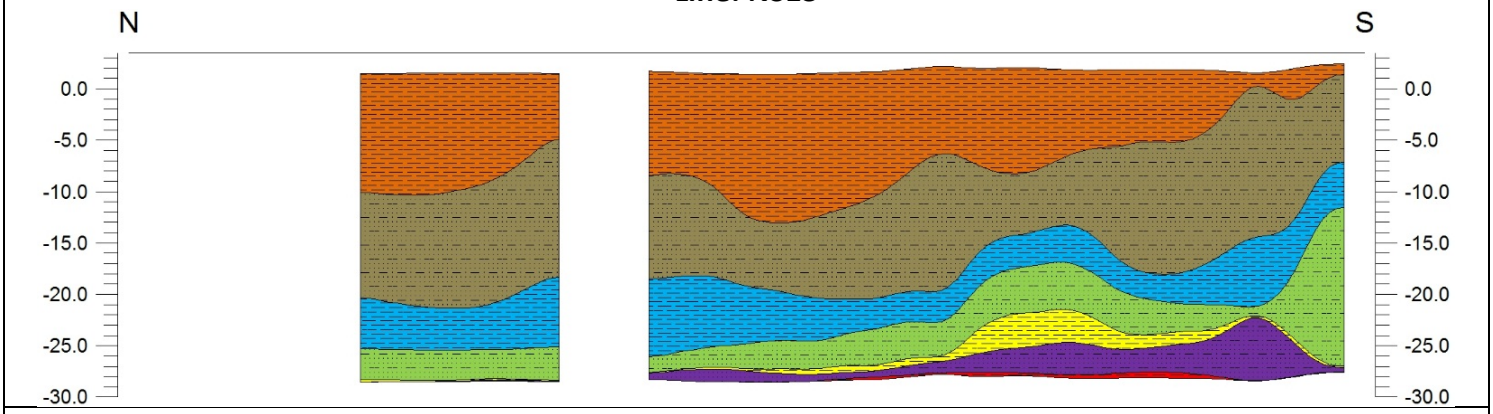

Line: NS14

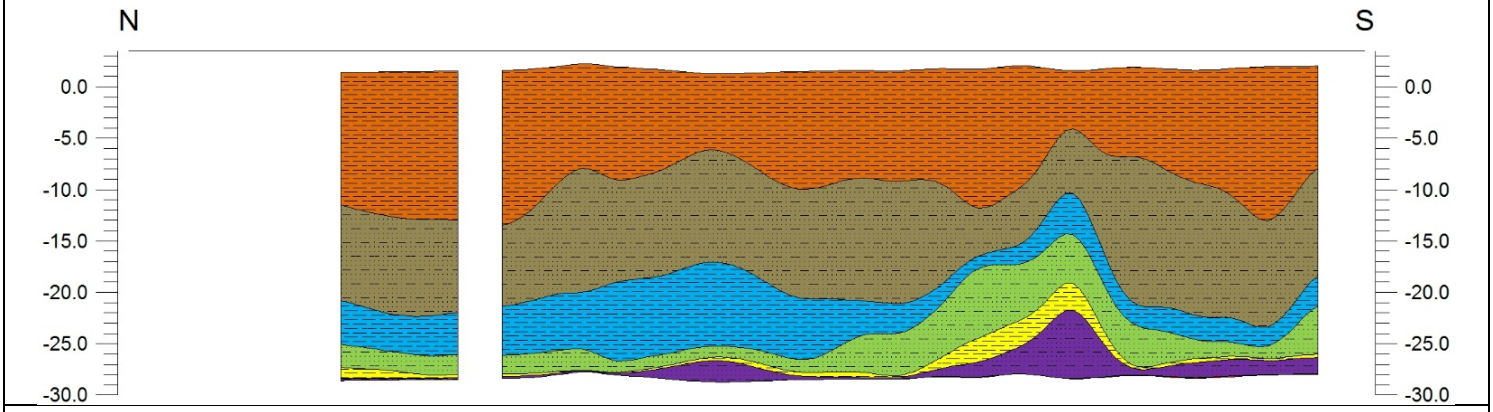

Line: NS15

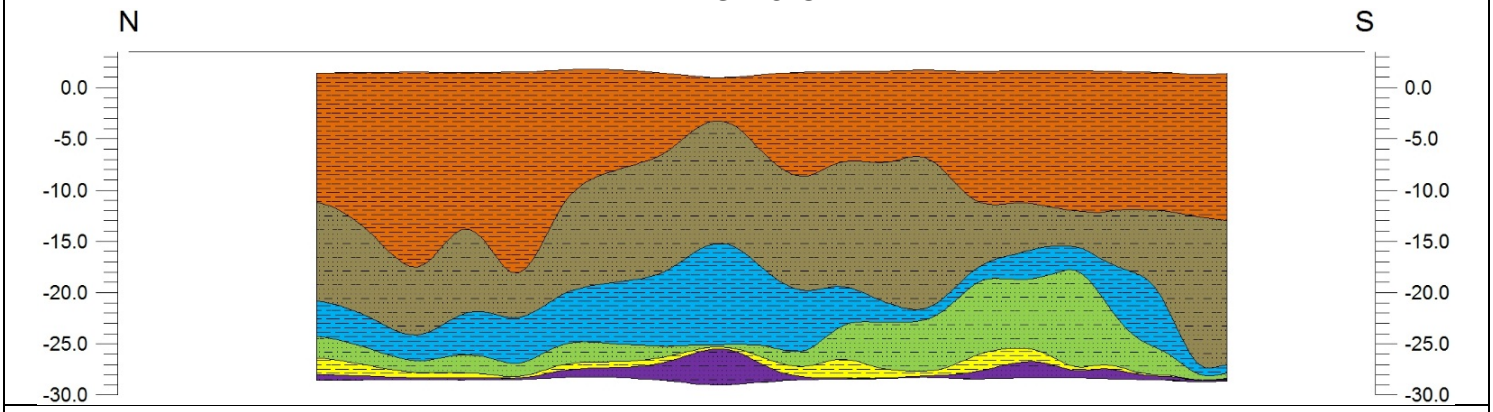

Line: NS16

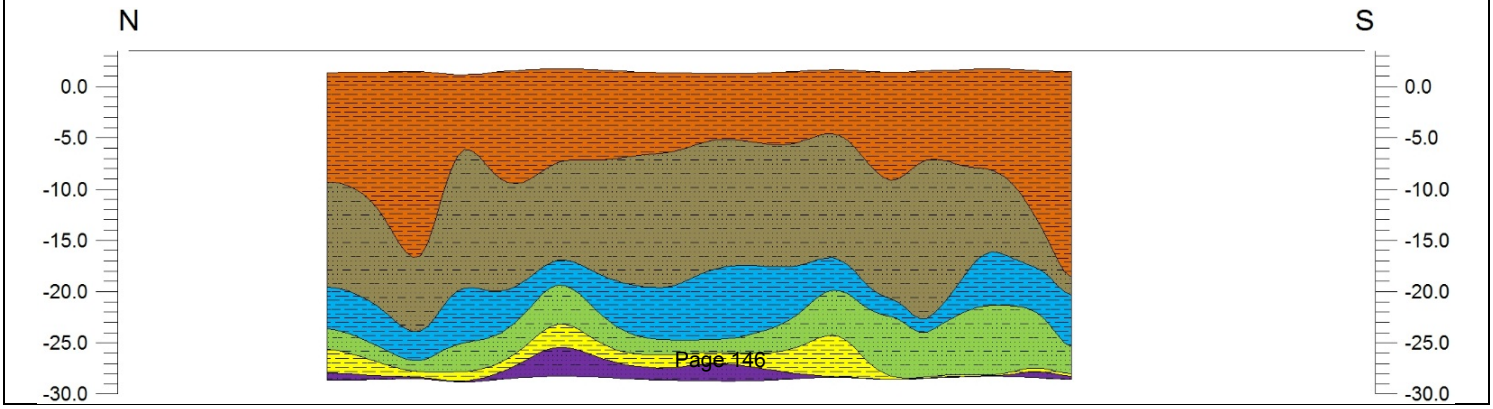

V.Soft to M.Stiff Clayey SILT/Silty CLAY	M.Stiff to Hard Silty CLAY/SILT
V.Loose to M.Dense V.Fine to Fine SAND	M.Dense to V.Dense V.Fine to M. SAND
M.Stiff to Stiff Clayey SILT/Silty CLAY	M.Stiff toV.Stiff Silty CLAY/Clayey SILT
M.Dense to Dense V.Fine to M. SAND	

Line: NS17

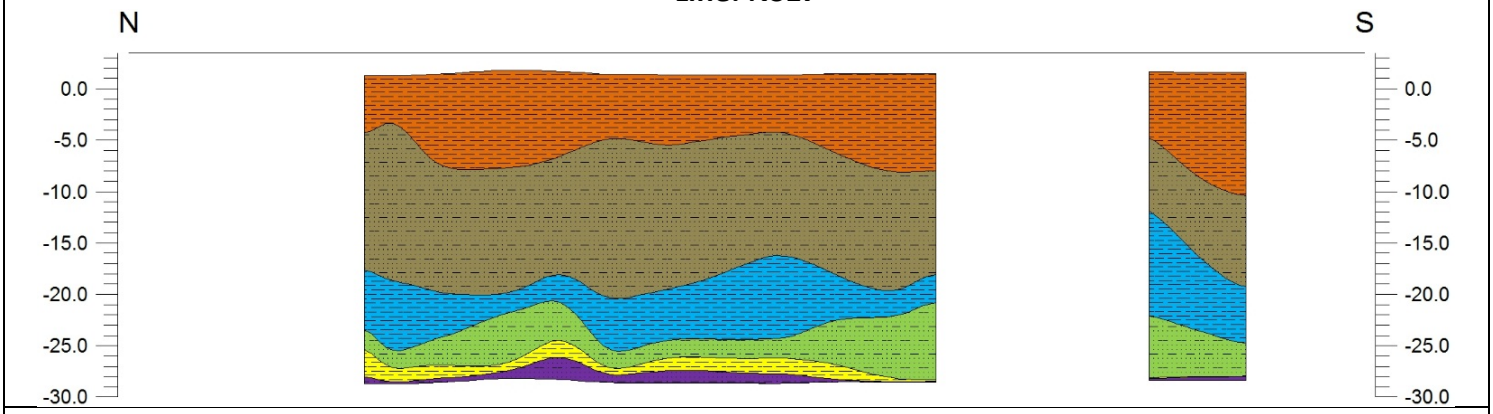

Line: NS18

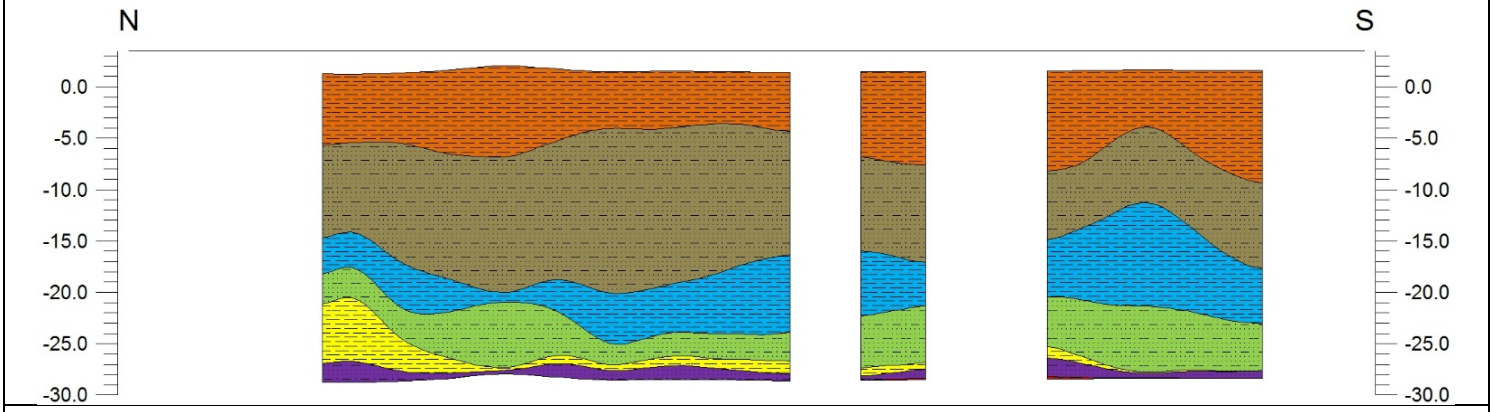

Line: NS19

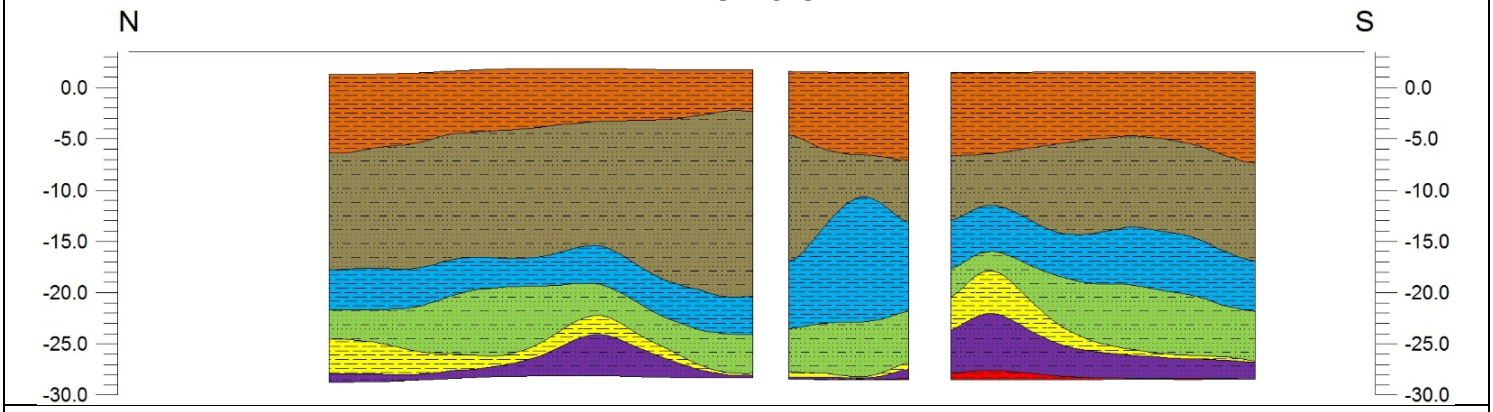

Line: NS20

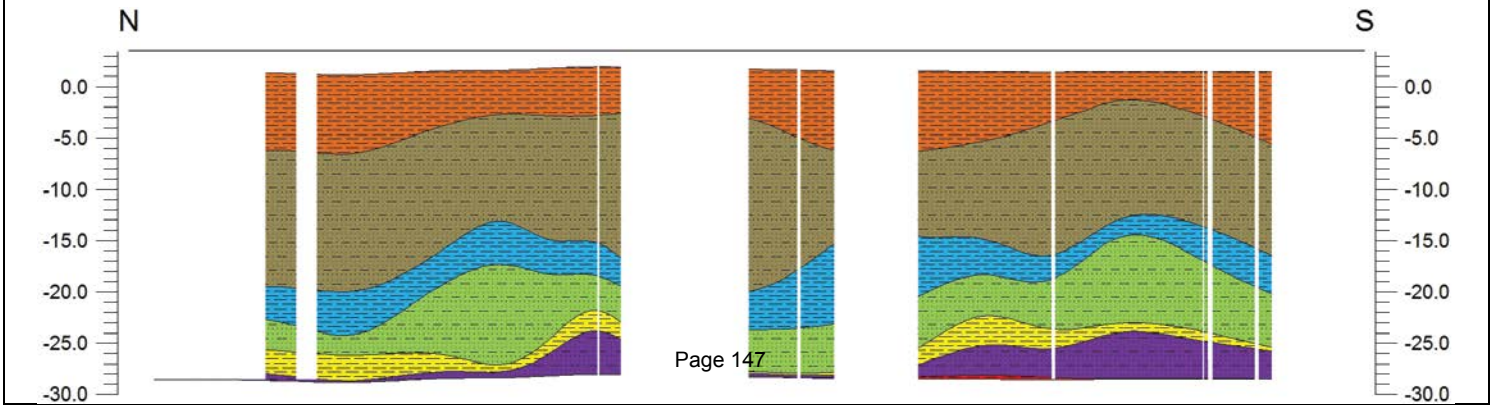

V.Soft to M.Stiff Clayey SILT/Silty CLAY	M.Stiff to Hard Silty CLAY/SILT
V.Loose to M.Dense V.Fine to Fine SAND	M.Dense to V.Dense V.Fine to M. SAND
M.Stiff to Stiff Clayey SILT/Silty CLAY	M.Stiff toV.Stiff Silty CLAY/Clayey SILT
M.Dense to Dense V.Fine to M. SAND	

Line: NS21

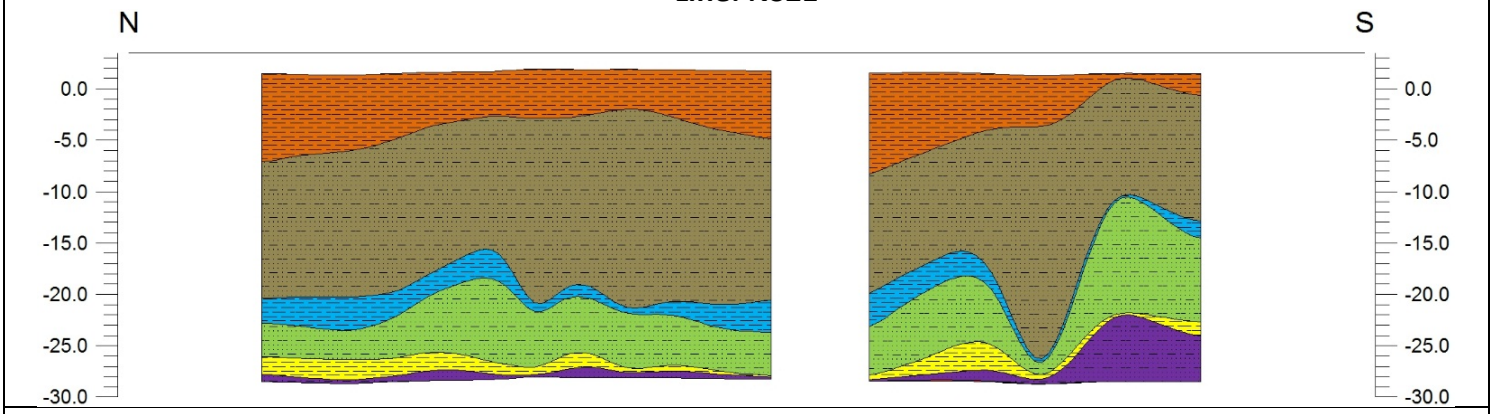

Line: NS22

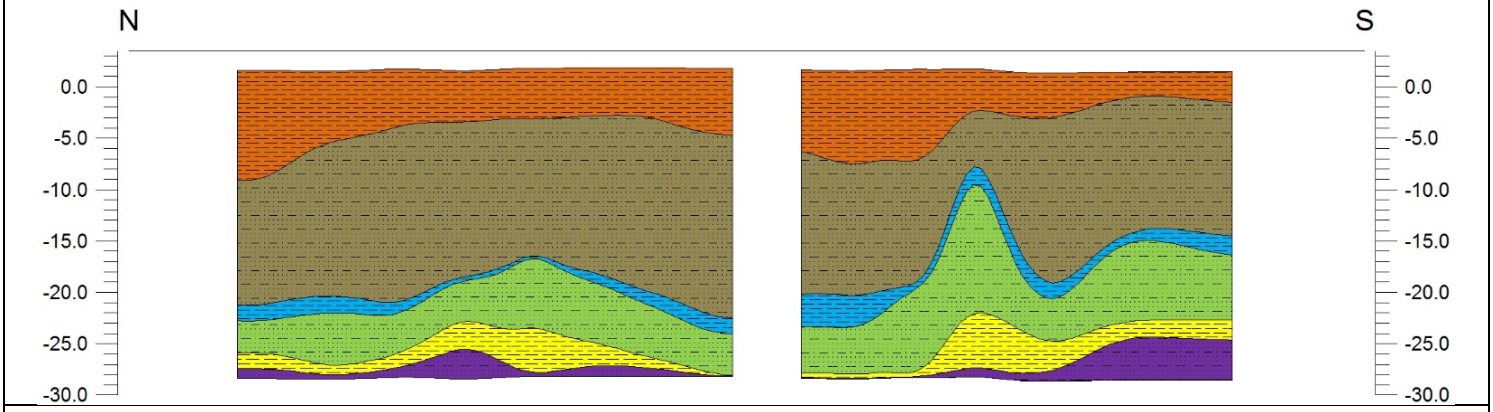

Line: NS23

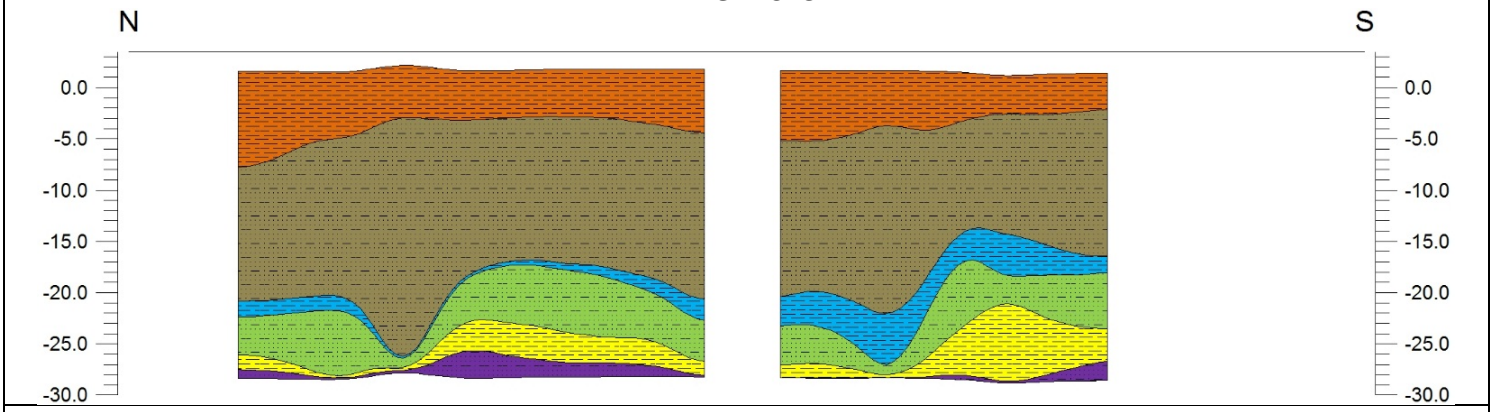

Line: NS24

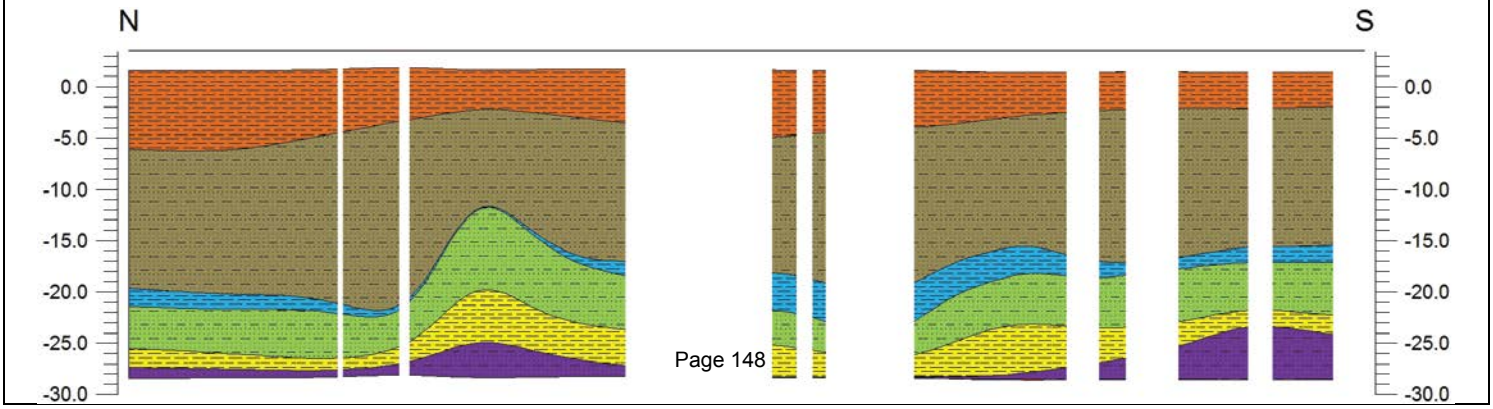

V.Soft to M.Stiff Clayey SILT/Silty CLAY	M.Stiff to Hard Silty CLAY/SILT
V.Loose to M.Dense V.Fine to Fine SAND	M.Dense to V.Dense V.Fine to M. SAND
M.Stiff to Stiff Clayey SILT/Silty CLAY	M.Stiff toV.Stiff Silty CLAY/Clayey SILT
M.Dense to Dense V.Fine to M. SAND	

Line: NS25

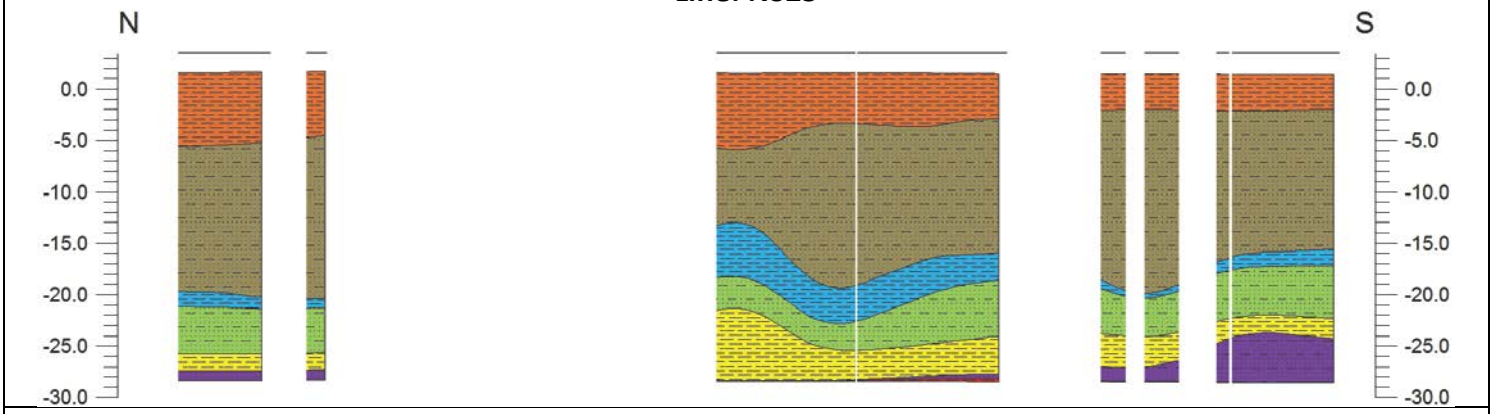

Line: NS26

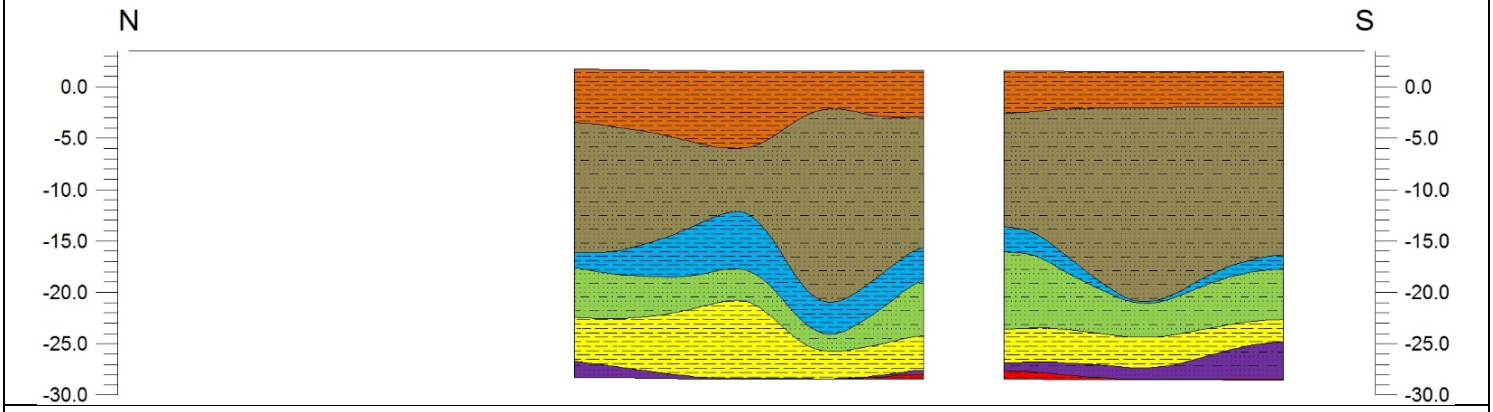

Line: NS27

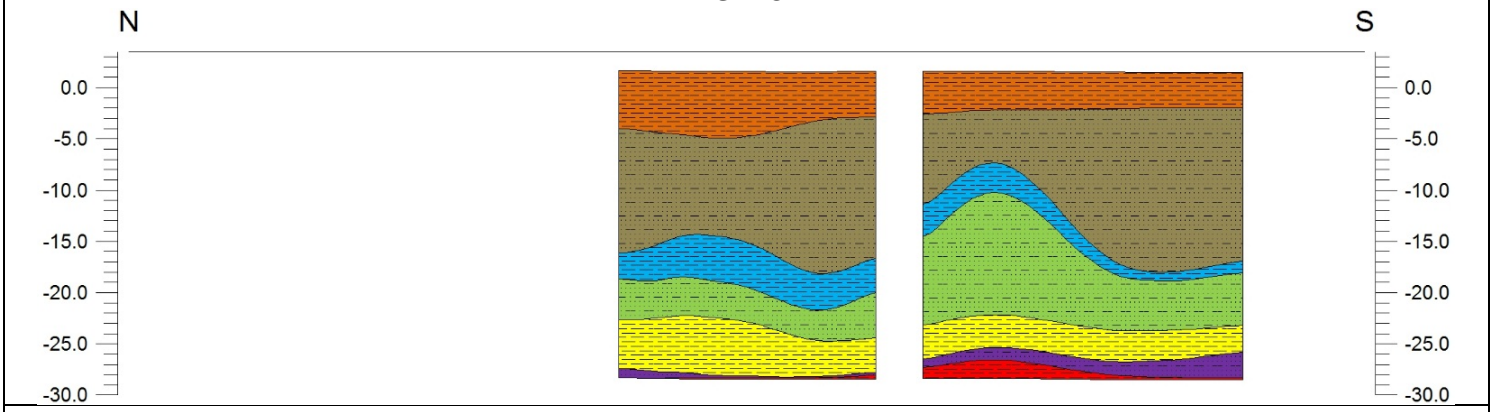

Line: NS28

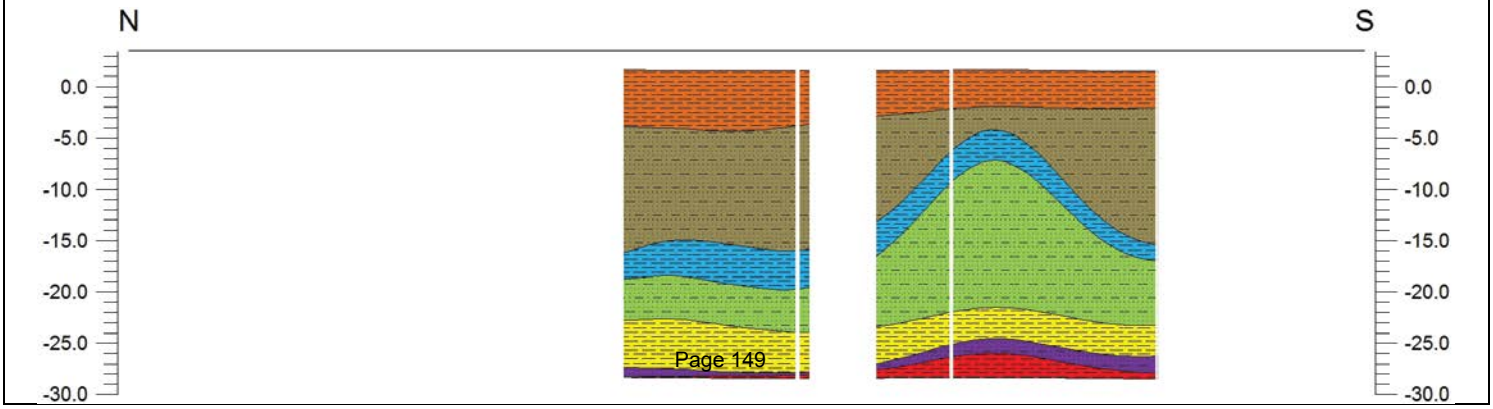

V.Soft to M.Stiff Clayey SILT/Silty CLAY	M.Stiff to Hard Silty CLAY/SILT
V.Loose to M.Dense V.Fine to Fine SAND	M.Dense to V.Dense V.Fine to M. SAND
M.Stiff to Stiff Clayey SILT/Silty CLAY	M.Stiff toV.Stiff Silty CLAY/Clayey SILT
M.Dense to Dense V.Fine to M. SAND	

Line: NS29

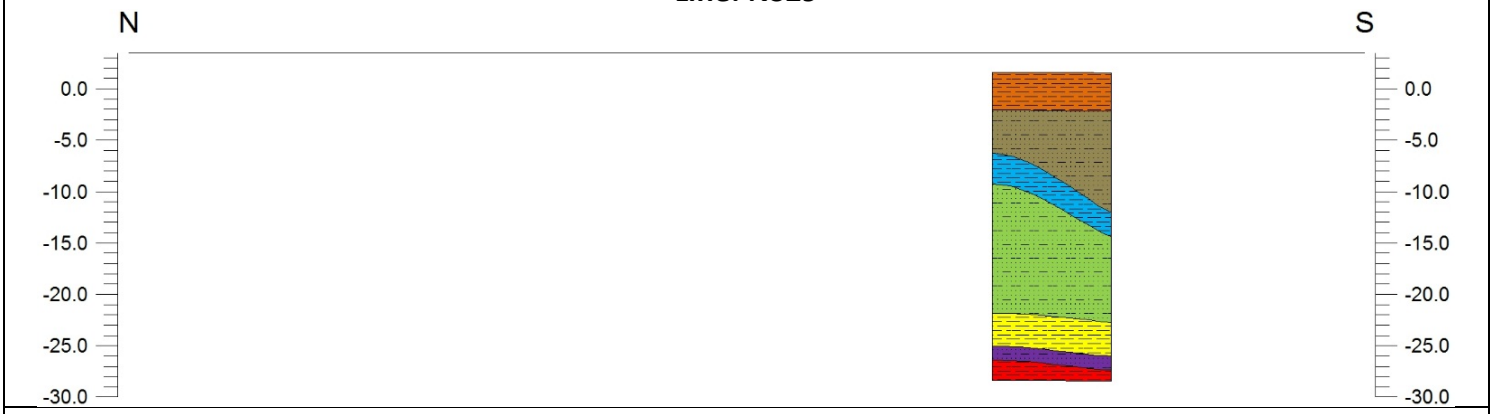

Line: EW01

Line: EW02

Line: EW03

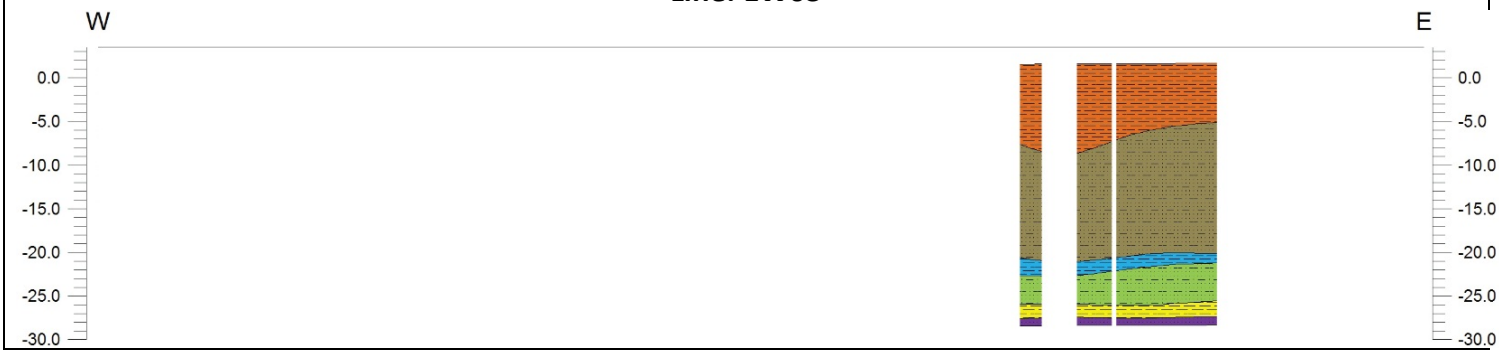

V.Soft to M.Stiff Clayey SILT/Silty CLAY	M.Stiff to Hard Silty CLAY/SILT
V.Loose to M.Dense V.Fine to Fine SAND	M.Dense to V.Dense V.Fine to M. SAND
M.Stiff to Stiff Clayey SILT/Silty CLAY	M.Stiff toV.Stiff Silty CLAY/Clayey SILT
M.Dense to Dense V.Fine to M. SAND	

Line: EW04

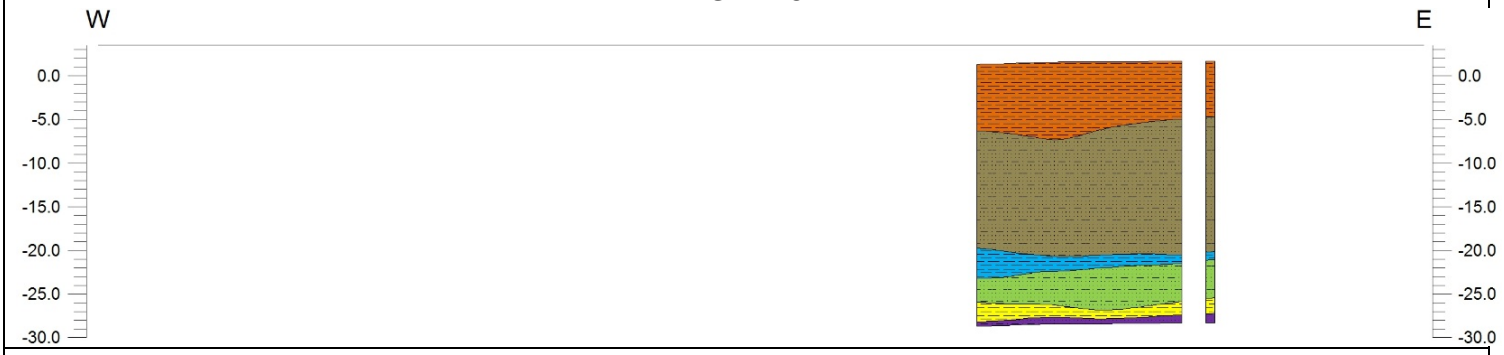

Line: EW05

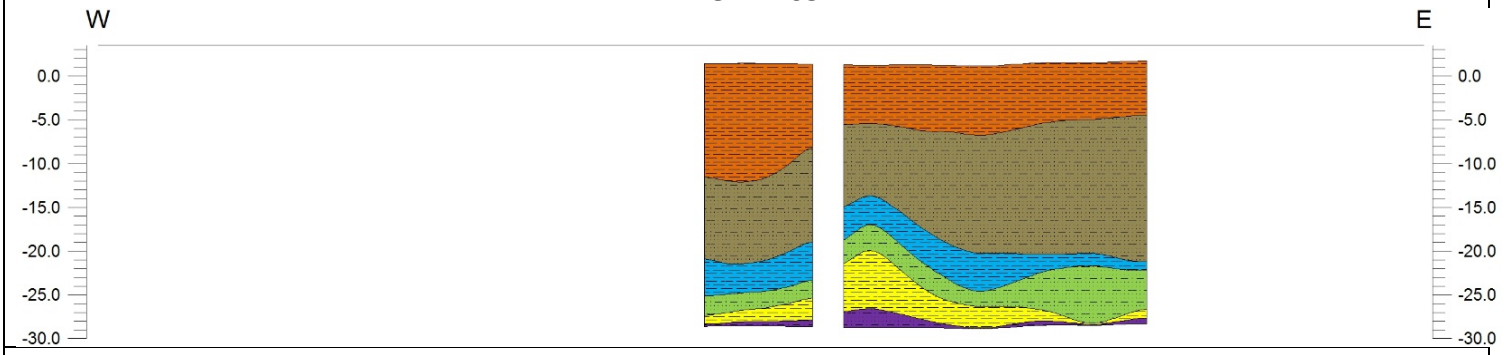

Line: EW06

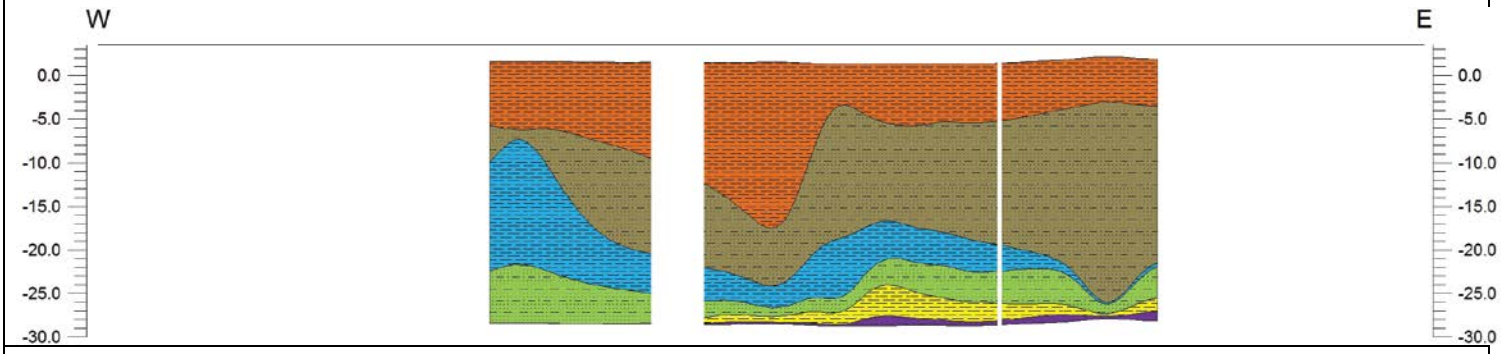

Line: EW07

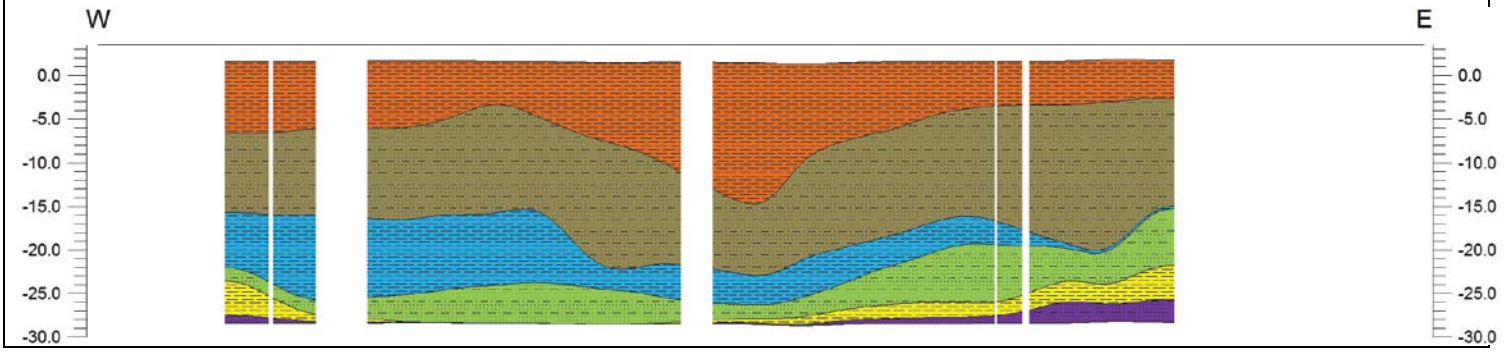

V.Soft to M.Stiff Clayey SILT/Silty CLAY	M.Stiff to Hard Silty CLAY/SILT
V.Loose to M.Dense V.Fine to Fine SAND	M.Dense to V.Dense V.Fine to M. SAND
M.Stiff to Stiff Clayey SILT/Silty CLAY	M.Stiff toV.Stiff Silty CLAY/Clayey SILT
M.Dense to Dense V.Fine to M. SAND	

Line: EW08

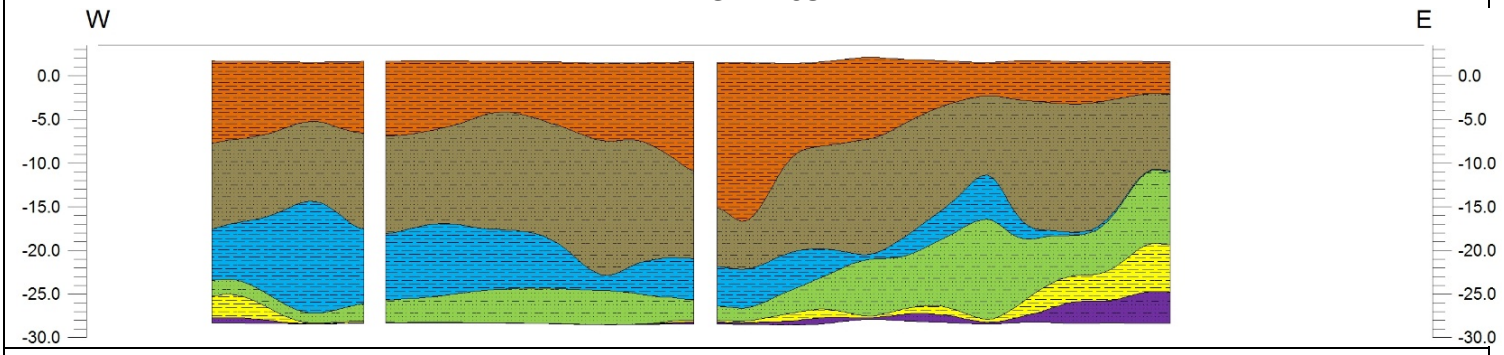

Line: EW09

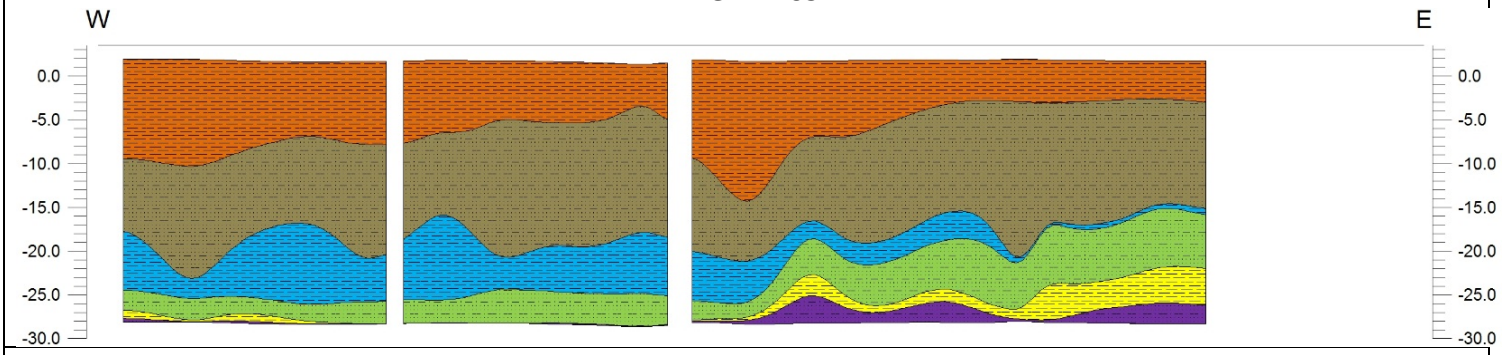

Line: EW10

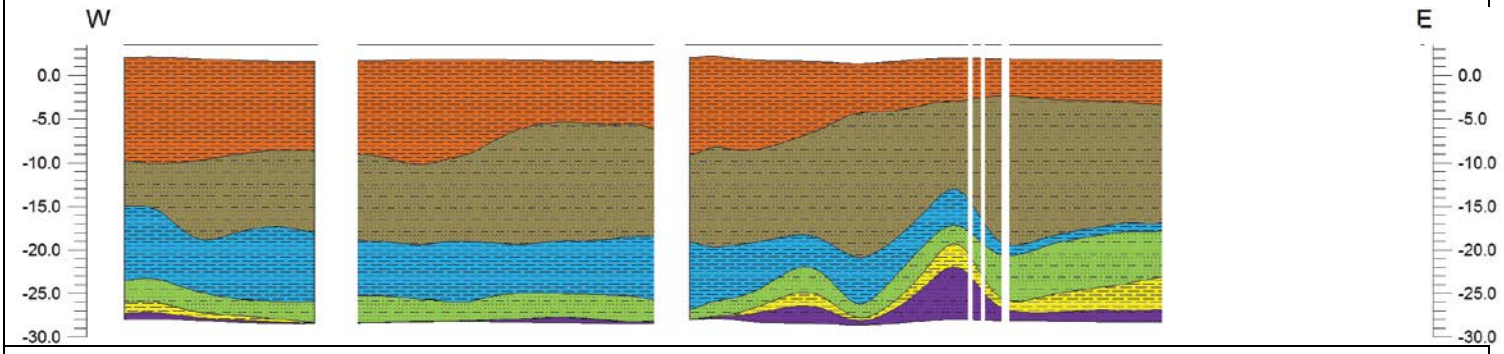

Line: EW11

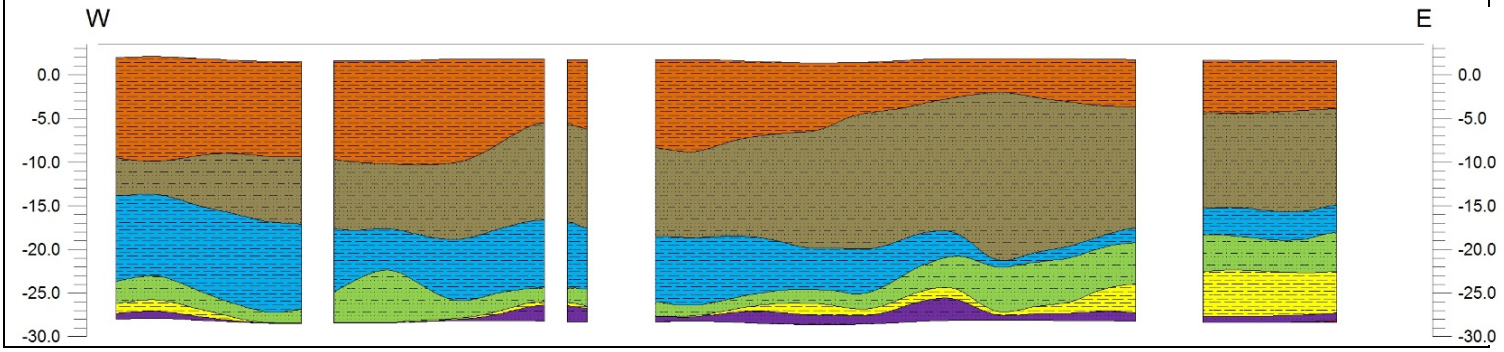

V.Soft to M.Stiff Clayey SILT/Silty CLAY	M.Stiff to Hard Silty CLAY/SILT
V.Loose to M.Dense V.Fine to Fine SAND	M.Dense to V.Dense V.Fine to M. SAND
M.Stiff to Stiff Clayey SILT/Silty CLAY	M.Stiff toV.Stiff Silty CLAY/Clayey SILT
M.Dense to Dense V.Fine to M. SAND	

Line: EW12

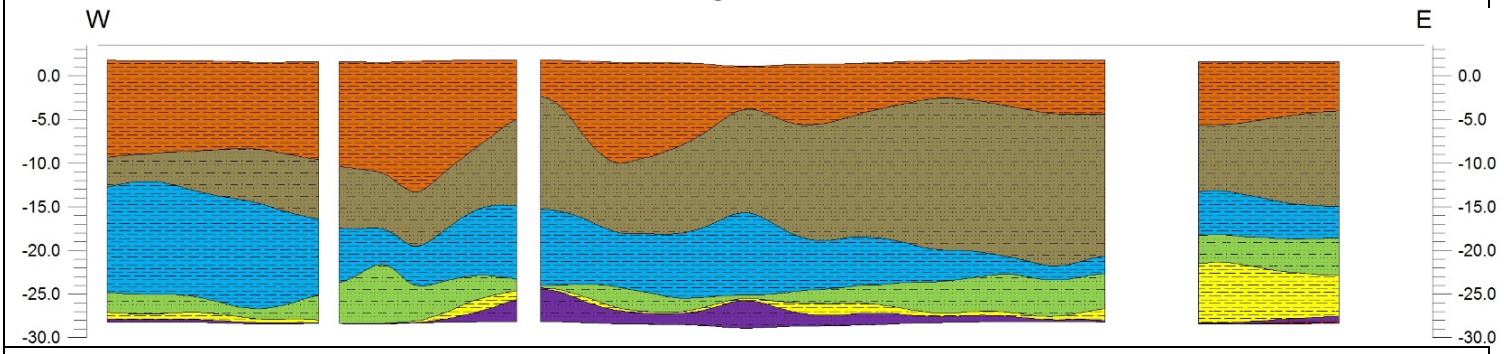

Line: EW13

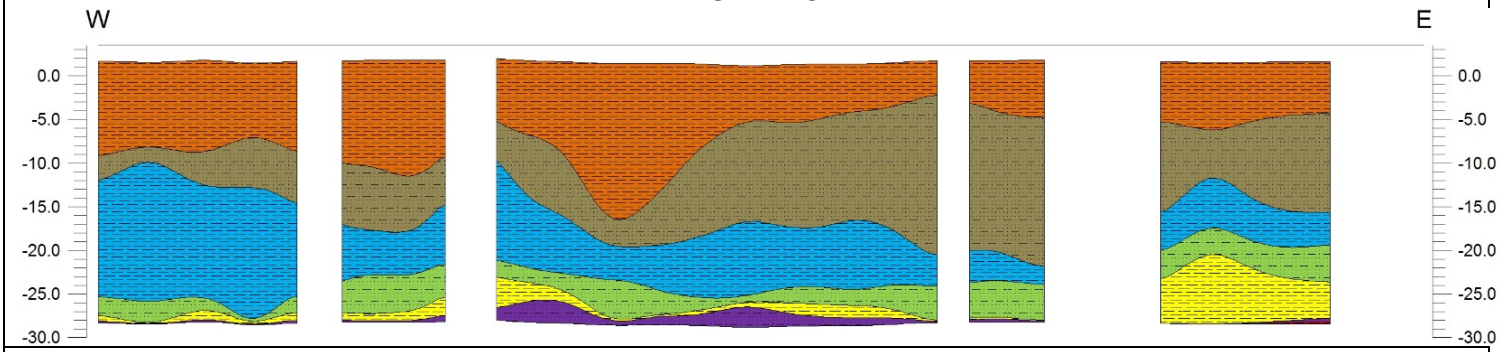

Line: EW14

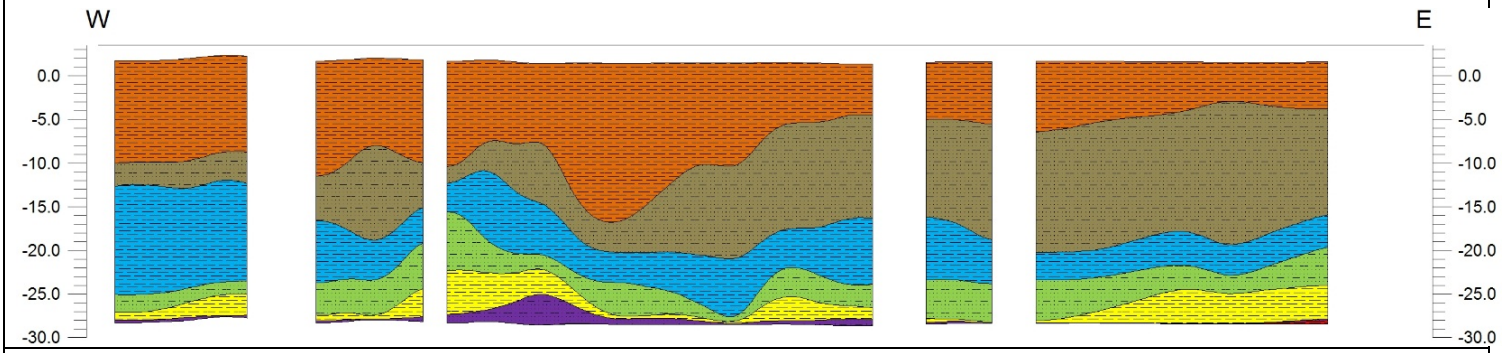

Line: EW15

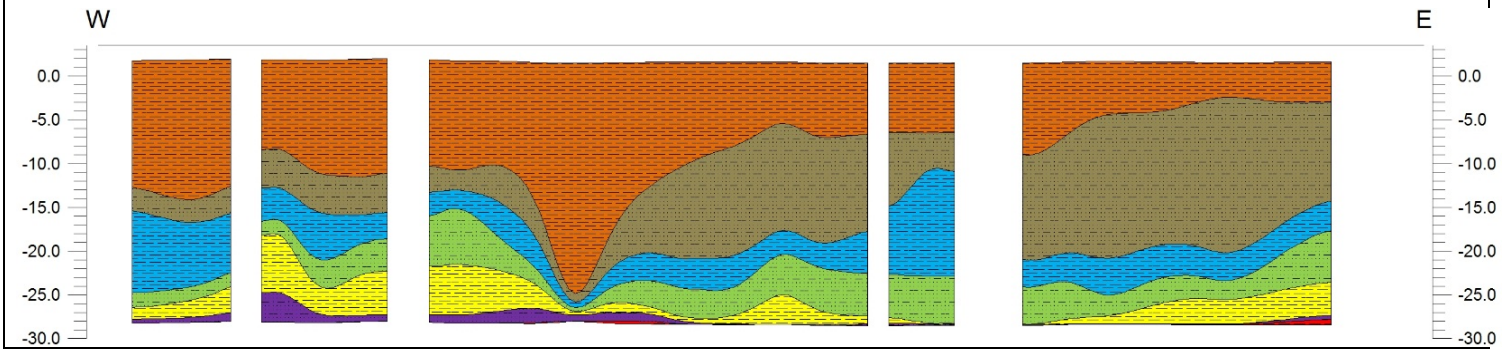

V.Soft to M.Stiff Clayey SILT/Silty CLAY	M.Stiff to Hard Silty CLAY/SILT
V.Loose to M.Dense V.Fine to Fine SAND	M.Dense to V.Dense V.Fine to M. SAND
M.Stiff to Stiff Clayey SILT/Silty CLAY	M.Stiff toV.Stiff Silty CLAY/Clayey SILT
M.Dense to Dense V.Fine to M. SAND	

Line: EW16

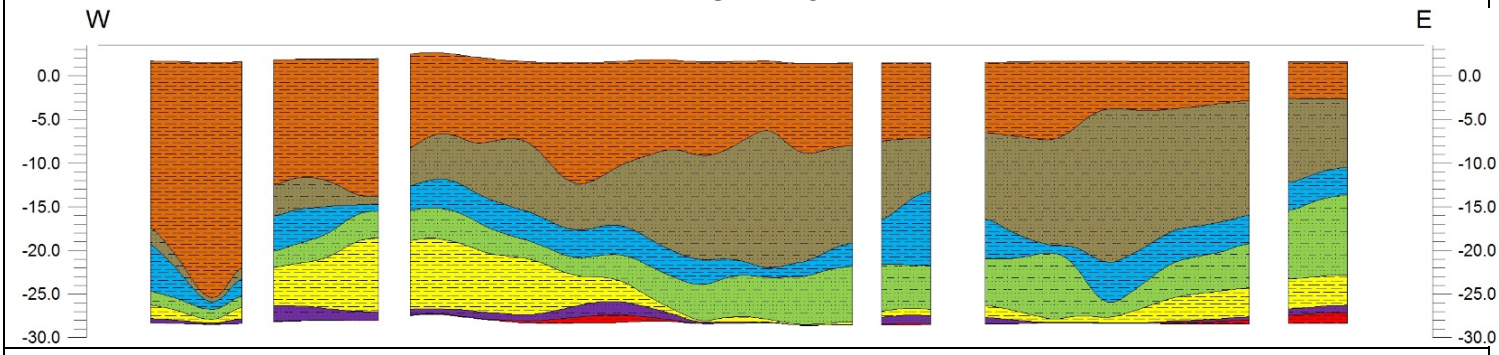

Line: EW17

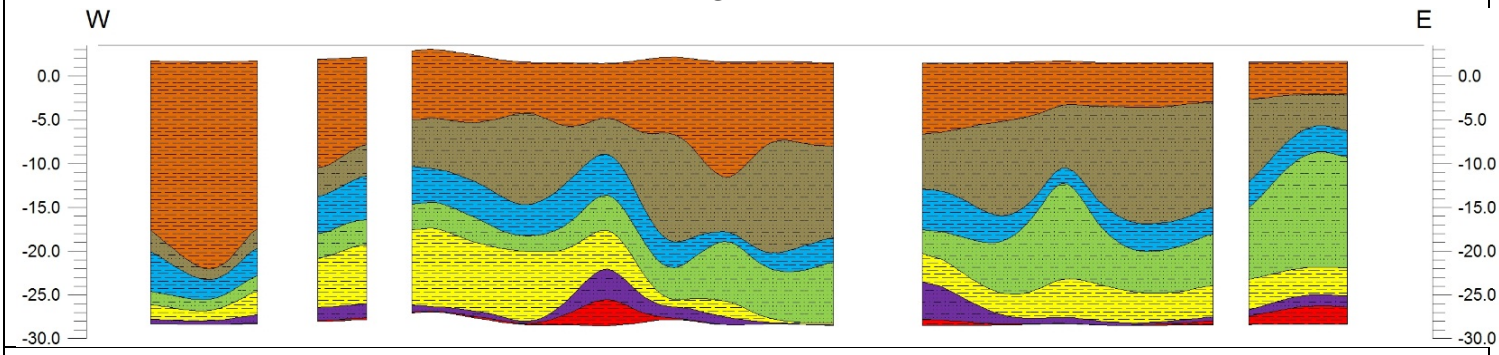

Line: EW18

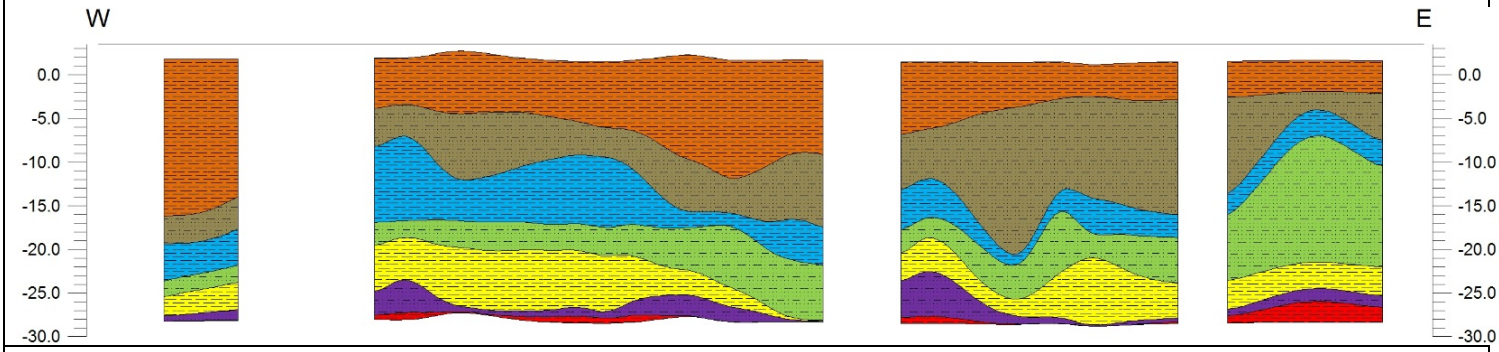

Line: EW19

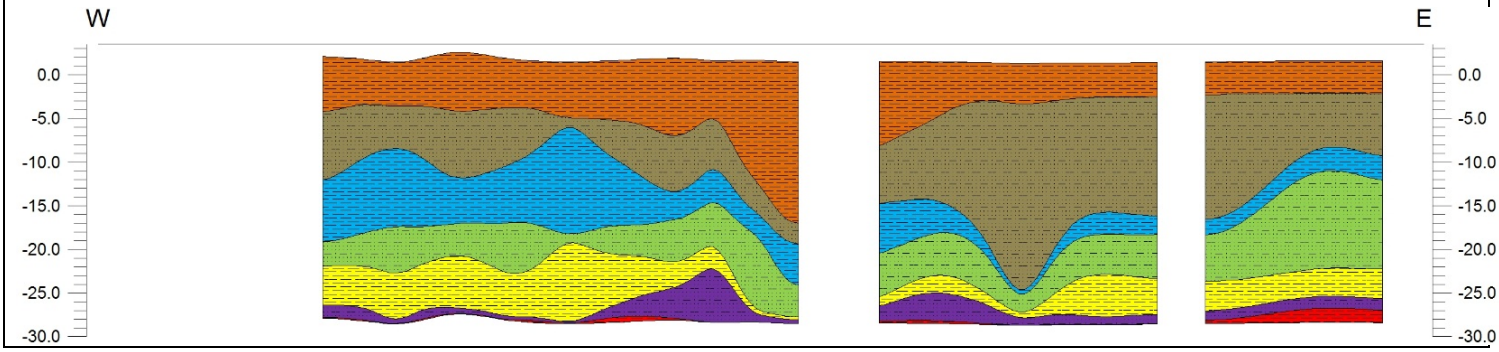

V.Soft to M.Stiff Clayey SILT/Silty CLAY	M.Stiff to Hard Silty CLAY/SILT
V.Loose to M.Dense V.Fine to Fine SAND	M.Dense to V.Dense V.Fine to M. SAND
M.Stiff to Stiff Clayey SILT/Silty CLAY	M.Stiff toV.Stiff Silty CLAY/Clayey SILT
M.Dense to Dense V.Fine to M. SAND	

Line: EW20

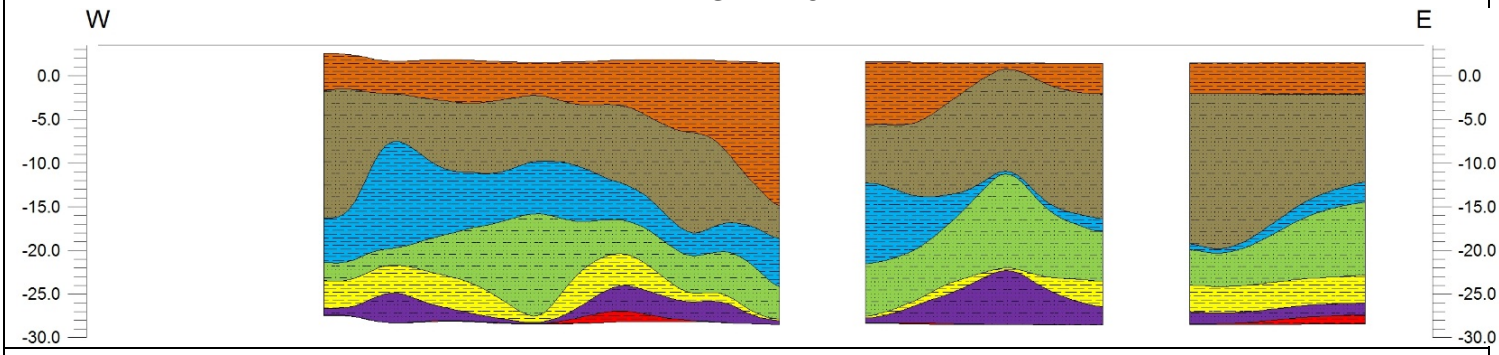

Line: EW21

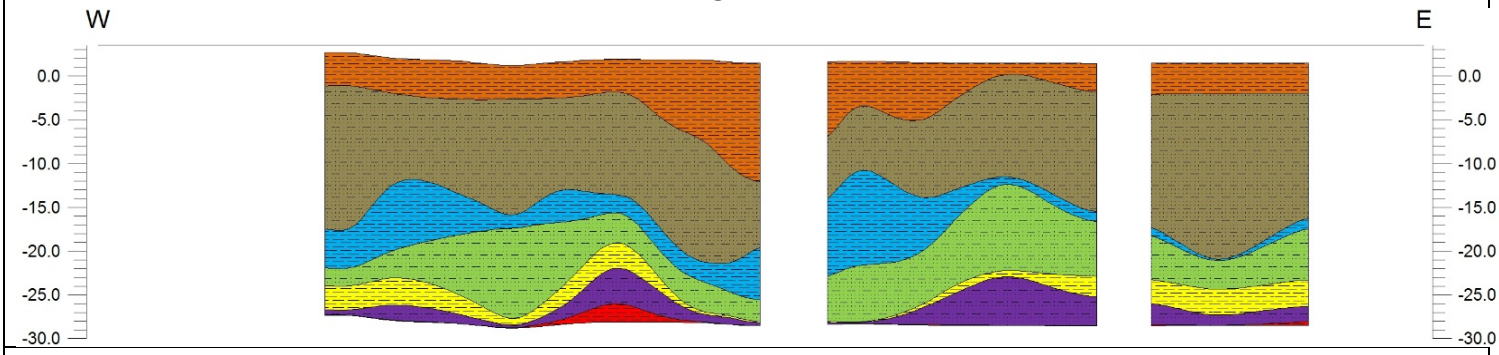

Line: EW22

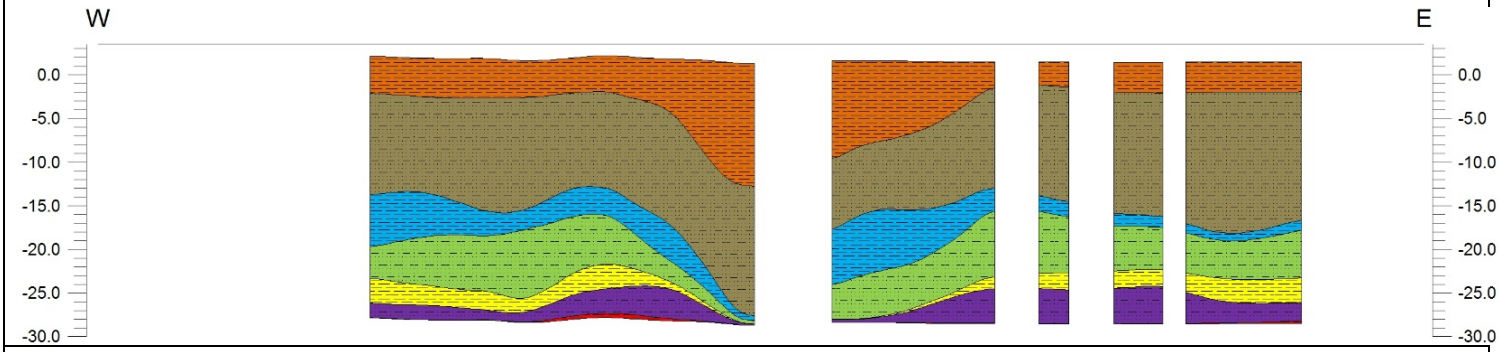

Line: EW23

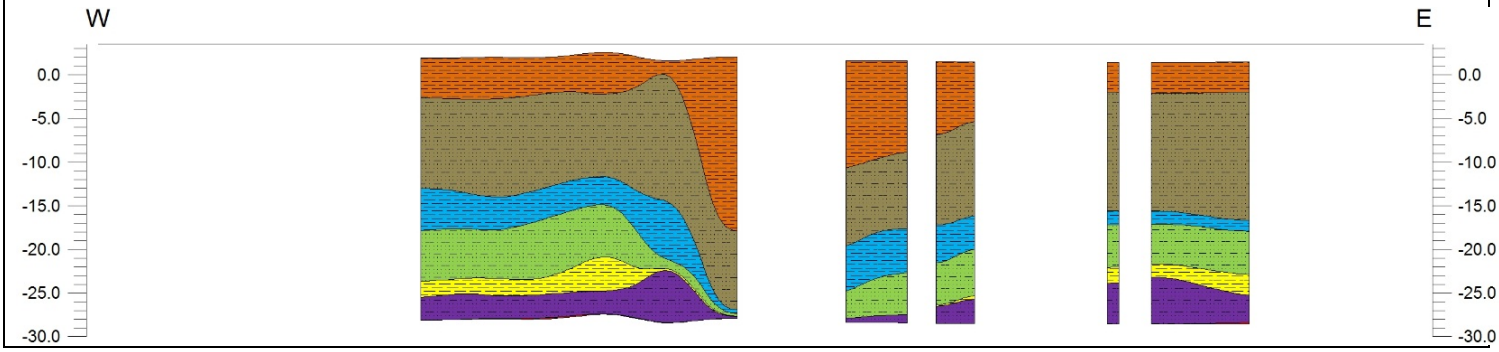

V.Soft to M.Stiff Clayey SILT/Silty CLAY	M.Stiff to Hard Silty CLAY/SILT
V.Loose to M.Dense V.Fine to Fine SAND	M.Dense to V.Dense V.Fine to M. SAND
M.Stiff to Stiff Clayey SILT/Silty CLAY	M.Stiff toV.Stiff Silty CLAY/Clayey SILT
M.Dense to Dense V.Fine to M. SAND